



Durham E-Theses

Configuration and diffusion of trapped polymer molecules

Davison, Donald

How to cite:

Davison, Donald (1995) *Configuration and diffusion of trapped polymer molecules*, Durham theses, Durham University. Available at Durham E-Theses Online: <http://etheses.dur.ac.uk/5134/>

Use policy

The full-text may be used and/or reproduced, and given to third parties in any format or medium, without prior permission or charge, for personal research or study, educational, or not-for-profit purposes provided that:

- a full bibliographic reference is made to the original source
- a [link](#) is made to the metadata record in Durham E-Theses
- the full-text is not changed in any way

The full-text must not be sold in any format or medium without the formal permission of the copyright holders.

Please consult the [full Durham E-Theses policy](#) for further details.

Configuration and Diffusion of Trapped Polymer Molecules

September 1995

The copyright of this thesis rests with the author.
No quotation from it should be published without
his prior written consent and information derived
from it should be acknowledged.

**Donald Davison
Hatfield College
University of Durham**

**Supervisor
Dr. Randal Richards**

A thesis submitted to the University of Durham in partial fulfilment of the regulations for
the Degree of Doctor of Philosophy



17 MAY 1996

Configuration and Diffusion of Trapped Polymer Molecules

Donald Davison

PhD Thesis, September 1995

Abstract

The purpose of this work was to study both the static and dynamic behaviour of polymer chains "trapped" within polymeric networks. In recent years there has been a large amount of theoretical work dedicated to towards the study of polymer chains in concentrated, entangled media and quantitative theories have been advanced describing both the mechanism of diffusion of polymer chains within a polymeric network as well as the size of the loose chain within the network. There have, however been relatively few experimental studies of the properties of such systems, due to considerable the difficulties involved in the preparation of suitable samples.

This work has centred on the preparation of model polymer networks containing a very low sol fraction and the trapping of a series of probe chains within these networks to determine the properties of the probe chain. A series of well characterised polymer networks containing probe chains have been prepared by anionic polymerisation using a novel difunctional initiator recently developed in another laboratory. Properties of the networks alone have been measured by both SANS and QELS and analysed in terms of renormalisation group and mean-field theories. Good agreement has been found with theory, though the correlation length of the network has been found not scale as predicted and appears to be determined by the synthetic conditions employed in the preparation of the network.

SANS has been used to determine the size of the probe chain in bulk networks, the results of which have been found to be different to that predicted by the theories of a chain in a "random medium". In solvent swollen networks, the size of the chain has been found to be independent of the cross link density, the behaviour being associated with that of a semi-dilute solution and the appropriate region of the polymer phase diagram has been identified.

QELS has been used in an attempt to determine the mechanism of diffusion of the probe chain within the network and in semi-dilute solutions so as to ascertain any differences between the two cases. Analysis centred around deconvolution of the autocorrelation function its components (the probe chain and the collective motions of the network). However difficulties in the interpretation of the data have prevented a full clarification of the experimental situation.

Acknowledgements

Firstly the usually understated expressions of thanks go to my supervisor, Randal Richards for his continual help, support, guidance and relentless enthusiasm through the project, even when it was "only" to teach the famous RTFM lesson.

Without the efforts of several people, much of the work outlined here would not be possible and I thank them gratefully. Tom Kiff who prepared many of the initiators, provided a great deal of invaluable experience, without which my life would have been substantially more difficult. Likewise, Dr. Steve King, instrument scientist at R.A.L., proved to be an essential ingredient of all S.A.N.S. experiments. Thanks go to Terry Harrison for fixing the computer whenever it decided not to work and to Gordon "Trigger" Forrest for providing a S.E.C. service and for (almost) backing up the data. Many thanks are also due to Ray Hart and Gordon Haswell, the Chemistry Department glassblowers for producing and repairing equipment with such speed, they have a talent that I can only watch in amazement.

Thanks have to go to the people that made three years in the IRofC pass with such ease. Norman Clough, who repeatedly attempted to teach me his eight jokes, Cecilia Backson and Ian Hopkinson all managed to keep me at least relatively sane, while Sian Davies, Andy Grainger, PD, Mark Taylor, Tall Paul, Steve Edge, John Holland, Stella Gissing, Lian Hutchings, Frank Davies (and even Lesley Hamilton...) all helped to pass the time with the odd joke (well not many from Marky T actually).

Without the efforts of several good friends, Richard (Captain Birdseye) Towns, Brian (Roach) Rochford, Ian (Weeman) Reynolds, Nick (Ronnie) Haylett, Simon Tasker, Richard McGowan and Steven Snaith I doubt that I'd have consumed as much beer in the last three years. Thanks go to them for keeping me straight, (well maybe not).

Thanks also go to Rorie, Pete and Rob, who put up with me in the three years of living at 36 Sutton Street, a household that produced many memorable moments, (not least the incident with the bath), it was a truly good place to live.

Finally thanks go to everyone at Courtaulds who have made working there a reasonably enjoyable experience over the last year, even Les Clark, for despite all the verbal abuse on a Monday morning he's actually quite a good bloke to work for.

Declaration

All work contained in this thesis is, unless stated otherwise, the sole work of the author and has been carried out in the laboratories of the Interdisciplinary Research Centre in Polymer Science and Technology (University of Durham) and at the Rutherford Appelton Laboratory (Harwell, Oxfordshire) and remains the copyright of the author. No quotation from it should be published without the prior written consent of the author and information derived from it should be acknowledged. No work contained in this thesis has previously been submitted for any other qualification.

Contents

Abstract	i.
Acknowledgements	ii.
Declaration	iii.
Contents	iv.
Appendices	viii

Chapter 1, General Introduction

1.1	Background	1
1.2	The Structure of Polymer Networks	1
1.3	The Conformation of Polymer Chains	8
1.3.1	Theoretical Modelling of the Conformation of Polymer Chains	9
1.3.2	The Excluded Volume Effect	10
1.3.3	The Conformation of Real Chains in the Bulk and in Dilute Solution	11
1.3.4	The Conformation of a Chain in a Random Medium	12
1.3.5	Polymer Concentration Regimes	14
1.3.6	The Properties of Semi-Dilute Solutions and Polymer Gels	16
1.3.6.1	The Correlation Length	19
1.3.6.2	The Blob Model Of Chain Statistics	21
1.3.6.3	The Polymer Phase Diagram	23
1.3.6.4	The c^* Theorem	26
1.4	The Dynamics of Polymer Chains	27
1.4.1	Models of Hydrodynamic Behaviour in Dilute Solution	28
1.4.2	Hydrodynamic Behaviour in Semi-Dilute Solution	30
1.4.3	Models of Hydrodynamic Behaviour in Concentrated Systems	32
1.4.4	The Reptation Model	33
1.5	Aims and Objectives	40
1.5.1	The Choice of System	42
1.6	References	44

Chapter 2, Sample Preparation and Characterisation

2.1	Introduction	48
2.2	Anionic Polymerisation	48
2.2.1	Difunctional Anionic Polymerisation Initiators	51
2.3	Experimental	53
2.3.1	Preparation of Solvent	53
2.3.1.1	Tetrahydrofuran (THF)	53
2.3.1.2	Benzene	54
2.3.2	Preparation of Monomer	54
2.3.2.1	Preparation of Deuterated Monomer	55
2.3.3	Preparation of Initiator	55
2.3.3.1	(s) Butyllithium	55
2.3.3.2	Sodium Napthalene	56
2.3.3.3	Disodium Tetramer of α -Methyl Styrene	56
2.3.3.4	1,3-Phenylenebis(3-methyl-1-phenylpentylidene)dilithium	57
2.3.4	Preparation of Cross linking Agent	59
2.3.4.1	Triallyloxytriazene (TAT)	59
2.3.4.2	Divinylbenzene (DVB)	59
2.3.5	Polymerisation Procedure	62
2.3.5.1	Preparation of Linear Polystyrene	64
2.3.6	Preparation of Polystyrene Networks	64
2.4	Characterisation of Polymers by Size Exclusion Chromatography	68
2.4.1	Chloroform SEC	68
2.4.2	Results of SEC Analysis of Linear Polymers	69
2.5	Characterisation of Polystyrene Networks	69
2.5.1	Characterisation of Precursor Polymer to Blank Networks	69
2.5.1.1	SEC Analysis of Networks Containing Deuterated Probe Chains	70
2.5.1.2	SEC Analysis of Networks Containing Hydrogenous Probe Chains	72
2.5.2	Sol Fraction of Polymer Networks	73
2.5.2.1	Extraction of the Sol Fraction	73

2.5.3	Equilibrium Swelling Measurements	75
2.5.3.1	Determination of the Volume Fraction in Swollen Networks	76
2.5.3.2	Evaluation of Swelling Equilibrium	77
2.5.3.3	Results of Swelling Measurements	78
2.5.3.4	Polymer Molecular Weight From Swelling Measurements	81
2.6	Conclusions	85
2.7	References	86

Chapter 3, Small Angle Neutron Scattering

3.1	Introduction	87
3.2	Theoretical Aspects of Small Angle Neutron Scattering	89
3.3	Instrumentation	98
3.3.1	The Small Angle Spectrometer-LoQ	99
3.3.2	Calibration of the Spectrometer	100
3.4	Experimental	103
3.5	Determination of the Correlation Length of Solvent Swollen Gels	106
3.6	Determination of the Radius of Gyration of a Trapped Probe Chain	114
3.6.1	Initial Experiments on the Probe Chain Size	116
3.6.2	Probe Chain Size Measured in the Bulk State Using Probe PSD2	117
3.6.3	Probe Chain Size in Solvent Swollen Networks	124
3.7	Conclusions	137
3.8	References	139

Chapter 4, Quasi-Elastic Light Scattering

4.1	Introduction	142
4.2	Theoretical Aspects of QELS	143
4.2.1	The Origin of the Scattering of Light by Macromolecules	143
4.2.2	Quasi-Elastic Light Scattering	147
4.2.3	Homodyne and Heterodyne Correlation Functions	149
4.2.4	Data Reduction and Analysis	151

4.2.4.1	Cumulants	153
4.2.4.2	The Kohlrausch-Williams-Watts Stretched Exponential Function	154
4.2.4.3	Inverse Laplace Transformation of QELS Data	155
4.3	Instrumentation	155
4.3.1	Alignment of the Spectrometer	159
4.3.2	Calibration of the Spectrometer	160
4.4	Experimental	165
4.4.1	Preparation of Solvents and Glassware for QELS Studies	165
4.4.2	Dilute Solution Measurements of the Tracer Diffusion Coefficient	166
4.4.3	Preparation of Semi-Dilute Solutions for QELS Study	167
4.4.4	Preparation of Swollen Gels for QELS Study	168
4.5	The Probe Chain Tracer Diffusion Coefficient	169
4.5.1	Tracer Diffusion Coefficients in Cyclohexane Solution	173
4.6	QELS From Model Polystyrene Networks	178
4.6.1	General Features of the QELS Spectra	181
4.6.2	The Co-operative Diffusion Coefficient	184
4.6.3	The Longitudinal Osmotic Modulus	189
4.7	The Co-operative Diffusion Coefficient of "Equivalent" Solutions	193
4.7.1	General Features of the Spectra from Cyclohexane Solutions	193
4.7.2	General Features of the Spectra from Toluene Solutions	197
4.7.3	The Co-operative Diffusion Coefficient	200
4.8	QELS from Networks and Solutions Containing Probe Chains	205
4.9	Conclusions	209
4.10	References	212

Chapter 5, Conclusions and Suggestions for Future Work

5.1	General Discussion	216
5.2	Conclusions	220
5.3	Suggestions for Future Work	221

Appendices

Appendix A: Glossary of Terms and Symbols Used

Appendix B: Volumetric Swelling Results

- B1: Swelling Results in Cyclohexane at 308K
- B2: Swelling Results in Cyclohexane at 313K
- B3: Swelling Results in Cyclohexane at 318K
- B4: Swelling Results in Cyclohexane at 323K
- B5: Swelling Results in Toluene at 298K

Appendix C: Quasi-Elastic Light Scattering Results

- C1: Dilute Solution QELS Results from the Probe 3 Polymer
- C2: Dilute Solution QELS Results from the Probe 4 Polymer
- C3: Dilute Solution QELS Results from the Probe 5 Polymer
- C4: QELS Results from PBMPPD/DVB Networks Swollen in Cyclohexane in the Temperature Range 308-323K
- C5: QELS Results from AMS/DVB Networks Swollen in Cyclohexane in the Temperature Range 308-318K
- C6: QELS Results from AMS/DVB networks Swollen in Cyclohexane at 323K, in Toluene at 298K and from PBMPPD/DVB Networks Swollen in toluene at 298K
- C7: Longitudinal Osmotic Modulus Results from AMS/DVB and PBMPPD/DVB Series Networks in Cyclohexane in the Temperature Range 308-323K
- C8: QELS Results from Equivalent Solutions in Cyclohexane at 308K
- C9: QELS Results from Equivalent Solutions in Cyclohexane at 313K
- C10: QELS Results from Equivalent Solutions in Cyclohexane at 318K
- C11: QELS Results from Equivalent Solutions in Cyclohexane at 323K
- C12: QELS Results from Equivalent Solutions in Toluene at 298K

Appendix D: Lectures, Conferences and Courses Attended

CHAPTER 1.

GENERAL INTRODUCTION.

1. Background.

It is only in recent years that the theoretical and experimental study of polymer molecules at concentrations intermediate between the bulk and dilute solution has progressed. One stimulus for these experimental advances has been provided by the availability of high flux neutron beams that have allowed the development of small angle neutron scattering (SANS) spectrometers¹. Over roughly the same time scale, advances in digital electronics have allowed the measurement of the line width broadening of Rayleigh scattered radiation and the development of photon correlation spectrometry (PCS)². The development of these two important techniques has allowed the study of concentrations above the dilute limit and has tested theoretical predictions of the properties of semi-dilute solutions and polymer gels which were advanced at a remarkable pace during the 1970's by many researchers but predominantly by several French groups culminating in the publication in 1979 of de Gennes' book³ "Scaling Concepts in Polymer Physics".

2. The Structure of Polymer Networks.

Although many of the remarkable features exhibited by polymer molecules arise from the properties of linear polymer chains, many more applications, particularly in the rubber, biochemical, adhesives and coatings industries⁴⁻⁶ rely on the joining together of large numbers of polymer molecules to form networks of polymeric material. Such networks consist of precursor polymer chains that are in essence cross linked to such an extent that the resulting three-dimensional network can be envisaged as being a single covalently bonded molecule.

Such molecules, as typified by elastomers, exhibit many remarkable properties. Elastomeric networks produce large reversible deformations following the imposition of an external stress, behaviour that arises from both the nature of the polymer and the



presence of the cross links in the network. Two features are the key to the understanding of this behaviour. Elastomers consist of long chain macromolecules above the polymer glass transition temperature that have a large number of easily accessible spatial arrangements, thus allowing the change in conformation of the polymer. Secondly, the polymer chains comprise a three dimensional network that extends continuously throughout the material, providing permanence to the structure for recovery on the removal of the external stress. This is achieved by linking the chains together at positions along the chain backbone-cross linking. Changes in the cross link density can be brought about by changing the separation of the cross links within the network which (by decreasing the chain separation) leads to the formation of a more highly cross linked network that is more resistant to imposed stresses as the polymer chains are unable to relax fully and adopt as many conformations as less highly cross linked networks.

Production of polymeric networks can be achieved by a number of different chemical pathways, however all strategies produce networks of two structural types^{7,8}. The most commonly found type of polymeric network is known as a random network where the chains of the network are joined together with no regard being paid to the homogeneity of the network. Randomly cross linked networks, typified by the case of the vulcanised rubber, consist of polymer chains joined to each other by covalent bonds distributed randomly along the polymer backbone as shown in figure 1.1. below.

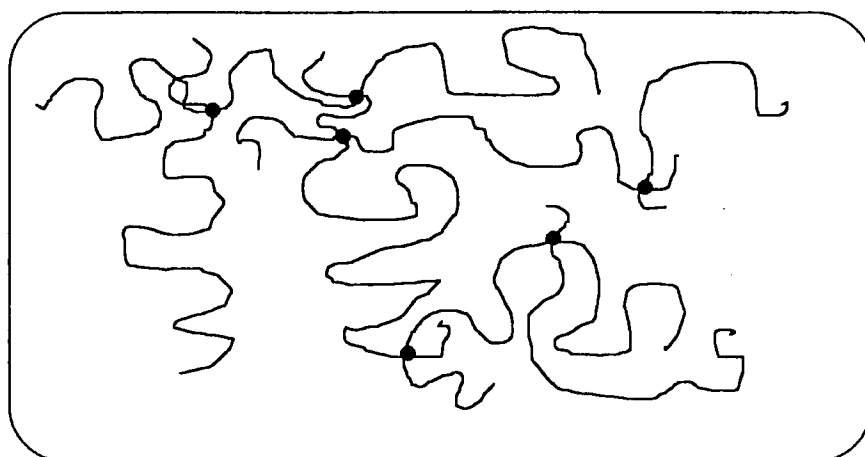


Figure 1.1.: In-homogeneous Distribution of Cross links in Random Networks.

This produces regions having differing cross link homogeneities where the molecular weight between cross links and hence the cross link density is not fixed. A second feature of randomly cross linked networks concerns the number of chains emanating from the cross links-the junction functionality. For randomly cross linked networks the functionality is not fixed and only junctions with a functionality greater than two act as cross links and are elastically effective.

Although the functionality of the junctions of the network plays an important part in determining the properties of the network, the most important structural characteristic is the concentration of the cross links connecting the polymer chains^{9,10}. There are a number of ways of expressing the extent of cross linking¹¹ within the network.

1. The density of cross links, (μ_e / V_0) where μ_e is the number of elastically effective cross links within the network and V_0 is the undeformed volume of the dry network.
2. The concentration of elastic chains, (v_e / V_0) where v_e is the number of chains connecting two elastically effective junctions.
3. The cycle rank density, (ξ_N / V_0) , where ξ_N is the cycle rank of the network¹², which is the number of cuts required to reduce the network to an acyclic structure
4. The molecular weight between cross links M_c , where $\left(M_c = \frac{\rho}{v_c / V_0} \right)$ and ρ is the density of the polymer network, this is an inverse measure of the degree of cross linking of the network.

Possibly the most important measure of the cross link density is the molecular weight between cross links as its measurement is the most simple, however it should be noted that relation of experimentally measurable quantities to the cross link density is invariably model dependent.

Characterisation of the structure of a real network requires the consideration of imperfections or defects in the network⁵⁻⁹. Any real network will contain terminal or pendant chains that do not fully participate in the elastic response of the network—they are bound to the network at only one end. A second class of defects within networks that provide no contribution to the elasticity of the network is the intramolecular loop where two points on a single chain are joined at the same junction. The same effect is obtained by the joining of an elastically effective chain to a chain that is unconnected to the network. Both types of defects can be seen in figure 1.2. below.

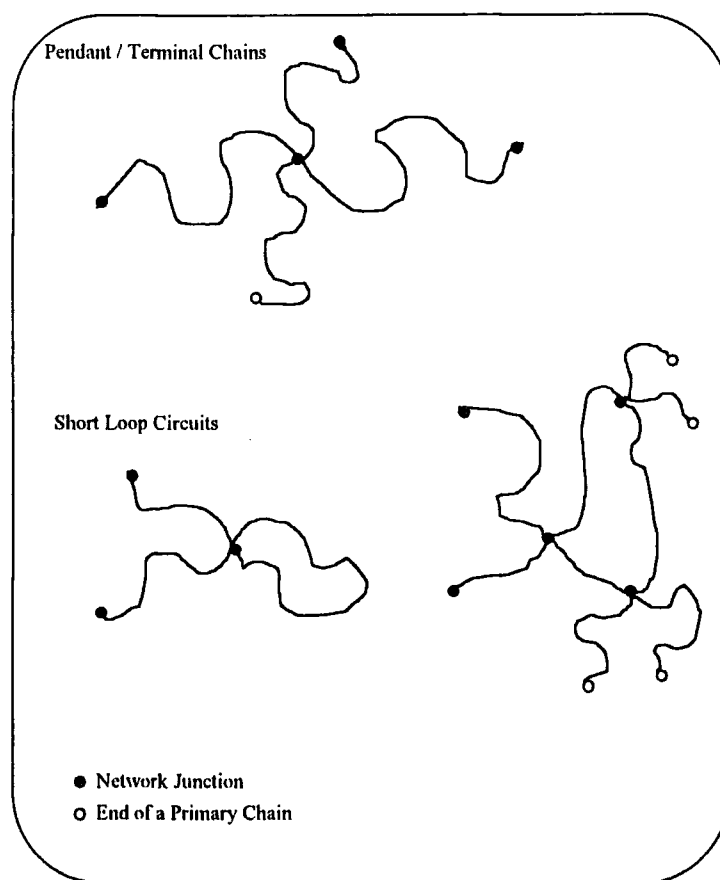


Figure 1.2.: Schematic Diagram of Defects Present in Randomly Cross linked Networks.

The structural defects present in randomly cross linked networks are however eliminated in *model* networks^{7,8}, which by definition are homogeneous and have no defects in the network structure. Such networks have formed the basis of many of the

theoretical studies trying to understand further the elasticity of rubber. Four criteria can be applied to model networks.

1. They should be homogeneous, microsinerisis (local expulsion of solvent) should be avoided and both the segment and cross link density be constant throughout the material.
2. They should consist of elastically effective chains only and hence pendant chains and loops should be eliminated.
3. The elastically effective chains should obey Gaussian statistics and therefore the chains should have a known molecular weight with a narrow distribution.
4. The functionality of the cross links should be known and constant throughout the sample, the functionality being the number of elastically effective network chains that are attached to one given cross link.

Several methods have been outlined for the preparation of model networks, however all follow the same general two step procedure where firstly a precursor polymer chain of known molecular weight and low polydispersity is prepared which is subsequently linked to the other polymer chains in a controlled manner, generally this being known as an end linking process. Two such methods are anionic block copolymerisation and anionic deactivation cross linking⁷. Both methods involve the Anionic polymerisation of a suitable monomer as the anionic technique offers a reliable method for the generation of the precursor polymer, producing a polymer that not only has a known molecular weight and a narrow distribution but is also reactive and therefore capable of being cross linked into a network structure. Reaction of the anion produced from the first polymerisation step can then be employed in a cross linking reaction to produce a network. Anionic block copolymerisation relies on the first stage polymerisation of a monomer such as styrene to produce a polymer with carbanionic sites at both chain ends. These *living* anionic chain ends⁷ can then be used to initiate the

polymerisation of a small amount of a bifunctional monomer such as divinylbenzene (DVB) the polymerisation of which forms small cross linked nodules, each connected to the f chain ends that have participated in the initiation process. Such methods have been used to produce various networks with elastic chains having different structures, however it should be noted that the method of cross linking employed allows no control over the junction functionality of the resulting network.

Similarly the method of anionic deactivation cross linking relies on an anionic polymerisation stage to produce a precursor polymer of known molecular weight with living carbanionic chain ends. Cross linking then proceeds in a more controlled manner by reaction of the living anions with a plurifunctional electrophilic reagent. As the functionality of the cross linking agent is fixed by the number of electrophilic sites in the molecule, the junction functionality of the network is in principle fixed. Such methods utilising organofunctional silane cross linking molecules have been found to prepare networks, however it has been found that some difficulty can arise over the relative reactivity of electrophilic sites in the cross linking molecule.

While swelling experiments have been used to confirm the homogeneous nature of "model" networks⁷, the presence of loops and pendant chains cannot be avoided. The former are most likely to occur when the polymer concentration of the reaction medium is low, the latter when it is very high. Such defects cannot be avoided during the preparation of any real network, however their presence can at least be minimised by the use of the correct reaction conditions.

As with any polymeric network, chains not cross linked into a model network can be removed from the network by the repeated extraction of this "sol fraction". Such material, the portion of polymeric chains not bound into the network during the cross linking process, can be extracted by Soxhlet extraction with solvent which swells the network. A qualitative link can be drawn to the quality of the produced network and the proportion of macromolecular sol extracted from the network. For networks containing

a high degree of a sol fraction a relatively poor network might be expected to have been formed, conversely for a network containing only a small fraction of a macromolecular sol, the cross linking reaction can be thought as having proceeded to completion and it can be envisaged that the number of pendant chains within the network might have been minimised.

As noted earlier, probably the most commonly expressed quantity measuring the degree of cross linking of a network is the molecular weight between cross links, M_c . One of the most common methods for the measurement of M_c relies upon the determination of the degree of swelling of the polymer network. Polymer networks absorb compatible diluents for essentially the same reasons as an analogous linear polymer chains dissolves in solvent to form an ordinary polymer solution. The entropy of the system is increased due to the larger volume of the polymer throughout which the solvent may spread, this may be either augmented or diminished by the enthalpy of dilution of the system. At the same time, the network chains are deformed and an elastic retractive force caused by the cross links in the system begins to develop. The equilibrium value of the amount of solvent absorbed is determined by the condition that under constant thermodynamic conditions, the free energy is at a minimum with respect to changes in the composition of the mixed phase (equation 1.1).

$$\left(\frac{\partial G}{\partial n_1} \right)_{n_2} = \mu_1 - \mu_1^0 = 0 \quad 1.1$$

where $\left(\frac{\partial G}{\partial n_1} \right)_{n_2}$ is the change in the Gibbs free energy with respect to the number

of solvent molecules,

μ_1 is the chemical potential of the solvent in the swollen network,

and μ_1^0 is the chemical potential of the pure solvent.

The theoretical treatment of the swelling of polymeric networks was developed some time ago by Flory and Rehner¹³ who described the swelling of the network on the

assumption that the free energy consists of two separable and additive contributions from the elementary mixing and elastic retractive forces. In this classical treatment, the mixing term was taken from the Flory-Huggins theory¹⁵⁻¹⁷ of polymer solutions and the elastic term from classical rubber elasticity theory^{9,18}. The Flory-Rehner expression given below in equation 1.2., was derived specifically for the case of a network cross linked in the bulk state and as such is inapplicable to the case of model networks prepared by the end linking of a semi-dilute solution of a polymer. A modification to the Flory-Rehner theory has been advanced by Rotstein and Lodge¹⁴ who have added a prefactor to the classical equation to describe the behaviour of a network prepared in the presence of a diluent. Both versions of the Flory-Rehner equation are discussed further in chapter 2, where the modified theory has been used to determine the molecular weight between cross links of "model" networks.

$$M_c = \rho \bar{V}_1 \phi^{1/3} \left[\frac{-\left(\phi^{1/3} - \frac{\phi}{2}\right)}{\ln(1-\phi) + \phi + \chi\phi^2} \right] \quad 1.2.$$

where \bar{V}_1 is the molecular volume of the solvent molecule,

ϕ is the polymer volume fraction in the swollen gel,

χ is the Flory-Huggins interaction parameter

and ρ is the density of the polymer network in the bulk state.

3. The Conformation of Polymer Chains.

Possibly the single most significant structural characteristic of a long chain macromolecule is its capacity to assume an enormous number of possible conformations as a direct consequence of the considerable degree of rotational freedom about single main chain bonds. The total number of conformations of the chain increases dramatically with increasing numbers of segments on the macromolecule and is amazingly large for polymers containing between 100 and 10,000 repeat units. Knowledge of the conformation of the chain is therefore of the utmost importance as many physical properties (viscosity, diffusion, tensile strength) are found to be dependent on the length

of the polymer chain. Detailed analysis of the conformation depends particularly on the use of molecular modelling, the most simple model of a polymer chain being the freely jointed chain.

3.1. Theoretical Modelling of the Conformation of Macromolecules.

The freely jointed chain model^{9,19} consists of a polymer chain of x links, each of length l , joined in a linear sequence with no restrictions on the angles between successive bonds-i.e. only the bond length is fixed. Description of the freely jointed chain model involves essentially the same arguments used for a random flight such as that found in the Brownian motion of gas molecules. The root mean square end-to-end distance, $\sqrt{r^2}$, is given by 1.3.

$$\sqrt{r^2} = l\sqrt{x} \quad 1.3.$$

However, although simplistic the freely jointed chain model does not describe accurately the conformation of real macromolecules, as short range steric hindrances between monomer units on the polymer chain restrict the angles available for bond rotations. Short range steric effects cause an expansion of real polymer chains, the degree of which can be estimated from the characteristic ratio⁹ C_∞ which is given by equation 1.4. and expresses the ratio of the measured mean square end-to-end distance in the absence of long range effects to the value that would be found if all interactions (i.e. both long and short range) were absent and only the lengths of the bonds fixed. The characteristic ratio varies from about 5 to upwards of 10, depending upon the precise chemical nature of the polymer⁶ (side groups on the polymer, "rigid" bonds present in the backbone etc.).

$$C_\infty = \frac{\overline{r^2}}{l^2 x} \quad 1.4.$$

More complicated models of the conformation of macromolecules aim to account for short range steric effects by the inclusion of parameters decreasing the local flexibility of the polymer chain. In the second most simplistic model, the freely rotating chain^{6,9},

the bond angle θ is fixed along with the bond length and only the torsion angle ϕ is allowed to vary. Although better this model is still not entirely satisfactory and to obtain an accurate picture of molecules with hindered internal rotations the Rotational Isomeric State theory⁹ is often invoked. However, although complicated by the effects of short range interactions, the statistical properties of real flexible chains will not be different in character from the freely jointed chain model and behaviour seen in equation 1.3. (where the size of the polymer is proportional to the square root of the number of bonds) is frequently seen.

3.2 The Excluded Volume Effect.

One problem exists with the random walk description of the polymer chain conformation, this is the neglect of interactions between monomer units far apart along the contour of the chain, which by the very nature of the chain can be close together in space. Briefly, two segments remote from one another along the chain contour cannot occupy the same volume element at the same time, repulsive Van der Waals forces act between the segments and cause the chain to expand to a size greater than its unperturbed dimension^{3,6}. Interactions such as these are known as excluded volume interactions. The problem now becomes that of a self-avoiding walk, i.e. a random walk with certain restrictions that once a volume element has been occupied it cannot be revisited⁹.

Possibly the most important influence on the excluded volume effect is the presence of a solvent medium surrounding the polymer chains. A solvent is said to be "good" if the monomer-solvent interactions are favourable compared to the monomer-monomer interaction. Conversely the solvent is said to be poor if the monomer-solvent interactions are weaker than the monomer-monomer interaction. ... Therefore good solvents tend to be favoured by the polymer and cause the polymer chain to become expanded. For a chain with excluded volume interactions, the end-to-end distance is given by equation 1.5.

$$\langle r^2 \rangle = \alpha^2 \langle r_0^2 \rangle \quad 1.5.$$

where $\langle r^2 \rangle$ is the mean square end-to-end distance in the perturbed state,

α is the linear expansion factor,

and $\langle r_0^2 \rangle$ is the mean square end-to-end distance in the unperturbed state.

From this it can be seen that a condition is predicted ($\alpha = 1$) where the excluded volume effect vanishes and the chain adopts an essentially unperturbed conformation.

3.3. The Conformation of "Real" Chains in the Bulk and in Dilute Solution.

In the bulk state, the conformation of amorphous polymers such as polystyrene, polymethyl methacrylate and polyvinyl chloride are found to be dependent upon the molecular weight of the polymer under study⁶. Experimentally the conformation is studied using small angle neutron and/or small angle X-ray scattering. Techniques such as these have produced information on the variation of the radius of gyration of the polymer as a function of the molecular weight of the polymer²⁰⁻²³. The radius of gyration, the mean square distance from the centre of gravity of the N (where N is the degree of polymerisation) scattering points of the polymer, is found to be related to the molecular weight of the polymer through equation 1.6.

$$\sqrt{\frac{R_g^2}{M_w}} = k \quad 1.6.$$

where R_g is the radius of gyration,

and k is a constant.

Values of k are found to be dependent upon the system under study and for polystyrene^{20,21} is found to be $0.275 \text{ \AA} (\text{mol g}^{-1})^{0.5}$. The end-to-end distance of the polymer chain described in the freely jointed model is related to the radius of gyration of the polymer through equation 1.7⁹.

$$\langle r^2 \rangle = 6R_g^2 \quad 1.7.$$

The conformation of polymer chains in dilute solution has also been investigated, utilising light scattered from the solution to determine the radius of gyration of the polymer²⁰. In theta solvents¹⁵⁻¹⁷, where the chemical potential due to monomer-solvent interactions is zero, the radius of gyration is found to be the same as that found in the bulk and behaves in a manner given by equation 1.6. Values of k determined for polystyrene in cyclohexane at the theta temperature of 308K, are found to be the same as for those determined by SANS on the bulk polymer (0.275). These results are not surprising when it is considered that the polymer chain in dilute solution at the theta point exists in a medium that is thermodynamically equivalent to the bulk state, a situation which was described by Flory over twenty years before any experimental evidence became available.

Changing the quality of the solvent, either by increasing or decreasing the temperature of the system changes the dimensions of the polymer molecules. At temperatures higher than 308K, solutions of polystyrene in cyclohexane have radii of gyration which are greater than the "ideal" dimensions obtained in the bulk. The reason for this lies in the excluded volume interactions described earlier. Increasing the temperature increases the relative strength of the monomer-solvent interaction and causes the solvent to occupy regions normally favoured by segments of the chain. Expulsion of the monomer from those regions causes an expansion of the chain and hence an increase in the size of the polymer²⁰. Measurement of the radius of gyration of a polymer in a good solvent using intensity light scattering shows the size of the chain not to be dependent upon the square root of the chain length, but instead to be proportional to the chain length raised to the power 0.6¹⁹, confirming the predictions of the self avoiding walk for a chain subject to excluded volume interactions.

3.4. The Conformation of A Chain in a Random Medium.

Although much of the theoretical work above was first described over 50 years ago, there is one situation which has not been considered by theoreticians until very recently and for which no experimental work has been completed. The theoretical

discussions above pertain to the case of polymer chains in either the bulk amorphous state, in a theta solvent or dilute polymer solutions subjected to excluded volume effects. The case of a polymer chain within a *random medium* has not been considered. A random medium is one wherein regions of space are defined by fixed obstacles, examples being membranes, chromatography columns and polymer networks in the bulk and when swollen with solvent. In the case of a polymer network the fixed obstacles are provided by the cross links of the network and the network chains which provide barriers through which the polymer chain cannot pass.

Early computer modelling experiments showed the polymer to have slightly reduced dimensions in such random media²⁴. Subsequently to these experiments, the magnitude of the contraction of the polymer has been quantified by two groups. Edwards²⁵ found the end-to-end distance of the polymer to be related to the mean obstacle density through equation 1.8.

$$\frac{\langle r^2 \rangle}{\langle r^2 \rangle_{\theta}} = \frac{6.5}{N\rho_0^2} \left[1 - \exp\left(\frac{-N\rho_0^2}{6.5}\right) \right] \quad 1.8.$$

where $\langle r^2 \rangle$ and $\langle r^2 \rangle_{\theta}$ are the mean square end-to-end distance of the polymer in the random medium and the theta state respectively,
 N is the number of segments in the polymer chain
 and ρ_0 is the mean obstacle density of the network.

For a polymer network, the mean obstacle density is proportional to the volume fraction of polymer in the network and hence the cross link density of the network. A similar expression to equation 1.8, though expressed in terms of the correlation length, has been derived independently by Vilgis²⁶. A further prediction of the Edwards' expression relates to the scenario of a "probe" polymer chain within a medium of high obstacle density (i.e. high cross link densities). At a critical cross link density, the interstitial space defined by the network chains is predicted to become so small that the percolation threshold is crossed and the probe chain becomes confined to a region the

dimensions of which are given by the correlation length of the network. Consequently, no matter how large the probe chain, its dimensions will be approximately that of the correlation length, the mesh size of the network.

3.5. Polymer Concentration Regimes.

The properties of a polymer solution depend strongly upon the concentration of the solution, different regimes being identified with a particular type of behaviour^{5,6}. The purpose of this section is to introduce these various regimes and to provide quantitative description of their boundaries.

On increasing the concentration of a polymer solution from the limit of infinite dilution, the separation of the coils decreases. Within the concentration region where the coils are widely separated the solution is said to be dilute and the solution can be treated as a gas of hard spheres. The fundamental length scale applicable to the polymer is the end-to-end distance of the chain, the size of the chain (and the radius of the hypothetical hard sphere) being determined by the degree of polymerisation and the relative strength of the excluded volume effects present with the solvent.

As the concentration of the polymer is increased the chains (which do not in reality behave as hard impenetrable spheres) begin to overlap and the excluded volume effects on individual chains become attenuated by the presence of other chains³. This region of behaviour is known as the semi-dilute region and the characteristic length scale pertaining to the polymer is the screening length ξ_c (defined in section 3.6.). Finally when the polymer concentration becomes so high that each segment is no longer surrounded by solvent molecules, the solution is considered to be concentrated and the fundamental length scale reduces to that of the statistical step length²⁷.

The concentration at which the crossover between dilute solution and semi-dilute solution behaviour occurs is known as the critical overlap concentration³ and is denoted by the symbol c^* . The critical overlap concentration occurs when the concentration of

the polymer chains increases to such an extent that the polymer chains just begin to overlap and the "hard spheres" of polymers are in close contact. Clearly in real solutions c^* does not have a specific value, it is instead a region of crossover between the two regimes. However, c^* is expected to be comparable to the monomer concentration in a dilute solution. From this assumption a value of c^* can be determined, the value of c^* being expected to decrease with the size (and hence molecular weight of the polymer) and the degree of swelling of the polymer coil. Equation 1.9. below gives a quantitative expression for c^* ^{14,27,28}.

$$c^* = \frac{M_w}{\frac{4}{3}\pi N_A R_g^3} \quad 1.9.$$

where M_w is the molecular weight of the polymer,
and N_A is the Avogadro constant.

Schematically, the transitions between a dilute and a concentrated solution are shown in figure 1.3. parts a-c where the dilute (Part A), c^* (Part B) and semi-dilute (Part C) solutions can be seen.

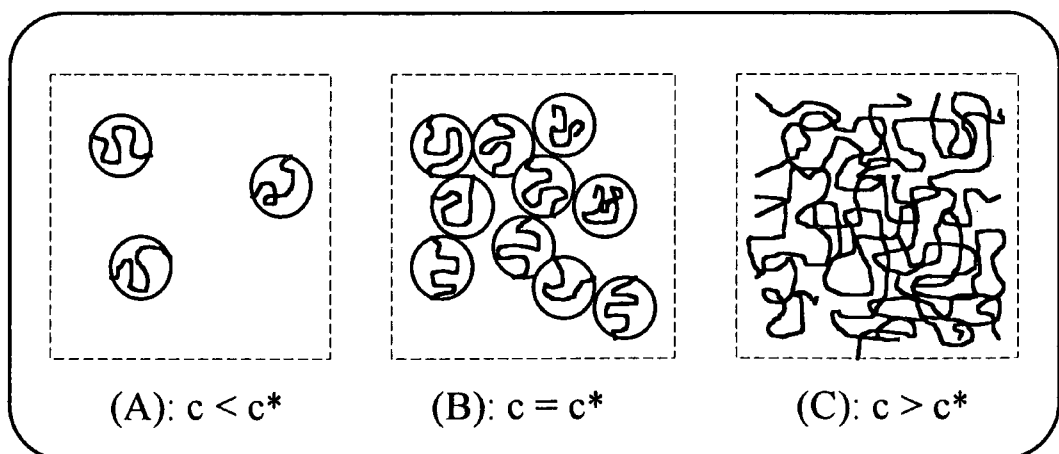


Figure 1.3.: Crossover Between Dilute, Onset of Overlap and Semi-dilute Regions.

Therefore from the molecular weight of a given polymer, both the radius of gyration and the onset of overlap can be determined allowing the prediction of the boundaries of the dilute and semi-dilute solution regimes.

3.6. The Properties of Semi-Dilute Solutions and Polymer Gels.

The properties of polymer gels at swelling equilibrium have been described by de Gennes following an intuitive argument relating the properties of the gel to those of solutions of weakly overlapping linear chains. This analogy, supported by both SANS and QELS experiments, explains both static and dynamic behaviour over a wide range of thermodynamic environments. The purpose of this section is to introduce some of these concepts and to provide an insight into the *scaling* properties of semi-dilute solutions and polymer gels.

The classical model of the thermodynamics of polymer solutions, due to Flory and Huggins¹⁵⁻¹⁷, was based on a lattice model and assumed an average polymer segment density constant over the entire lattice. The uniformity of interaction is a mean field approach and only truly valid at high polymer concentrations such as those in molten polymer blends and concentrated solutions. The expression for the free energy of mixing is given as:

$$\frac{\Delta G_{mix}}{k_B T} = n_1 \ln \phi_1 + n_2 \ln \phi_2 + \chi n_1 \phi_2 \quad 1.10.$$

where T is the absolute temperature,

k_B is the Boltzmann constant,

ΔG_{mix} is the free energy of mixing,

n_1, n_2 is the number of molecules of solvent and solute,

ϕ_1, ϕ_2 is the volume fraction of solvent and solute respectively

and χ is a dimensionless quantity characterising the interaction per solvent molecule.

An ideal polymer solution, in which the chain is not subject to excluded volume interactions, and hence expansion of its size, is one which has a zero heat of mixing. Flory-Huggins theory introduces χ to describe the heat of mixing of the solution:

$$\chi = \frac{\Delta H_{mix}}{k_B T n_1 \phi_2} \quad 1.11.$$

where ΔH_{mix} is the heat of mixing.

By manipulation of equations 1.10 and 1.11. equations relating thermodynamic parameters such as the osmotic pressure can be obtained:

$$\pi = \frac{RT}{\bar{V}_1} \left[\left(\frac{1}{2} - \chi \right) \phi_2^2 + \frac{\phi_2^3}{3} + \dots \right] \quad 1.12.$$

where π is the osmotic pressure,

R is the gas constant

and \bar{V}_1 is the molar volume of the solvent.

By comparison with the virial expansion for the osmotic pressure^{5,6}, χ can be expressed in terms of the second virial coefficient, equation 1.13.

$$A_2 = \frac{v_2}{N_A \bar{V}_1} \left(\frac{1}{2} - \chi \right) \quad 1.13.$$

where A_2 is the second virial coefficient

and v_2 is the specific volume of the polymer

From 1.13. it can be seen that the Flory θ temperature (the point where the excess chemical potential due to segment-solvent interactions is zero) occurs at the point where χ equals 0.5 i.e. A_2 equals zero. The theta point occurs when the enthalpic and entropic contributions to χ balance. Values of χ are possibly the most widely used measurement of the interaction between the polymer and solvent, values less than 0.5 correspond to values of A_2 greater than zero and occur for polymers which are soluble in the solvent under consideration.

It has been realised for some time that the Flory Huggins mixing expression is not adequate at low concentrations due to the inherent non uniformity of the polymer concentration. Flory and Krigbaum have studied this problem using a smoothed density model in which the polymer is considered as a continuous cloud of segments distributed with a Gaussian probability over a sphere located about the molecular centre of mass^{9,19}. The excluded volume expansion of the chain is described by a uniform potential in a mean field approximation, the equilibrium conformation of the chain being determined by

equating the osmotic swelling of the coil with the elastic reaction developed by the coil trying to restore itself to a less expanded conformation.

The magnitude of the osmotic pressure developed depends upon the difference in the energy of the interaction between components in the system, which is directly analogous to the macroscopic equilibrium swelling of a network described by the Flory-Rehner equation. The osmotic term was found using the mean field approach above, while the elastic term found following the assumption of an affine deformation of the end-to-end chain vector. An expression for the free energy of the coil can then be determined and by manipulation an equation relating the end-to-end distance of the chain found (equation 1.14).

$$\langle r^2 \rangle \approx \left(\frac{1}{2} - \chi \right)^{\frac{1}{5}} a N^{\frac{3}{5}} \quad 1.14.$$

where a is a constant dependent on the polymer under study.

Although this approach leads to the correct exponent relating the coil size to the chain length in solution, it does so by a remarkably fortuitous cancellation of two strong assumptions³. Firstly, the osmotic energy is overestimated by the neglect of the correlation between segments within the chain, while the elastic energy is also overestimated by the assumption of affine distortion of Gaussian chain statistics.

During the early 1970's an alternative approach to the problem of polymer chain statistics, accounting for correlation's between monomer units within a chain was developed by several French research groups based upon a mathematical analogy with critical phenomena in magnetic systems^{27,29,30}. Some general results were provided by the use of re normalisation group theory developed for the study of critical phenomena. de Gennes used these results along with scaling arguments and extrapolations to develop the laws and to predict new scaling exponents, the results of which are summarised in the book *Scaling Concepts in Polymer Physics*³. The purpose of this section is not to derive all scaling relationships applicable to the cases of semi-dilute solutions and

polymer gels, instead it serves identify those areas most important for the work described later in this thesis and to provide an insight into the origins of their behaviour.

When the polymer concentration is increased from the dilute solution, there comes a point when the domains of the polymer coil begin to overlap. This threshold, described earlier as the critical overlap concentration can also be expressed as a critical volume fraction, ϕ^* , again comparable to the local segment concentration within a single dilute coil. A quantitative expression for c^* was given earlier in equation 1.9., here it is presented in a different manner showing the scaling nature of the critical overlap concentration. For a good solvent where the end-to-end distance scales as $N^{0.6}$ c^* is given by:

$$c^* \approx \frac{N}{\langle r^2 \rangle^3} \approx \frac{N}{a^3 N^{\frac{9}{5}}} \approx a^{-3} N^{-\frac{4}{5}} \quad 1.15.$$

For a theta solvent where $\langle r^2 \rangle$ scales as $N^{0.5}$, c^* is given by

$$c^* \approx \frac{N}{\langle r^2 \rangle^3} \approx \frac{N}{a^3 N^{\frac{3}{2}}} \approx a^{-3} N^{-\frac{1}{2}} \quad 1.16.$$

By inspection of equations 1.15. and 1.16., equation 1.17. can be written for the general case of a chain in any solvent.

$$c^* \approx \frac{N}{\langle r^2 \rangle^3} \approx a^{-3} N^{1-3\nu} \quad 1.17.$$

where ν , the excluded volume exponent, is 0.6 for good and 0.5 for theta solvents.

3.6.1. The Correlation Length.

As seen schematically in figure 1.3 part c, chains in semi-dilute solution do not act as hard spheres, instead the chains interpenetrate one another forming what can be viewed as a lattice, which when photographed at a single time will look very similar to a polymeric network having a certain mesh size, ξ -the correlation length of the solution.

This is best explained schematically in figure 1.4. below.

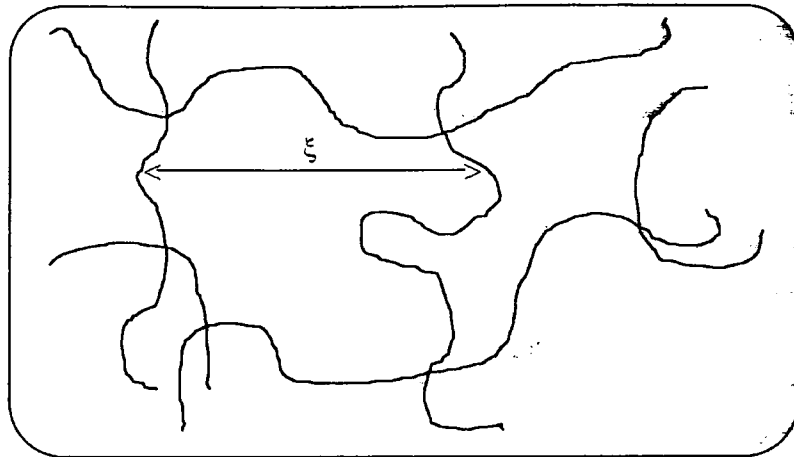


Figure 1.4.: Schematic Diagram of the Correlation Length of Semi-Dilute Solutions.

The importance of the correlation length of the semi-dilute solution will be realised in the following discussion. Clearly from figure 1.4. the magnitude of the correlation length, the mesh size, is related to the concentration of the polymer chains. At the critical overlap concentration, the mesh has its largest size as the polymer chains are only just in contact, increasing the concentration reduces the separation of the chains and therefore decreases the correlation length. At c^* the correlation length can be seen to be the size of one coil, $\langle r^2 \rangle$. For concentrations above c^* , the transient network structure will depend only upon the concentration and not upon the molecular weight of the polymer, the chains being much longer than the mesh size. From these two assumptions, the following scaling relationship can be written for the correlation length (assuming good solvent conditions).

$$\xi(c) = \langle r^2 \rangle \left(\frac{c^*}{c} \right)^m \quad 1.18.$$

where m is chosen such that powers of N from $\langle r^2 \rangle$ and c^* cancel.

For good solvent conditions, substituting 1.14 and 1.15 into 1.18. leads to equation 1.19.

$$\xi(c) \approx c^{-\frac{3}{4}} \quad 1.19.$$

Similar arguments can be used for the case of a semi-dilute chain in a theta solvent, except in this case the chains are ideal and by use of the appropriate scaling forms for $\langle r^2 \rangle$ and c^* (1.14 and 1.16) the correlation length is given by equation 1.20.

$$\xi(c) \approx \langle r^2 \rangle \left(\frac{c^*}{c} \right)^m \approx c^{-1} \quad 1.20.$$

3.6.2. The "Blob" Model Of Chain Statistics.

Consider a single chain within a semi-dilute solution of a polymer in a good solvent. It is known that the chain in dilute solution has a conformation where the size of the chain scales with the degree of polymerisation to the power 3/5. Yet by increasing the concentration of the system to the bulk, the size of the chain is found to scale with the degree of polymerisation to the power of 1/2. The question therefore arises of what happens at concentrations intermediate between the dilute regime and the concentrated regime-the semi-dilute region.

The size of the chain in the semi-dilute region can be understood by using the "blob model" first introduced by Daoud²⁹ in 1976. In the model, the chain is considered to consist of a succession of subunits known as blobs, shown schematically by figure 1.5.

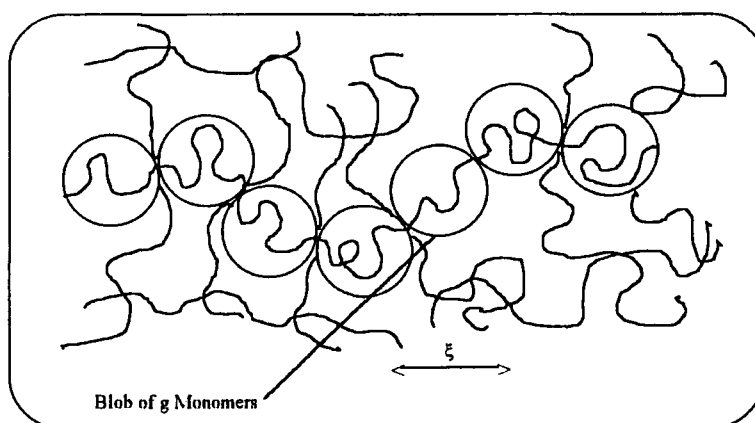


Figure 1.5.: The Excluded Volume "Blob" in Semi-Dilute Solution.

Within the subunit, the polymer chain does not interact with other chains and is swollen by excluded volume effects, while outside the blob radius, the excluded volume

interactions between segments of the same chain (but arising from different blobs) are screened out by the overlapping chains of the semi-dilute solution. As the excluded volume effects are screened out by the overlapping chains of the semi-dilute solution, it is natural to take the size of the blob to be the mesh size or correlation length of the transient network. The number of monomers per blob, g , is related to the correlation length by the law of swollen coils, whereby the size of the blob (the correlation length) is obtained by direct analogy to equation 1.14.

$$\xi \approx ag^{\frac{3}{5}} \quad 1.21.$$

where a is the same constant as given in equation 1.14. measuring the chain stiffness.

Similarly, the size of the blob in a theta solvent is given by equation 1.22.

$$\xi \approx ag^{\frac{1}{2}} \quad 1.22$$

By combination of equation 1.19. with equation 1.21., the number of monomers per blob can be seen to be dependent upon the concentration of the solution, equation 1.23.

$$g \approx \left(\frac{\xi}{a}\right)^{\frac{5}{3}} \approx \left(\frac{c^{-\frac{3}{4}}}{a}\right)^{\frac{5}{3}} \approx c^{-\frac{5}{4}} \quad 1.23.$$

By taking the excluded volume blob as being the basic units of the semi-dilute solution it can be shown that the solution behaves as a close packed system of blobs and as such the problem returns to that of the of the ideal chain. In such a case the chains can then be considered as being ideal on length scales greater than the blob radius, the mean square end-to-end size being estimated from the ideal chain formula for N/g blobs of size ξ .

$$\langle r^2 \rangle(c) \approx \left(\frac{N}{g}\right) \xi^2 \quad 1.24.$$

By combination of equations 1.21., 1.22 and 1.24. the end-to-end size of the chain can be seen to scale with the polymer concentration.

$$\langle r^2 \rangle(c) \approx N a^2 c^{-\frac{5}{4}}$$

1.25.

Equation 1.25. was first derived by Daoud and has been experimentally verified by SANS studies of semi-dilute solutions of polystyrene in benzene²⁹. Clearly for semi-dilute solutions in a theta solvent where the chains are ideal, the notion of the blob does not need to be invoked in order to describe the static properties of the solution.

3.6.3. The Polymer Phase Diagram.

The predictions of the scaling theories outlined above have been studied for a number of chemical systems in the dilute and semi-dilute regimes, though polystyrene systems have been by far the most studied. Transitions between the different modes of behaviour are brought about by changes in the solvent quality of the system. Different regimes of concentration and solvent quality can be qualitatively associated with different types of behaviour following the temperature-concentration phase diagram shown below in figure 1.6^{30,35}.

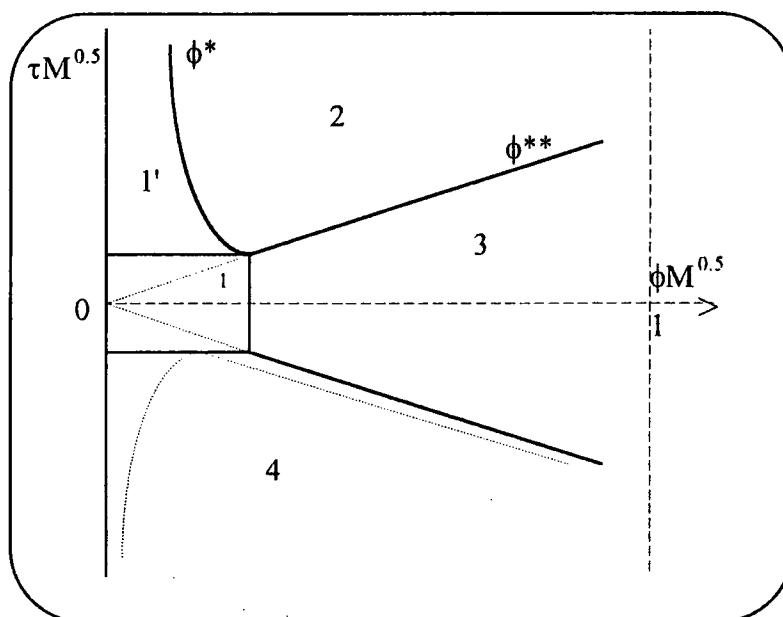


Figure 1.6.: Temperature-Concentration Phase Diagram due to Daoud.

The phase diagram shown in figure 1.6 is given as a function of two variables, the concentration (denoted here by the polymer volume fraction) and the reduced

temperature of the system, τ , given by equation 1.26. Both quantities have been multiplied by the square root of the molecular weight in order to remove any dependence on M_w . Consequently the point $\tau M^{0.50}$ corresponds to the theta point of the solution.

$$\tau = \left(\frac{T - T_\theta}{T_\theta} \right) \quad 1.26.$$

Five distinct regions of behaviour have been identified by Daoud³⁰:

Region 1: The dilute theta region, here the polymer chain has unperturbed dimensions over a small range of temperature and concentration due to the finite molecular weight.

Region 1': The dilute good solvent region, here the polymer chains are widely separated and subject to excluded volume effects.

Region 2: The semi-dilute region of intermediate concentration where molecules overlap under good solvent conditions.

Region 3: The concentrated region where each monomer is in contact with many others and the conformation of the chain approaches that of the bulk.

Region 4: The two phase region below the theta point where the polymer precipitates out of solution.

Daoud and Jannink have obtained expressions for the correlation length and the radius of gyration of polymer chains in regions 1' to 3 in terms not only of the polymer concentration but also of the reduced temperature τ . These predictions are outlined in table 1.1.

Region	R_g^2	ξ^2
1	N	Not Applicable
1'	$N^{6/5} \tau^{2/5}$	Not Applicable
2	$Nc^{-1/4} \tau^{1/4}$	$c^{-3/2} \tau^{-1/2}$
3	N	c^{-2}

Table 1.1: Scaling Theory Predictions for the Polymer Phase Diagram of Daoud.

In addition to the predictions of scaling theory, Edwards³¹ and co-workers have re-examined mean field theoretical predictions on the semi-dilute regime and have found relationships which are effectively identical to those of scaling theory. Perhaps more importantly, the relationships obtained were derived from a single formula which can be applied from the most dilute solution to the bulk polymer. The various regions of behaviour are obtained by setting specific conditions for c and τ . From the approach a picture emerges where changes between regions occur not as distinct barriers but instead as gradual changes.

The exponents obtained from mean field theory are generally in good agreement with those of scaling theory, except in the so-called region 2A, which is not predicted by scaling theory where there is a much higher monomer density than in region 2. This region, known as the semi-concentrated region has been studied by SANS where some evidence for its existence has been found³².

A further refinement to the predictions of scaling theory has been made by Schaeffer^{33,34} in which a departure from the predictions of the scaling laws is attributed to restricted flexibility on a local scale of real chains, perturbative corrections in a mean field analysis then being considered as appropriate. Although the argument has some theoretical justification it presents difficulties in defining the degree of flexibility of real chains. The Schaeffer approach makes use of the blob model and predicts a phase diagram somewhat more complicated than that due to Daoud. Although there is some theoretical justification for the Schaeffer model, experimental evidence remains scarce.

The scaling theories due variously to de Gennes, Cotton, Daoud etc. have also been used to make predictions of other static and dynamic properties, controlled by the concentration and degree of excluded volume in the solution. Properties such as the osmotic pressure, osmotic modulus as well as the collective diffusion coefficient of the polymer chains of either the swollen network or semi-dilute solution are related to the polymer concentration, the results of which are presented in table 1.2. below.

Experimentally Observable Quantity	Polymer Concentration Scaling Exponent	
	Good Solvent	Theta Solvent
Screening Length, ξ_c	-3/4	-1
Osmotic Pressure, π	9/4	3
Collective Diffusion Coefficient, D_c	3/4	1
Osmotic Modulus, M_{os}	9/4	3

Table 1.2.: Exponents for the Power Law Dependence of Various Quantities on Polymer Segment Concentration in the Swollen Gel/Semi-Dilute Regime.

3.6.4. The c^* Theorem.

Many of the properties of polymer solutions described above are rationalised by considering the semi-dilute solution to be a transient network formed by interchain contacts between the polymer chains, the unconnected chains being able to disentangle over long time scales, while new interchain contacts form over roughly the same time scale. Clearly the semi-dilute solution exhibits many structural properties reminiscent of a swollen polymer gel. The connection between the polymer gel at swelling equilibrium and polymer solutions is stated formally in de Gennes c^* theorem³. Polymer chains in a good solvent repel one another and form a positive osmotic pressure, π . If the chains are attached to one another at their ends then although they would like to separate as much as possible they are restricted in doing so by the cross links which impose a permanence to the structure.

The result is a system of closely packed coils analogous to the overlap concentration separating the dilute and semi-dilute regions. The gel is predicted to maintain automatically a concentration which is proportional to the overlap concentration.

$$c \approx k(f)c^* \approx k(f)N^{-\frac{4}{5}}v^{\frac{3}{5}}a^{-\frac{6}{5}} \quad 1.27.$$

where $k(f)$ is a constant dependent on the functionality of the junctions of the network

Equation 1.27. summarises the Flory theory of gels⁹, increasing the quality of the solvent and hence ν , causes a decrease in the overlap concentration of the polymer and hence causes the network to become more swollen. Macroscopic swelling experiments have in the main confirmed the relationship between the degree of polymerisation and the concentration of polymer in the swollen network^{7,8}, an area which is returned to later in chapter 2.

4. The Dynamics of Polymer Chains.

Many of the industrial applications of polymers are related to their unusual rheological and hydrodynamic properties, one method of increasing the viscosity of a liquid being to introduce a polymeric additive with its associated long relaxation times due to the effects of intramolecular motion of the polymer. However, the processes controlling the dynamic properties of polymer solutions are, similarly to the conformation of polymers, dependent on the concentration of the polymer in solution.

The hydrodynamic properties of dilute polymer solutions are relatively well understood due to the ease of study by techniques such as dilute solution viscometry and concentration gradient diffusion, the data of which is interpreted in terms of the theoretical models of Zimm³⁶ and Kirkwood³⁷. However the understanding of the properties of non-dilute polymer solutions and melts is less well understood due to both the difficulties in experimental design and theoretical interpretation of the data.

The recent development of techniques such as quasi elastic light scattering (QELS), forced rayleigh scattering and pulsed field gradient NMR techniques have alleviated some of these experimental problems and have provided results which have been discussed in terms of the scaling theories and the reptation model of polymer diffusion in concentrated systems advanced by de Gennes³.

The purpose of this section is to provide an introduction to the theory of macromolecular dynamics in dilute systems as well as concentrated media and to

describe the experimental efforts to validate those theories used in such systems. A basic introduction to the theories of hydrodynamic behaviour is provided, a more rigorous treatment being found in the literature³⁸⁻⁴¹.

4.1. Models of Hydrodynamic Behaviour in Dilute Solution.

The hydrodynamic properties of dilute solutions are both experimentally and theoretically easily studied as the motions of separate chains can be studied independently of one another. Essentially the most important microscopic parameter is the monomer friction coefficient ζ , which describes the motion of a single monomer in the solvent. ζ depends upon the solvent viscosity η_0 and can be related to the radius a of a hydrodynamic sphere through equation 1.28⁴⁰.

$$\zeta = 6\pi\eta_0 a \quad 1.28.$$

In the simplest model of the hydrodynamic behaviour in solution, the Rouse model⁴², the polymer is considered to act as a coupled harmonic oscillator moving through the solution, the $(N+1)$ monomers of the polymer being connected by N linear elastic springs. All of the mass of the polymer is contained in the monomers which experience a frictional interaction with the solvent.

The motions of the different monomers are considered to be independent in that the frictional force of a given monomer unit depends solely in the velocity of the monomer and not on that due to the other monomers. This approach is said to be a *free draining model* and neglects the hydrodynamic interactions due to the different segments of the polymer chain.

The dynamics of the Rouse model have been extensively studied, only the main results of which are presented here

$$D_{Rouse} \cong \frac{k_B T}{(N+1)\zeta} \quad 1.29.$$

$$[\eta] = \lim_{c \rightarrow 0} \frac{\eta - \eta_0}{c\eta_0} \approx R_g^2 \approx N \quad 1.30.$$

where D_{Rouse} is the diffusion coefficient of the chain due to the model

T is the Absolute Temperature

$[\eta]$ is the intrinsic viscosity

and η is the shear viscosity.

However, the predictions of the Rouse model are not found in experimental studies of dilute solutions, in particular the behaviour of the polymer chain is found to scale with the molecular weight, not with a scaling exponent of 1 as predicted but with an exponent of between 0.5 and 0.6 depending on the quality of the solvent.

The behaviour of polymer chains in dilute solution can however be well understood in terms of the non-free draining Zimm model³⁶, where it is considered that not all monomers feel the same hydrodynamic friction due to shielding from viscous drag interaction by neighbouring monomer units, thus reducing the molecular weight dependence of the diffusion coefficient to that of the reciprocal size of the chain. Again only the main predictions of the model are described here.

$$D_{\text{Zimm}} \cong \frac{k_B T}{6\pi\eta_0 R_H} \quad 1.31.$$

where D_{Zimm} is the diffusion coefficient of the chain

and R_H is the Hydrodynamic radius of the polymer.

A number of experimental studies on solutions of polystyrene in both good and theta solvents have shown the Zimm model to be applicable in the description of the hydrodynamic behaviour in dilute solution. Generally for polymer-good solvent systems, light scattering, sedimentation and viscometric measurements have shown the scaling exponent to be only very slightly smaller than that predicted by the Zimm model^{43,44}. Similarly, results obtained from theta systems show the model to be valid for the dilute chain in the ideal state^{45,46}.

However, it should be noted that Zimm treats the polymer in terms of a hard sphere model, clearly this is not the case for semi-dilute solutions and discrepancies might be expected for more concentrated systems where the polymer chains overlap and entangle in the medium.

4.2. Hydrodynamic Behaviour in Semi-Dilute Solution.

In dilute solutions only the motions of single chains have been considered and dynamic properties are studied in the limit of infinite dilution. However when the concentration is non-zero, interactions between other chains both static and hydrodynamic in nature must be taken into account. When the concentration is lower than the critical overlap threshold these interactions can be classified as perturbations and considered to be small. When the concentration of the solution is above c^* in the semi-dilute regime, the motions of the chains become collective and the monomer friction coefficient ζ becomes concentration dependent.

In the semi-dilute regime two distinct types of hydrodynamic processes are prevalent, collective motions due to the co-operative motions of the solution and single chain processes involving the motion of a single labelled chain³. Two diffusion coefficients can be defined, a collective (or co-operative) diffusion coefficient D_c which characterises the relaxation of the concentration fluctuations and the self (or tracer) diffusion coefficient (D_s or D_t) characterising the motion of the labelled chain. The dynamic collective motions of semi-dilute solutions and swollen gels in both good and theta solvents can be considered independently from the case of the single chain motion. The collective motions of the chain are essentially different from the cases outlined above for dilute solution behaviour due to the effects of hydrodynamic interactions and the screening of these effects.

Experimental evidence from dilute solutions reinforces the Zimm approach where each moving monomer in the solvent creates a backflow field which decays slowly with the distance from the monomer. In the semi-dilute regime, the interference between

these fields induces a screening of the solvent backflow field of the monomer, which falls off exponentially beyond a characteristic distance, λ , the screening length of the hydrodynamic interactions⁴⁰. The theory of the collective motion of semi-dilute solutions of ideal Gaussian chains has been proposed by Edwards and Freed⁴⁷. Only the main predictions of the model are described here, a full discussion being available in the literature. The Edwards' theory relates the hydrodynamic screening length λ to the effective monomer friction coefficient ζ .

$$\lambda = \left(\frac{\eta_0}{c\zeta} \right)^{0.5} \quad 1.32.$$

From this expression, de Gennes has used self consistent field arguments to show that λ is only dependent on the monomer concentration c and that λ follows the same scaling structure as the correlation length. In a semi-dilute solution of a good polymer-solvent system, the following scaling form is predicted.

$$D_{\infty} \approx \frac{k_B T}{\eta_0 \xi} \approx c^{0.75} \quad 1.33.$$

Experimentally the predictions of the hydrodynamic scaling theory have been confirmed, where QELS measurements indicate that the collective diffusion coefficient scales with the polymer concentration raised to the power 0.7^{48,49}. However some discussion occurs in the literature over the shape of the autocorrelation function obtained from the QELS experiment. Some authors claim the autocorrelation function to be composed of two relaxation modes^{50,51} while others claim only one^{52,53}, the concentration of the semi-dilute solution under study being a major source of discussion. The area of QELS from semi-dilute solutions is discussed further in chapter 4.

Scaling theory can also be used to predict a linear dependence of the collective diffusion coefficient upon the concentration in theta solutions. However a similar situation exists in the experimental study of semi-dilute theta solutions, where experimental difficulties are prevalent and two relaxation modes are again⁵⁴⁻⁵⁷ noted in

the autocorrelation function of the QELS spectra, the mode with the longest relaxation time being thought to be due to the viscoelastic motions of the polymer in solution. Again the experimental situation is complicated and is discussed further in chapter 4.

4.3. Models of Hydrodynamic Behaviour in Concentrated Systems.

Although it was shown that the Rouse model is a poor model of polymer behaviour in dilute solutions where its neglect of hydrodynamic effects leads to incorrect predictions, the Rouse model is found to provide a more accurate description of the dynamic behaviour of the polymer as the concentration is increased. The reason for this can be understood qualitatively. Increasing the density of the chains causes the polymer coils to interpenetrate one another which induces a screening of the hydrodynamic interactions between the monomer units. This leaves all monomer units equally susceptible to hydrodynamic drag effects, due both to the polymer-polymer as well as the polymer-solvent drag⁵⁸. When the polymer chains are not too long, (below the molecular weight at which chains become entangled M_c), the predictions of the Rouse model are experimentally verified³⁹. However above the entanglement molecular weight, the dynamics of polymer chains in the melt cannot be described by the Rouse model.

The Rouse model predicts that the shear stress modulus $G(t)$, decays to zero after the imposition of the shear strain without any dependency on the molecular weight of the polymer⁴¹. However, above a critical molecular weight (M_c) a plateau modulus exists causing a slowing down of the stress modulus relaxation, similar to the behaviour of cross linked polymers. The plateau is due to the entanglement of the polymer chains above M_c , producing behaviour which can be understood in terms of temporary cross links causing the formation of a transient network. Hence above M_c behaviour not consistent with the Rouse model is found, which is understood in terms of the entanglements of the chains in the melt state⁵⁸.

However, de Gennes in 1971 introduced an alternative explanation of the dynamic processes controlling polymer diffusion in concentrated media. Called *reptation*⁵⁹, the motions of loose polymer chains inside a polymer network are assumed to proceed by a snake like motion along the backbone of the "loose" chain. Transverse motion of the chain is not possible as the chains surrounding the loose chain form obstacle to its path preventing sideways motion, thereby forcing the reptative motion along the chain backbone. Understanding of the reptation theory was made somewhat more simple by the introduction of the tube model by Edwards⁶⁰, where polymer chains in concentrated media are considered to be confined to a tube formed by the adjacent polymer chains. The following sections describe the reptation model in some detail and provide an introduction into the experimental controversy surrounding the model as applied to many different systems of interest.

4.4. The Reptation Model.

In polymer melts or concentrated solutions, the complex topological constraints imposed by chain entanglements are in the reptation model considered to restrict each chain to motion along its own contour except at the chain ends. This is often referred to as the tube model due to Edwards⁶⁰, where excursions of the monomer segments of the chain at right angles to the axis of the tube are forbidden by the presence of the chains forming the tube. Schematically, this can be seen by figure 1.7. below where entanglements of the type shown in figure 1.4. provide the "walls" of the tube.

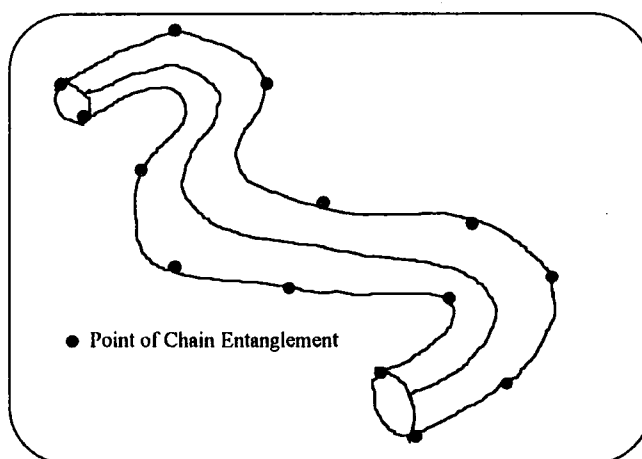


Figure 1.7.: Schematic Diagram of Entanglements Producing a Confining Tube.

Motion of the chain is then expected only to occur in a direction parallel this the axis of the tube and proceeds by the motion of a "defect" along the chain backbone towards one of the chain ends. The defect is in reality a "stored length" in the backbone of the chain which moves by a "snake-like" motion (reptation). Thus as the defect moves along the tube, one part of the tube at the trailing end of the chain is destroyed and a section of tube of corresponding size is created at the forward end. This can be seen in figure 1.8. below.

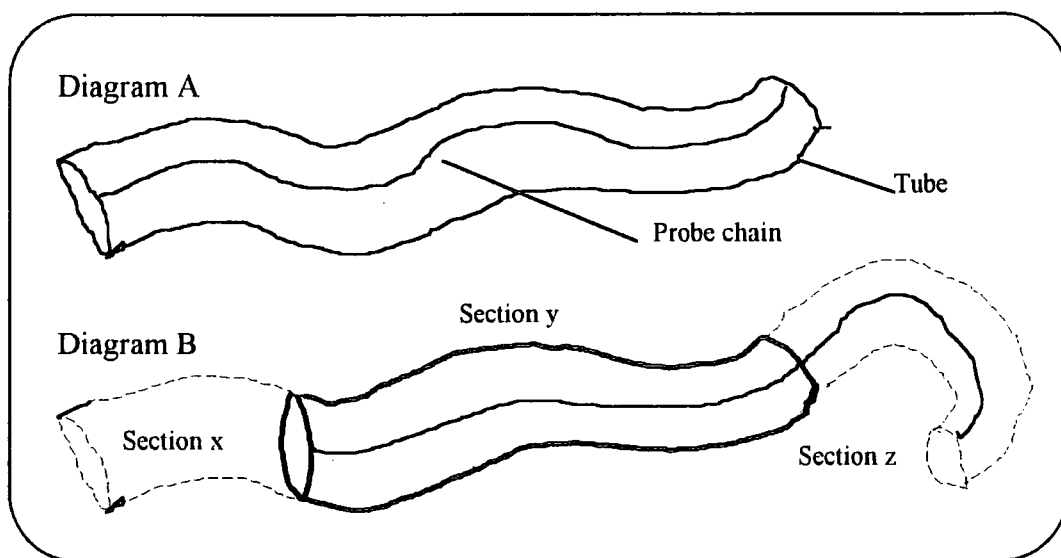


Figure 1.8.: Creation and Destruction of Sections of Tube Due to Chain Reptation.

In diagram A of figure 1.8., the diffusing "probe" chain can be seen to be confined to a tube like region formed by the neighbouring polymer chains around the probe chain. In diagram B the diffusing probe chain is shown some time later having moved along its own axis. This motion causes several effects. Firstly the leading edge of the probe chain "creates" a new section of tube around itself (section z). The trailing end of the probe chain moves into the original tube, causing the destruction of part of the original tube (section x). Finally the centre portion of the probe correspondingly moves along the original tube and is displaced by an amount (equivalent to the amount moved by the chain end) relative to its position within the original tube. The section of the original tube still occupied by the probe chain is highlighted in bold face (section y).

The diffusive motion of the chain can be characterised by a mobility which gives the curvilinear velocity under an external force. The mobility, μ_t is inversely proportional to the length of the tube, i.e. the degree of polymerisation of the chain^{3,59}.

$$\mu_t = \frac{\mu_0}{N} \quad 1.34.$$

where μ_0 is the microscopic mobility which depends only upon the local friction.

The Einstein relationship relates μ_t to the curvilinear diffusion coefficient D_t

$$D_t = k_B \mu_t T = \frac{k_B \mu_0 T}{N} \quad 1.35.$$

The reptation time, T_r is the time taken for the chain to disentangle itself from the tube made up from the local chains. The relaxation (or reptation) time is given by 1.36.

$$T_{rep} \approx \frac{N^2}{D_t} \approx \tau_0 N^3 \quad 1.36.$$

The constants appearing in equation 1.36. can be chosen such that during one relaxation time, the test chain has moved over a distance of the order of its radius of gyration (during one relaxation time the chain moves along the tube length L -given by $L \approx Na$), however in space the tube is contorted and during one relaxation time the probe chain moves through a distance given by its radius of gyration).

$$R_g^2 = D_{self} T_{rep} \quad 1.37.$$

where D_{self} is the self diffusion coefficient

By combination of equations 1.36 and 1.37 and recalling the dependence of the radius of gyration upon the molecular weight of the polymer, equation 1.38 describing the diffusion of the probe chain can be written.

$$D_{self} \approx \frac{Na^2}{\tau_0 N^3} \approx \frac{a^2}{\tau_0 N^2} \quad 1.38.$$

Equation 1.38. forms the basis of de Gennes theory for the diffusion of a chain in a concentrated, entangled system. Its M^{-2} dependence contrasts with the M^{-1} dependence of the Rouse model. Equation 1.38. applies to the case considered by de Gennes of a probe chain diffusing through a very concentrated medium such as a polymer network (or through the melt state well above the critical entanglement weight). Similar chain entanglements exist in semi-dilute solutions, however as was shown earlier in section 3.6.1. these entanglements are dependent on the concentration of the semi-dilute solution and therefore scaling arguments relating the diffusion of the probe to the concentration of the semi-dilute matrix can be derived. A semi-dilute solution can be considered to be a melt of blobs, size ξ , each containing g monomers. The tube diameter in the semi-dilute solution can be taken as being the size of the blob^{3,40}. In this case the overall contour length of the tube is $N\xi/g$, the local mobility μ_0 is the blob mobility given by equation 1.39.

$$\mu_0 = \frac{1}{6\pi\eta_0\xi} \quad 1.39.$$

Using the Einstein relationship, the diffusion coefficient and relaxation time of the chain can then be determined.

$$D_t = k_B\mu_0T = \frac{k_BgT}{\eta_0N\xi} \quad 1.40.$$

$$T_{rep} = \frac{6\pi\eta_0N^3\xi^3}{k_Bg^3T} \quad 1.41.$$

Again following the arguments presented in equations 1.37. and 1.38 the self diffusion coefficient of the chain can be determined.

$$D_{self} \approx \frac{k_B T g^2}{6\pi\eta_0\xi N^2} \quad 1.42.$$

However, as noted earlier both g and ξ scale with the polymer concentration of the semi-dilute solution. Therefore for a good solvent equation 1.43 is obtained while for a theta solution equation 1.44. is obtained.

$$D_{self} \approx M^{-2}c^{-9/4} \quad 1.43.$$

$$D_{self} \approx M^{-2}c^{-3} \quad 1.44.$$

The discussions above provide predictions for the dynamic behaviour of polymer chains from the reptation model in concentrated systems where chain entanglements provide topological constraints upon chain motion. Although derived specifically for the case of a chain diffusing through a bulk polymeric network where cross links provide the topological constraints to chain motion, there has until recently been very little experimental evidence for the dynamic behaviour of a probe chain inside a network. The reason for this is primarily due to the difficulties of sample preparation. It is not sufficient to simply prepare a network and then allow probe chains to diffuse into the network as thermodynamics does not favour diffusion into the network and the kinetics of chain diffusion are sufficiently slow to hinder the development of a small concentration of probe chain within the network. In reality networks need to be prepared around the probe chain, i.e. by either the anionic block copolymerisation or deactivation routes incorporating a known fraction of the probe chain into the living reaction medium and cross linking around the probe chain.

Such systems have until recently not been studied and the focus of attention for those investigating the reptation mechanism has been in those systems where the cross links are replaced by chain entanglements, thus providing the topological constraints for reptation. Such cases are typified by polymer melts, where the probe chain is immersed inside a melt of chemically identical chains, the molecular weight of which is substantially higher than the probe and therefore provides temporary cross links which do not disentangle over the time scales of interest.

Above the critical entanglement molecular weight, the reptation predictions for the viscosity of the polymer melt are broadly speaking, in agreement with the data available⁵⁸. Results indicate the viscosity of the melt to be dependent upon the molecular weight of the matrix raised to the power of 3.4, in a manner seemingly regardless of the chemical structure of the polymer⁵⁸, samples of polystyrene, polyethylene, polyisoprene being amongst those studied⁶³⁻⁶⁵. Reptation theory predicts $\eta \approx M_w^3$ in the limit of infinite molecular weight as compared with the value from Rouse theory which predicts a linear dependence.

Experiments testing the reptation mechanism in semi-dilute and concentrated solutions have been performed on a variety of systems using a number of experimental methods, however all have one common feature in that none equivocally prove the existence of the mechanism. Leger has studied the polystyrene-benzene system and has measured the self diffusion coefficient of the polymer as a function of the matrix polymer concentration and molecular weight as well as a function of the probe molecular weight⁶⁶. For the system where the matrix and probe molecular weights are equal, the self diffusion coefficient was found to scale as expected with no dependence upon the matrix molecular weight. However later studies by the same group found a dependence upon the matrix molecular weight when the ratio of the matrix molecular weight to the probe molecular weight was less than 5⁶⁷.

Ternary solutions have been studied by several groups. Lodge has examined the compatible system, of PS/PVME/o-fluorotoluene⁶⁸ and found a complex dependence of the tracer diffusion coefficient upon the probe molecular weight ($M^{-0.5}$ - $M^{-2.3}$), with a small inverse dependence on the matrix molecular weight. However no scaling with the polymer concentration was reported. Brown has also studied the homopolymeric ternary PIB/PIB/chloroform system⁶², reporting a dependence upon the polymer concentration which increased smoothly with the concentration, the predicted dependence being found over only a very narrow concentration region. The situation concerning the dynamic processes of semi-dilute and concentrated solutions can be seen to be complicated which

has prompted several authors to propose modified reptation models. Phillies has advanced an alternative approach to the dynamics of semi-dilute solutions⁶⁹. The "hydrodynamic scaling model" has proved to be quite successful, though cannot explain the retardation of the diffusion coefficient that occurs for branched polymers as compared to linear polymers of the same molecular weight.

It is only in recent years that studies of probe chains trapped inside networks have progressed with experiments being carried out to examine the reptation mechanism. Cohen⁷⁰ has studied the diffusion of polystyrene through model poly(dimethylsiloxane) networks and has determined the diffusion coefficient of the probe polymer with QELS, utilising THF as the solvent (PDMS being isorefractive in THF) for the gel, however no scaling behaviour was reported between the molecular weight of the probe and the tracer diffusion coefficient. Haggerty⁷¹ has studied the diffusion of poly(acrylic acid) through poly(acrylamide) gels by measuring the rate of diffusion out of the gel, the diffusion coefficient of the low molecular weight probe being found to be inversely dependent upon the square root of the molecular weight of the probe. QELS has also been used to study the behaviour of polystyrene diffusing through PMMA gels by Bansil⁷² who measured the diffusion coefficient directly from the decay of the autocorrelation function, the solvent for the experiment being chosen such that the PMMA was isorefractive and thus the relaxation of the gel not seen in the experiment. Behaviour consistent with reptation having a scaling exponent of -1.8 was found between the tracer diffusion coefficient and the probe molecular weight, the difference between the experimentally obtained relationship and that predicted (-2) being attributed to the expansion of the probe chain.

Possibly the most comprehensive study of the behaviour of probe chains inside polymer networks has recently been reported by Lodge and Rotstein¹⁴. They have studied the behaviour of polystyrene polymers diffusing through poly(vinylmethylether) (PVME) end linked gels by QELS. The tracer diffusion coefficient of the polystyrene was obtained from the decay of the autocorrelation function, the solvent for the

experiment being toluene which is isorefractive with PVME under the conditions used. The diffusion of the probe chain was however found to be somewhat more highly dependent upon the probe molecular weight (scaling exponents of -2.7 and -2.8 being found for gels of concentration 0.2 and 0.235g/ml respectively) than predicted. The diffusion of the probe polymer was also obtained in PVME solutions of the same concentration, where it was found that the diffusivity in the gel was in all cases slower than or equal to that obtained in free solution. From the entire series of measurements, behaviour was found which was not consistent with any model however it should be noted that although the polymers are compatible under the conditions used, the reptation model was envisaged for the case of a polymer diffusing through a matrix of chains identical to itself.

5. Aims and Objectives.

The study of polymeric networks and semi-dilute polymer solutions has in the main been concerned with the examination of the theories of rubber elasticity and scaling relationships respectively. One of the most important theoretical predictions made during the last twenty or so years has been the reptation mechanism advanced by de Gennes for the dynamic behaviour of a polymer in a concentrated entangled medium. Although this theory was derived more than twenty years ago and considerable experimental effort imparted into the study of systems where reptation might be expected to be seen, there has been little experimental evidence in support of the theory in its most applicable case, that of a chain moving through a polymer network.

As noted earlier, the reason for this lack of attention has predominantly been due to the difficulty of experimental design. Considerable difficulties exist in the preparation of samples suitable for study containing a known fraction of polymer molecules of which the molecular weight is known and well defined. Such "loose" polymers must be the only chains capable of moving through the network, as resolution of the various motions need to be related to the molecular weight of the probe chain. In addition to this, the cross link density of the polymeric network through which the loose chain moves must be known and carefully controlled, for if the sample were not homogeneous the probe chain might be expected to diffuse at different rates through the network. Therefore, in order to study the diffusive processes controlling the motion of probe chains within networks, three criteria must be satisfied.

The probe chains must be monodisperse in order to relate the motion of the probe to its molecular weight, the network through which the probe chain moves must be homogeneous (i.e. the cross link density controllable) and finally the probe chain moving through the network must not be attached to the network and must be the only chain moving through the network. Therefore in order to satisfy the final two criteria, the network through which the probe chain to be studied is moving must be a model network where the chains of the network are cross linked only at the chain end and the molecular weight of the network chains easily controlled in order to control the cross link density of the network.

Samples for study must therefore be good quality model networks not containing a sol fraction associated with the network. The network must then be doped with a known fraction of the monodisperse probe polymer which must be compatible with the network in order to prevent expulsion of the probe polymer from the network. Such a situation can only truly be realised by the use of a probe polymer having the same chemical constituency as the network. In this case, the motions of the probe chain can be studied by QELS and the diffusion coefficient of the probe chain extracted from the

autocorrelation function by the use of Inverse Laplace Transformation (ILT) methods as typified by CONTIN⁶¹.

Therefore by controlling the cross link density of the network and the molecular weight of the probe, the predictions of the reptation theory can be studied for the ideal case of a probe chain trapped within a network, which can also be studied as a function of the solvent quality of the system by changing the swelling solvent and thermodynamic conditions. Extraction of the diffusion coefficient of the probe chain from the QELS spectrum with relaxation modes due to both the gel and the probe relies on the ILT routine being able to deconvolute the spectrum into its components. This has been shown by Brown⁶² for ternary semi-dilute solutions of poly(isobutylene) where the relaxation of the two constituent polymers (matrix and probe) were resolved and tracer diffusion coefficients obtained.

Theoretical predictions of the conformation of a probe chain within a random medium have been advanced in recent years²⁴⁻²⁶ which suggest that the size of the probe chain is dependent upon the number of obstacles in its path. A random medium is one in which regions of space are defined by fixed obstacles which are incapable of moving, an example of one such system being a polymer network where the obstacles are provided by the cross links of the network. For such a network, the obstacle density is proportional to the cross link density of the network and as such the size of the probe chain is predicted to decrease as the cross link density increases, which for a model network is inversely proportional to the molecular weight between cross links.

Whilst in recent years there have been a number of studies regarding the size of polymer chains in semi-dilute solutions, there have been no studies of the size of probe chains entrapped within swollen polymer networks of equivalent concentration to the semi-dilute solution. In such a case, an argument could be made over the applicability of the Edwards predictions as the mean obstacle density of the network decreases dramatically as the network becomes swollen with solvent. By changing the quality of the solvent by changes in solvent type and temperature it should then be possible to examine the effects of solvent quality on the size of the probe chain within the swollen network.

5.1. The Choice of System.

The system which was chosen to be studied consisted of model polystyrene networks cross linked in semi-dilute solution by the end linking of 'living' anionically prepared linear polystyrene polymers. For the study of the dynamic processes controlling the diffusion of probe chains, it was decided to trap monodisperse hydrogenous polystyrene polymers within the network and to then study the diffusive

processes of the system using QELS. In the determination of the size of the probe chain, a monodisperse perdeuterated polystyrene polymer was introduced into the network, so as to provide a contrast for SANS to selectively "pick out" the probe chain.

Polystyrene was chosen for study for several reasons. Firstly, styrene is relatively easily polymerised anionically and there exists a large volume of literature describing the synthesis of linear polystyrene polymers and model polystyrene networks. Secondly, both hydrogenous and perdeuterated monomer are commercially available at relatively low cost, allowing a cost effective preparation of a range of samples having different characteristics. Finally, there have been several investigations of the properties of polystyrene utilising both SANS and QELS and there exists a large amount of data within the literature describing the behaviour of the polymer.

Polystyrene polymers exist at room temperature below the glass transition temperature of 393K and therefore polystyrene networks are not elastomeric at ambient conditions. However, polystyrene networks can be plastisised by the addition of low molecular weight diluents when the network becomes swollen to an equilibrium value dependent upon the strength of the polymer solvent interactions. Toluene was used here to create a good solvent environment at 298K, whilst cyclohexane has been used to provide theta conditions at 308K and to provide weak solvent conditions by increasing the temperature of the system above the theta point in the range 313-323K.

For SANS experiments measuring the size of the probe chain in swollen networks, deuterated analogues were found to be commercially available and used to produce conditions where only the perdeuterated probe chain was visible to the neutron beam.

6. References.

- 1 Willis B.T.M., *Chemical Applications of Neutron Scattering*, Oxford University Press, Oxford, 1973
- 2 Berne B.J. and Pecora R., *Dynamic Light Scattering*, Wiley Interscience, New York, 1976
- 3 deGennes P.G., *Scaling Concepts in Polymer Physics*, Cornell University Press, Ithaca, N.Y., 1979
- 4 Port A.B. in *The Chemistry and Physics of Coatings* (Ed Marrion A.R.), Royal Society of Chemistry, Cambridge, 1994
- 5 Cowie J.M.G., *Polymers: Chemistry and Physics of Modern Materials*, Intertext, Aylesbury, 1973
- 6 Sperling L.H., *Introduction to Physical Polymer Science*, Wiley Interscience, New York, 1992
- 7 Rempp P., Herz J.E. and Borchard W., *Adv. Polym. Sci.*, **26**, 105, (1978)
- 8 Rempp P. and Herz J.E., *Die Angewandte Makromol. Chem.*, **76/77**, 373, (1979)
- 9 Flory P.J., *Principles of Polymer Chemistry*, Cornell University Press, Ithaca, N.Y., 1953
- 10 Treloar L.R.G., *The Physics of Rubber Elasticity*, Clarendon Press, Oxford, 1975
- 11 Mark J.E., *Rubber Chem. Technol.*, **55**, 762, (1982)
- 12 Flory P.J., *Macromolecules*, **15**, 99, (1982)
- 13 Flory P.J. and Rehner J., *J. Chem. Phys.*, **11(11)**, 521, (1943)
- 14 Rotstein N.A. and Lodge T.P., *Macromolecules*, **25**, 1316, (1992)
- 15 Flory P.J., *J. Chem. Phys.*, **10**, 51, (1942)
- 16 Huggins M.L., *J. Chem. Phys.*, **46**, 151, (1942)
- 17 Huggins M.L., *J. Am. Chem. Soc.*, **64**, 1712, (1942)
- 18 Wall F.T., *J. Chem. Phys.*, **11**, 527, (1943)
- 19 Flory P.J., *Statistical Mechanics of Chain Molecules*, Wiley Interscience, New York, 1969

- 20 Cotton J.P., Decker D., Benoit H., Farnoux B., Higgins J., Jannink G., Ober R, Picot C. and desCloizeaux J., *Macromolecules*, 7, 863, (1974)
- 21 Wignall G.D., Ballard D.G. and Schelten J., *Eur Polym. J.*, 10, 861, (1974)
- 22 Kirste R.G., Kruse W.A. and Ibel K., *L. Polym. Sci. Polym. Lett.*, 13, 39, (1975)
- 23 Allen G., *Proc. R. Soc. Lond. Ser. A.*, 351, 381, (1976)
- 24 Baumgartner A. and Muthukumar M., *J. Chem. Phys.*, 87, 3082, (1987)
- 25 Edwards S.F. and Muthukumar M., *J. Chem. Phys.*, 89, 2435, (1988)
- 26 Vilgis T., *J. Phys. (Paris)*, 50, 3243, (1989)
- 27 Cotton J.P., Nierlich M., Boue F., Daoud M., Farnoux B., Jannink G., Duplessix R., and Picot C., *J. Chem. Phys.*, 65(3), 1101, (1976)
- 28 Brown W., Mortenson K. and Floudas G., *Macromolecules*, 25, 6904, 1992
- 29 Daoud M., Cotton J.P., Farnoux B., Jannink G., Sarma G., Benoit H., Duplessix R., Picot C. and deGennes P.G., *Macromolecules*, 8, 804, (1975)
- 30 Daoud M. and Jannink G., *J. Phys.(Paris)*, 37, 973, (1976)
- 31 Edwards S.F. and Jeffers E.F., *J. Chem. Soc. (Farad. Trans. II)*, 75, 1020, (1979)
- 32 Richards R.W., Maconnachie A. and Allen G., *Polymer*, 22, 147, (1981)
- 33 Schaeffer D.W., *Polymer*, 25, 387, (1984)
- 34 Scheaffer D.W., *Macromolecules*, 13, 1280, (1980)
- 35 Farnoux B., Boue F., Cotton J.P., Daoud M., Jannink G., Nierlich M. and deGennes P.G., *J. Phys. (Paris)*, 39, 77, (1978)
- 36 Zimm B.H., *J. Chem. Phys.*, 24, 269, 1956
- 37 Kirkwood J.G. and Reisman J., *J. Chem. Phys.*, 16, 565, 1948
- 38 Lodge T.P., Rotstein N.A. and Prager S., in *Advances in Chemical Physics, Vol 79*, (Eds. Prigogine I. and Rice S.A.), Wiley Interscience, New York, 1990
- 39 Merrill W. and Tirrel M. in *Kinetics of Nonhomogeneous Processes* (Ed. Freeman G.R.) Wiley Interscience, New York, 1987
- 40 Joanny J-F. and Candau S.J., in *Comprehensive Polymer Science, Volume 2*, (Ed. Allen G.) Pergamon, Oxford, 1989
- 41 Bird B., Hassager O., Curtiss F. and Armstrong H., *Dynamics of Polymeric Liquids*, Wiley Interscience, New York, 1974

- 42 Rouse P.E., J. Chem. Phys., 21, 1272, 1953
- 43 Meyerhoff G. and Appelt B., Macromolecules, 12, 968, 1979
- 44 Meyerhoff G. and Appelt B., Macromolecules, 13, 657, 1980
- 45 Nystrom B., Roots J. and Bergman R., Polymer, 20, 157, (1979)
- 46 Flory P.J. and Wagner H.L., J. Am. Chem. Soc., 74, 195, (1952)
- 47 Edwards S.F. and Freed K.F., J. Chem. Phys., 61, 1189, 1974
- 48 Nystrom B. and Roots J., Macromolecules, 13, 1595, 1980
- 49 Adam M., Delsanti M. and Pouyet G., J. Phys. Lett. (Orsay Fr.), 40, 435, 1979
- 50 Amis E. and Han C.C., Polymer, 23, 1403, (1982)
- 51 Brown W., Polymer 24, 680, (1984)
- 52 Munch J.P., Candau S., Herz J. and Hild G., J. Phys. (Orsay Fr.), 38, 971, (1977)
- 53 Munch J.P., Candau S., Herz J. and Lemarchal P., J. Phys. (Orsay Fr.), 38,
1499, (1977)
- 54 Adam M. and Delsanti M., Macromolecules, 18, 1760, (1985)
- 55 Brown W., Macromolecules, 19, 387, (1986)
- 56 Hecht A.M., Bohidar H.B. and Geissler E., J. Phys. Lett. (Orsay Fr.), 45,
121, (1984)
- 57 Stepanek P., Konak C. and Jakes J., Polym. Bull. (Berlin), 16, 73, (1986)
- 58 Ferry J. D. *Viscoelastic Properties of Polymers*, Wiley Interscience, New York,
1981
- 59 de Gennes P.G., J. Chem. Phys., 55, 572, (1971)
- 60 Edwards S.F. and Doi M., *The Theory of Polymer Dynamics*, Oxford University
Press, Oxford, 1986
- 61 Provencher S.W., Makromol. Chem., 180, 201, (1979)
- 62 Brown W. and Zu P., Macromolecules, 22, 4031, (1989)
- 63 Berry G.C. and Fox T.G., Adv. Polym. Sci., 5, 261, (1968)
- 64 Nemoto N., Moriwaki M., Odani H. and Kurata M., Macromolecules, 4,
215, (1971)
- 65 Rudin A. and Chee K.K., Macromolecules, 6, 613, (1973)
- 66 Leger L. et al, Macromolecules, 14, 1732, (1981)

- 67 Marmonier M., Leger L. et al, Phys. Rev. Lett., 55, 1078, (1985)
- 68 Wheeler L.M. and Lodge T.P., Macromolecules, 22, 3489, (1989)
- 69 Phillis G.D., Macromolecules, 19, 2367, (1986)
- 70 Aven M.R. and Cohen C., Polymer, 31, 778, (1990)
- 71 Haggerty, L., Sugarman J.H. and Prudhomme R.K., Polymer, 29, 1058, (1988)
- 72 Bansil R., Pajevic S. and Konak C., Macromolecules, 23, 3380, (1990)

CHAPTER 2

SAMPLE PREPARATION AND CHARACTERISATION

1. Introduction

Methods used to synthesise polymer networks generally provide very little control over the structure of the network obtained. Radical and anionic copolymerisation as well as polycondensation processes produce networks where cross links are distributed randomly throughout the sample, hence the molecular weight between cross links (M_c) is an average and the distribution of chain lengths is quite broad¹. Networks can also be obtained by the cross linking of linear 'precursor' chains by both vulcanisation and γ -irradiation techniques. In both cases, cross linking occurs randomly along the precursor chain backbone and again there is a broad distribution of M_c within the network. Further to this, the junction functionality of the network is unknown and a fraction of the precursor chains will be attached to the network at one end only, forming pendant chains within the network.

'Model' polymer networks have a defined structure where the cross links are distributed homogeneously throughout the network. These can be prepared by a two stage 'end linking' process where in the first stage a linear precursor chain of known DP and narrow polydispersity is prepared having reactive groups at both chain ends. In the second stage, a suitably reactive cross linking agent is introduced and the reactive groups at the chain ends are 'end linked' together to form the cross links of the network.

2. Anionic polymerisation

Polymers unlike small molecules do not have a specific molecular weight, instead they consist of a distribution of chain lengths that can be described by various averages.^{2,3} As many of the properties including the size and diffusion of macromolecules are dependent upon the molecular weight of the polymer it would be useful to be able to prepare polymers of known molecular weight having a narrow molecular weight distribution. For many vinyl monomers capable of sustaining a

nucleophilic centre, the technique of anionic polymerisation provides a quick and efficient method of preparing polymers of predictable molecular weight, having a narrow polydispersity. The reaction is a homogeneous addition polymerisation, which in the absence of compounds containing an active hydrogen has no termination step and can be said to be a 'living' polymerisation⁴.

There are two stages in the living polymerisation. Firstly the initiating species adds across the double bond of the monomer to produce an anionic species, which in the second propagation step reacts with the monomer until all of the monomer is consumed. If the initiation of the chains occurs over a relatively short interval of time, the chains will all have an equal probability of growth and the molecular weight distribution of the resulting polymer will be narrow, approaching Poisson statistics⁵.

Initiator species for anionic polymerisation are frequently organolithium compounds, which are useful as they are soluble in a wide range of organic solvents and initiate the polymerisation by direct anionic attack on the monomer to produce the propagating species⁶. In the anionic polymerisation of styrene, (secondary)-butyllithium has been found to be highly effective in the production of 'monodisperse' polystyrene samples. The initiation step proceeds by nucleophilic attack at the vinyl bond by the (s)-butyllithium-figure 2.1. The resultant anionic species is stabilised by the electron withdrawing effect of the phenyl ring adjacent to the anion.

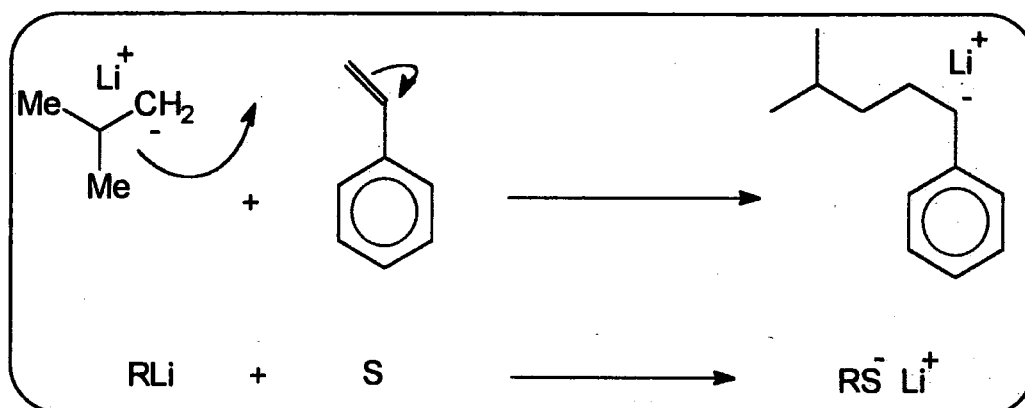
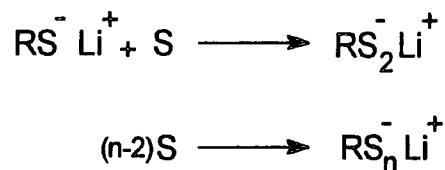


Figure 2.1: Initiation of styrene with s-butyllithium to form poly(styryllithium)

Propagation of the polystyrene chain then proceeds by subsequent addition of monomer to the poly(styryllithium) until there is complete consumption of the monomer by the growing polymer chain.



The propagating centre of the living polymer will then remain intact in the absence of any proton source. Termination of the living chain can then be brought about by the addition of a proton source such as methanol.

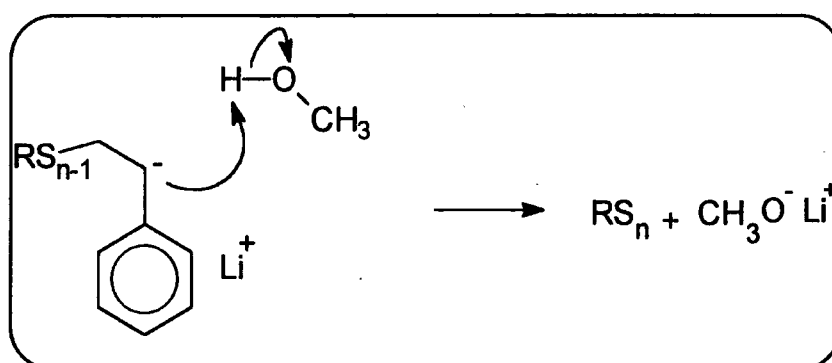


Figure 2.2.: Termination of living poly(styryllithium) with methanol

'Monofunctional' initiators such as (s)-butyllithium induce the propagation of the living anion along the growing chain from the α to the ω position, i.e. from one end to the chain to the other producing monofunctional polystyryl anions, the size of these polymer chains being related to the ratio of monomer and initiator:

$$DP = \frac{\text{mols monomer}}{\text{mols initiator}} \quad 2.1.$$

Similarly:

$$M_n = \frac{\text{mass monomer (g)}}{\text{mols initiator}} \quad 2.2$$

2.1. Difunctional anionic polymerisation initiators

In order to prepare model polystyrene networks, it is necessary to prepare α,ω polystyryl dianions that can be then be cross linked to form a network. This is only possible by the use of a difunctional initiator species, where the polymer chain grows from the centre outwards to both chain ends, as opposed to the chain growing from one end as with a monofunctional initiator.

Three types of difunctional initiator are available for the preparation of α,ω polystyryl dianions:

1. Sodium naphthalene.

Sodium naphthalene exists in polar solvents as a radical anion and initiates a living polymerisation by a rapid electron transfer from the naphthalene ring to the styrene, forming a second radical anion. This styrene radical anion rapidly dimerises to form a dianion capable of propagating a poly(styrene) chain^{4,7}-see figure 2.3. below.

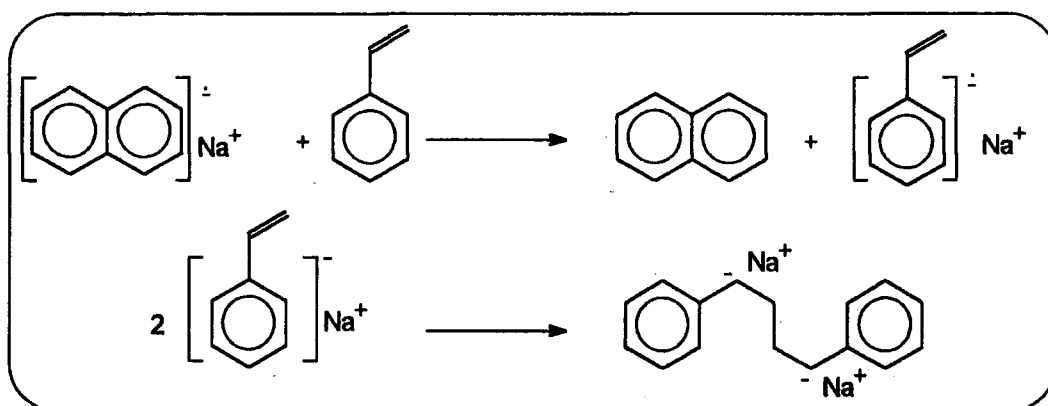


Figure 2.3.: Initiation mechanism of sodium naphthalene with styrene

2. The disodium tetramer of α -methylstyrene.

The disodium tetramer of α -methylstyrene (figure 2.4.), exists in polar solvents as a dianionic low molecular weight polymer, which can initiate the living anionic polymerisation of styrene⁴. The polymerisation of α -methylstyrene by sodium in polar solvents at room temperature produces a low molecular weight polymer as the low

ceiling temperature of poly(α -methylstyrene) prevents the formation of a high molecular weight polymer^{9,10}.

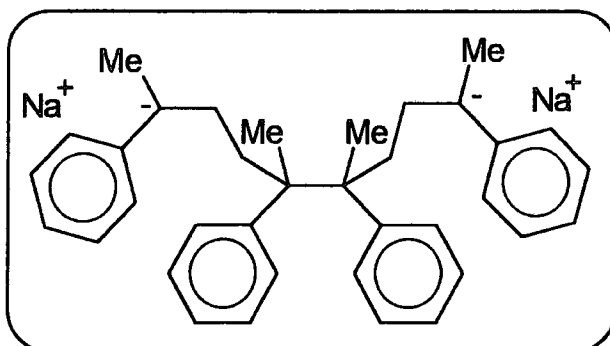


Figure 2.4.: The disodium tetramer of α -methylstyrene

The disodium tetramer formed is particularly effective in the difunctional polymerisation of styrene. As the dianionic species is already in solution, there is no initiation step and the propagation reaction proceeds instantaneously to produce a living polymer with a narrow molecular weight distribution.

3. Difunctional organolithium initiators.

Similarly to the butyllithium initiators used for the preparation of monofunctional polystyrene, a series of difunctional dilithium initiators has been prepared which will initiate the polymerisation of styrene^{11,12}. One of the most commonly used of these initiators is 1,3-phenylenebis(4-methyl-1-phenylpentylidene)dilithium^{13,14} which is prepared by reacting a divinyl compound, 1,3-bis(1-phenylethenyl)benzene with two equivalents of *s*-butyllithium. Self polymerisation of the diolefin is prevented by the large steric bulk of the phenyl rings adjacent to the vinyl groups¹³.

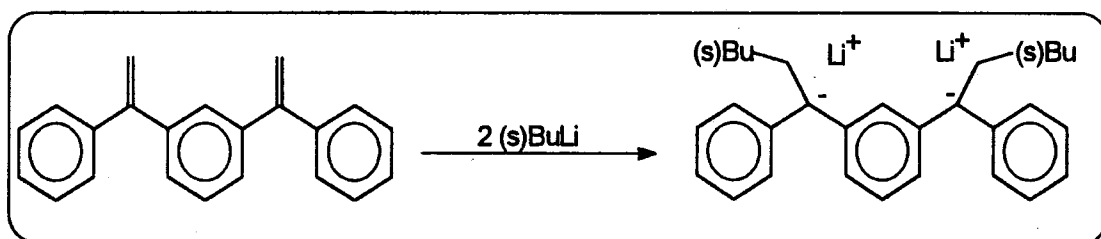


Figure 2.5.: Preparation of the difunctional lithium initiator 1,3-phenylenebis(4-methyl-1-phenylpentylidene)dilithium from 1,3-bis(1-phenylethenyl)benzene

The dilithium initiator, soluble in both polar and non polar solvent initiates the styrene polymerisation by direct anionic attack upon the vinyl group of the styrene. Propagation then proceeds as described earlier.

The molecular weight of a polymer prepared using a difunctional initiator follows the simple relationship:

$$M_n = \frac{\text{mass monomer (g)}}{0.5 \text{ mols initiator}} \quad 3.3.$$

3. Experimental

In order to be able to prepare monodisperse polymers reliably by anionic polymerisation, two experimental criteria must be satisfied. Firstly the rate of initiation should be comparable or preferably faster than the rate of propagation. This can be achieved by a careful choice of initiator and solvent. Secondly the monomers and solvents used must be extremely dry and free from polar impurities so as to prevent abortion of the polymerisation. This can only be achieved using specially dried monomers and solvents and by polymerising them under either an inert atmosphere or under high vacuum.

3.1. Preparation of solvent

3.1.1. Tetrahydrofuran (THF)

'Anhydrous' THF supplied by Mr. B. Hall (Chemistry Department, University of Durham) was refluxed over sodium wire and benzophenone for around three hours under a dry nitrogen atmosphere until a dark blue-purple colouration dominated, indicative of the formation of a complex between the sodium and benzophenone that exists only in the absence of water and polar impurities. The dried THF was then distilled under a dry atmosphere and separated into 250 cm³ portions to which a small amount of benzophenone was added as well as a slight excess of sodium wire, again a purple colouration dominated. The distillate flask was then connected to the vacuum line and

the THF thoroughly degassed by repeated freeze-thaw cycles until a pressure of 10^{-2} mbar was maintained above the frozen solvent.

3.1.2. Benzene

Benzene (Hopkin and Williams) was freed from sulphurous impurities by washing with concentrated sulphuric acid. The sulphur free benzene was then washed with distilled water until all the acid had been removed and was subsequently dried over magnesium sulphate for 24 hours. The benzene was then filtered and distilled under a dry nitrogen atmosphere, the fraction boiling at 350K was collected and separated into 250 cm³ portions. Freshly ground calcium hydride was then added to the distillate flask to dry the benzene further prior to connection of the flask to the high vacuum line. The benzene was then degassed by repeated freeze-thaw cycles until a pressure of 10^{-2} mbar was maintained above the frozen benzene. The benzene was rapidly stirred in between freeze-thaw cycles and was degassed immediately before use in a polymerisation.

3.2. Preparation of monomer

Styrene (BDH) was firstly freed from inhibitor (~15 ppm di-tert-butyl catechol) by a thorough washing with a 10% NaOH solution. The inhibitor free styrene was then washed with distilled water until all of the NaOH had been removed and was then dried over magnesium sulphate for 24 hours before vacuum distillation at a pressure of 40 mbar. The fraction boiling at 338 K was collected and was separated into 125 cm³ portions. Freshly ground calcium hydride was then added to the distillate flask and the flask connected to the high vacuum line. The styrene was then degassed by repeated freeze-thaw cycles until a pressure of 10^{-2} mbar was maintained over the styrene. The styrene was stirred vigorously in between freeze-thaw cycles and was kept covered between degassing cycles. After some time the styrene became viscous due to the formation of small amounts of low molecular weight polymer via photoinitiation. The styrene was always degassed immediately prior to use in a polymerisation.

3.2.1. Preparation of deuterated monomer

A different procedure was used to purify the deuterated styrene monomer (Aldrich styrene-d₈ 98+ atom % D) as it was used in considerably smaller quantities and contained higher concentrations of impurities than the hydrogenous monomer. The monomer was initially dried over calcium hydride and degassed frequently for around two days prior to use. In order to remove the inhibitor (0.5% di-tert-butyl catechol) the deuterated styrene was transferred under vacuum into a pre-polymerisation flask of the type shown below in figure 2.6.

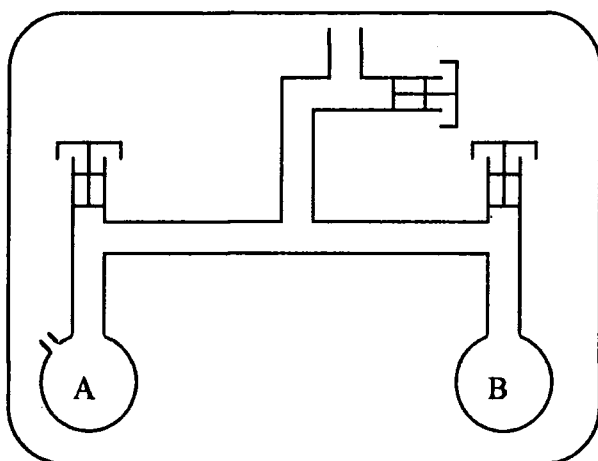


Figure 2.6.: Pre-polymerisation Flask
Used to Remove Inhibitor
from Deuterated Styrene

The monomer was introduced into bulb A which contained a small rubber septum. The bulb was isolated from the remainder of the apparatus which was maintained under vacuum and a volume of n-butyllithium introduced into the bulb. When an orange colour, typical of polystyryl anions was noted, the remaining monomer was rapidly transferred under vacuum into bulb B. Typically there was a 90% yield of purified monomer which was then transferred into the polymerisation flask.

3.3. Preparation of initiator

3.3.1 (s)-Butyllithium

The s-butyllithium initiator (Aldrich, 1.3M solution in cyclohexane) was used as received. Required aliquots were withdrawn using gas tight syringes through a self sealing membrane from the solution stored under nitrogen.

3.3.2. Sodium naphthalene

An approximately 2 molar solution of sodium naphthalene in THF was prepared by adding a 50% excess of sodium to a solution of naphthalene (Aldrich 99%) in anhydrous THF, freshly distilled from sodium-benzophenone solution. The solution was then refluxed under a dry nitrogen atmosphere for around 4 hours until all of the sodium appeared to have reacted^{7,8}. The solution was then transferred into a sealed flask (purged with dry nitrogen gas) by cannular wire. Appropriate amounts of initiator were then withdrawn by gas tight syringe as required through a rubber septum.

3.3.3. Disodium tetramer of α -methyl styrene

An approximately 2 molar solution of the disodium tetramer of α -methyl styrene (AMS) was prepared by the reaction of a solution of α methyl styrene in THF with sodium wire. α -methyl styrene (Aldrich 99%), previously freed from inhibitor (15 ppm of di-tert-butyl catechol), dried and degassed over calcium hydride on a vacuum line was transferred under vacuum into a preweighed flask. To this was added an amount of anhydrous THF, distilled directly from sodium-benzophenone solution, such that the final concentration of α -methyl styrene was approximately 4 Molar. Freshly pressed sodium wire was added to a flask of the type shown below in figure 2.7., which was found to be convenient for the preparation and filtration of air sensitive materials.

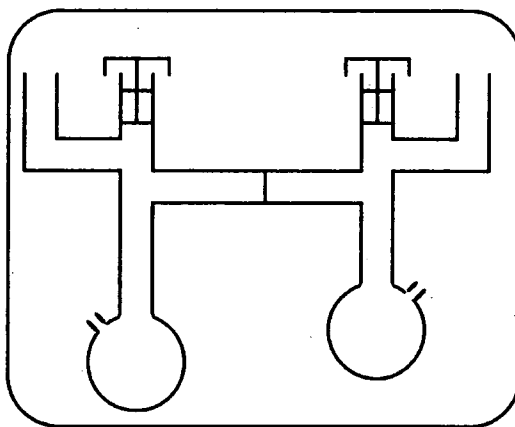


Figure 2.7.: Apparatus used for the preparation of initiators under an inert atmosphere

Briefly, the flask consists of two bulbs connected by a sintered glass disc, which allows for the filtration of material between the two bulbs. The flask has two vacuum tight PTFE 'Youngs' taps which isolate the flask from the atmosphere and two 'Youngs' sliding joints which give a gas tight connection of the flask to the vacuum line. Each bulb is also equipped with a small hole to accommodate a rubber septum.

The flask was then purged with dry nitrogen gas and the solution of α -methyl styrene-THF introduced into the bulb through the septum via a cannular wire transfer under nitrogen pressure. An immediate red colouration was noticed as the disodium α -methyl styrene tetramer began to form. The reaction was allowed to proceed at 313K for around 6 hours before the mixture was filtered to remove any remaining sodium.⁹

The concentration of the initiator was then estimated by titration of a small portion of the initiator against a 1 molar solution of butanol in toluene, the result of the titration was found to give a good correlation with the molecular weight of the polymer obtained. It was however noticed that the 'shelf-life' of the initiator was rather short and because of this a fresh solution was prepared as required.

3.3.4 1,3-Phenylenebis(3-methyl-1-phenylpentylidene)dilithium

1,3 phenylenebis(4-methyl-1-phenylpentylidene)dilithium (PBMPPD) was prepared by the reaction of 1,3-bis(1-phenylethenyl)benzene (BPEB) with (s)-butyllithium. BPEB is not commercially available and was prepared by Mr. F. T. Kiff at the I.R.C. in Polymer Science and Technology, University of Durham. The procedure used to prepare BPEB has been outlined in the literature¹⁴ and is shown below in figure 2.8. The starting material, 1,3 diacetylbenzene (Aldrich) is reacted with two equivalents of phenyl magnesium bromide in a Grignard reaction to produce 1,3-di(1-phenyl-1-hydroxy ethyl) benzene. This is subsequently dehydrated with p-toluene sulphonic acid to prepare BPEB which is then stored under nitrogen to prevent oxidation.

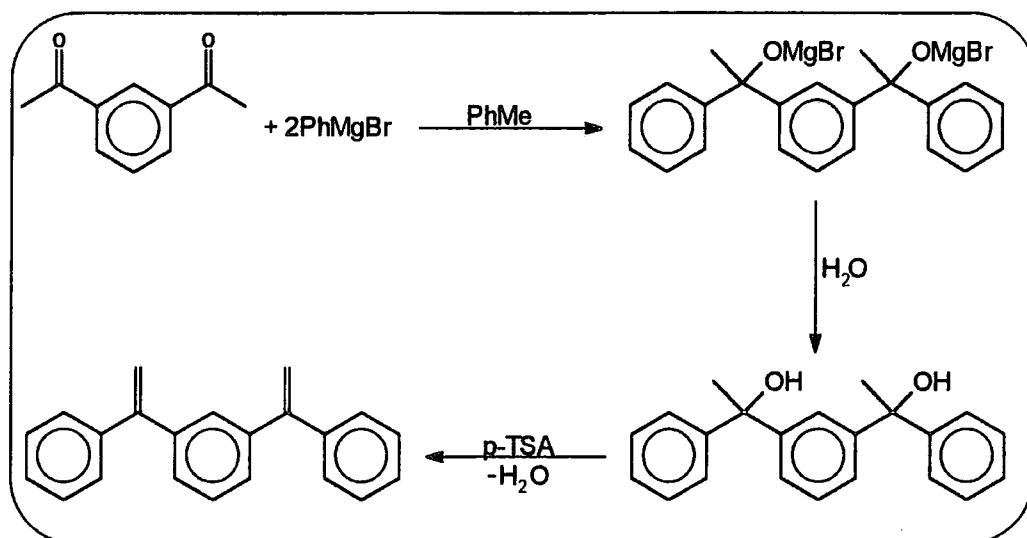


Figure 2.8.: Synthetic route to 1,3-bis(1-phenylethenyl)benzene

The addition of *s*-butyllithium to a solution of BPED produces an intensely red coloured compound which is the difunctional initiator PBMPPD. However the addition of either too much or too little *s*-butyl lithium will give rise to the presence of a monofunctional initiator in addition to the difunctional product. It is therefore of great importance to attain the correct stoichiometric ratio between BPED and *s*-butyllithium. Several methods have been developed to achieve this¹⁴, including SEC analysis of the quenched initiator¹³, though the technique used here is dependent upon the low solubility of PBMPPD in heptane¹².

Apparatus of the type shown in figure 2.7. above was used in the preparation of the PBMPPD. A known amount of the BPEB was weighed into the flask and was dissolved in approximately 50 cm³ of anhydrous heptane transferred into the flask by cannular wire having been dried over calcium hydride on the vacuum line. To this solution was added exactly twice the equivalent of *s*-butyllithium, which produced an intensely dark red solution immediately. However the reaction was allowed to proceed at 333K for 2 hours.

At this point a dark red precipitate(PBMPPD) was observed and the mother liquor removed by filtration. Further heptane was transferred into the flask to wash the precipitate and was again filtered off. The PBMPPD was then dissolved in

approximately 80 cm³ of benzene and was then filtered and transferred into a storage flask by cannular wire. As with the AMS initiator, the strength of the initiator was estimated by titration with a solution of (s)-butanol in toluene. The solubility of PBMPPD in benzene is however quite low and the concentration of the initiator is around 0.08 Molar.

3.4. Preparation of cross linking agent

3.4.1. Triallyloxytriazine (TAT)

Triallyloxytriazine (Aldrich, 98+%) was purified by recrystallisation from HPLC grade heptane at 300K, followed by drying under vacuum at 323K for 24 hours. An approximately 1 molar solution of TAT in anhydrous THF was then prepared by distilling THF directly onto TAT from sodium-benzophenone solution. The flask, equipped with a rubber septum, was then refilled with dry nitrogen gas and the required amounts of TAT solution withdrawn with a gas tight microlitre syringe as necessary.

3.4.2. Divinylbenzene (DVB)

Divinylbenzene, was obtained commercially as a technical grade material (Merck-Schuchardt, a 60% solution of meta and para isomers in ethylvinylbenzene) and although methods are available for the isolation of the DVB component¹⁶ these were not used in this work. The solution was freed from inhibitor (0.2% di-tert-butyl catechol) by a thorough washing with a 10% solution of sodium hydroxide followed by distilled water.

The DVB was then dried over magnesium sulphate for approximately 2 hours before the addition of a quantity of freshly ground calcium hydride to the cross linking agent. The flask was then connected to the vacuum line where the DVB was dried and degassed for around 24 hours by repeated freeze-thaw cycles before transferring the DVB under vacuum to a separate flask equipped with a small self-sealing rubber septum which was then refilled with dry nitrogen gas.

The composition of the solution prior to and after vacuum transfer was determined by Gas Chromatography(GC) and Nuclear Magnetic Resonance(NMR) spectroscopy. GC analysis was performed using a Hewlett Packard 5890A machine containing a 0.25 μ m SE 30 column and a flame ionisation detector. Nitrogen was used as the carrier gas in the analysis.

¹H NMR spectroscopy was carried out using a Varian 'Gemini' 200 spectrometer operating at a proton resonance frequency of 200 MHz. Results of the GC analysis are shown below in table 2.1., from which it can be seen that there is no change in the composition of the liquid mixture on vacuum transfer.

Before Vacuum Transfer		After Vacuum Transfer	
Retention Time/min	% Area	Retention Time/Min	% Area
9.26	0.509	9.26	0.498
9.36	0.645	9.36	0.664
9.49	0.280	9.48	0.286
9.66	0.297	9.66	0.306
9.76	29.559	9.76	28.994
9.90	8.447	9.89	8.337
10.25	43.306	10.25	44.926
10.44	16.140	10.44	15.187
11.68	0.814	11.73	0.799

Table 2.10.: GC analysis of DVB solution before and after vacuum transfer.

The ratios of the major peaks in the GC (9.76 and 9.90 mins to 10.25 and 10.44 mins) indicate that the DVB content of the solution is 60% as claimed. This is also confirmed by the ratio of the peak areas from the proton NMR data in figures 2.9. and

2.10. Figure 2.9. shows the NMR spectrum of the DVB solution prior to vacuum transfer, while figure 2.10. shows the spectrum after transfer.

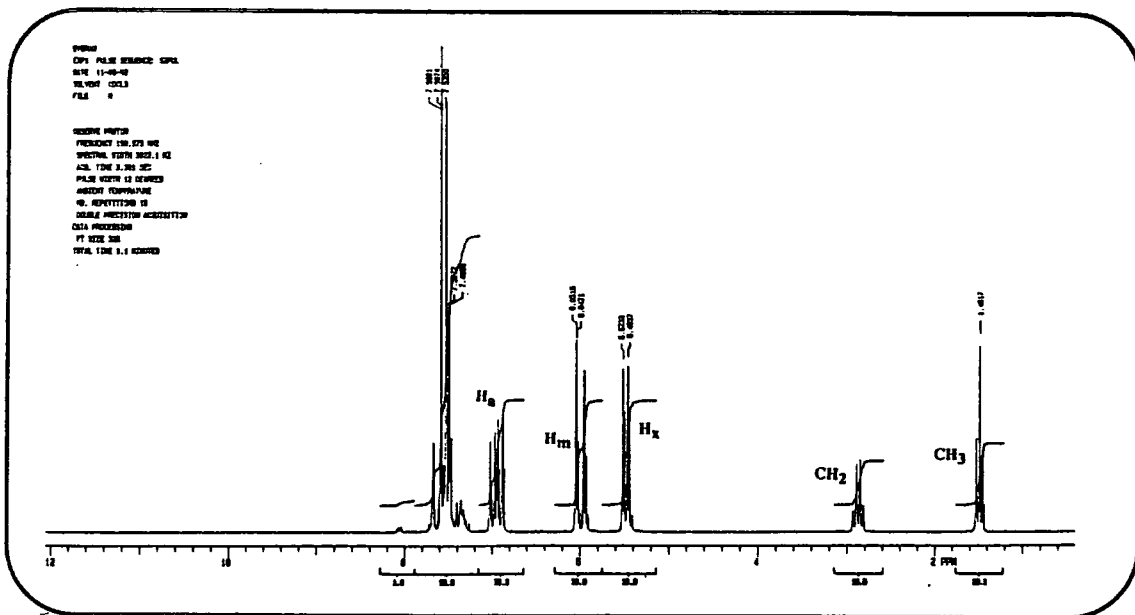


Figure 2.9.: Proton NMR spectrum of DVB solution before vacuum transfer

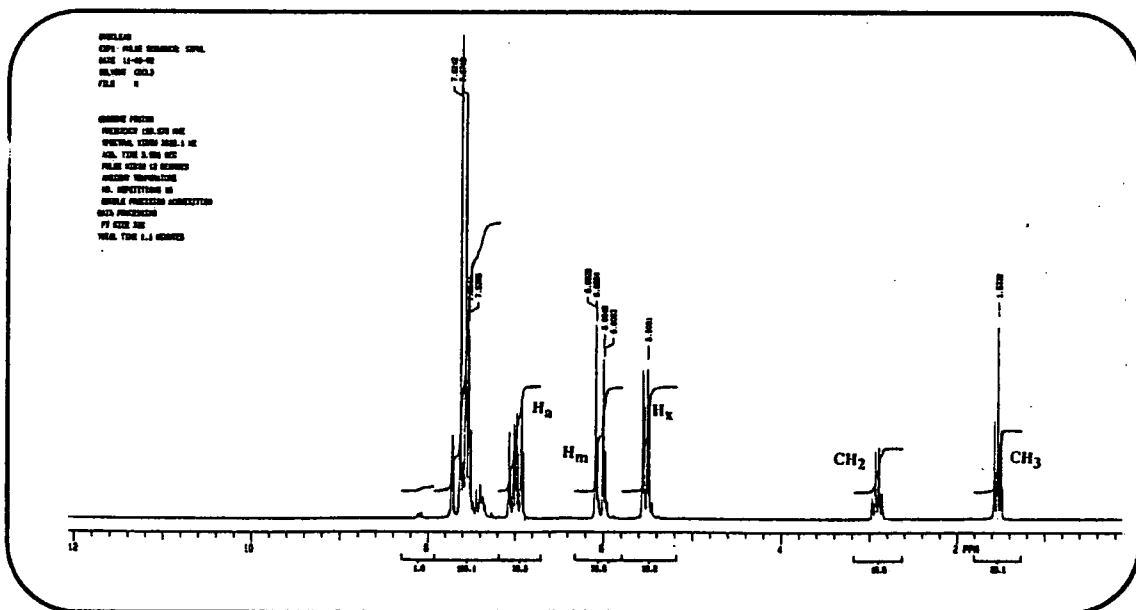
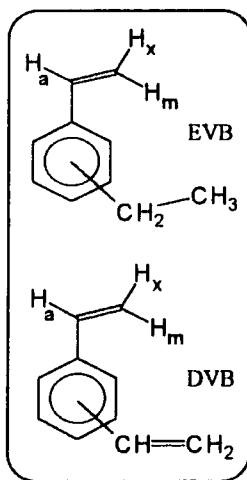


Figure 2.10.: Proton NMR of DVB after vacuum transfer.

From the ratio of the integrals of the methylene resonance at 2.9 ppm (due to ethylvinyl benzene) to the vinylic resonance (H_a in figure 3.11. below) at 7.0 ppm (due to

the vinyl groups of both divinyl benzene and ethylvinyl benzene), no change in the composition of the solution is observed after vacuum transfer.



Resonance/ppm	Assignment
1.49 (m)	Methyl CH ₃
2.85 (q)	Methylene CH ₂
5.5 (m)	H _x
6.05 (m)	H _m
6.9 (m)	H _a
7.5 (m)	Benzene ring

Figure 2.11.: NMR assignments for DVB/ EVB solution

Examination of the ratio of the integrals of the methylene to the vinylic resonance shows the ratio of DVB to ethylvinyl benzene to be 1.75:1. Theoretically this ratio should be 1.5:1, however the NMR spectra support the GC data in showing that no depletion of the DVB occurs on purification.

3.5. Polymerisation procedure

The procedure used to prepare both linear polymers and model networks followed an established technique used in this laboratory for the preparation of polymers and copolymers by anionic methods. As noted earlier, one of the main difficulties in anionic polymerisation is the need for scrupulously clean equipment and reagents.

Here, a high vacuum method has been used to prevent abortion of the polymerisation by reactive impurities. A pressure of 10^{-7} mbar was maintained by the use of rotary (Edwards E2) and oil diffusion pumps (Edwards 63/150 'Diffstack') operated in series. Flasks of the type shown below in figure 2.12. were used to prepare both the polymers and networks.

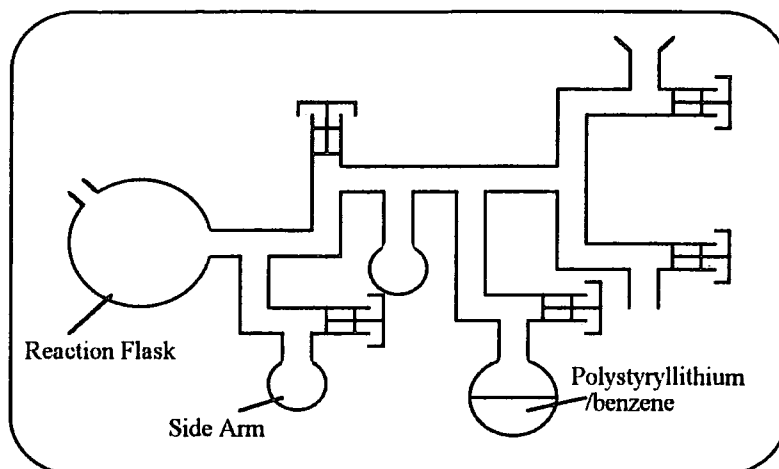


Figure 2.12: Reaction flask of the type used to prepare polymers and networks

The flask was cleaned thoroughly by washing with permanganic acid to remove both organic and inorganic residue, followed by rinsing with a large volume of distilled water and methanol. The 'clean' flask was then dried before being attached to one of the secondary manifolds of the vacuum line as shown in figure 2.13.

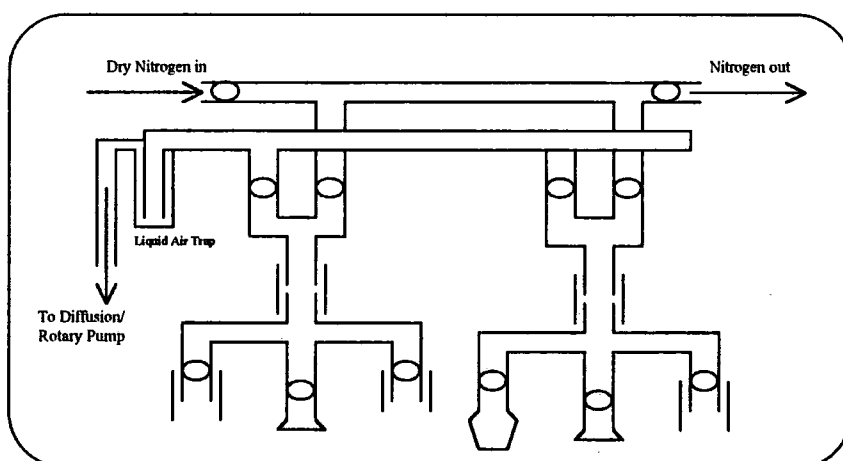


Figure 2.13.: High vacuum anionic polymerisation line

The flask was then heated under vacuum so as to remove any atmospheric contaminants present upon the surface which would otherwise not have been removed. A living solution of poly(styryllithium) in benzene was then introduced into the flask and all surfaces of the glassware and vacuum taps were thoroughly washed to remove any remaining polar impurities. The poly(styryllithium) solution was then returned to the bulb and all traces of the living polymer removed by washing the flask with solvent

distilled from the poly(styryllithium) solution. This procedure is particularly important as the poly(styryllithium) is capable of initiating the polymerisation of the monomer to be introduced into the flask. The reaction flask was degassed finally before the addition of solvent and monomer by vacuum transfer prior to polymerisation with the appropriate initiator.

3.5.1. Preparation of linear polystyrene

Suitable combinations of initiator and solvent for the preparation of linear polystyrene samples have been described in the literature. One frequently used method is the polymerisation of styrene in benzene using *s*-butyllithium as the initiator^{4,5,6}. This combination has been shown to produce polymers of predictable molecular weight and low polydispersity and for these reasons was chosen to be used here for the synthesis of linear polystyrene samples to be used in this project.

Sufficient solvent was transferred into the clean reaction flask to give as final polymer concentration of approximately 5% w/v. A preweighed amount of monomer was then introduced into the reaction flask by vacuum transfer and the flask degassed prior to bringing the reaction mixture to room temperature, where the polymerisation was initiated by addition of the appropriate volume of initiator as given by equation 2.2. A characteristic orange colouration indicative of the formation of polystyryl anions was observed and the propagation reaction allowed to proceed for upwards of 2 hours before termination of the reaction with methanol.

3.6. Preparation of polystyrene networks

Several combinations of initiator, solvent and cross linking agents have been investigated here for the preparation of model networks, a brief summary of which is given here. Initial attempts centred around cross linking with triallyloxytriazine (TAT) of α,ω polystyryldianions in THF prepared from the sodium naphthalene initiator. TAT is a trifunctional molecule, its use as a coupling agent in the preparation of star polystyrene having been described in the literature¹⁵.

However attempts here to develop its use as a cross linking agent using sodium naphthalene as the difunctional initiator proved fruitless. Although high molecular weight polymer was produced by the sodium naphthalene, on addition of TAT no sign of gelation was observed, though SEC analysis of both the parent polymer and the 'cross linked' product indicated an increase in molecular weight upon coupling with TAT. Cross linking with TAT was also investigated using the disodium tetramer of α -methyl styrene (AMS) as the difunctional initiator of polystyrene in THF. Again although a high molecular weight polymer was obtained, no cross linking occurred with the introduction of the TAT.

At this point, efforts to obtain cross linking with TAT (which should produce networks with a well defined junction functionality of 3) were abandoned in favour of the more conventional cross linking agent divinylbenzene (DVB) which produces networks from a block copolymerisation reaction in which the DVB polymerises to form intermolecular nodules which act as cross links (the functionality of which is varied and unknown) for the polystyrene block. The reaction of 3 equivalents of DVB per living chain end with polystyryl dianions prepared from sodium naphthalene in THF again failed to produce a network, though SEC analysis of the polymers indicated a substantial rise in the molecular weight had occurred upon the introduction of the DVB.

The introduction of 3 equivalents of DVB per living anion was found to induce the gelation of a solution of polystyryl dianions prepared from either the AMS or PBMPPD initiators in benzene solvent. A series of networks were prepared using these schemes where the precursor chain molecular weight ranged from 10,000 to 100,000 g mol⁻¹. Initially the AMS/DVB combination was investigated for the preparation of polystyrene networks, however this method was not entirely satisfactory as the reliability of the system was rather poor and the networks obtained were found to be of poor quality in that large quantities of material could be extracted from the networks, resulting from incomplete incorporation of the precursor polymer into the network (sections 5.2.

and 5.3.). The most efficient method of producing polystyrene networks was found to be the end linking with DVB of α,ω dianionic polystyryl lithium chains, prepared in benzene from the PBMPPD initiator. Networks were produced where only a small trace of material could be extracted from the network, indicating that all of the precursor polymer had been cross linked.

Although it is not fully understood why the AMS/DVB system produced networks sporadically, it seems feasible that the problem with the system lies with the AMS initiator used for the polymerisation, a fresh solution of initiator being prepared for each polymerisation. It would seem possible that some batches might not be as effective in the difunctional initiation of polystyrene as others since α -methyl styrene can also react with alkali metals to produce a disodium dimer, which may be present in the initiator solution and does not initiate the difunctional polymerisation of styrene^{4,9,10}. As the shelf life of the PBMPPD initiator was quite long (stable for upto 3 months at 273K) the initiator was prepared as required, the same batch being used for repeated polymerisation's. Further to this, the synthetic route employed to PBMPPD prevented the presence of any monofunctional species in the initiator solution, which contained only one difunctional initiator species.

The AMS and PBMPPD initiators have been used to prepare a series of polystyrene networks with M_c ranging from 10,000 to 100,000 g mol^{-1} , either containing one of a series of probe chains (M_p 30,000 to 1,000,000 g mol^{-1}) or containing no trapped chain ('blank networks'). For the AMS/DVB system, the solvent used for the polymerisation reaction was anhydrous benzene prepared as in section 3.1.1. For the PBMPPD/DVB system the polymerisation solvent was benzene doped with 1% v/v of anhydrous THF to prevent the aggregation of the PBMPPD initiator, which may adversely affect the polydispersity of the polymer produced¹¹⁻¹⁴.

Two series of polymer networks have been prepared for use in this project:

1. Synthesis of 'blank' networks.

A preweighed amount of monomer was distilled into a cleaned reaction flask together with sufficient solvent to give a 10% (w/v) concentration of polymer in solution. The appropriate volume of initiator was then added and the propagation reaction allowed to proceed to completion. Prior to the addition of the cross linking agent, a small volume of the polymer solution was withdrawn into a sidearm and terminated with methanol to facilitate SEC analysis of the precursor chain molecular weight.

The appropriate volume of cross linking agent was then added to the remainder of the precursor polymer solution and gelation allowed to proceed for around 12-14 hours (overnight). The living gel was then terminated by the addition of methanol and was subsequently recovered by cutting the flask open after releasing the vacuum.

2. Synthesis of networks containing trapped chains.

A preweighed amount of monomer was transferred under vacuum into a cleaned reactor flask. The appropriate quantity of the probe polymer to give a trapped chain concentration of 10% (w/w) within the dry network was added to a small flask equipped with a rubber septum. A known amount of the polymerisation solvent was then distilled into the flask, producing a solution of the probe polymer which was then purged with dry nitrogen. Sufficient solvent (accounting for the volume of the probe polymer solution and the polymerisation initiator) to give a 10% (w/v) concentration of the network polymer was distilled into the reactor flask and the flask then brought to atmospheric pressure with dry nitrogen.

The solution of the probe polymer was then transferred into the reaction flask by cannular wire and polymerisation under the inert atmosphere initiated by addition of the appropriate volume of initiator. After completion of the propagation reaction, a small

volume of the polymer solution was removed from the flask and terminated with methanol for SEC analysis of the parent polymer.

The appropriate volume of the cross linking agent was added to the remaining precursor solution and the end linking of the living chains allowed to proceed around the probe chains, thus trapping the probe within the network. The 'living' network was terminated after around 12 hours by the addition of methanol and was again cut free from the reaction flask.

4. Characterisation of polymers by Size Exclusion Chromatography

Size exclusion chromatography (SEC) was used to determine the molecular weight characteristics of the linear polystyrene polymers chains prepared in this project. SEC analysis was carried out on samples of polymers in chloroform solution.

4.1. Chloroform SEC

Samples for SEC analysis were dissolved in filtered and degassed chloroform (distilled GPR grade) and made up to a concentration of 0.1% w/v. Sample solutions (100 μ l) were filtered through 0.2 μ m polypropylene backed PTFE membrane filters to remove any dust and particulate matter.

The solutions, containing a toluene flow rate marker, were pumped to a Waters differential refractometer detector (R401) through three polymer laboratories PL gel columns (pore size: 10²Å, 10³Å and 10⁵Å with 5 μ m bead size) by a Waters model 590 pump operating at 1 cm³/minute. Calibration of the SEC detector system was relative to various narrow molecular weight polystyrene standards obtained from Polymer Laboratories.

4.2. Results of SEC analysis of linear polymers

Several linear polystyrene samples were prepared to be used in the project, the molecular weight characteristics as determined by chloroform SEC are listed below in table 2.2.

Polymer	M_n	M_w	M_w/M_n	Comment
PS 11	24,700	61,600	2.49	Not Used
PS 12	56,900	96,800	1.70	Not Used
PS 13	63,100	73,700	1.17	H-PS
PS 14	108,800	113,400	1.04	H-PS
PS 18	21,800	22,000	1.01	H-PS
PS 19	10,500	10,700	1.01	H-PS
PSD 1	30,000	30,500	1.02	D-PS
PSD 2	24,800	26,000	1.05	D-PS
PROBE 3	118,800	125,000	1.03	See Below
PROBE 4	316,400	326,600	1.04	See Below
PROBE 5	1,015,500	1,063,300	1.05	See Below

Table 2.2.: Chloroform SEC analysis of linear polystyrene polymers

Samples in bold face were purchased from Polymer Laboratories Ltd, whose own SEC analysis of molecular weight is given here.

5. Characterisation of polystyrene networks

The molecular weight between cross links of the networks were determined by SEC on the precursor chains prior to cross linking, as well as from the equilibrium swelling ratio of the solvent swollen network. The degree of uncross linked material was also evaluated by quantitatively measuring the sol fraction of the 'blank' networks.

5.1.1. Characterisation of precursor polymers to 'blank' networks

The molecular weight characteristics of the precursor polymers obtained from the AMS/DVB system are described below in table 2.3., whilst table 2.4. shows the SEC analysis of the PBMPPD/DVB system.

Network	M_n	M_w	M_w/M_n
AMS 4	87,800	109,900	1.25
AMS 5	41,900	48,700	1.16
AMS 6	8,700	10,400	1.20
AMS 7	17,700	20,100	1.14
AMS 11	36,300	37,900	1.04
AMS 16	50,000	53,600	1.07
AMS 19	11,600	12,700	1.10

Table 2.3.: SEC analysis of precursor chains to the AMS/DVB 'blank' networks

Table 2.4.: SEC analysis of PBMPPD/DVB 'blank' network precursor polymers

Network	M_n	M_w	M_w/M_n
DLB 1	16,300	17,800	1.09
DLB 2	45,600	53,000	1.16
DLB 3	81,100	102,800	1.27
DLB 4	9,000	10,600	1.18

5.1.2. SEC of precursor chains to networks containing deuterated trapped chains

Two series of networks containing perdeuterated trapped chains were prepared for SANS investigation of the size of the probe chain. Firstly, a series of networks containing the PSD 1 polymer as the perdeuterated probe chain were prepared with M_c ranging from 10,000 to 50,000 g mol⁻¹. SEC data from the precursor polymers are shown below in table 2.5., however the presence of the probe chain (10% of the total polymer mass) influences the molecular weight distribution of the precursor polymer as SEC is unable to resolve the PSD 1 peak (M_n 30,000 g mol⁻¹).

Network	M_n	M_w	M_w/M_n
AMSD 1	8,900	9,800	1.11
AMSD 2	15,600	17,000	1.09
AMSD 4	25,200	27,000	1.07
AMSD 5	45,800	46,400	1.01

Table 2.5.: SEC data from AMS/DVB networks containing the PSD 1 probe chain.

The second series of networks containing perdeuterated probe chains were prepared using the PBMPPD/DVB system, and contained the PSD 2 polymer as the

probe chain. Again the SEC analysis of the precursor chain molecular weight was influenced by the presence of the probe polymer, figure 2.14 shows the SEC data of network TCD 4, where the higher molecular weight probe polymer can be seen to be causing an increase in both the molecular weight of the sample as well as broadening the polydispersity.

Network	M_n	M_w	M_w/M_n
TCD 1	42,500	53,100	1.25
TCD 2	26,400	28,300	1.07
TCD 3	12,500	14,700	1.17
TCD 4	12,300	14,100	1.15
TCD 5	18,000	19,800	1.10
TCD 6	7,900	10,000	1.26

Table 2.6.: SEC data for PBMPPD/DVB networks containing PSD 2 probe

As SEC is does not give a true representation of the precursor chain molecular weight, M_c cannot be solely evaluated from SEC data and has also been determined from the equilibrium volume fraction of polymer in the solvent swollen network (section 5.3.).

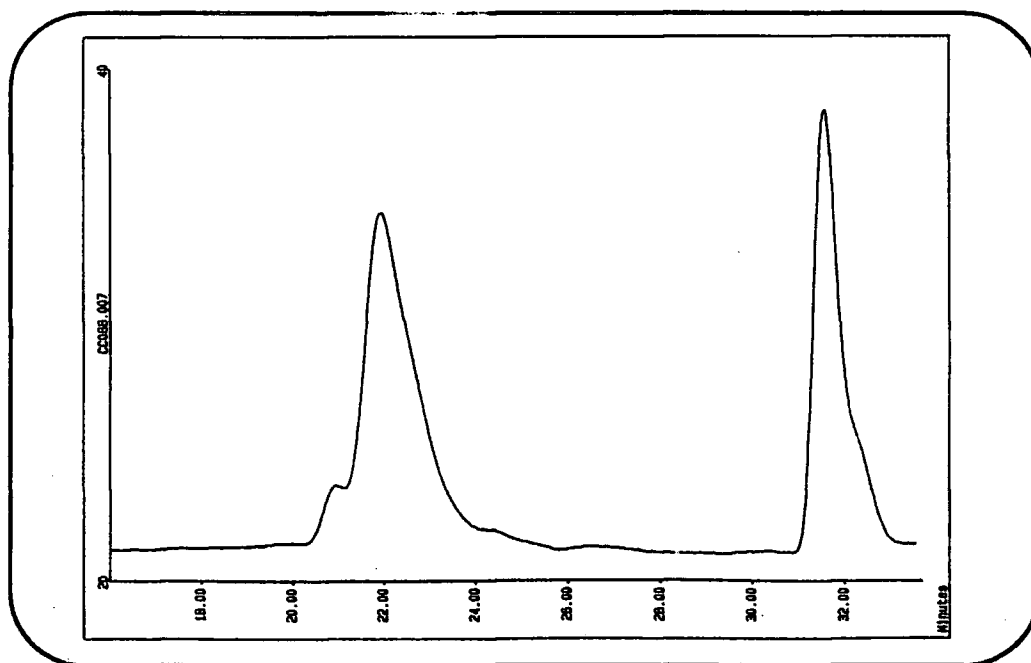


Figure 2.14.: SEC trace of network TCD 4

5.1.3. SEC analysis of networks containing hydrogenous probe chains

A series of networks containing probe chains of various molecular weights were prepared by the PBMPPD/DVB system for a QELS study of the diffusion of the trapped chain. Results of the SEC analysis of the precursor chain molecular weight are given in table 2.7. Networks TCH 1, 2 and 3 contained probe 5 as the trapped chain whilst TCH 4, 5 and 6 contained probe 4 and networks TCH 7, 8 and 9 contained probe 3.

Network Precursor Polymer				Probe Polymer		
Network	M_n	M_w	M_w/M_n	M_n	M_w	M_w/M_n
TCH 1	8,700	10,100	1.17	1,268,300	1,389,300	1.09
TCH 2	38,000	44,500	1.17	1,634,400	1,789,900	1.09
TCH 3	87,400	112,000	1.28	1,725,300	1,860,700	1.08
TCH 4	8,500	9,800	1.15	273,400	299,600	1.09
TCH 5	37,100	44,100	1.19	348,900	367,000	1.05
TCH 6	111,100	171,700	1.54	-----	-----	-----
TCH 7	11,800	20,200	1.71	-----	-----	-----
TCH 8	43,000	56,200	1.31	-----	-----	-----
TCH 9	94,300	129,000	1.37	-----	-----	-----

Table 2.7.: SEC analysis of networks containing hydrogenous probe chains

As the molecular weights of these probe chains are considerably higher than the perdeuterated chains, SEC has been able, in many cases to resolve two separate peaks, as in figure 2.15 where the less intense peak is due to the probe polymer and the main peak due to the network precursor chains. Where possible both peaks have been analysed, the results of which are shown in table 2.7., the data in bold type refers to the probe chain incorporated into the network.

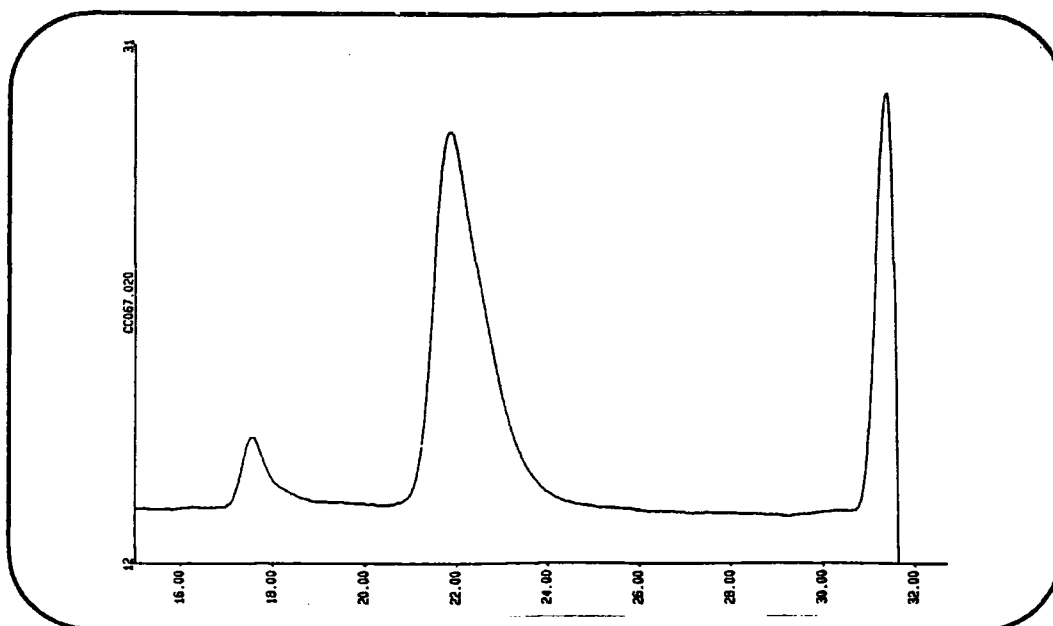


Figure 2.14.: SEC of TCH 4 network containing probe 4 as the trapped chain

5.2. Sol fraction of polymer networks

The amount of uncross linked material in the 'blank' networks was determined by the extraction of the sol fraction of the networks. Two separate procedures were used to determine the sol fraction. For the AMS/DVB system this relied upon continual extraction of the as produced network with cyclohexane, whilst for the PBMPPD/DVB networks a Soxhlet extraction was performed after initial drying of the network to constant weight.

5.2.1 Extraction of the sol fraction

After cutting the benzene swollen AMS/DVB network from the reaction flask, the network was deswollen by immersion in cyclohexane at ambient temperature for several days. The solvent was changed at regular intervals and the excess solvent collected at each stage. When the benzene solvent had been completely extracted, the network was placed inside a Soxhlet apparatus and extracted with cyclohexane for around 7 days until the sol fraction had been completely extracted.

The gel was slowly dried to constant weight, firstly in air for several days followed by drying in a vacuum oven at approximately 350K for 24 hours. The

combined washings from the deswelling process and the Soxhlet extraction were evaporated to dryness and dried overnight in a vacuum oven at 370K. The weight of the dry extracted material was then noted and the sol fraction determined.

A different procedure was however adopted for the PBMPPD/DVB networks. After removal from the reaction flask, the gels were dried in air and under vacuum to constant weight. A preweighed sample of the network was then placed into a small packet formed from a fine mesh stainless steel sheet. This was then placed inside a Soxhlet apparatus and extracted with cyclohexane for 7 days. After complete extraction of the sol fraction, the network was again dried to constant weight and any change in mass noted. Similarly to above the extracted material was collected by evaporation of the solvent, followed by drying at 370K. The amount of extracted material was again noted and the sol fraction determined. The amount of the sol fraction removed from the networks is shown in table 2.8., both methods for the determination of the sol fraction are shown. Method A used the amount of collected material while method B measured the difference in gel weights before and after extraction.

Network	Sol Fraction 'A' (%)	Sol fraction 'B' (%)
AMS 4	12.1	-----
AMS 5	16.8	-----
AMS 6	24.9	-----
AMS 7	21.0	-----
AMS 11	17.7	-----
AMS 16	15.5	-----
AMS 19	23.7	-----
DLB 1	0.3	0.5
DLB 2	0.7	1.0
DLB 3	0.5	0.9
DLB 4	0.4	1.5

Table 2.8.: Amount of sol fraction extracted from 'blank' networks.

As can be seen from the data of table 2.8., a large difference in the amount of the sol fraction exists for the two series of samples. Whilst nearly no extractable material was found for the PBMPPD/DVB system, the AMS/DVB system was found to give rise to a considerably larger sol fraction. Measurement of the sol fraction, expressed as a percentage of the initial sample weight, was however subject to several sources of error. In drying the network to constant weight it was difficult to remove the last traces of solvent trapped within the network, whilst in the measurement of the extracted material care was needed to avoid loss of any of material, which as the quantities of extracted material were generally small was a significant amount of the sol fraction. In all cases only a small portion of each gel was evaluated and sample homogeneity was assumed throughout.

5.3. Equilibrium swelling measurements

The purpose of these experiments was to measure the equilibrium swelling ratio so as to correlate other measurements on the gels with the polymer concentration in the swollen network. The degree of swelling of the network is generally defined in terms of the volumetric swelling ratio, Q which relates the volume of the dry network to the volume of the swollen gel.

$$Q = \frac{V_g}{V_0} = \frac{V_p + V_s}{V_0} \quad 2.4.$$

An alternative measure used is the polymer volume fraction, ϕ_p which is given by:

$$\Phi_p = \frac{V_p}{V_p + V_s} \quad 2.5.$$

Where $V_p = v_p m_d$ is the swollen volume of polymer

$V_s = v_s m_s$ is the volume of solvent

$V_0 = v_0 m_d$ is the dry volume of polymer

and v is the partial specific volume and m is the mass.

The equilibrium degree of swelling of the network can be related to the cross link density of the network by the Flory-Rehner model²¹ which states that the free energy of mixing is zero at swelling equilibrium. Furthermore, the Flory-Rehner model assumes that the free energy of mixing arises from a heat of mixing term and two separable and additive entropic terms describing the increase in entropy of the polymer chains on mixing with solvent and also the entropic change arising from the decrease in the numbers of possible chain conformations on swelling. The first of the two entropic terms, the mixing term is taken from the Flory-Huggins theory of polymer solutions, while the second entropic term arises from the elastic retractive forces opposing the deformation of the polymer chains and is taken from the affine model of rubber elasticity (chapter 1).

At swelling equilibrium the Flory-Rehner equation is given by:

$$M_c = \bar{V}_s \rho_p \left[\frac{-\left(\phi^{1/3} - \frac{\phi}{2}\right)}{\ln(1-\phi) + \phi + \chi\phi^2} \right] \quad 2.6.$$

Where M_c is the effective molecular weight between cross links

\bar{V}_s is the molar volume of the solvent

ρ_p is the density of the dry network

χ is the polymer solvent interaction parameter

and ϕ is the polymer volume fraction at swelling equilibrium

5.3.1. Determination of the polymer volume fraction in solvent swollen networks

The swelling ratio of each individual network was determined in cyclohexane between 308K and 323K and in toluene at 298K. The swelling ratio was evaluated by a weighing method¹⁷ where a preweighed portion of the dry network (dried under vacuum at approximately 340K for 4 days), was immersed in an excess of solvent and allowed to

reach constant weight. The swollen gel was then removed from the excess solvent and any adhering surface film of solvent removed before weighing the gel in a sealed bottle.

The swollen weight of the gel was taken as an average of several weighings so as to account for errors arising from solvent evaporation and incomplete removal of the surface solvent film. For the calculation of the polymer volume fraction, values of the specific volume of polymer in bulk and in solution were obtained from the data of Sarazin¹⁸ while values of χ used for the determination of M_c were obtained from the work of Orwoll¹⁹. It was assumed that the specific volume of the polymer in the swollen gel was independent of concentration and polymer molecular weight over the range of polymer volume fractions used.

5.3.2. Evaluation of Swelling Equilibrium

Some preliminary swelling experiments were performed in order to determine the length of time required for networks to reach swelling equilibrium. Figures 2.16. and 2.17. show the swelling curves for networks TCH 3 and TCD 4 swollen to equilibrium (directly from the dry state) in toluene and cyclohexane at 298K respectively.

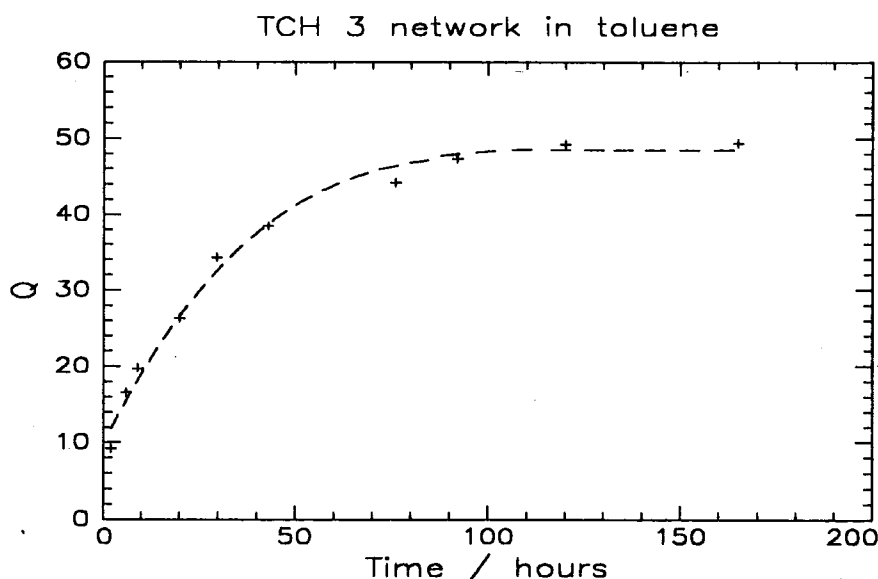


Figure 2.16.: Swelling curve for network swollen in toluene at room temperature

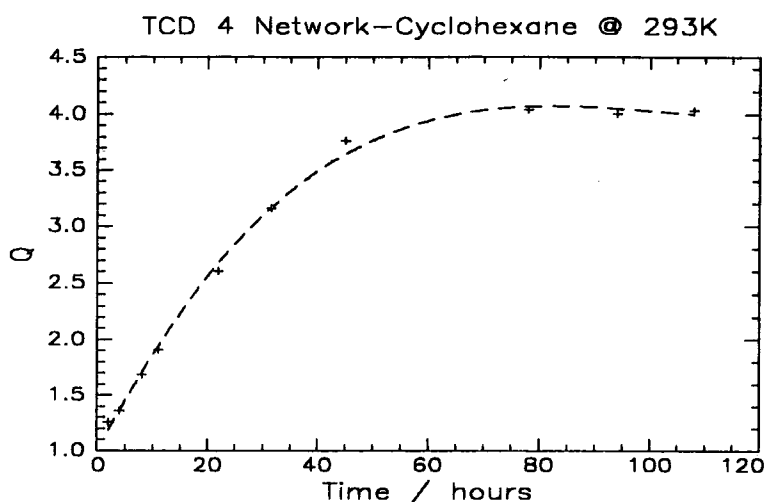


Figure 2.17.: Swelling curve for TCH 4 network swollen in cyclohexane

As can be seen from figure 2.16. the TCH 3 sample swollen in toluene was found to reach constant weight in approximately 6 days, however since samples of the networks varied in both shape and volume, all samples were left for a period of 10 days to ensure that swelling equilibrium had been reached. Networks swollen in cyclohexane were found to reach swelling equilibrium more rapidly than when swollen in toluene. Figure 2.17. shows the swelling curve for a extracted sample of network TCD 4, as can be seen constant weight was reached in around 4 days, however samples were left for a period of 7 days to again ensure that swelling equilibrium had been attained. Upon changing the temperature of networks swollen in cyclohexane, only a few hours were needed for the gels to reach the new swelling equilibrium and consequently samples were allowed to equilibrate for around 12 hours to ensure constant weight.

5.3.3. Results of Swelling Measurements

The equilibrium swelling ratio was measured for all gels at temperatures of 308K, 313K 318K and 323K in cyclohexane as well as at 298K in toluene. As expected, the volumetric swelling ratio of the PBMPPD/DVB networks increased with the precursor chain molecular weight. Figures 2.18. and 2.19. respectively show the variation in Q with precursor chain M_n for networks swollen in toluene and cyclohexane. As can be seen in figure 2.19., the swelling ratio increased most dramatically for gels with a low cross link density as the quality of the solvent was improved by increasing the

temperature of the cyclohexane system, however even when swollen to equilibrium in cyclohexane at 323K, the degree of swelling was considerably lower than that in toluene at 298K.

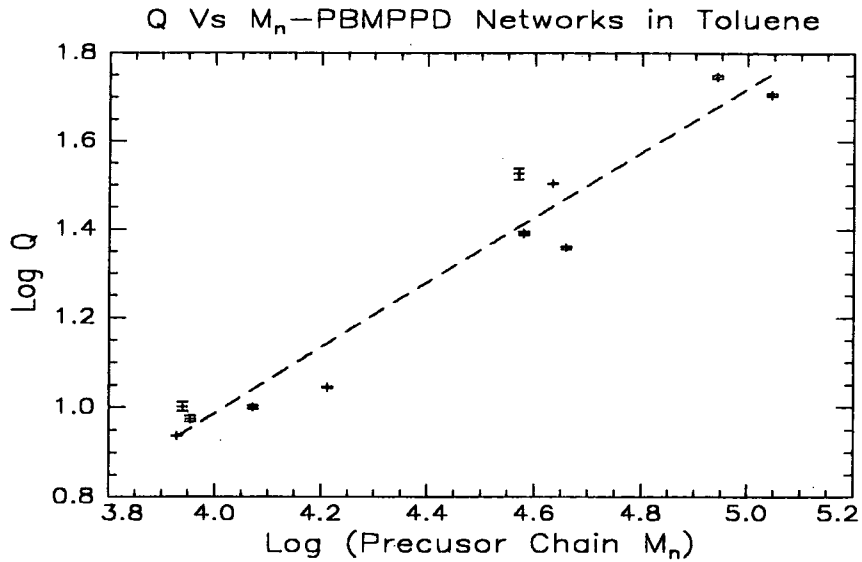


Figure 2.18.: Equilibrium swelling of PBMPPD series networks in toluene at 298K.

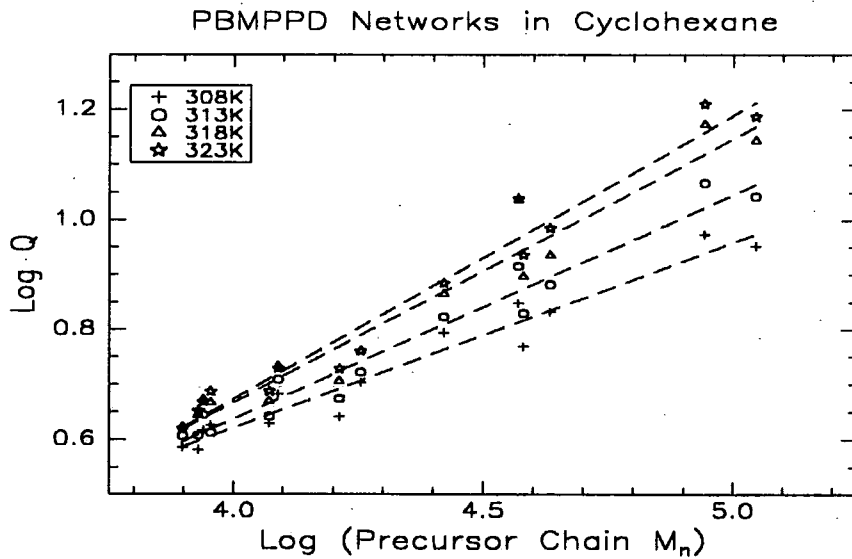


Figure 2.19.: Equilibrium swelling of PBMPPD networks in cyclohexane

Figures 2.18. and 2.19. have both been plotted in double logarithmic format, showing that the equilibrium swelling ratio of the gels follow the scaling arguments of de Gennes²⁰, which predicts that Q scales as $N^{0.8}$ for gels swollen in good solvents. Using similar arguments scaling theory predicts that Q is proportional to $N^{0.5}$ for a theta system.

For networks in toluene the following relationship was observed.

$$\text{Log}(Q) = (-1.95 \pm 0.26) + (0.74 \pm 0.06) \text{Log}(M_n)$$

While in cyclohexane:

$$308\text{K}: \text{Log}(Q) = (-0.73 \pm 0.09) + (0.34 \pm 0.02) \text{Log}(M_n)$$

$$313\text{K}: \text{Log}(Q) = (-0.99 \pm 0.10) + (0.41 \pm 0.02) \text{Log}(M_n)$$

$$318\text{K}: \text{Log}(Q) = (-1.28 \pm 0.15) + (0.48 \pm 0.03) \text{Log}(M_n)$$

$$323\text{K}: \text{Log}(Q) = (-1.39 \pm 0.12) + (0.52 \pm 0.03) \text{Log}(M_n)$$

As can be seen Q was found to scale with the precursor chain M_n for networks swollen in cyclohexane over the entire temperature range studied, the magnitude of the scaling exponent being found to increase with the solvent quality of the system. The determined scaling exponent for gels swollen in cyclohexane at the theta temperature was however found to be lower than that predicted by theory. In all cases the scaling exponent was considerably lower than that found for gels swollen in toluene, where the determined value of the scaling exponent was found to correlate well with that predicted by theory. The equilibrium swelling of networks prepared from the AMS/DVB system was also investigated in toluene at 298K and in cyclohexane at 308K, 313K, 318K and 323K. Unlike the results obtained from the PBMPPD/DVB system, the swelling of the gels was found not to scale with the precursor chain molecular weight, -see figures 2.20. and 2.21. below.

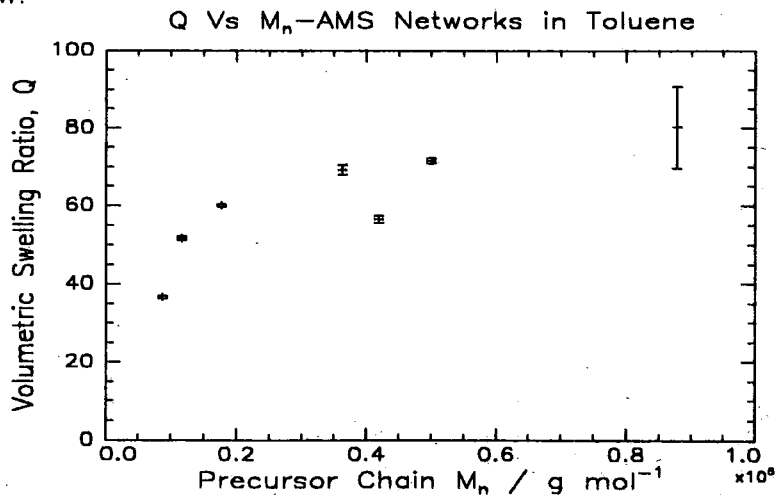


Figure 2.20.: Equilibrium Swelling of AMS/DVB networks in toluene at 298K

Again, the swelling of networks in cyclohexane was found to increase with the solvent quality of the system, though here the degree of swelling was found to be much higher than that obtained than that for networks prepared from the PBMPPD/DVB system under the same conditions.

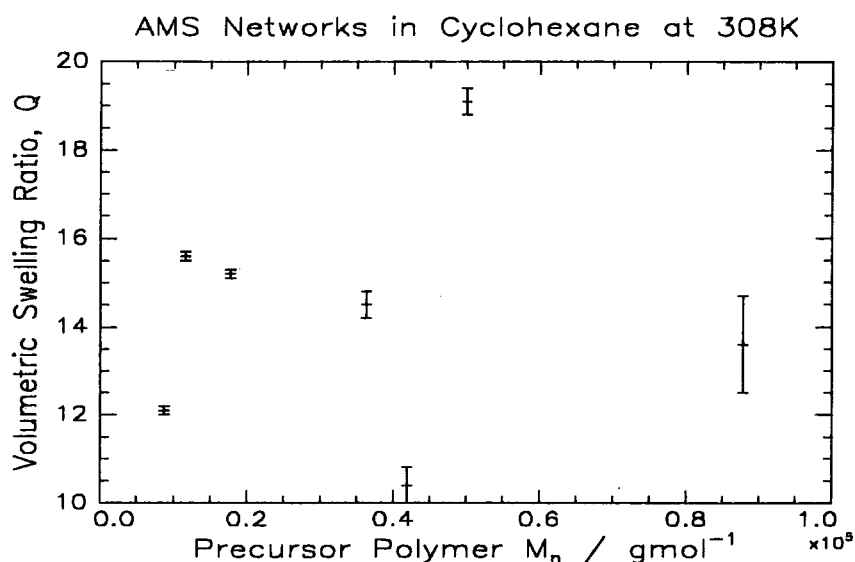


Figure 2.21.: Equilibrium Swelling of AMS/DVB Networks in Cyclohexane at 308K

The higher degree of swelling and the lack of scaling behaviour shown by the AMS/DVB series of networks has been attributed to the large amounts of uncross linked polymeric material (table 2.8.) which is extracted from the networks prior to the swelling measurements. As some of the precursor polymer is not incorporated into the network at cross linking, the volume fraction of polymer in the system will be lower and hence the volumetric swelling ratio higher. Since the amount of extracted material appears to be independent of the precursor chain molecular weight, the swelling behaviour of the AMS/DVB networks does not seem to reflect the cross link density in terms of the precursor chain molecular weight as might be expected for a model network.

5.3.4. Determination of Molecular Weight from Swelling Measurements.

Although the Flory-Rehner model has been used to determine M_c of polystyrene networks in cyclohexane and toluene²³, it has been found here that the results obtained

from the model are highly dependent upon the value of χ used as the interaction parameter in the model. Figure 2.22. shows a generalised plot of the Flory-Rehner model using various values for χ .

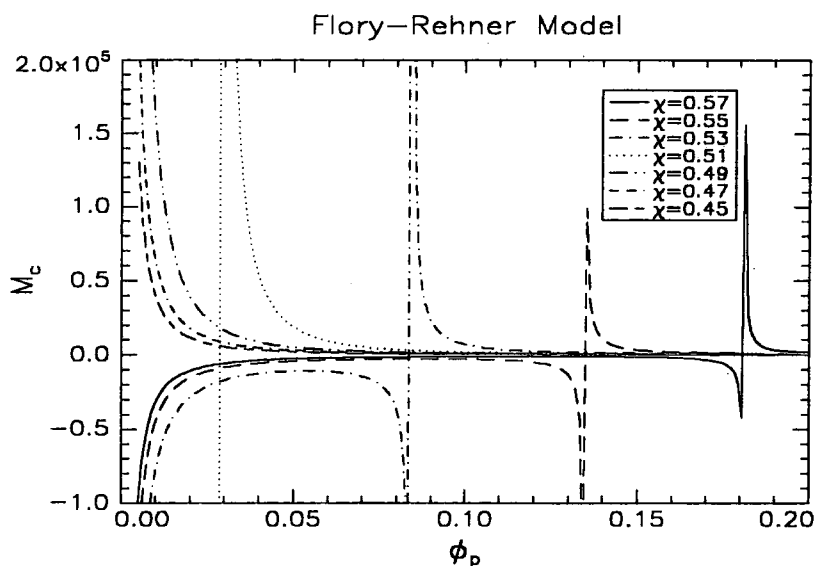


Figure 2.22.: General Flory-Rehner function for various χ values

As can be seen, values of χ greater than 0.5 produce a function with a discontinuity in the region of ϕ_p between 0.05 and 0.2. Below the discontinuity, the function is invalid and leads to negative values for M_c , hence the condition must be applied to the function that M_c should be positive and therefore the model used for sufficiently high values of ϕ_p above the discontinuity. Decreasing the value of χ can be seen to shift the invalid region to lower volume fractions, such that at values of χ less than 0.49, the invalid region only extends upto $\phi_p \sim 0.005$, which is much below the range of volume fractions under consideration here.

Values of χ for polystyrene in cyclohexane as quoted in the literature^{19,24,25} are quite limited and are found to vary considerably with the source, while literature values of χ for polystyrene in toluene are consistent and believed to be more reliable^{19,24}. Therefore M_c has only been evaluated here for polystyrene networks swollen to equilibrium in toluene where χ is substantially lower than 0.5 (0.42).

The Flory-Rehner equation as discussed above was originally derived for the case of networks cross linked in the bulk state such as vulcanised rubbers and as such is not applicable to the case of model networks prepared by end linking in solution since the presence of solvent increases the separation of the cross links within the network structure and thus the contour length of the chain and M_c will be increased by dilution prior to cross linking. However, a modified version of the Flory-Rehner equation has been derived by Rotstein and Lodge²² for the generalised case of networks cross linked in the presence of low molecular weight solvents and it is this version, equation 2.7. which has been used to determine the cross link density from swelling measurements.

$$M_c = \bar{V}_s c_0 \left(\frac{V_o}{V_d} \right)^{1/3} \left[\frac{-\left(\phi^{1/3} - \frac{\phi}{2} \right)}{\ln(1-\phi) + \phi + \chi\phi^2} \right] \quad 2.6.$$

Where V_s is the molar volume of solvent

c_0 is the polymer concentration at cross linking

V_o is the volume of the system at cross linking

V_d is the volume of the dry network

and ϕ is the equilibrium volume fraction of polymer in the swollen gel

However,

$$c_0 = \frac{m_d}{V_o}, \quad \mathbf{A} \quad \text{where } m_d \text{ is the mass of polymer}$$

$$\text{and } V_d = \frac{m_d}{\rho_b} \quad \mathbf{B} \quad \text{where } \rho_b \text{ is the density of the dry network}$$

By substituting **A** and **B** into equation 2.6., equation 2.7. is obtained.

$$M_c = \bar{V}_s c_0 \left(\frac{\rho_b}{c_0} \right)^{1/3} \left[\frac{-\left(\phi^{1/3} - \frac{\phi}{2} \right)}{\ln(1-\phi) + \phi + \chi\phi^2} \right] \quad 2.7.$$

The cross link densities of both the AMS/DVB and PBMPPD/DVB series of networks were determined from the equilibrium swelling ratio of gels swollen in toluene at 298K and is shown below in table 2.9 along with the weight average molecular weight of the precursor chain.

Network	Precursor Chain M_w	Swelling M_c
DLB 1	17,800	11,100
DLB 2	53,000	45,400
DLB 3	102,800	51,100
DLB 4	10,600	8,000
TCH 1	10,100	9,200
TCH 2	44,500	52,200
TCH 3	112,00	228,000
TCH 4	9,800	6,700
TCH 5	44,100	92,400
TCH 6	171,700	194,000
TCH 7	20,200	9,000
TCH 8	56,200	84,400
TCH 9	129,000	66,100
AMS 4	109,900	430,000
AMS 5	48,700	233,000
AMS 6	10,400	108,000
AMS 7	20,100	259,000
AMS 11	37,900	332,000
AMS 16	53,600	353,000
AMS 19	12,700	199,000

As can be seen in table 2.9., the large degree of swelling exhibited by all of the AMS/DVB networks is reflected in the high M_c 's determined from the Flory-Rehner model, from which it can be seen that the precursor chain molecular weight does not influence the cross link density of the network produced. However networks prepared from the PBMPPD initiator, which after cross linking show only a small amount of extractable polymer, have cross link densities which are in good agreement with the SEC analysis of the precursor chain molecular weight. Generally the molecular weight obtained from the swelling measurements is slightly lower than that from the SEC measurements, indicating that

there are very few chains within the network which do not contribute to the elastic properties of the network, i.e. the number of pendant chains within the network is limited. Taking these results in conjunction with the sol fraction measurements, it can be seen that the PBMPPD/DVB system produces networks which meet the main criteria for model networks, in that polymer chains are quantitatively end linked into a network structure containing very few defects.

6. Conclusions.

Two series of model polymer networks have been prepared by anionic polymerisation of styrene using a difunctional initiator and divinylbenzene as the cross linking agent. The series of networks prepared using the PBMPPD initiator have been found to contain relatively small amounts of extractable material and the networks produced found to swell upon addition of suitable solvent in the manner as predicted by scaling arguments. The series of networks produced from the AMS initiator have however been found to have relatively poorer properties, due to incomplete incorporation of the precursor polymer in the cross linking reaction, where a large amount of material has subsequently been *washed out* of the networks with a consequent effect upon the swelling ratio of the network. For these reasons, networks prepared from the AMS/DVB system were unsuitable for the study of trapped chain molecules as it would be impossible to differentiate between the properties of the sol fraction of the network and those chains introduced as trapped chains within the network.

7. References.

1. Herz J.E., Rempp P., Borchard W, Adv. Poly. Sci., 26, 105, (1978)
2. Flory P.J., *Principles of Polymer Chemistry*, Cornell University Press, Ithaca, N.Y., 1953
3. Cowie J.M.G., *Polymers: Chemistry and Physics of Modern Materials*, Blackie, London, 1991
4. Morton M., *Anionic Polymerisation: Principles and Practice*, Academic Press, New York, 1983
5. Morton M. and Fetters L.J., Macromol. Revs., 2, (1967)
6. Morton M. and Fetters L.J., Rubber Chem. and Technol., 48, 359,
7. Wegner F., Macromol. Chemie., 64, 151, (1963)
8. Morton M. and Milkovich R., J. Polym. Sci. A., 1, 443, (1963)
9. Lee C.L., Smid J. and Szwarc M., J. Phys. Chem. 66, 904, (1962)
10. Richards D.H. and Williams R.L. J. Polym. Sci. Poly. Chem., 11, 89, (1973)
11. Tung L.H. and Lo G.Y.S. Macromolecules, 27, 2219, (1994)
12. Nugay T. and Kucukyavuz S., Polymer International, 29, 195, (1992)
13. Quirk R. P. and Ma J.J. , Polymer International, 24, 197, (1991)
14. Tung L.H., Lo G.Y.S. and Beyer D.E. U.S. Pat. 4-172190 (1979)
15. Herz J. Hert M. and Strazielle C., Makromol. Chem, 160, 213, (1972)
16. Wiley R.H., Jin J. and Kamath Y., J. Polym. Sci. A-1, 6, 1065, (1968)
17. Weiss P., Herz J., Hild G., and Rempp P., Makromol. Chem, 135, 249, (1970)
18. Sarazin D., Herz J.E. and Francois J., Polymer, 23, 1317, (1982)
19. Orwoll R.A., Rubber Chem. and Technol., 50, 451
20. deGennes P.G., *Scaling Concepts in Polymer Physics*, Cornell University Press, Ithaca, N.Y., 1979
21. Flory P.J. and Rehner J., J. Chem. Phys., 11, 521, (1943)
22. Rotstein N.A. and Lodge T. P., Macromolecules, 25, 1316, (1992)
23. Davidson N.S., PhD Thesis, University of Strathclyde, (1984)
24. Brandrup J. and Immergut E.H., *Polymer Handbook*, Wiley, New York, 1989
25. Krigbaum W.R. and Geymer D.O., J. Amer. Chem. Soc., 6, 1063, (1970)

CHAPTER 3

SMALL ANGLE NEUTRON SCATTERING.

1. Introduction.

The scattering of neutrons by condensed matter is broadly analogous to the more conventional scattering techniques of X-ray and light scattering in that all three methods offer the possibility of probing the structure of matter at the atomic/molecular level. However, certain properties of the neutron mean that the scattering of neutrons can provide unique information in the study of condensed matter¹⁻⁴.

1. The absorption of neutrons is generally low and thus large sample volumes can be studied.
2. The wavelength of thermal neutrons (2-20 Å) is appropriate to the study of atomic and macromolecular dimensions.
3. The magnetic moment of the neutron may interact with any unpaired electrons to provide information on the magnetic structure of matter.
4. The interaction of the neutron and nucleus does not vary in a systematic manner within the periodic table, the interaction is an isotopic property and as such can be dramatically changed by isotopic substitution.

Interaction of the neutron with matter can occur in one of two ways⁵. Interaction with any unpaired electrons gives rise to magnetic scattering while most importantly, interaction with the nucleus can occur giving rise to nuclear scattering. Similarly to the scattering of electromagnetic radiation, energy can be exchanged between the sample and the neutron giving rise to inelastic scattering arising from transitions between quantised vibrational or rotational energy levels or if the energy of the neutron is unchanged the scattering process is said to be elastic and the static structural properties of the sample can be determined. If there is a small change in the energy of the neutron, the scattering is termed quasi-elastic and reflects a broadening of the elastically scattered peak and is due to diffusive motion of the scattering centres. Although both quasi-elastic and inelastic scattering have been applied to the study of

polymeric systems, by far the most frequently applied and useful technique has been due to elastic scattering of the neutron.

There is however one inherent difficulty in all neutron scattering experiments. The generation of a suitable flux of neutrons is by no means an easy or cheap task and generally requires the use of either a nuclear reactor or a synchrotron spallation source for a continuous or pulsed beam of neutrons respectively. These are both extremely expensive and require centralised funding, hence the demand for experimental 'beam' time is usually high and thus the amount of time allocated to an experiment is limited.

As with any scattering experiment, the most important variable is the modulus of the scattering vector \bar{Q} ¹⁻⁶, which is defined (equation 3.1.) as the resultant between the vector for the incident radiation \bar{k}_i and the scattered radiation \bar{k}_s .

$$Q = |\bar{Q}| = |\bar{k}_s - \bar{k}_i| = \frac{4\pi n}{\lambda} \text{Sin}\left(\frac{\theta}{2}\right) \quad 3.1.$$

Where $|\bar{Q}|$ is the modulus of the scattering vector,

λ is the neutron wavelength (Å),

n is the refractive index, taken to be 1 in a neutron scattering experiment,

and θ is the angle between \bar{k}_i and \bar{k}_s , as shown below in figure 3.1.

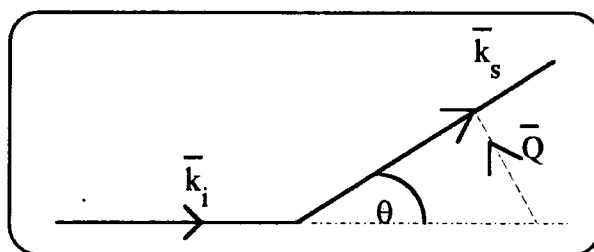


Figure 3.1.: Vector representation of the scattering geometry.

The intensity of radiation scattered by systems with *large* dimensions (such as polymers) takes the form of a small peak at low values of Q . Low values of Q are generally obtained at small angles in the forward direction and with incident radiation

having a long wavelength. This technique for probing long range spatial correlation's is known as Small Angle Neutron Scattering.

Here Small Angle Neutron Scattering has been used to determine the correlation length of a series of polymer networks having various cross link densities, as well as determining the static properties of a dilute solution of polymer chains trapped within a polymer network.

2. Theoretical Aspects of SANS

In any neutron scattering experiment (shown schematically in figure 3.2.) an incident neutron, wave vector \vec{k}_i is incident upon a target and is scattering by the target such that the wave vector of the scattered neutron is \vec{k}_s and the transfer of momentum to the target is $\hbar \vec{Q}$

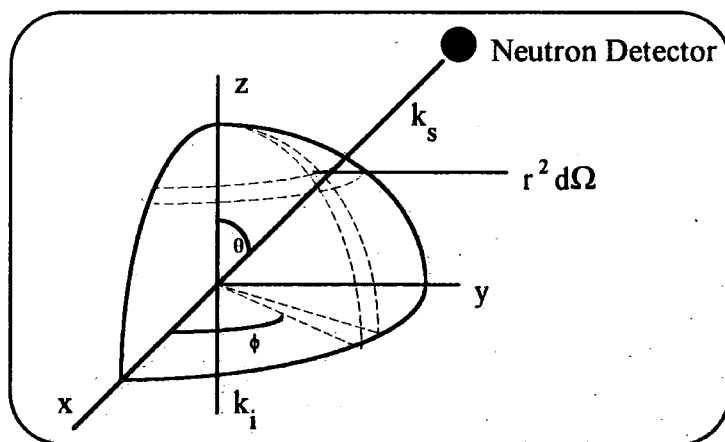


Figure 3.2.: Scattering geometry for a neutron scattering experiment.

The quantity measured in any scattering experiment is the partial differential scattering cross-section, denoted by 3.2., which describes the fraction of neutrons (of incident energy E) scattered into a solid angle $d\Omega$ (equal to $\sin\theta d\theta d\phi$), with a change in energy between E' and $E + dE'$.

$$\frac{d^2\sigma}{d\Omega dE'}$$

3.2.

For elastic scattering, no energy is transferred between the target and the incident neutron and equation 3.2 reduces to the differential scattering cross-section ($d\sigma/d\Omega$). If the flux of incident neutrons is I_0 then the flux scattered into a detector located at an element $d\Omega$ is given by:

$$I_0 \left(\frac{d\sigma}{d\Omega} \right) d\Omega \quad 3.3.$$

An expression for the differential cross-section can be calculated from quantum mechanical arguments. The probability of scattering a neutron of wave vector \bar{k}_i to a wave vector \bar{k}_s (both of energy $\hbar^2 k^2/2m$) is given by Fermi's golden rule, 3.4.

$$W_{k_i \rightarrow k_s} = \frac{2\pi}{\hbar} \left| \int d\bar{r} \bar{\Psi}_{\bar{k}_s}^* \hat{V} \bar{\Psi}_{\bar{k}_i} \right|^2 \rho_{\bar{k}_s}(E) \quad 3.4.$$

Where \hat{V} is the interaction potential associated with the transition

$\bar{\Psi}_{\bar{k}_n}$ is the Hamiltonian operator associated with the n^{th} wave,

and $\rho_{\bar{k}_s}(E)$ is the density of the final scattering states and is given by 3.5.

$$\rho_{\bar{k}_s} = \left(\frac{L}{2\pi} \right)^3 \frac{mk}{\hbar^2} d\Omega \quad 3.5.$$

Where L^3 is the volume of the target,

m is the mass of the neutron,

and k is the magnitude of the wave vector of the neutron

The flux of incident neutrons is given by the number passing the target per second (the velocity) per unit area, given by 3.6. and the cross-section is therefore given by 3.7.

$$I(0) = \frac{\hbar k}{mL^3} \quad 3.6.$$

$$d\sigma = \frac{W_{k_i \rightarrow k_s}}{I(0)} = \frac{\frac{2\pi}{\hbar} \left| \int d\bar{r} \bar{\Psi}_{\bar{k}_s}^* \hat{V} \bar{\Psi}_{\bar{k}_i} \right|^2 \frac{L^3 mk}{(2\pi)^3 \hbar^2} d\Omega}{\frac{\hbar k}{mL^3}} \quad 3.7.$$

Using the notation,

$$\left(\frac{L^3 m}{2\pi\hbar^2}\right)^2 \int d\bar{r} \Psi_{\bar{k}_i} \hat{V} \Psi_{\bar{k}_i} = \langle \bar{k}_s | \hat{V} | \bar{k}_i \rangle \quad 3.8.$$

Then equation 3.7. can be rewritten as 3.9.

$$\frac{d\sigma}{d\Omega} = \left| \langle \bar{k}_s | \hat{V} | \bar{k}_i \rangle \right|^2 \quad 3.9.$$

Scattering depends upon the nature of the neutron-nucleus interaction, the form of which is unknown although experimental results show that it is a short range interaction⁵. As the interaction is much shorter range (10^{-13} m) than the wavelength of the incident neutron, the scattering contains only an S-wave component and is therefore isotropic and characterised by a single parameter-the scattering length b . The only model of the interaction potential which gives rise to isotropic scattering is the Fermi-pseudo potential and for the interaction between a neutron and a single nucleus this is given by equation 3.10.

$$\hat{V}(r) = \frac{2\pi\hbar^2}{m} b \delta(\bar{r} - \bar{R}) \quad 3.10.$$

Where \bar{R} is the position of the nucleus and is usually taken to be the origin ($\bar{R}=0$).

Combining 3.8. and 3.10. and setting \bar{R} to zero

$$\langle \bar{k}_s | \hat{V} | \bar{k}_i \rangle = \left(\frac{m}{2\pi\hbar^2}\right) \frac{2\pi\hbar^2}{m} b \int d\bar{r} \exp(-i\bar{k}_s \cdot \bar{r}) \delta(\bar{r}) \exp(i\bar{k}_i \cdot \bar{r}) = b \quad 3.11.$$

Which gives:

$$\frac{d\sigma}{d\Omega} = |b|^2$$

And hence the total scattering cross-section as

$$\sigma = 4\pi |b|^2$$

If the same potential is applied for a rigidly fixed array of N nuclei the potential has the form⁵:

$$\hat{V}(\vec{r}) = \frac{2\pi\hbar^2}{m} \sum_i b_i \delta(\vec{r} - \vec{R}_i) \quad 3.12.$$

Where \vec{R}_i is the position of the i^{th} nucleus of scattering length b_i .

Therefore, substituting 3.12. into 3.8., equation 3.13. is obtained

$$\langle \vec{k}_s | \hat{V} | \vec{k}_i \rangle = \sum_i b_i \exp(i\vec{k} \cdot \vec{R}_i) \quad 3.13.$$

For elastic scattering from a rigidly bound array of nuclei (with nuclei at positions defined by i and j), the differential scattering cross-section is given by:

$$\frac{d\sigma}{d\Omega} = \sum_{ij} \exp[i\vec{k} \cdot (\vec{R}_i - \vec{R}_j)] \overline{b_i * b_j} \quad 3.14.$$

The values of b_i and b_j depend upon the isotope and its spin at positions i and j and the quantity $\overline{b_i * b_j}$ is the average over random nuclear spin orientations and random isotope distributions.

$$\text{For } i \neq j \quad \overline{b_i b_j} = \overline{b_i} \overline{b_j} = |\overline{b}|^2$$

$$\text{For } i = j \quad \overline{b_i b_j} = \overline{|b|^2}$$

$$\text{Therefore } \overline{b_i b_j} = |\overline{b}|^2 + \left[\overline{|b|^2} - |\overline{b}|^2 \right] \quad 3.15$$

Substituting 3.15. into 3.14. the differential scattering cross-section can be written as the sum of two components-equation 3.16.

$$\frac{d\sigma}{d\Omega} = \left(\frac{d\sigma}{d\Omega} \right)_{coh} + \left(\frac{d\sigma}{d\Omega} \right)_{incoh} \quad 3.16.$$

Where the coherent scattering cross-section is given by:

$$\left(\frac{d\sigma}{d\Omega}\right)_{coh} = |\bar{b}|^2 \left| \sum_l \exp(i\bar{k} \cdot \bar{R}_l) \right|^2 \quad 3.17.$$

and the incoherent scattering cross-section is given by:

$$\left(\frac{d\sigma}{d\Omega}\right)_{incoh} = N \left[|\bar{b}|^2 - |\bar{b}|^2 \right] = N |\bar{b} - \bar{b}|^2 \quad 3.18.$$

These two contributions to the differential scattering cross-section are greatly different⁵. Incoherent scattering is isotropic, having no phase term and hence no dependence upon Q. The coherent scattering term contains all the structural information about the scattering species, describing the interference effects between waves scattered from different nuclei in the target. Both the coherent and the incoherent differential scattering cross-sections are dependent upon the scattering lengths of the nuclei present in the target, which describe the interaction of the neutron with the sample, tables of scattering lengths for many isotopes are available in the literature⁵.

The total scattering cross-section σ is given by 3.19.

$$\sigma = 4\pi |\bar{b}|^2 \quad 3.19.$$

While the coherent scattering cross-section is given by:

$$\sigma_c = 4\pi |\bar{b}|^2 \quad 3.20.$$

The incoherent cross-section is therefore given by

$$\sigma - \sigma_c = \sigma_i \quad 3.21.$$

Equations 3.16., 3.17., and 3.18. form the basis of elastic neutron scattering theory and when applied to scattering from a pure material, either crystalline or a liquid predicts that coherent scattering is only observed when strict geometric conditions are

obeyed, thus giving rise to Bragg peaks for crystalline materials and structure factors for liquids⁵. However, in small angle scattering, it is the diffuse scattering around the direct beam which is measured. This arises from the variation of the scattering length density over distances which exceed the normal inter atomic spacing of condensed matter and as such is ideal for the study of small particles, macromolecules and molecular aggregates.

The coherent scattering from a dilute solution (such that intermolecular interference between coherent scattering from particles is absent due to the large intermolecular distances) of a macromolecule in a solvent is given by equation 3.17.. The sum in equation 3.17. can be separated into contributions arising from the solvent and the macromolecule-equation 3.22.

$$\frac{d\sigma}{d\Omega} = \left[\left[\rho_s \int \exp(i\bar{k} \cdot \bar{R}) d\bar{R} - \int_V \exp(i\bar{k} \cdot \bar{R}) d\bar{R} \right] + \rho(\bar{R}) \int_V \exp(i\bar{k} \cdot \bar{R}) d\bar{R} \right]^2 \quad 3.22.$$

Where ρ_s is the scattering length density of the solvent (the scattering length averaged over the solvent molecular volume),

and $\rho(\bar{R})$ is the scattering length density of the macromolecule.

The first term in equation 3.22. is an integral over the entire scattering volume and approximates to a δ function which is zero for all values of Q except zero. Therefore equation 3.22. can be rewritten as:

$$\frac{d\sigma}{d\Omega} = \left| \int_V [\rho(\bar{R}) - \rho_s] \exp(i\bar{k} \cdot \bar{R}) d\bar{R} \right|^2 \quad 3.23.$$

Assuming that each segment acts as a point scatterer, $\rho(\bar{R})$ can be averaged over the segment volume to give a scattering length density ρ_p , hence 3.23. can be rewritten as equation 3.24.

$$\frac{d\sigma}{d\Omega} = \left| V(\rho_p - \rho_s) \frac{1}{V} \int \exp(i\bar{k} \cdot \bar{R}) d\bar{R} \right|^2 \quad 3.24.$$

This can itself be rewritten as equation 3.25.

$$\frac{d\sigma}{d\Omega} = V^2 (\rho_p - \rho_s)^2 P(Q) \quad 3.25.$$

$$\text{Where } \frac{1}{V} \int \exp(i\bar{k} \cdot \bar{R}) = P(Q) \quad 3.26.$$

and $(\rho_p - \rho_s)$ is the contrast factor.

$P(Q)$ is referred to as the particle form factor and contains all the structural information of the conformation of the scattering particle^{6,7,8,11}. The contrast factor simply describes the ability of the neutron radiation to see the scattering species against a background.

The scattering length of a particular segment or molecule is simply the sum of the component scattering lengths over the n atoms in the molecule-equation 3.27.

$$b = \sum_{i=1}^n n_i b_i \quad 3.27.$$

The scattering length density is the scattering length of a segment or molecule per unit of molecular volume, given by 3.28. Tables of the scattering length densities for a range of polymers and solvents are available in the literature²².

$$\rho = \frac{N_A b}{vM} \quad 3.28.$$

Where N_A is Avogadro's Number,

\bar{M} is the (segment) molecular weight

and v is the partial specific volume

A more general equation for elastic scattering from macromolecules can be written so as to account for the possibility not only of intramolecular interference (as described by the particle form factor) but also intermolecular interference as would be seen in a non-dilute or interacting system. The coherent scattering is then described in terms of a structure factor which for an incompressible binary mixture can be written as:

$$\left(\frac{d\sigma}{d\Omega}\right)_{coh} = (b_1 - b_0)^2 S(Q) \quad 3.29.$$

Where b_1 and b_0 are the scattering lengths of species 1 and 0 respectively

$S(Q)$ is the structure factor (also known as the coherent scattering law) describing both the intramolecular and intermolecular interference effects and is given by equation 3.30.

$$S(Q) = Nz^2 P(Q) + N^2 z^2 Q(Q) \quad 3.30.$$

Where N is the number of scattering polymers molecules,

z is the number of segments in the polymer,

$P(Q)$ is the particle form factor,

and $Q(Q)$ is the normalised interference term describing the interaction of the scattering molecules and is given by equation 3.31.

$$Q(Q) = \frac{1}{z^2} \sum_{i=1}^z \sum_{j=2-1}^z \left\langle \exp(-i\bar{k} \cdot \overline{r_{ij}}) \right\rangle \quad 3.31.$$

Equation 3.30. is a general equation describing the coherent scattering from any macromolecular system. It can be shown that the particle form factor, $P(Q)$ can be extracted at any concentration of labelled species when the hydrogenous and deuterated components are identical (except for the difference in the scattering length density). However this is not generally the case as both the degree of polymerisation and the polydispersity of the hydrogenous and deuterated materials are usually different. In this case it is possible to extract the particle form factor for a low concentration of labelled

species where the concentration is such that the labelled molecules are spread randomly throughout the material and are dilute with respect to one another, therefore the probability of contacts and correlation's between labelled species is low. In this case equation 3.30 can be written as:

$$\left(\frac{d\sigma}{d\Omega}\right)_{coh} = (b_d - b_h)^2 z^2 NP(Q) \quad 3.32.$$

In the case of scattering arising from a single polymer in solution, equation 3.30. can be written as equation 3.29. which in the dilute solution limit reduces to the single chain scattering law.

The form of P(Q) is determined by the shape of the scattering particle, and a wide variety have been tabulated for particle shapes such as rods, discs, cylinders and spheres²³. In the limit as Q approaches zero, all forms of the particle form factor tend to one and within the range $0 < Q < R_g^{-1}$, the scattering from any polymer can be described by the Guinier approximation⁷ given below in equation 3.33.

$$\frac{d\sigma}{d\Omega}(Q) = \left(\frac{d\sigma}{d\Omega}\right)_{Q=0} \exp\left(\frac{-Q^2 R_g^2}{3}\right) \quad 3.33.$$

Therefore if a sufficiently small range of Q can be studied, the radius of gyration of the polymer can be determined.

A similar expression also valid in the Guinier Q region is that due to Zimm, more frequently seen in intensity light scattering²⁴ which not only allows the determination of the radius of gyration but also measurement of the polymer molecular weight given below in equation 3.34.

$$\frac{K^*c}{d\sigma_{d\Omega}(Q)} = \frac{1}{M} \left[1 + \frac{Q^2 R_g^2}{3} \right] + 2A_2c \quad 3.34.$$

The Gaussian coil model of a polymer chain can also be used to determine the polymer radius of gyration, following the model developed by Debye¹⁵, valid in the so called intermediate Q region ($R_g^{-1} < Q < b^{-1}$, where b is the statistical segment length) as well as the Guinier region, given by equation 3.35.

$$\frac{d\sigma}{d\Omega}(Q) = \left(\frac{d\sigma}{d\Omega}\right)_{Q=0} \frac{2}{Q^2 R_g^2} \left[\exp(-Q^2 R_g^2) + Q^2 R_g^2 - 1 \right] \quad 3.35.$$

The coherent scattering law for a semi-dilute solution or a swollen polymer gel can be written in terms of a pair correlation function describing the screening or correlation length of the semi-dilute solution/polymer gel^{11,25}. For distances less than ξ , the total pair correlation function is dominated by scattering from the chain containing the reference point, while at distances greater than ξ the segments of the reference chain will be uncorrelated as other polymer chains intervene. For regions where ($Q < \xi^{-1}$), the scattering can be described in terms of equation 3.36.

$$S(Q) = \frac{f(T, c)}{Q^2 + \xi^{-2}} \quad 3.36.$$

3. Instrumentation

As noted earlier, the use of small angle neutron scattering as a technique is reliant upon the production of a suitable flux of neutrons to be scattered from the target. There are two methods for producing a suitable flux, the most common being the use of a nuclear reactor, where neutrons are released by the fission of uranium-235 producing a continuous beam of neutrons⁶.

A second type of neutron source is the pulsed source where a short burst of neutrons is produced as a high energy proton beam impinges upon a target of heavy nuclei. Providing the kinetic energy of the proton beam is high enough to overcome the intrinsic short range nuclear and electrostatic repulsive forces, the nuclei of the target will be "blasted apart" in the spallation process.

3.1. The Small-Angle Spectrometer-LoQ.

Currently the most powerful spallation neutron source in the world is located at the ISIS facility at the Rutherford-Appleton Laboratory in Chilton, Oxfordshire. At ISIS an 800MeV proton synchrotron operating at 50Hz produces 200 μ A pulses of protons which are directed at a tantalum target where on impact around 25 neutrons per incident proton are released which are then passed down the various beam-lines surrounding the target station^{9,10}. The small angle spectrometer at ISIS is known as LoQ and it is this instrument which has been used for all the SANS work in the study.

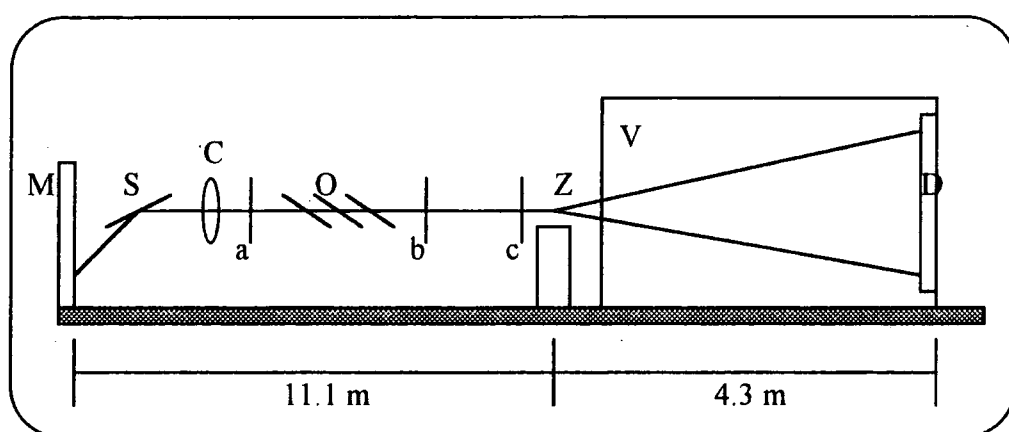


Figure 3.3.: Schematic Diagram of the LoQ spectrometer.

Figure 3.3. shows a schematic diagram of the LoQ spectrometer⁹. The primary flight path (the section before the sample stage) contains various devices to collimate the incident beam, which initially passes through a liquid hydrogen moderator (M) operating at 25K to reduce the velocity distribution of the as produced neutrons.

Neutrons are then incident upon a Soller bending mirror (S) which removes short wavelength ($<2\text{\AA}$) neutrons and prevents the detector viewing directly the target station thus reducing the background intensity, long wavelength neutrons ($>12\text{\AA}$) are removed by a frame overlap mirror (O). The neutron beam is collimated by three apertures (a, b and c) which produce a beam at the target with a diameter of 11mm. The disc chopper (C) operates at 25 Hz thus selecting alternate pulses from the target station, producing a neutron pulse with a wavelength range from 2 to 10 \AA .

Both the primary and the secondary flight paths are evacuated so as to reduce flux losses due to collisions between neutrons and air molecules. The secondary flight path is simply an evacuated vacuum tank (V) 4.3 metres in length placed immediately in front of the detector. Both the primary and secondary flight paths are heavily shielded by solid steel and borated wax to reduce the background flux of radiation.

Neutrons scattered by the sample fall into one of the $^3\text{He-CF}_4$ filled 1cm^2 pixels of the two dimensional area detector (D), the active region of which is 64cm by 64 cm. Together with the range of wavelengths available from the collimation system, the geometry of the instrument permits a Q range from 0.006\AA^{-1} to 0.22\AA^{-1} to be studied.

Samples were placed on a nine position, temperature controlled sample holder (\bar{Z}), the temperature of which was measured by a thermocouple mounted at the centre of the rack. For the temperatures studied here (308K to 313K), the rack temperature was found to vary sinusoidally by $\pm 1\text{K}$ over a period of around 3 minutes. The position of the rack was aligned using a laser beam co-linear with the incident neutron beam to ensure that the full sample volume was exposed to the flux of neutrons.

Data was collected in time of flight (ToF) mode, whereby the scattered intensity was measured as a function not only of θ and ϕ but also as a function of λ , which as described above influences the magnitude of the scattering vector. The raw ToF spectrum was corrected for this wavelength dependence and also for effects of transmission and sample thickness using the COLETTE¹² program at the Rutherford-Appleton Laboratory which converts the ToF spectrum into the more conventional picture of scattering cross-section in terms of Q.

3.2. Calibration of the Spectrometer.

Although the output from COLETTE is nominally in units of absolute intensity, a further calibration is required if accurate values of the radius of gyration, correlation length and particularly the polymer molecular weight are to be obtained. Calibration of a

SANS instrument using a monochromatic beam of neutrons is relatively straightforward as a sample of a flat isotropic scatterer is used to normalise the data for detector efficiency¹¹. The procedure normally used for this is to run a sample of water, however on a pulsed source this procedure is not applicable as the scattering cross-section is dependent upon the wavelength of the incident neutrons.

An alternative calibration procedure which can be used on a pulsed source is to measure the scattering from a polymer blend. Here the scattering from a 0.47 volume fraction blend of d-PS in h-PS was measured and then analysed in terms of de Gennes Random Phase Approximation (RPA)¹³. Two samples were run in order to determine the normalisation constant, a blend of d-PS and h-PS and also a random copolymer having the same composition as the blend which is used to measure the incoherent scattering of the blend. The coherent scattering cross-section for a two component blend can be given in terms of de Gennes incompressible Random Phase Approximation by equation 3.37.¹⁴

$$\frac{d\sigma}{d\Omega}(Q) = k_d v_0 \left(\frac{b_a}{v_a} - \frac{b_b}{v_b} \right)^2 \left(\frac{v_0}{\phi v_a N_a g_d(R_{ga}, Q)} + \frac{v_0}{(1-\phi)v_b N_b g_d(R_{gb}, Q)} - 2\chi \right)^{-1} \quad 3.37.$$

Where k_d is the normalisation constant

b_a and b_b are the scattering length's of the respective components

N_a and N_b are the degree's of polymerisation of both components

χ is the interaction parameter

v_0 is a reference volume given by equation 3.38.

and $g_d(R_g, Q)$ is the Debye function¹⁵ given by equation 3.39.

$$v_0 = \left(\frac{\phi}{v_a} + \frac{(1-\phi)}{v_b} \right)^{-1} \quad 3.38.$$

$$g_d(R_g, Q) = \left(\frac{2}{(Q^2 R_g^2)^2} \right) \left(\exp(-Q^2 R_g^2) + Q^2 R_g^2 - 1 \right) \quad 3.39.$$



The scattering of any blend can then be fitted to determine χ and the radii of gyration of the components. Conversely, from a knowledge of χ and polymer molecular weight, the normalisation constant can be determined.

The molecular weights of the polymers used here were determined by S.E.C. in tetrahydrofuran solution and values from these results have been used to determine the degree of polymerisation of the blend components. The scattering of the blend (after background subtraction) was then fitted to equation 3.37. using the FORTRAN program BANTAM¹⁶, allowing the normalisation constant and the radii of gyration of both the hydrogenous and deuterated components to vary, although the constraint $R_{g,h}=R_{g,d}$ was applied. Values of b_h and b_d used in the fitting procedure were 2.328×10^{-12} cm and 10.66×10^{-12} cm respectively, the reference volume was taken as 1.725×10^{-22} cm³, the average degree of polymerisation (for both h-PS and d-PS) was taken to be 800 and χ was fixed at zero. Values of the radii of gyration and k_n obtained from the fitting routine are given below in table 3.1., the value of k_n obtained being that which the model data is multiplied by in order to fit the data. To correct raw data obtained from COLETTE into absolute values of the differential scattering cross-section, the data is simply *divided* by k_n .

Experiment Date	$R_g/\text{\AA}$	k_n
October 1992	67.9	0.8145
December 1992	68.3	0.841
November 1993	68.9	0.839
March 1994	69.2	0.843

Table 3.1.: Values of the radii of gyration and normalisation constant fitted from the R.P.A.

All data was normalised using this procedure, however there are several sources of error which may lead to inaccuracies in the normalisation constant. Firstly some error may be present in the value of the average segmental volume used in the fitting routine, which is calculated from the densities of d-PS and h-PS given by Russell¹⁷. Values of the densities of both deuterated and hydrogenous polystyrene calculated by Davidson¹⁸ are in agreement with those quoted in Polymer Handbook¹⁹ and have been found to lead to a 4% difference in k_n .

The main source of error in the determination of k_n is likely to arise from the values used for the degree of polymerisation. As described above, the molecular weights of the polymers were evaluated by S.E.C. in THF solution, the results used to calculate the degrees of polymerisation being an average of several measurements. However, data was also obtained from S.E.C. in chloroform solution and was found to lead to somewhat lower values of the molecular weight and hence the degree of polymerisation. As the THF S.E.C. apparatus employed a double (both refractive index and viscosity) detection system rather than the single refractive index detector used in the chloroform machine, data from the THF system was relied upon to give a more accurate value of the polymer molecular weight. Data from the chloroform system was found to lead to a 20% increase in the fitted value of k_n .

The final source of error in the determination of k_n arises from the assumption that the interaction parameter between the hydrogenous and deuterated components is zero. Wignall²⁰ states that the effect of χ on the scattering of low molecular weight polymers is negligible, hence χ was initially set to zero. However values of χ for the d-PS/h-PS system have been given by Bates²¹ ($\sim 1.6-3.7 \times 10^{-4}$) which lead to values of k_n which are around 10% lower than that calculated where χ equalled zero. A detailed study of all of these effects has been performed, where it has been shown that the most important parameter in the determination of k_n is due to the uncertainty in the molecular weight of the components, this could of course be improved by determining the absolute molecular weight of the components by intensity light scattering.

4. Experimental

In all experiments on swollen gels, small samples of polystyrene networks cut from the network as prepared in chapter 3 were dried to constant weight, firstly in air for around 7 days and secondly under vacuum at 350K for 24 hours. The dried, bulk samples were then reswollen in the appropriate solvent. In the measurement of the correlation length of the 'blank' networks, the hydrogenous polystyrene networks were

reswollen to equilibrium in perdeuterated cyclohexane or toluene solvents obtained from Cambridge Isotope Laboratories, (99+% atom d).

In all measurements on swollen samples, it was assumed that there was no difference in the equilibrium swelling ratio of the networks when swollen in perdeuterated solvents as compared to the swelling ratios obtained using hydrogenous solvents (chapter 2, section 5.3.) Samples in toluene were allowed to reach swelling equilibrium over a period of 5 days while those in cyclohexane were allowed to reach swelling equilibrium at room temperature for 5 days before being equilibrated at 308K for 12 hours prior to study. Unfortunately, due to the lack of experimental time available it was not possible to allow 12 hours for equilibration of the gels as in the measurements detailed in chapter 2, it was only possible to allow 1 hour for equilibration of the cyclohexane swollen samples upon increasing the temperature of the gels. However, from the results of the swelling measurements described in chapter 2 it is thought that this will not have adversely affected the results of the experiment as in such cases only a short time was required to reach equilibrium on changing the temperature.

All samples were placed between two quartz discs (1mm thick) separated by a 2mm thick PTFE washer (inner diameter, 14mm) and were contained in a brass holder (inner diameter, 14mm). Samples were cut from the swollen gels so as to fit the sample volume defined by the inner volume of the spacer and were therefore in intimate contact with the quartz windows. The sample holder was then filled with an excess of solvent prior to scattering to allow for evaporation of the solvent during scattering runs at elevated temperatures.

Bulk samples of networks containing deuterated probe chains were dried to the bulk state as outlined in the above procedure and were then carefully cut to the shape of a circular disc around 13mm diameter with a thickness of approximately 1mm (measured accurately with a micrometer). The samples were then placed into the sample cell between two quartz windows separated by a 1mm spacer.

Solvent swollen samples of networks containing deuterated probe chains were prepared by swelling suitable samples of the bulk network dried following the procedure outlined above. Samples were swollen in both cyclohexane and toluene for SANS experiments and were allowed to equilibrate for a minimum of 5 days before study. It was again found that due to the lack of experimental time available, only one hour could be allowed for equilibration of the samples between temperature changes. Samples were again cut to the appropriate dimensions following the procedure outlined above.

The isotopic composition of the swelling solvent for the measurement of the probe chain size in the swollen gel was chosen such that the mean scattering length density of the solvent mixture was equal to the scattering length density of hydrogenous polystyrene, therefore no coherent scattering was observed from the network chains and coherent scattering was seen only from the deuterated probe chain. The mean scattering length density of the solvent mixture is given below in equation 3.40.¹⁸

$$\overline{\rho_s} = \phi\rho_{s,d} + (1-\phi)\rho_{s,h} \quad 3.40.$$

where $\overline{\rho_s}$ is the mean scattering length density

$\rho_{s,x}$ is the scattering length density of component x

and ϕ is the volume fraction of the deuterated component

In order to contrast match any scattering from the hydrogenous polystyrene of the network, a 0.268 mole fraction solution of C_6D_{12} in C_6H_{12} was prepared for measurements of the deuterated probe chain size in cyclohexane swollen networks, whilst any resultant scattering from hydrogenous polystyrene was eliminated by the use of a 0.099 mole fraction solution of C_7D_8 in C_7H_8 for networks swollen to equilibrium in toluene.

Polystyrene discs approximately 12 mm diameter and 1mm thick were required for use as calibrants for the SANS experiments. A suitable blend of the deuterated and hydrogenous polymers was prepared by dissolving the appropriate amounts of the

homopolymers in chloroform solution such that a 5% solution of polymer in solution resulted. The blend was then precipitated by pouring into a non-solvent, in this case chilled methanol and the precipitate filtered before being dried under vacuum at 330K for 2 days.

Discs of both the blend and copolymer were prepared by pressing the appropriate amounts of polymer in a heated press. The polymer was initially pressed under vacuum for a few minutes with an applied load of two tonnes, followed by removal of the vacuum and an increase in the die temperature to around 550K, where the temperature was held constant under the same applied load for around 1 hour. The die was then allowed to cool to ambient temperature (with no increase in the applied load) when the discs of polymer were removed from the die. The as prepared samples were found to be free from any macroscopic air bubbles and uniform in thickness, the thickness of the samples being determined by the average of 5 readings using a micrometer. The discs were then placed in the SANS cells described above between two 1mm thick quartz windows separated by a 1mm thick spacer.

5. Determination of the Correlation Length of Solvent Swollen Gels

In these experiments, information on the characteristic length scale (that where excluded volume interactions on a polymer chain are screened out by the presence of other polymer chains) the correlation length, of hydrogenous polystyrene networks swollen to equilibrium in deuterated solvents was obtained by measuring the coherent scattering from the network in the intermediate Q region and then fitting the data to the model proposed by Daoud²⁵. One of the main difficulties in these experiments was the extraction of the coherent scattering from the raw data by removal of the large incoherent background arising from the protons of the network. Mixtures of low molecular weight hydrogenous molecules in perdeuterated solvents were used to estimate this, where the hydrogenous material had a similar structure to the segmental units of the polymer chain. For measurements on networks swollen in d-cyclohexane, a series of mixtures of h-cyclohexane and d-cyclohexane varying in composition were

prepared, whilst for networks swollen in d-toluene mixtures of h-toluene and d-toluene were used to estimate the background level.

Scattering from the mixtures of the hydrogenous and deuterated solvents was found to be flat over the range of scattering vector used, the scattering from a 1mm path length cell filled with the solvent mixture being measured at 308K for cyclohexane solutions and at 298K in toluene. A mean value of the incoherent background was then determined from the SANS spectrum using a linear fitting procedure with the GENPLOT³⁸ program. The incoherent background was found to vary in a linear manner over the composition range studied.

A total of five solutions of hydrogenous and deuterated cyclohexane were prepared, the relative ratio's of hydrogenous to deuterated components being chosen following the swelling measurements described in chapter 2. The solvent mixture with the most similar composition to the swollen gel was chosen as the background for the sample and was subtracted from the spectrum of the gel while accounting for both sample thickness and transmission. The corrected data was then normalised to values of absolute scattering following the procedure outlined above.

Previous SANS studies on swollen polymer networks have also been directed upon the determination of the correlation length of the polymer network. Randomly cross linked polystyrene networks have been studied by Davidson¹⁸ who found that the correlation length as determined by SANS scaled with the volume fraction of polymer in a manner predicted by de Gennes scaling theories¹³. Studies on model networks prepared by end linking methods have however proved more difficult.

Both Bastide^{26,27} and Mendes²⁸ have studied end linked polystyrene networks produced in thermodynamically good solvents and have reported that no measure of the correlation length could be made due to anomalous scattering at low values of Q . Mendes reports that the scattering from end linked polystyrene networks at swelling

equilibrium in toluene is dominated by a shoulder region at intermediate Q values followed by a strong increase in the scattered intensity at low Q values around 10^{-2} \AA^{-1} .

Although the polystyrene networks studied here were prepared by a very similar method to both those used by Bastide and Mendes, no evidence of any anomalous scattering was found in the Small Angle Scattering studied here, though it is noted that the Q range explored here using the LoQ instrument ($0.01\text{-}0.22 \text{ \AA}^{-1}$) is somewhat different to that probed by both Mendes and Bastide ($0.003\text{-}0.25 \text{ \AA}^{-1}$) who used the D11 and D17 diffractometers at the ILL in Grenoble.

Corrected data from the measurement of the total correlation function can be seen below in figure 3.4. the errors of which are propagated from those quoted by the COLETTE program which arise from Poisson counting statistics. Whilst almost all of the gels studied here exhibited an upturn in the scattered intensity at low Q values, these data points were neglected as the statistical uncertainty in those data points was rather high due to the radial averaging of the scattered intensity (collected on a square detector) carried out by the COLETTE program.

As described earlier, the correlation length is extracted from the coherent scattering law in the intermediate Q region, following equation 3.35. ξ is determined from the ratio of the slope to intercept of a plot of reciprocal intensity versus Q^2 . Figure 3.5. below shows this plot of the reciprocal scattering intensity against the square of the scattering vector, the errors of which have been propagated from the Poisson counting statistics produced by COLETTE.

At high values of the scattering vector a relatively large error in the reciprocal intensity is found. This is most probably due to a slight error in the subtraction of the large incoherent scattering background from the original plot of scattering intensity against Q which although small in the conventional picture of scattering intensity against Q is somewhat larger in the Zimm plot.

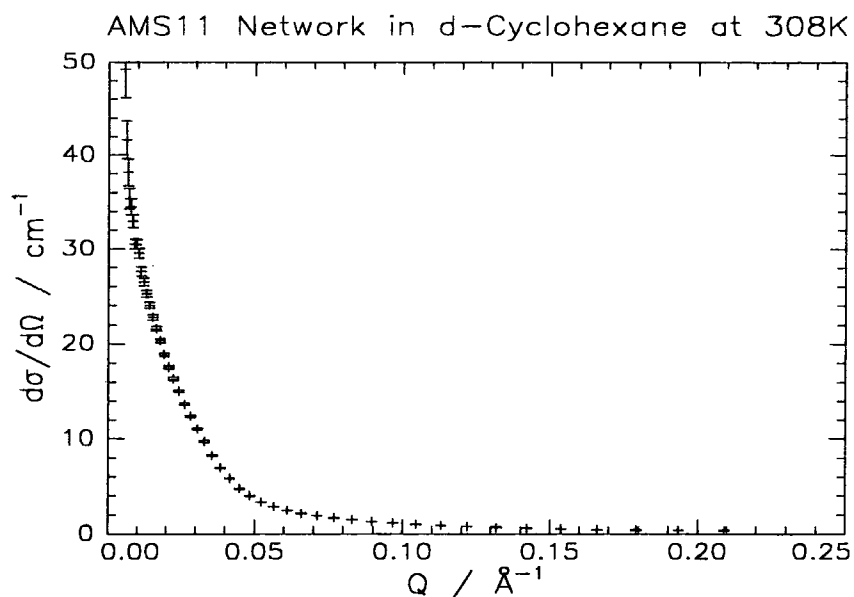


**Figure 3.4.: Corrected Scattering from AMS 11 Network
swollen in d-Cyclohexane at 308K.**

Figure 3.5. shows one such Zimm plot in the intermediate and high Q region for a network swollen to equilibrium in cyclohexane at 308K. At higher scattering vectors there is a departure from the linear behaviour observed in the intermediate region as the scattering vectors probe length scales smaller than the correlation length, where the structure of the polymer chain is subject to excluded volume interactions.

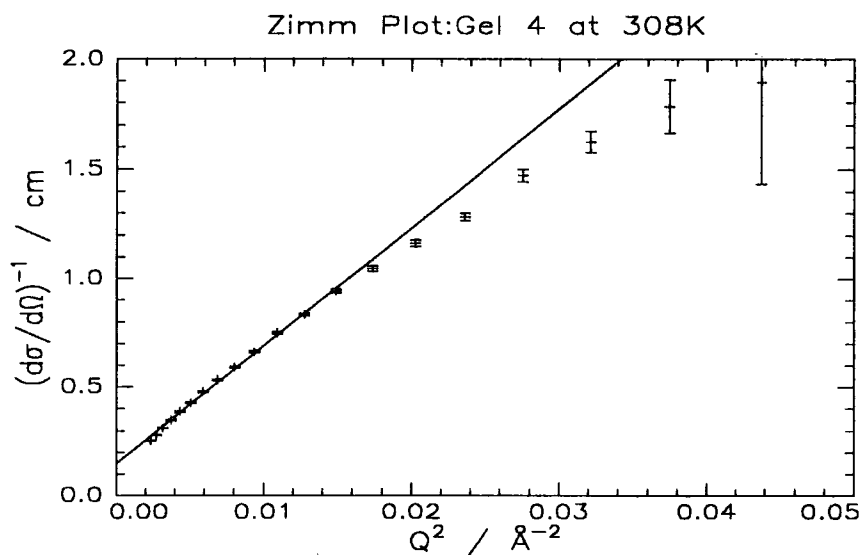


Figure 3.5.: Zimm Plot of Data and Fit in the Intermediate Q Region

Values of ξ determined from the Zimm plots are given below in table 3.2. along with the error in ξ arising from the errors in the slope and intercept of the best-fit line to the data. Table 3.2. correlates ξ with the precursor chain molecular weight, which in principle determines the polymer volume fraction of the network to which ξ is related through a scaling law.

Correlation length of Swollen Networks \pm Error (\AA)										
Precursor Chain M_w	Cyclohexane 308 K		Cyclohexane 313 K		Cyclohexane 318 K		Cyclohexane 323 K		Toluene 298 K	
	10,400	23.7	4.3	23.0	5.2	20.8	4.7	15.0	1.4	10.2
12,700	27.9	6.3	25.8	4.7	23.6	4.8	20.6	4.0	10.8	0.8
20,100	17.9	1.8	15.5	2.2	16.6	1.2	16.4	1.4	12.5	0.7
37,900	15.9	1.4	15.8	1.8	14.9	1.7	14.6	0.8	12.3	1.0
48,700	26.7	3.3	24.2	2.9	23.2	2.3	22.2	2.2	10.6	0.7
53,600	22.9	2.7	23.6	1.8	20.5	2.3	19.9	1.7	12.7	1.2
109,900	20.4	1.0	18.1	0.9	17.3	0.7	16.6	0.7	10.5	0.8

Table 3.2.: Variation of the Correlation Length of Swollen Gels

Three features are immediately noticeable from this data. Firstly, under constant thermodynamic conditions in either cyclohexane or toluene, the correlation length is found to be constant within the margins of error of the experiment, ξ is not found to scale with either the volume fraction or the precursor chain molecular weight.

Secondly although under constant thermodynamic conditions the correlation length is constant, increasing the solvent quality causes a decrease in the correlation length. Increasing the solvent quality causes two opposing effects in a decrease the polymer volume fraction and an increase in the degree of excluded volume in the system. A decrease in the polymer concentration might be expected to result in an increase in the correlation length of the network while increasing the solvent quality would be expected to cause a decrease in the correlation length as the chains expand in the better quality solvent. The net effect observed here is a decrease in the correlation length of the network.

Finally, it can be seen that for networks swollen to equilibrium in toluene, corresponding to the limit of excluded volume interactions, the correlation length is constant at $11 \pm 1 \text{ \AA}$. This value for the correlation length is quite small and indicates an inter chain distance of the order of a few repeat units.

The results of table 3.2 are shown graphically in figures 3.6 a-e where the measured values of ξ are again correlated against the precursor chain molecular weight, the least squares fit to the data being included as the solid line through the data.

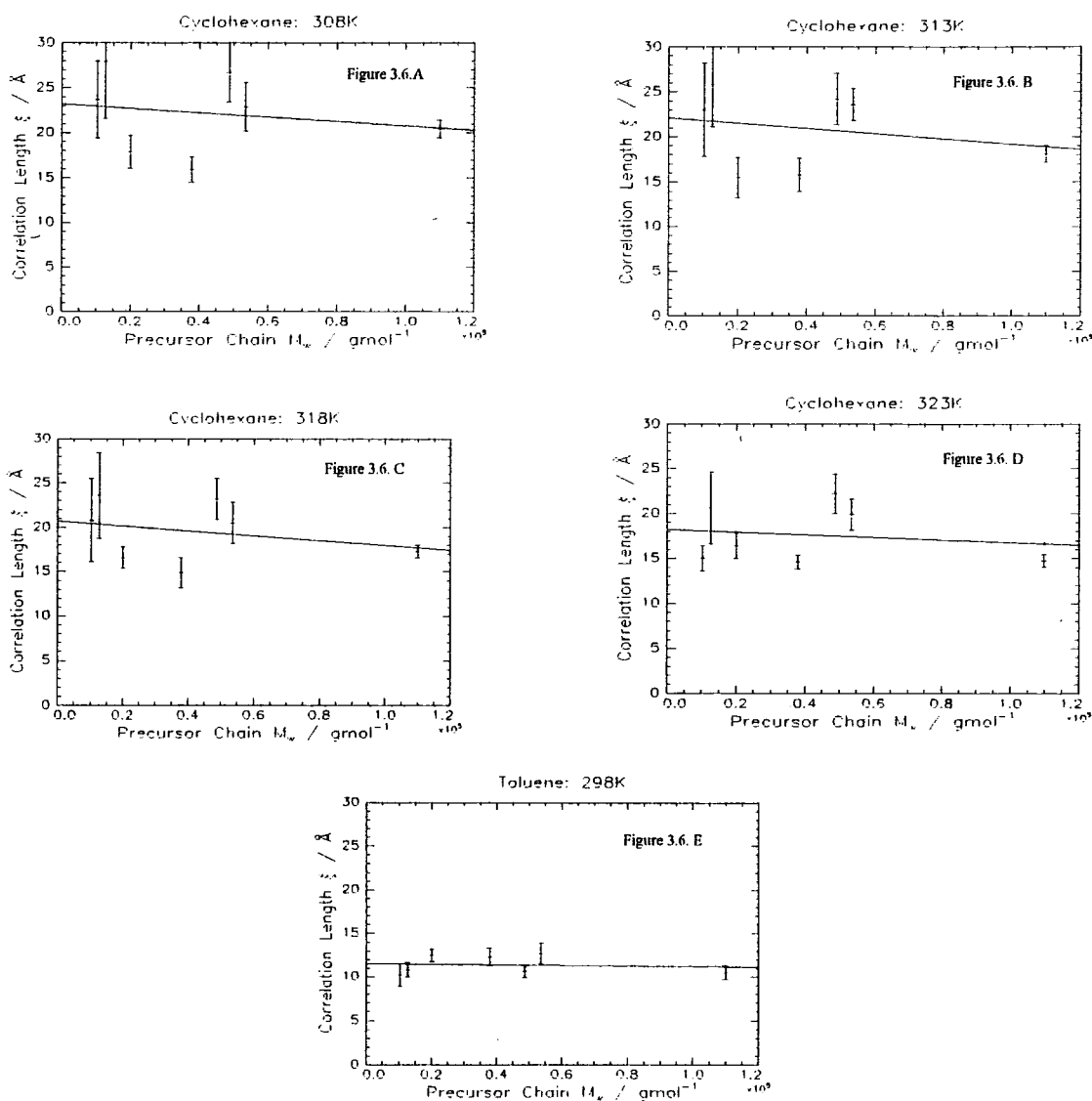


Figure 3.6 a-e: Correlation Length of Networks as Determined by SANS Against Precursor Chain Molecular Weight for all Polymer-Solvent Conditions.

The most noticeable feature of figure 3.6 is the lack of scaling behaviour obtained between the correlation length and the precursor chain molecular weight, similar behaviour being found between the correlation length and the polymer volume fraction in the swollen network. This is in direct contrast to the results of the measurement of the correlation length in randomly cross linked networks where scaling behaviour was observed¹⁸. Hence the density-density correlation length would appear to only be dependent upon the quality of the solvent and hence the degree of excluded volume present in the system.

The lack of any dependence of ξ in the precursor chain molecular weight becomes clarified when it is recalled that the correlation length of a semi-dilute solution, describing temporary inter chain contacts, is dependent only upon the concentration of the solution (as the inter chain contacts occur frequently along the chain backbone, not on the molecular weight of the chain) and is not influenced by the chain molecular weight as the length of the chain is much greater than the separation of the chain contacts¹³.

Here, all networks were prepared under essentially the same conditions (i.e. at the point of cross linking a 10% w/v solution of polystyrene in benzene). It would seem reasonable that the correlation length of the highly expanded chains (just prior to gelation, i.e. a semi-dilute solution) is constant and describes the separation of temporary chain entanglements along the polymer backbone. Therefore in the end linking step the introduction of the cross linking agent to the solution causes the ends of the polymer chains to become tied into the network structure therefore preventing the temporary chain entanglements of the former semi-dilute solution from disentangling and thus 'freezing' the correlation length of the semi-dilute solution into the network structure.

Changes in the correlation length after cross linking reflect only a change in the solvent quality of the system. For a semi-dilute solution at the theta point, such as polystyrene in cyclohexane at 308K, the polymer chains are Gaussian in nature with no excluded volume present. Upon increasing the temperature of the cyclohexane system,

the semi-dilute chains develop excluded volume interactions and expand, causing the intermolecular separation of the chains to decrease and therefore the mesh size and ξ to decrease.

Evidence for this hypothesis arises from the values of the correlation length for a series of semi-dilute solutions determined by other authors. King²⁹ has measured the correlation length for polystyrene in toluene as a function of concentration in the range ($0.02 < c < 0.22 \text{ gml}^{-1}$). As predicted by scaling theory, ξ was found to decrease with the polymer concentration in the system, however more importantly, the correlation length of a 0.12 gml^{-1} solution of polystyrene in toluene was reported to be 13.3 \AA .

Similar results for the correlation length of polystyrene in toluene have been reported by Brown³⁰, who again found that the correlation length of a 0.1 gml^{-1} solution of polystyrene in toluene was 15.1 \AA at room temperature. The correlation length of polystyrene in benzene has also been measured by Cotton³¹ who found for a 0.08 gml^{-1} concentration solution the correlation length was 14 \AA . Since all networks were synthesised in benzene solution, both toluene and benzene are thermodynamically good solvents for polystyrene and therefore the measured values of the correlation length in both solutions should be equal as is indicated by the experimental data available.

The correlation length of polystyrene in cyclohexane has also been investigated as a function of polymer concentration and temperature. For a fixed concentration, the correlation length of polystyrene in cyclohexane has been found to decrease with increasing temperature as the excluded volume interactions increase in a manner predicted by scaling theory³².

A comprehensive study of the correlation length of semi-dilute solutions of polystyrene in cyclohexane has been carried out by Cotton³³ who not only confirms the results of Davidson³², but also shows that ξ for polystyrene in cyclohexane is again dependent upon the polymer concentration. For a 0.082 gml^{-1} solution of polymer, ξ is

reported to be 66Å at 308K decreasing to 45Å at 323K. These values for ξ in solution are somewhat higher than those measured for gels here under the same conditions, a difference which is attributed to the presence of the cross links in the gel which prevent full relaxation of the chains into the structure found in a semi-dilute solution.

It was noted in chapter 2 (section 5.2.) that a large sol fraction was extracted from the AMS/DVB networks prior to the measurement of the correlation length of the solvent swollen networks. While in some cases this sol fraction was up to 25% of the mass of the network, it seems apparent that the correlation length of the network does not proportionately increase with any extracted material.

This is due in the main to the fact that those chains cross linked into the network are end linked in the presence of chains which do not participate in the cross linking reaction and therefore the semi-dilute correlation length is still constant and does not differentiate between living chains to be cross linked and dead chains which go to form the sol fraction.

After cross linking, the same number of chain entanglements are present upon those chains cross linked into the network structure, the process of extracting the sol fraction not affecting the number of chain entanglements. Hence after cross linking and sol fraction extraction the correlation length is still dependent upon concentration of polymer at cross linking.

6. Determination of the Radius of Gyration of a Trapped Probe Chain.

In this series of experiments, the size of a polystyrene probe chain immersed inside a model polystyrene network was determined in order to ascertain the dependence of the probe chain size on the cross link density of the network. To facilitate this, the coherent scattering of a perdeuterated polystyrene chain *trapped* inside a hydrogenous network was measured and the radius of gyration of the probe chain analysed in terms of equations 3.33., 3.34. and 3.35.

As described earlier in chapter 1 the size of a probe chain in a random medium is given by equation 3.41.

$$\frac{\langle r^2 \rangle}{\langle r^2 \rangle_{\theta}} = \frac{6.5}{N\rho_0^2} \left[1 - \exp\left(\frac{-6.5}{N\rho_0^2}\right) \right] \quad 3.41.$$

Where $\langle r^2 \rangle$ and $\langle r^2 \rangle_{\theta}$ are the mean square end to end distances of the polymer chain in the random medium and in the unperturbed (θ) state respectively,

N is the number of segments in the probe chain

and ρ_0 is the mean obstacle density.

Equation 3.41. predicts a decrease in the probe chain size with increasing obstacle density of the medium. However there is no direct measure of the density of the fixed obstacles, though for a network the obstacle density can be replaced by the cross link density of the network which itself is inversely proportional to the molecular weight between cross links. As the mean square end to end distance of the polymer chain is experimentally difficult to quantify and is related to the radius of gyration, it is the measurable R_g of the polymer chain which is determined and related to the molecular weight between cross links of the network.

Although it was shown in chapter 2 that for PBMPPD/DVB networks the swelling M_c correlates well with the precursor chain molecular weight from S.E.C. measurements, it is the directly determined value of the M_c (S.E.C..) rather than the model dependent value (swelling measurements) that the radii of gyration are correlated against.

The size of the probe chain has been studied in two series of experiments. Firstly, the radius of gyration has been determined for networks dried to the bulk state, where equation 3.41. is theoretically most applicable. Secondly, the size of the probe chain has been measured for networks swollen to equilibrium in cyclohexane and

toluene. In principle, the probe chain experiences the same interactions when the network is swollen to the theta point in cyclohexane at 308K. By increasing the temperature above the theta temperature, the effects of any excluded volume interactions upon the probe chain size can be studied.

A series of six polymer networks containing the perdeuterated PSD2 polymer as the probe chain were prepared in order to determine any size changes of the probe polymer, of which only five were studied by SANS. The molecular weights between cross links of these networks are given below in table 3.3.

Network	$M_c / (\text{gmol}^{-1})$
TCD 1	42,500
TCD 2	26,400
TCD 5	18,000
TCD 4	12,300
TCD 6	7,900

Table 3.3.: Molecular Weight Characteristics of Networks Containing the PSD2 Probe Polymer

The molecular weight of the PSD2 probe polymer has also been determined by S.E.C. and M_w has been found to be $26,000 \text{ gmol}^{-1}$. Theta dimensions for this sample are predicted to be 44\AA^2 .

6.1. Initial Experiments on the Probe Chain Size.

It was initially intended to study the perdeuterated polystyrene polymer PSD1, trapped inside a series of hydrogenous networks prepared from the AMS/DVB system in the dry and solvent swollen states. A series of networks were prepared for this study (AMSD1-AMSD5) containing 5% by mass of the probe polymer. These were studied by SANS and the coherent scattering determined by removal of an incoherent background arising from the protons of the hydrogenous material. However, the scattering from the probe polymer was found to be particularly weak and the probe chain size was only evaluated in the dry state as the probe concentration was too low in the swollen samples to allow a determination of the radius of gyration.

The low degree of scattering from these samples has been attributed to the conditions used to prepare the AMS/DVB samples. Networks prepared from the AMS/DVB system were deswollen by solvent exchange with cyclohexane. This procedure, whilst deswelling the network, was found (rather unexpectedly) to extract not only the sol fraction of the network but also to wash the trapped chain out of the network. The resulting concentration of the probe polymer was estimated to be approximately 1-1.5% in the dried samples from the amount of extracted material and the relative peak areas of the probe polymer and the sol fraction from S.E.C. measurements.

However, an estimation of the probe chain R_g for the dried samples was possible by fitting the scattering in the intermediate region to the Debye function (equation 3.35.), the R_g being found to increase with the cross link density of the network as shown below in table 3.4. Theta Dimensions for the PSD1 probe polymer are expected to be 52Å.

Network	M_c/gmol^{-1}	$R_g \pm \text{Error} / \text{Å}$
AMSD1	8,900	106 ± 25
AMSD4	25,200	49 ± 14
AMSD5	45,800	52 ± 10

Table 3.4.: R_g Measurements of the Probe PSD1 Trapped in AMS/DVB Networks.

6.2. Probe Chain Size Measured in the 'Bulk' State Using Probe Polymer PSD2.

The coherent scattering of the perdeuterated probe chain was extracted from the scattered intensity by removal of an incoherent background arising from the protons of the hydrogenous polystyrene in the network. The concentration of the probe chain was determined at synthesis and was set for all networks to be 10% of the total polymer mass.

Hence an incoherent background (corrected for the volume fraction of the hydrogenous polymer) was removed before conversion of the corrected data to units of absolute scattering as described above. A typical corrected data set is shown below in

figure 3.7., the errors of which again arise from Poisson counting statistics produced by the COLETTE program.

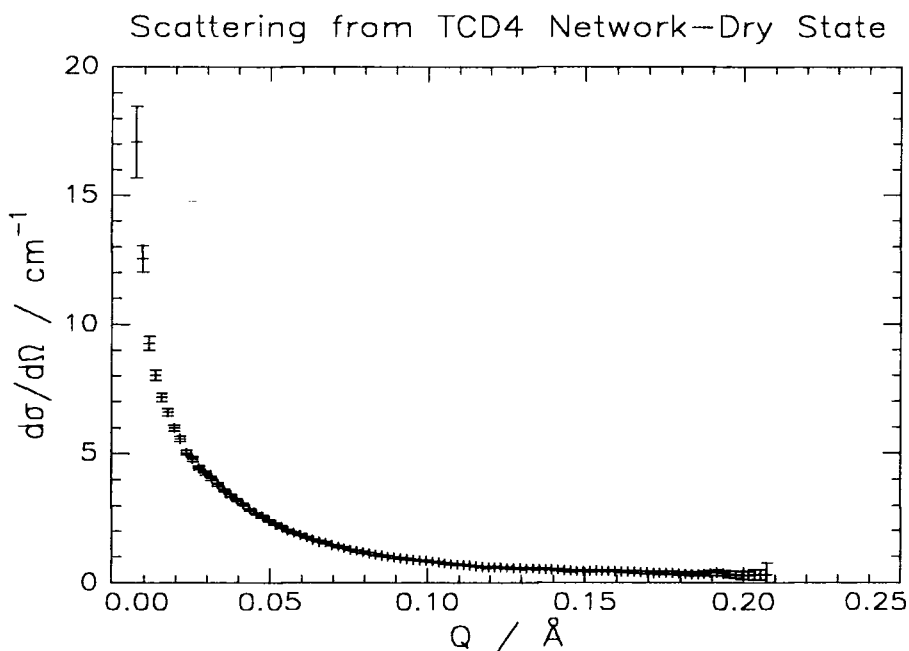


Figure 3.7.: Corrected Small Angle Scattering from Probe Chains Trapped in Polymer Network

The radius of gyration was determined using three methods. In the Guinier region, (where $Q < R_g^{-1}$) the R_g is evaluated from both the Guinier approximation (equation 3.33) and the Zimm expression (equation 3.34). The Zimm expression has also been used to determine the molecular weight of the probe chain from the scattered intensity extrapolated to zero scattering vector.

In the intermediate Q region ($R_g^{-1} < Q < b^{-1}$) the scattering of the polymer can be modelled as a Gaussian coil and the Debye equation (3.35) can be used to determine the radius of gyration of the probe chain. Figure 3.8 shows a representative data set in the Guinier representation used to determine the polymer chain size. In the Guinier approximation, R_g is determined from the slope of a plot of $\ln(Q)$ versus Q^2 , whilst in the Zimm expression the R_g is determined from the ratio of the slope to intercept in a plot of $I^{-1}(Q)$ versus Q^2 .

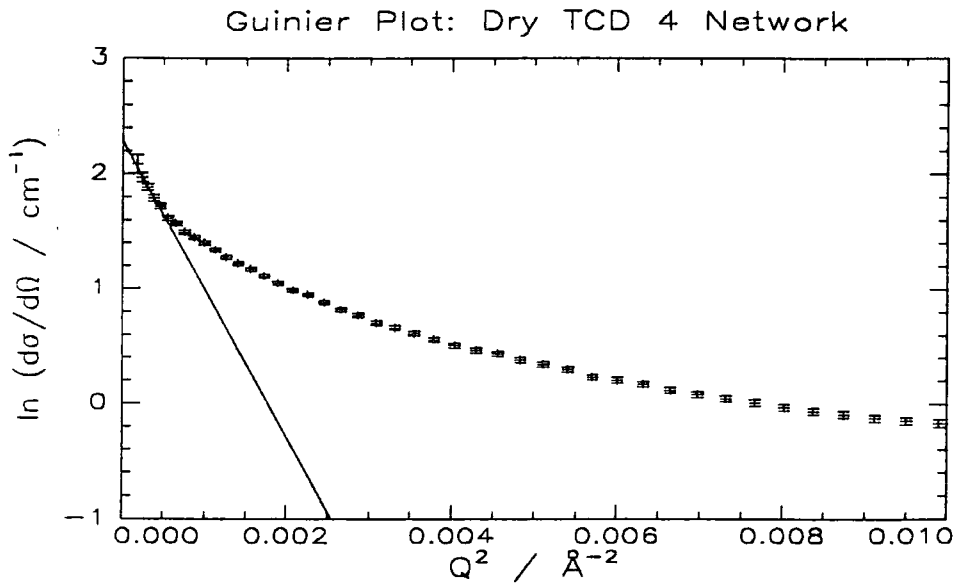


Figure 3.8.: Guinier Plot used to Determine the Radius of Gyration of the Probe Chain

The Zimm expression has also been used to determine the molecular weight of the polymer chain from the intensity at zero scattering vector³⁴ following equations 3.42. and 3.43.

$$\frac{K^*c}{d\sigma/d\Omega(Q)} = \frac{1}{M_w} \left(1 + \frac{Q^2 R_g^2}{3} \right) + 2A_2c \quad 3.42.$$

$$K^* = \frac{N_a \Delta b^2}{m_d^2} \quad 3.43.$$

Where m_d is the segment molecular weight of the deuterated polymer

N_a is Avogadro's number

and $\Delta b = (b_d - b_h)$ is the scattering contrast factor between deuterated and hydrogenous polymers.

By substituting 3.43 into 3.42 and neglecting the final term in the limit of $Q=0$ the polymer molecular weight can be obtained from equation 3.44.

$$\frac{1}{M_w} = \frac{cN_a \Delta b^2}{m_d^2 \left(d\sigma/d\Omega \right)_{Q=0}} \quad 3.44.$$

For data fitted at a single concentration a correction needs to be used for R_g to replicate the result of a full Zimm plot where the concentration is extrapolated to zero. This correction requires a value for A_2 and is given by equation 3.45.

$$(R_g)_{True} = (R_g)_{Meas} (1 + 2A_2M_w c) \quad 3.45.$$

Since in any scattering experiment, it is the z-average R_g that is measured, a correction is employed to relate this to the weight average radius of gyration^{18,35} given by equation 3.46.

$$R_{g,z} = R_{g,w} \left[\frac{(x+2)}{(x+1)} \right]^{0.5} \quad 3.46.$$

Where $x = \frac{1}{(PD-1)}$

The radius of gyration has also been determined by fitting the corrected coherent scattering to the Debye function (equation 3.35.) in the Zimm and intermediate Q regimes ($0 \leq Q(\text{\AA}^{-1}) \leq 0.12$). using the GENPLOT software package³⁸. A typical fit to the data is shown below in figure 3.9.

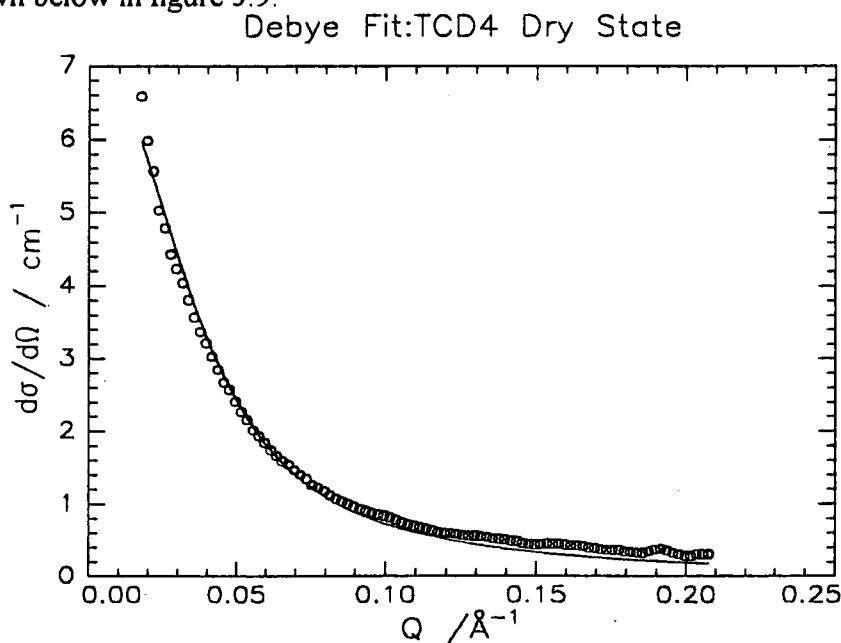


Figure 3.9.: Gaussian Fit to Corrected Scattering Data from the Debye Equation in the Intermediate Q Region.

Figure 3.10. shows the Zimm plots determined from the coherent scattering of the probe chain from which it can be seen that networks with higher cross link densities show an increase in the slope of the Zimm plot, resulting from an increase in the size of the probe chain. Values of the probe chain radius of gyration determined from the Guinier and Zimm approximations as well as from fitting the scattered intensity to the Debye function are shown below in table 3.5. along with the probe chain molecular weight determined by extrapolating the fitted Debye function to zero scattering vector.

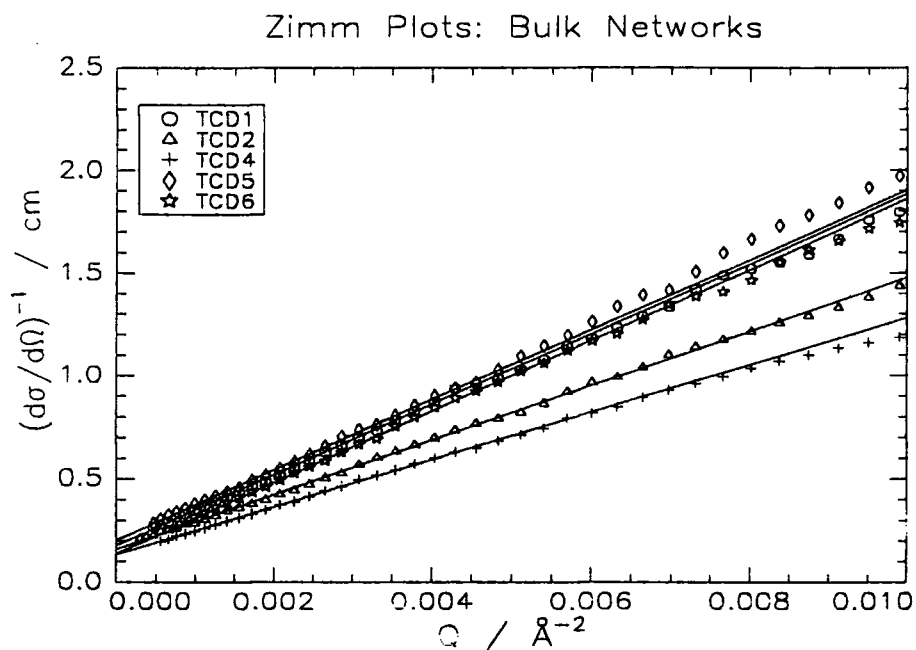


Figure 3.10.: Zimm Plots and Fits to Corrected Data from Dry Networks

Values of the radii of gyration quoted in table 3.5., determined from all methods have been corrected by equation 3.46. No correction was made for the data fitted from a single concentration to the Zimm equation using equation 3.45 as it was assumed, following the work of Cotton³⁹ that the second virial coefficient was zero for the deuterated probe chain trapped within the hydrogenous matrix. Values of the scattering lengths of PS-H and PS-D used to determine the contrast factor and hence the molecular weight of the deuterated polymer in equation 3.44. were taken from reference 11.

Polymer Network	Cross link Density- M_c	Probe Chain Size- $R_g \pm \text{Error} / \text{\AA}$			Molecular Weight-Probe
		Guinier	Zimm	Debye	
PSD2-PSH18	21,800*	39 ± 2	44 ± 2	38 ± 1	$14,900 \pm 300$
TCD 1	61,800	38 ± 3	48 ± 1	40 ± 1	$13,300 \pm 100$
TCD 2	30,600	38 ± 2	45 ± 2	39 ± 1	$15,500 \pm 100$
TCD 5	21,600	40 ± 4	50 ± 1	41 ± 1	$12,600 \pm 100$
TCD 4	14,300	46 ± 3	48 ± 3	45 ± 2	$18,400 \pm 300$
TCD 6	9,400	56 ± 3	61 ± 1	51 ± 1	$17,000 \pm 500$

Table 3.5.: Radii of Gyration and Probe Chain Molecular Weight for Dry Network Samples Containing PSD2 Probe Polymer.

***N.B. M_c Refers To The Molecular Weight Of The Matrix Polymer**

As seen in table 3.5., the molecular weight of the probe chain trapped within networks and in the uncross linked bulk state determined by S.A.N.S. is found to be consistent with the molecular weight of the probe polymer determined directly by the S.E.C. measurements detailed in chapter 2. From the result of the PSD2-PSH18 sample (probe polymer in an uncross linked matrix-note the term cross link density refers to the molecular weight of the matrix polymer), it is seen that the presence of the cross links within the networks does not cause any aggregation of the probe chains and the measured value of the radius of gyration determined corresponds reasonably well to the size of a single probe polymer chain.

Although table 4.5 shows broad agreement between the determined values of the radii of gyration from all three methods of analysis, it is the results from the fit to the Debye equation which are given more credence as the number of data points within the Guinier region (in the available Q range of the machine) are limited for a probe polymer having a radius of gyration around 50Å. However there are considerably more data points available in the intermediate Q region on the LoQ instrument and therefore results from the Debye fit are believed to be more reliable. Results from the Debye fit are shown below in figure 4.11. together with the associated errors arising from the fit to the data.

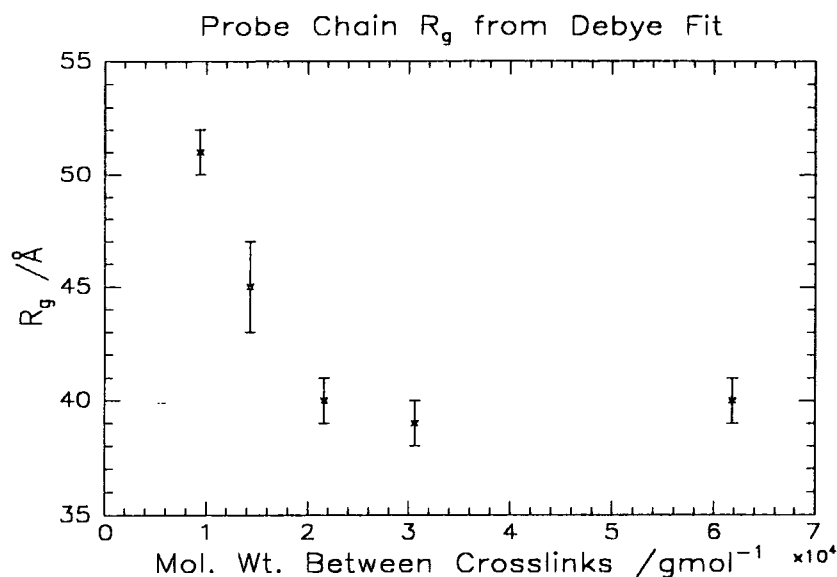


Figure 3.11.: Values of the Radius of Gyration Determined from the Debye Fit to Corrected Data.

Two distinct regions of behaviour can be seen in figure 3.11. At low cross link densities corresponding to a molecular weight between cross links higher than a critical value of M_c around $20,000 \text{ gmol}^{-1}$ the size of the probe chain is found to be given by the theta dimensions of the polymer-between 39 and 40\AA . The unperturbed Gaussian chain dimensions of the PSD2 probe chain have been measured in the bulk state in sample PSD2-PSH18 where the R_g of the probe polymer in an uncross linked matrix polymer ($M_w=22,000$) have been found to be 38\AA by fitting the scattered intensity to the Debye equation. Therefore it can be seen that in low cross link density networks the probe chains are not aggregated and the dimensions of the bulk probe chains are consistent with the assumption that the probe polymers adopt an unperturbed Gaussian conformation more frequently seen in the dimensions of polymers in the uncross linked bulk state where unperturbed Gaussian conformations have been observed for bulk samples of poly(styrene)³⁹, poly(methyl methacrylate)⁴⁰ and poly(ethylene)⁴¹.

However for networks where the M_c is lower than this critical cross link density, the radius of gyration of the probe polymer is found to increase with cross link density in a manner not predicted by the Edwards/Vilgis theories^{36,37} which suggest a decrease in the probe chain size with decreasing molecular weight between cross links. For the most

highly cross linked sample investigated here (network TCD 6- M_c 9,400 g mol⁻¹) the radius of gyration of the trapped chain has been found to be increased by more than 30% of the unperturbed dimensions of the probe chain.

The reason for the increase in the probe chain size is somewhat unclear. The molecular weight from the S.A.N.S. data indicates that the probe chains are not aggregated in any of the networks studied here and therefore the increase in size reflects direct increase in the size of the probe chains. Therefore, as the probe chains are not aggregated in high cross link density networks, it seems certain that the probe chain "expands" under the conditions of high cross link density, in a manner not explained by any current theoretical model. No reason for this behaviour can be advanced as none of the theoretical models currently available to describe the conformation of the chain consider the effect of cross links on the end-to-end distance and hence the radius of gyration of the probe chain. Clearly, the Edwards/Vilgis models do not provide an explanation of the behaviour of the chain within the polymer network and as such with only limited experimental evidence and no theoretical model, only limited conclusions regarding the behaviour of the probe chain within the bulk network can be drawn.

6.3. Probe Chain Size in Solvent Swollen Networks.

The size of a probe chain has been studied in networks swollen to equilibrium in both cyclohexane and toluene. Here the coherent scattering from the probe chain has been extracted from the SANS profile by removal of the "flat" background arising from the incoherent scattering of both the hydrogenous network polymer and the swelling solvent, the isotopic composition of the solvent being chosen such that the scattering length density of the solvent exactly matched that of the hydrogenous polystyrene, thus eliminating the coherent scattering of the hydrogenous polystyrene chains of the network.

The incoherent background removed from the measured SANS pattern was corrected for the volume fraction of the perdeuterated polystyrene probe chain in the

swollen network using data obtained from swelling measurements presented in chapter 2, section 5.3. A typical corrected data set is shown below in figure 3.12., the errors of which again arise from the Poisson counting statistics produced by the COLETTE program.

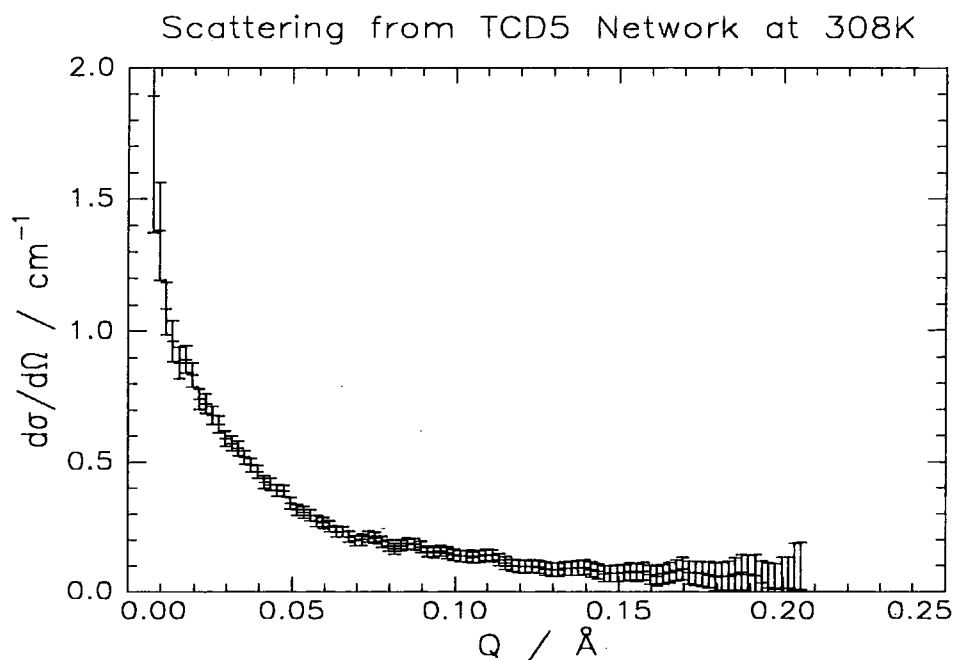


Figure 3.12.: Corrected Small Angle Scattering from the PSD 2 Probe Chain Trapped inside Network TCD 5 Swollen to Equilibrium in Cyclohexane at 308K

Examination of figure 3.12. shows clearly two important features of the coherent scattering arising from the trapped probe chains. Firstly the scattering from the trapped chains is found to be somewhat more noisy than that found from the bulk samples, and secondly the scattering is noted to be considerably weaker from probe chains in swollen networks when again compared to the dry samples.

Both of these features arise from the much lower concentration of the probe chain in the swollen networks, in all cases the probe chain concentration has been determined empirically from swelling measurements to be less than 2.5% (v/v). The low concentration of probe chain results in data of relatively poor quality, obtainable only by counting for significantly longer periods of time. Although it was originally intended to determine the probe chain size in networks swollen in cyclohexane at 308, 313, 318 and

323K, the lack of experimental time available coupled with the long acquisition times needed for the collection of data with acceptable signal to noise ratio's prevented the measurement of the probe chain size in networks swollen to equilibrium in cyclohexane at 323K. As noted above, figure 3.12. shows the coherent scattering from probe chains in cyclohexane swollen networks to be considerably weaker leading to data of noticeably poorer quality as compared to the bulk samples. For networks swollen in toluene this situation is accentuated to the point that after subtraction of the appropriate incoherent background no measure of coherent scattering could be observed from which to evaluate the probe chain size as shown below in figure 3.13.

The absence of any coherent scattering is again attributed to the low concentration of probe polymer in the gel. In toluene swollen networks the volume fraction of the probe polymer is in all cases calculated from swelling measurements to be less than 0.8% (v/v) and it is therefore assumed that the degree of contrast between the perdeuterated probe polymer and the 'hydrogenous' background is not sufficient to observe the scattering from such a low concentration of polymer.

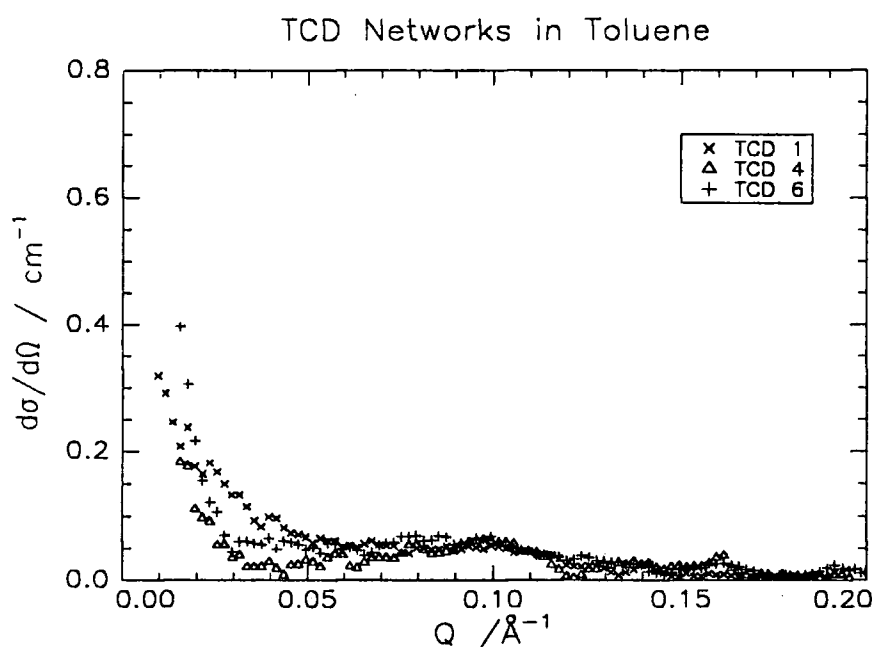


Figure 3.13.: Scattering from Networks TCD 1, TCD 4 and TCD 6 After Subtraction of the Incoherent Background from the Network and Swelling Solvent.

Small angle scattering data from experiments on networks swollen to equilibrium in cyclohexane at 308, 313 and 318K were analysed in both the Guinier and intermediate regions to determine the radius of gyration of the probe chain. In the intermediate Q region the observed coherent scattering was again fitted using equation 3.35. to the Debye function-a typical fit to this being shown in figure 3.14.

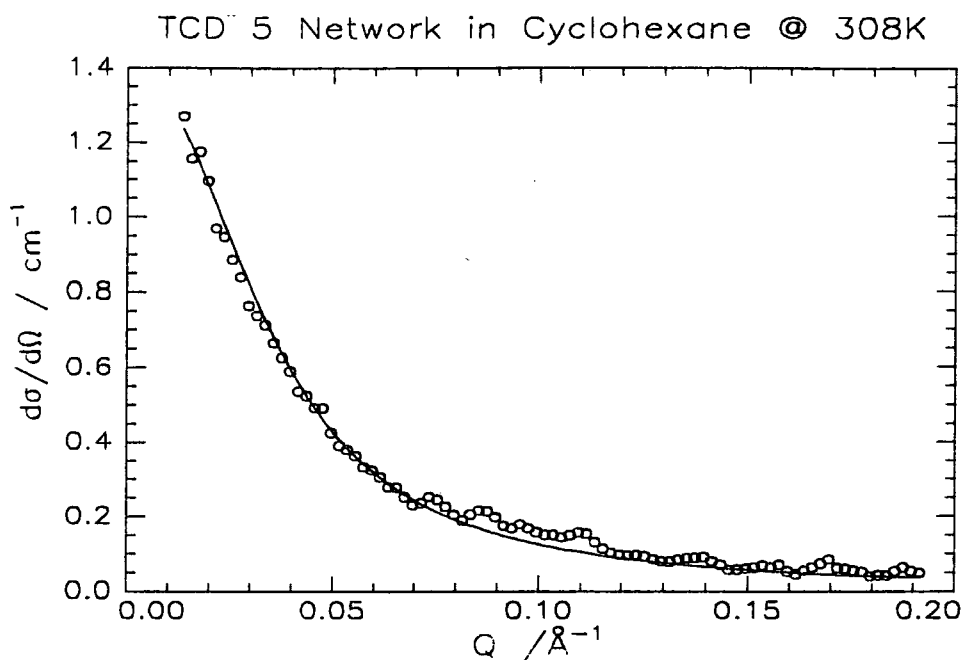


Figure 3.14.: Gaussian Fit in the Intermediate Q Region to Corrected Scattering Data from Probe Chain PSD 2 in Network TCD 5 Swollen in Cyclohexane at 308K.

In the Guinier Q region equation 3.34. has again been used to evaluate the probe chain size by fitting the data to a Zimm plot of the reciprocal intensity versus Q^2 in the range $0 \leq Q^2(\text{\AA}^{-2}) \leq 0.0004$. A typical fit to the Zimm expression is shown below in figure 3.15., the least squares fit to the data shown being obtained from fitting within the Guinier region only.

No use was made here of the Guinier approximation in the measurement of probe chain size as the relatively poor statistical quality of the data was found to lead to spurious results where the radius of gyration was measured to be of the order 300-800 \AA with an inherently large error associated with the fit of approximately $\pm 50\text{\AA}$.

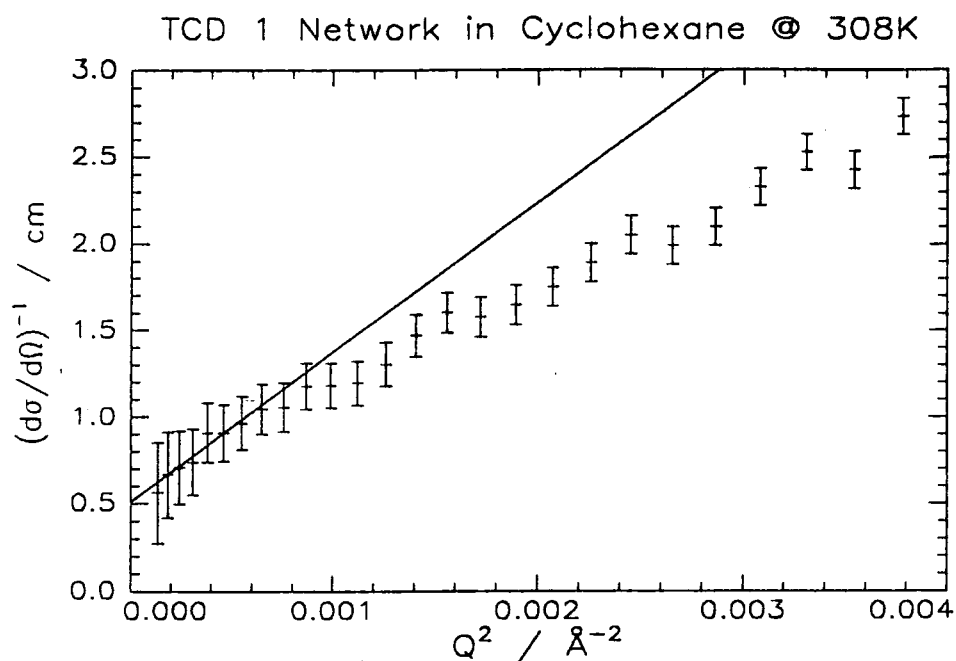


Figure 3.15.: Zimm Plot from PSD2 Probe Chain Trapped inside Network TCD 1 Swollen to Equilibrium in Cyclohexane at 308K

A similarly large uncertainty exists in the data fitted to the Zimm approximation, which although not as magnified as that found with the Guinier approximation highlights the noisiness of the data obtained from the swollen networks. These statistical errors are further augmented by the relatively few number of data points (within the available Q range of the machine) with which to study the Guinier scattering region of the probe polymer.

For polymer chains with an estimated radius of gyration of 50\AA there are as few as five data points lying within the Guinier region, however as the LoQ instrument produces around eighty data points within the intermediate region results from fitting to the Debye function are given more credence.

Values of the probe chain size as determined from both the Zimm and Debye expressions are shown below in table 3.6. All values of the radii of gyration have been converted to a weight average radius of gyration from the measured z-average radius of gyration following the correction given by equation 3.46, whilst values determined from the Zimm expression have been corrected by equation 3.45. for the effects of fitting the

data at a single concentration. Values of the second virial coefficient used in this correction were obtained from The Polymer Handbook¹⁹, while values of polymer concentration and the polymer molecular weight were taken from the swelling and S.E.C. results presented in chapter 2.

Polymer Network	$R_g \pm \text{Error} / \text{Å} \text{ (Zimm Model)}$			$R_g / \text{Å} \pm \text{Error} \text{ (Debye Model)}$		
	308K	313K	318K	308K	313K	318K
TCD 1	35 ± 4	31 ± 5	42 ± 5	42 ± 1	47 ± 1	46 ± 1
TCD 5	34 ± 5	37 ± 4	39 ± 5	42 ± 1	45 ± 1	48 ± 1
TCD 4	35 ± 5	43 ± 5	48 ± 6	44 ± 1	51 ± 1	52 ± 1
TCD 6	38 ± 4	42 ± 5	46 ± 4	45 ± 2	50 ± 2	49 ± 5

Table 3.6.: Radii of Gyration of the PSD 2 Probe Polymer Trapped in Networks Swollen in Cyclohexane Determined from the Zimm Equation and Debye Model.

The absolute intensity determined by extrapolation to zero scattering vector of the fit to the Debye equation has been used in equation 3.44. to determine the molecular weight of the probe polymer, the results of which are shown below in table 3.7.

Polymer Network	Probe Polymer Molecular Weight ± Error / gmol ⁻¹		
	308K	313K	318K
TCD 1	40,800 ± 1,000	37,600 ± 600	42,800 ± 700
TCD 5	20,300 ± 700	19,600 ± 500	30,300 ± 800
TCD 4	37,100 ± 300	35,100 ± 700	34,300 ± 400
TCD 6	18,400 ± 2,200	29,900 ± 8,000	23,400 ± 7,300

Table 3.7.: Probe Chain Molecular Weight Calculated from the Intensity at Zero Scattering Measured from the Debye Expression.

Two important features can be seen from the results of the fit to the Debye function presented in table 3.6. For networks swollen to any given temperature in cyclohexane the radius of gyration of the probe polymer is found to be independent of the cross link density of the network, it is noted that for networks swollen to equilibrium

in cyclohexane at 308K, (the theta point), the radius of gyration of the probe chain is found to take the value predicted from the ideal chain dimensions. Secondly, on increasing the temperature of any given network above the theta point, the size of the probe increases as might be expected following an increase in the quality of the solvent in the system.

Table 3.7. shows the molecular weight of the probe chain determined by SANS to correspond well to the value obtained from the S.E.C. measurement of the molecular weight. This is found to be in good agreement despite the errors introduced into the calculation from the determination of the probe chain concentration (via the swelling ratio of the network) and also from the lack of suitable data points in the Guinier region which would be expected to influence strongly the extrapolation of the Debye fit to zero scattering vector (and hence the molecular weight of the probe polymer).

These results indicate that the trapped probe chain is behaving in a manner similar to that of a flexible chain in a semi-dilute solution without cross links. Conformational studies of the behaviour of polymer chains in semi-dilute solutions have been undertaken^{25,31-33,42} and the results obtained compared to the predictions of both mean-field⁴⁴ and scaling theories^{13,43}. For semi-dilute solutions of flexible polymers in good solvents, scaling theory predicts that the radii of gyration and screening length of the polymer chains are dependent on the molecular weight and concentration of the polymer and the degree of excluded volume in the system (usually expressed as a function of the temperature of the system relative to the theta temperature of the system). For a semi-dilute solution of polymer in a good solvent (the so-called region 2 of reference 43), scaling theory predicts the radius of gyration to be given by equation 3.47.

$$R_g^2 \approx Mc^{-1/4} \tau^{1/4} \quad 3.47.$$

Where M is the molecular weight of the polymer,

c is the polymer concentration (g cm^{-3}),

and τ is the reduced temperature of the system given by equation 3.48.

$$\tau = \frac{T - \Theta_T}{\Theta_T} \quad 3.48.$$

where Θ_T is the theta temperature of the system.

These predictions of scaling theory for the effects of polymer molecular weight and concentration on the radii of gyration in semi-dilute solution have been confirmed by S.A.N.S. studies on solutions of polystyrene in carbon disulphide where Daoud²⁵ *et al* found the radius of gyration of hydrogenous polystyrene chains decreased with concentration with the predicted scaling exponent of -0.25. Cotton³³ *et al* further extended this work to study the temperature dependence of the radius of gyration and the screening length for solutions of polystyrene in cyclohexane in the temperature range 305K to 340K and from this constructed a phase diagram of the cross-overs between different regions as a function of polymer concentration and the reduced temperature.

The radii of gyration of a labelled fraction of perdeuterated polystyrene chains dissolved in a solution of hydrogenous polystyrene (total polymer concentration 0.15 gcm⁻³, concentration of PSD 0.01 gcm⁻³ i.e. c-PSD \ll c*), in hydrogenous cyclohexane was measured and it was found that the radius of gyration of the "probe" increased with the temperature of the system with the expected dependence upon the reduced temperature being observed for solutions between 313K and 340K. However, between the theta point (for PSD in cyclohexane $\Theta_T = 303.5 \pm 0.5$ K) and 313K, some deviation in behaviour was observed which was attributed to a crossover to a concentrated regime (region 3 of reference 43) where the radius of gyration of the polymer is dependent only on the molecular weight of the polymer chain.

In region 3, the so-called semi-dilute Θ region, the radius of gyration is predicted to be given by equation 3.49 where it can be seen that the radii of gyration are not expected to be dependent on the polymer concentration or the excluded volume of the system.

$$R_g^2 \approx M \quad 3.49.$$

While scaling theory predicts two semi-dilute regions of behaviour, mean-field theory predicts a further region of behaviour⁴⁴, region 2A-the so called semi-concentrated region not predicted by the re normalisation group theory approach. In region 2A the radius of gyration is expected to be given by equation 3.50.

$$R_g^2 = R_{g,0}^2 (1 + K\tau^{1/2}c^{-1/2}) \quad 3.50.$$

Evidence for this regime of behaviour has come from the work of Richards³² *et al* who studied the polystyrene cyclohexane system (again by doping a small fraction of the hydrogenous polymer with perdeuterated polymer) in the concentration range $0.5 \leq c$ (g cm^{-3}) ≤ 0.82 . at a temperature of 333K, where it was found that the radius of gyration was linearly dependent with the reciprocal of the square root of the total polymer concentration. Above this concentration range, the radius of gyration was found to be given by the unperturbed dimensions of the polymer.

The predictions of mean-field and re normalisation group theories for the behaviour of polymer chains in semi-dilute and concentrated polymer solutions are summarised below in table 3.8, showing the relationships between the screening length, radius of gyration, molecular weight, concentration and reduced temperature of the system.

Region	R_g^2 / SL	R_g^2 / MF	ξ^2 / SL	ξ^2 / MF
2	$\text{Mc}^{-1/4}\tau^{1/4}$	$\text{Mc}^{-1/5}\tau^{1/5}$	$c^{-3/2}\tau^{-1/2}$	$c^{-6/5}\tau^{-4/5}$
2A	-----	$R_{g,0}^2 [1 + kc^{-1/2}\tau^{1/2}]$	-----	$c^{-1}\tau^{-1}$
3	M	M	c^{-2}	-----

Table 3.8.: Theoretical Predictions for the Rg and Screening Length of Polymer Chains in Semi-Dilute Solutions Following the Phase Diagram of Daoud.

It might therefore be expected that the swollen gel could fall into any one of these three concentration regimes, depending upon the degree of swelling of the network and the temperature of the system. As noted earlier in section 5 of this chapter, the

correlation length of the networks are thought to be dependent only upon the synthetic conditions employed in the preparation of the networks and therefore the predicted scaling behaviour of the correlation length is of no use in the determination of the position of the swollen networks on the phase diagram. Therefore the variation in the radius of gyration of the probe chain with polymer concentration and reduced temperature is the only method of determining the position on the polymer phase diagram.

The variation of the radii of gyration of the probe chains with the polymer concentration at fixed temperatures are shown below in figures 3.16.a-c. All three graphs have been plotted in double logarithmic format so as to determine the scaling exponents of the radii of gyration.

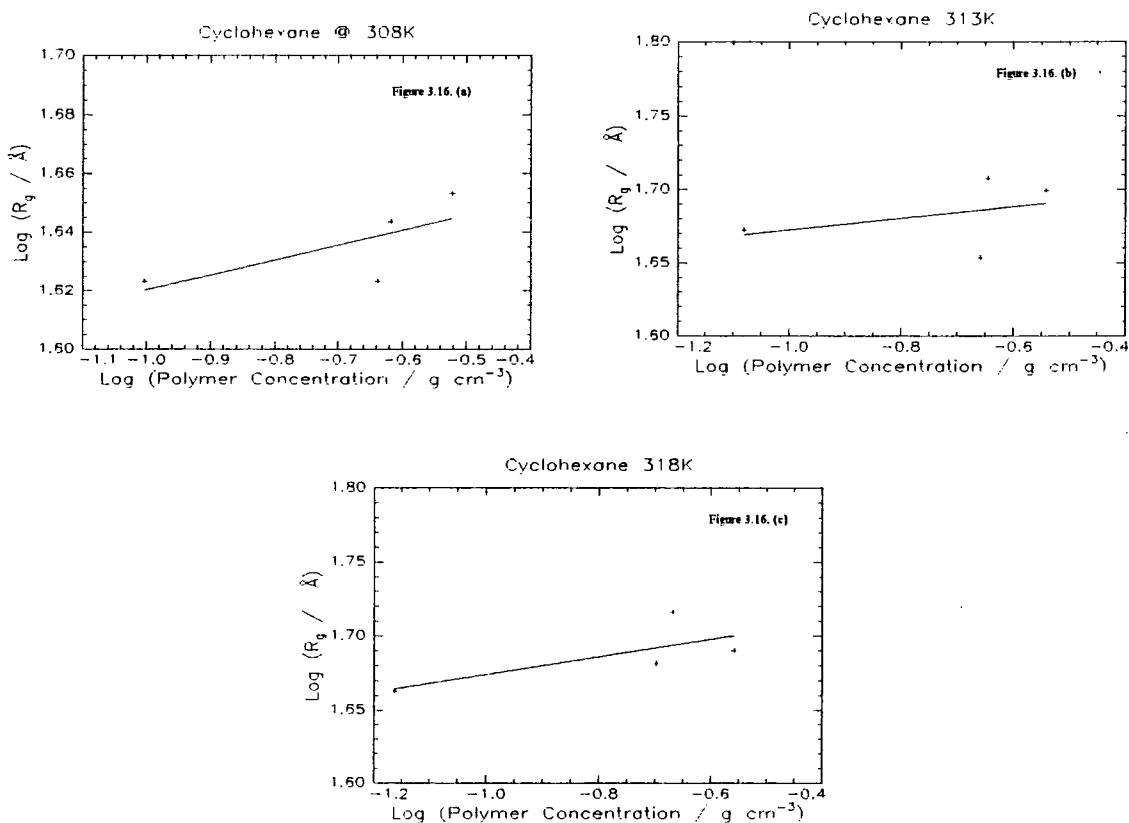


Figure 3.16. a-c: Variation in Probe Chain Size with Concentration for Fixed Temperatures at 308, 313 and 318K.

The following scaling relationships can then be deduced from the least-squares fit to the data.

Figure 3.16 a.: $\text{Log}(R_g) = (1.67 \pm 0.03) + (0.05 \pm 0.04) \text{Log}(c)$

Figure 3.16 b.: $\text{Log}(R_g) = (1.71 \pm 0.05) + (0.04 \pm 0.07) \text{Log}(c)$

Figure 3.16 c.: $\text{Log}(R_g) = (1.73 \pm 0.03) + (0.06 \pm 0.04) \text{Log}(c)$

Figures 3.17. parts a-d below show the variation of the radii of gyration of the probe chain as a function of the reduced temperature of the system for networks with a constant molecular weight between cross links. All figures are again plotted in double logarithmic format so as to determine the relative scaling exponents. The value of the theta temperature of PSD in cyclohexane was taken from the work of Cotton³³ who found the theta temperature to be $303.5 \pm 0.5\text{K}$.

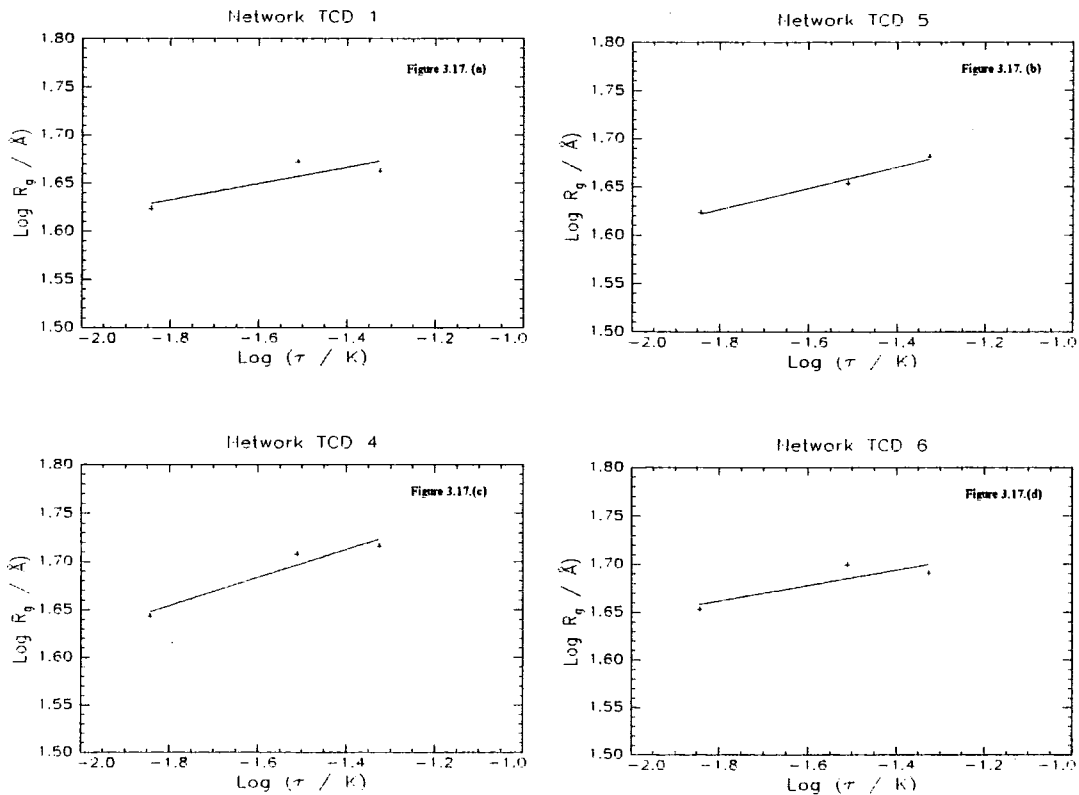


Figure 3.17. a-d: Variation in the Radii of Gyration of Probe Chains in Swollen Networks as a Function of the Reduced Temperature of the System.

The following scaling relationships were obtained from the least-squares fit to the data relating the probe chain radii of gyration to the reduced temperature of the system.

Figure 3.17 a.: $\text{Log}(R_g) = (1.78 \pm 0.08) + (0.09 \pm 0.05) \text{Log}(\tau)$

Figure 3.17 b.: $\text{Log}(R_g) = (1.82 \pm 0.02) + (0.11 \pm 0.02) \text{Log}(\tau)$

Figure 3.17 c.: $\text{Log}(R_g) = (1.92 \pm 0.06) + (0.15 \pm 0.04) \text{Log}(\tau)$

Figure 3.17 d.: $\text{Log}(R_g) = (1.80 \pm 0.07) + (0.08 \pm 0.05) \text{Log}(\tau)$

From the scaling exponents derived from figures 3.16. and 3.17. it can be seen that the changes in the radii of gyration of the probe chains are consistent with the behaviour expected for a flexible polymer in the semi-dilute theta region (region 3) of the polymer phase diagram. Figure 3.16 shows that the size of the probe chain increases by a small amount with an increase in the concentration of the polymer in the network. In region 2 it would be expected that the R_g^2 of the probe would decrease with the concentration following a scaling exponent of $-1/4$. Similarly if the probe chain were within region 2A, the square of the probe radius of gyration should increase with a scaling exponent of $-1/2$. Clearly the behaviour observed shows the size of the probe chain to be only slightly dependent on the polymer concentration, with the radius of gyration increasing with the volume fraction of polymer in the gel.

The scaling exponent is found to be zero within the large error associated with the fit to the data over the relatively small fitting region, therefore indicating that the network is within region 3 of the phase diagram. From figure 3.17. the radius of gyration is found to increase with the reduced temperature of the system, though the magnitude of the scaling exponent is found to be somewhat less than that expected for regions 2 and 2A on the phase diagram. Again within the margins of error associated with the fit to the data, the scaling exponents can be seen to be zero, further indicating that the probe chain is within the semi-dilute theta region.

It is noted however that both the excluded volume and concentration dependencies are inextricably linked and cannot be completely separated from each other. Thus as the temperature is increased the polymer concentration decreases (due to swelling of the network) as well as the increase in the excluded volume. As the concentration changes the influence of the excluded volume is changes due to the change in the number of intermolecular contacts. Consequently, the agreement with the hypothesis of region 3 behaviour arising from the data of figure 3.16. may be somewhat fortuitous, though given the nature of all of the available data, it is still thought that the gels behave as if in the semi-dilute theta regime.

7. Conclusions.

Small angle neutron scattering has been used to measure the correlation length of a series of end linked polymer networks swollen to equilibrium in cyclohexane in the temperature range 308K to 323K and in toluene at 298K. The measured correlation length was not found to be dependent upon the polymer concentration of the network as expected following the predictions of scaling and mean-field theory. The correlation length was found to be dependent only upon the conditions of synthesis employed in the preparation of the networks. The synthetic route to the networks relying upon the cross linking of a semi-dilute solution of polystyrene in benzene, where the correlation length describes the separation of temporary chain entanglements along the chain backbone and is fixed by the concentration of the solution.

In a semi-dilute solution these cross links can disentangle over long time scales as chains diffuse through the solution, however following the end linking of the chains into a network structure these temporary chain entanglements become frozen into the network structure and cannot disentangle due to the presence of the cross links in the solution. Variations in the correlation length with the temperature of the system after cross linking reflect only changes in the quality of the solvent in the system and follow the predictions of scaling theory for the correlation length of semi-dilute solutions.

Similar behaviour suggesting that the network behaves as a semi-dilute solution in region 3 of the polymer phase diagram are found from the determination of the radius of gyration of probe chains trapped within networks swollen in cyclohexane in the temperature range 308K to 318K. Here the radius of gyration of the probe is found to be independent of the cross link density of the network (and hence the volume fraction of polymer in the gel) following the predictions of scaling theory for the size of the probe chain in a semi-dilute solution at fixed temperature. Measurements of the radii of gyration as a function of temperature are somewhat ambiguous as increasing the temperature of the system causes a decrease in the polymer concentration of the gel as well as an increase in the solvent quality and hence excluded volume interactions in the

gel, however the results obtained from this measurement are fortuitously in line with the predictions of scaling theory for the semi-dilute theta regime.

The size of a probe chain trapped within a network has been measured by S.A.N.S. as a function of the cross link density of the network to establish the validity of the predictions for a chain in a random medium from Edwards and Vilgis. Whilst the theory of a chain in a random medium predicts a decrease in the probe chain size with increasing obstacle density, the situation found here is markedly different. With an increasing cross link density in the network, the radius of gyration of the probe chain has been found to be increased above the unperturbed theta dimensions of the network, though the molecular weight of the probe chain shows no evidence of phase separation and hence probe chain aggregation as the cross link density of the network is increased. For low cross link density networks theta dimensions are observed for the probe chain whilst for the most highly cross linked networks, radii of gyration approximately 30% greater than theta dimensions are found. Therefore it seems apparent that the predictions for a chain in a random medium cannot be applied to the case of a chain trapped within a network.

The reasons for the increase in the probe chain size are however somewhat poorly understood, as no current theories adequately describe the behaviour of the probe chain within a cross linked network and only a small amount of data was generated from the SANS experiments undertaken here. Clearly more work is needed in this area to understand fully the effects of cross link density on the conformation of chains trapped within model networks.

8. References.

1. Bacon G.E., *Neutron Diffraction*, Oxford University Press, Oxford, 1975
2. Willis B.T.M., *Chemical Applications of Neutron Scattering*, Oxford University Press, Oxford, 1973
3. Bacon G.E., *Neutron Scattering in Chemistry*, Butterworths, London, 1977
4. Squires G.L., *Thermal Neutron Scattering*, Cambridge University Press, Cambridge, 1978
5. Lovesey S.W., *Theory of Neutron Scattering from Condensed Matter*, Oxford University Press, Oxford, 1984
6. Higgins J.S. and Benoit H.C., *Polymers and Neutron Scattering*, Oxford University Press, Oxford, 1994
7. Richards R.W. in *Developments in Polymer Characterisation* (Ed Dawkins J.V.), Elsevier, New York, 1986
8. Maconnachie A. and Richards R.W. *Polymer*, **19**, 739, (1978)
9. King S.M. *Applications of SANS in Polymer and Colloid Science*, Rutherford-Appleton Laboratory, 1993
10. *ISIS User Guide and Experimental Facilities*, Rutherford-Appleton Laboratory, 1992
11. Richards R.W., in *Comprehensive Polymer Science Volume 1*, (Ed Allen G.), Pergamon, Oxford, 1989
12. King S.M., *COLETTE User Manual*, Rutherford-Appleton Laboratory, 1993
13. de Gennes P.G. *Scaling Concepts in Polymer Physics*, Cornell University Press, Ithaca, N.Y. 1979
14. Shikayama M., Yang H., Stein R.S. and Han C.C., *Macromolecules*, **18**, 2179, (1985)
15. Debye P., *J. Phys. Colloid Chem.*, **51**, 18, (1947)
16. Hopkinson I., PhD thesis, University of Durham, 1994
17. Russell T.P., *Mat. Sci. Reports*, **5**, 173, (1990)
18. Davidson N.S., PhD thesis, University of Strathclyde, 1984

- 19 Immergut E.H. and Brandrup J., *Polymer Handbook*, Wiley Interscience, New York, 1989
- 20 Wignall G.D. and Bates F.S., *J. Appl. Cryst.*, **20**, 28, (1987)
- 21 Wignall G.D. and Bates F.S., *Phys. Rev. Letts.*, **57(12)**, 1429, (1986)
- 22 Ullman R., *Ann. Rev. Mater. Sci.* **10**, 261, (1980)
- 23 Burchard W., in *Applied Fibre Science*, (Ed Happey F.), Academic Press, London, 1978
- 24 Zimm B.H., *J. Chem Phys.*, **16**, 1093, (1948)
- 25 Daoud M., Cotton J.P., Farnoux B., Jannink G., Sarma G., Benoit H., Duplessix R., Picot C., and deGennes P.G., *Macromolecules*, **8**, 804, (1975)
- 26 Bastide J., Duplessix R., Picot C. and Candau S., *Macromolecules*, **17**, 83, (1984)
- 27 Bastide J., Candau S. and Delsanti M., *Adv. Polym. Sci.*, **44**, 27, (1982)
- 28 Mendes E., Girard B., Picot C., Buzier M., Boue F. and Bastide J., *Macromolecules*, **26**, 6873, (1993)
- 29 King J.S., Boyer W., Wignall G.D. and Ullman R., *Macromolecules*, **18**, 709, (1985)
- 30 Brown W., Mortensen K. and Floudas G., *Macromolecules*, **25**, 6904, (1992)
- 31 Cotton J.P., Farnoux B. and Jannink G., *J. Chem. Phys.*, **57(1)**, 290, (1972)
- 32 Richards R.W., Maconnachie A. and Allen G., *Polymer*, **22**, 147, (1981)
- 33 Cotton J.P., Nierlich M., Boue F., Daoud M., Farnoux B., Jannink G., Duplessix R. and Picot C., *J. Chem. Phys.*, **65(3)**, 1101, (1976)
- 34 Wignall G.D., in *Encyclopedia of Polymer Science and Engineering Volume 10*, (Ed. Kroschwitz J.), Wiley Interscience, New York, 1985
- 35 Kurata M., Stockmeyer W.H., *Fortschr. Hochpolym. Forsch.*, **3**, 196, (1963)
- 36 Edwards S.F. and Muthukumar M., *J. Chem. Phys.*, **89(4)**, 2435, (1988)
- 37 Vilgis T.A., *J. Phys. France.*, **50**, 3243, (1989)
- 38 *GENPLOT User Manual*, Computer Graphic Service, 1991
- 39 Cotton J.P., Decker D., Benoit H., Farnoux B., Higgins J.S., Jannink G., Ober R., Picot C. and Des Cloiseaux J., *Macromolecules*, **7**, 863, (1974)

- 40 Kirste R.G., Kruse W.A. and Schelten J., Makromol. Chem: **162**, 299, (1973)
- 41 Lieser G., Fischer E.W. and Ibel K., J. Poly. Sci., Poly. Letters., **13**, 39, (1975)
- 42 Farnoux B., Boue F., Cotton J.P., Daoud M., Jannink G., Nierlich M., and deGennes P.G. J. Physique (Paris), **39**, 77, (1978)
- 43 Daoud M. and Jannink G., J. Physique (Paris), **37**, 973, (1976)
- 44 Edwards S.F. and Jeffers E.F., J. Chem. Soc.(Faraday Trans.II), **75**, 1020, (1979)

CHAPTER 4

QUASI-ELASTIC LIGHT SCATTERING.

1. Introduction.

The scattering of visible radiation by matter has been used for some time in the determination of molecular structure. Interaction between a photon and a molecule can take one of a number of forms, ranging from an exchange of energy between the photon and the translational, rotational, vibrational or electronic degrees of freedom of the molecule to elastic scattering where there is no absorption of the radiation impinging upon the molecules in its path, inducing an oscillation in the electron density of the molecule, which accelerates the particle causing it to radiate photons in all directions.

Where there is no absorption of the radiation the scattering is said to be elastic, a process which arises from interaction of the photon and the low energy rotational and translational degrees of freedom of the scattering molecule-the process being known as Rayleigh scattering¹. The determination of the peak intensity of the Rayleigh scattered radiation has been used to determine static properties such as the molecular weight, size, shape and the second virial coefficient of dilute polymer solutions. However, thermal motion of the scattering species causes the elastically scattered Rayleigh line to be broadened in frequency slightly, giving rise to Quasi-Elastic Light Scattering (QELS) from which information on the motion of the solute can be obtained.

It is only in recent times with the development of coherent light sources such as lasers that the study of the small frequency shifts and hence the optical line width has become possible, thus leading to the measurement of the dynamic properties of the polymer in solution with QELS. In dilute solution it is the translational diffusion coefficient which is determined, from which the particle size can be deduced as well as the polydispersity of the polymer. However in concentrated solutions, it is the collective diffusive motions of polymers that are studied.

In this work QELS has been used to study the dynamic behaviour of a series of model polymer networks having various cross link densities swollen in cyclohexane in the temperature range 308-323K and in toluene at 298K. The dynamic behaviour of a series of "equivalent" semi-dilute solutions having the same polymer concentration have also been studied under the same conditions and the differences in the dynamic properties established.

Further to this, a series of model polymer networks have been prepared containing a known fraction of unattached, "probe chains", which are free to diffuse through the network. These networks have been studied when swollen in cyclohexane and toluene and an attempt made to extract the diffusion coefficient of the trapped chain so as to relate this to the theories describing the dynamic behaviour of a polymer chain within a network. A series of equivalent ternary solutions having the same polymer concentration have been prepared and studied so as to ascertain any differences in the dynamic behaviour of the probe chain within the gel and the solution of the same polymer concentration.

In order to determine the effects of the polymer matrix (both cross linked and in semi-dilute solution) on the diffusion of the dilute probe, QELS has also been used to determine the diffusion coefficient of the probe chain in "free" solution in cyclohexane in the temperature range 308-323K and in toluene at 298K.

2. Theoretical Aspects of QELS.

In order to properly understand the theories describing QELS some knowledge of the origins of light scattering are required, a brief summary of which is given here, a more complete explanation being given in the literature²⁻⁴.

2.1. The Origin of the Scattering of Light by Macromolecules.

The first description of the scattering of light by gases was proposed over a century ago by Lord Rayleigh using classical electromagnetic theory⁵. In a simple

picture scattering particles with small dimensions ($< \lambda/20$) compared to the wavelength of the incident photons (λ) are considered to be optically isotropic and to scatter as individual points. When plane polarised light interacts with a particle of polarisability α , the sinusoidally oscillating incident electric field (E) impinging on the particle induces an electric dipole within the particle⁴, the dipole moment μ being given by equation 4.1.

$$\mu = \alpha E = \alpha E_o \exp(i\omega t) \quad 4.1.$$

The induced electric dipole behaves as a secondary source of radiation and radiates a plane polarised wave of exactly the same frequency as the incident beam in all directions. At any point P, the intensity of scattered light(I) at an angle θ to the incident beam arising from a unit scattering volume is given by equation 4.2.

$$I = \frac{2\pi^2 M I_o}{r^2 \lambda_o^4 N_A} \left(\frac{dn}{dc} \right)^2 \sin^2 \theta \quad 4.2.$$

where N_A is Avagadro's constant,

r is the distance between the scattering particle and the observer,

λ_o is the wavelength of the incident radiation,

θ is the scattering angle,

I_o is the intensity of the incident photon

M is the molecular weight of the scattering centre

and dn/dc is the refractive index increment

The dependence of the scattered intensity on the observation distance (r) and the incident intensity can then be removed by expressing the scattering in terms of the Rayleigh ratio R_θ given by equation 4.3.

$$R_\theta = \left(\frac{I r^2}{I_o} \right) \quad 4.3.$$

Therefore, equation 4.2. can be rewritten as equation 4.4.

$$R_\theta = \frac{2\pi^2 M c}{\lambda_o^2 N_A} \left(\frac{dn}{dc} \right)^2 \sin^2 \theta \quad 4.4.$$

Equation 4.4. has been verified experimentally by a light scattering determination of Avagadro's number, therefore from a knowledge of the mechanical and optical characteristics of the instrument used, the Rayleigh ratio can be determined for any gas.

The scattering of light by liquids is somewhat more complicated since the molecules are not independent of each other nor distributed at random. This leads to a reduction in the scattered intensity due to destructive interference between the scattered photons. The thermodynamic treatment of the scattering of light by liquids was developed independently by both Einstein⁶ and Smoluchowski^{7,8}. They described the scattering in terms of fluctuations in the refractive index increment (dn/dc) arising from Brownian motion of molecules in the liquid causing the formation (and destruction) of "holes" within the liquid leading to density fluctuations and hence changes in (dn/dc) which result in scattering from the liquid.

The scattering from a dilute solution containing *small particles* ($< \lambda/20$) has been described by Debye^{9,10} who showed that when a solute is dissolved in a liquid, the scattering from any volume element again arises from liquid inhomogeneities, however an additional contribution from fluctuations in the solute concentration is present above that from the solvent alone.

For much larger particles ($> \lambda/20$), scattering is not observed to be angularly symmetrical. This feature, known as Debye scattering takes the form of a decrease in the scattered intensity with increasing angle. This reduction of intensity arises from intramolecular effects occurring as the bigger particle can no longer be considered as a point scatterer, instead it is thought of as a collection of point scattering centres.

The interference effects can be seen below in figure 4.1. where the radiation arriving from the light source is incident simultaneously upon two scattering centres, A and B.

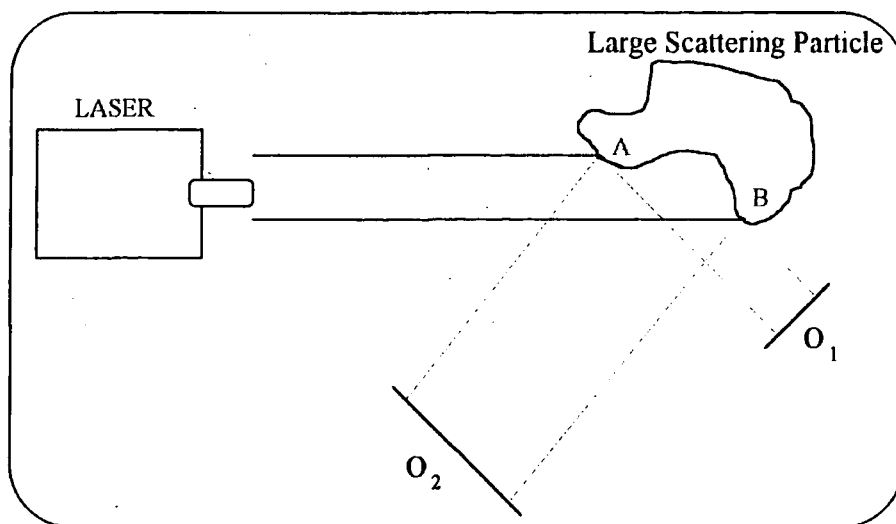


Figure 4.1.: Representation of the Geometry of Debye Scattering.

By analysing the path length difference between scattered radiation arriving at O_1 and O_2 from the two scattering centres, it can be seen that radiation arriving at O_2 will have a different phase to that at O_1 as the path length difference between waves scattered from the two centres increases. The angular distribution of the scattering is measured in terms of the particle scattering function $P(Q)^{11}$, which corresponds to the ratio of the real intensity of scattered radiation in a given direction to the theoretical intensity in the same direction measured in the absence of intramolecular interference-as defined by equation 4.5.

$$P(Q) = \frac{R_{\theta, \text{Experimental}}}{R_0} \quad 4.5.$$

As in any scattering experiment, the scattering is dependent on both wavelength and scattering angle, the modulus of the scattering vector Q being given by equation 4.6.

$$Q = \left(\frac{4\pi}{\lambda} \right) \sin\left(\frac{\theta}{2} \right) \quad 4.6.$$

The form of the $P(Q)$ depends upon the shape of the scattering particle, various models having been developed to describe the scattering from particles having different shapes¹². For a polymer such as polystyrene, the scattering is described in terms of a Gaussian coil model, the scattering function of which is given by equation 4.7.

$$P(Q) = \frac{2}{u^2} (\exp(-u) + u - 1) \quad 4.7.$$

where $u = Q^2 R_g^2$

and R_g is the mean square radius of gyration.

By studying the angular distribution of the scattered radiation it is therefore possible to deduce information on the shape of the scattering particle from the particle scattering function while determination of the molecular weight of a polymer is also possible by measuring the scattered intensity as a function of the scattering vector and concentration. In the limit of low Q , all scattering functions describing the various shapes of molecules reduce to the scattering function given in equation 4.8.

$$P(Q) = 1 - \left(\frac{Q^2 R_g^2}{3} \right) \quad 4.8.$$

2.2. Quasi Elastic Light Scattering.

Similarly to static light scattering, the technique of QELS involves the study of the scattering behaviour of polymer solutions. However, in QELS, the dynamic component of the scattered intensity is followed so as to determine the diffusive behaviour of the polymer chains. To this end, the technique is necessarily more technologically intense than static light scattering as the changes of the scattered intensity with time need to be considered. An introduction to the technique is given here, a more complete explanation of the method being given in the literature¹⁴⁻¹⁸.

On a macroscopic scale a polymer solution (above the theta point) is homogeneous as it is thermodynamically unfavourable in the absence of external forces for solute to preferentially occupy any one region. However, on a microscopic scale homogeneity cannot be assumed. Brownian motion is a thermally induced process which cannot be mathematically described and which causes random motion of the solute particles within the solution.

In a manner similar to the Doppler effect, the scattered light arriving at the photo detector is broadened in frequency with a frequency distribution centred upon ω_0 described by the function $S(\omega)$. The correlation function of the electric field $G^1(\tau)$, is also a measure of the frequency distribution and is the Fourier transform of the power spectrum $S(\omega)$. As the positions of the radiating charges are constantly changing the scattered electric field arriving at the detector changes with time in what would appear at first sight to be a noise pattern, figure 4.2.

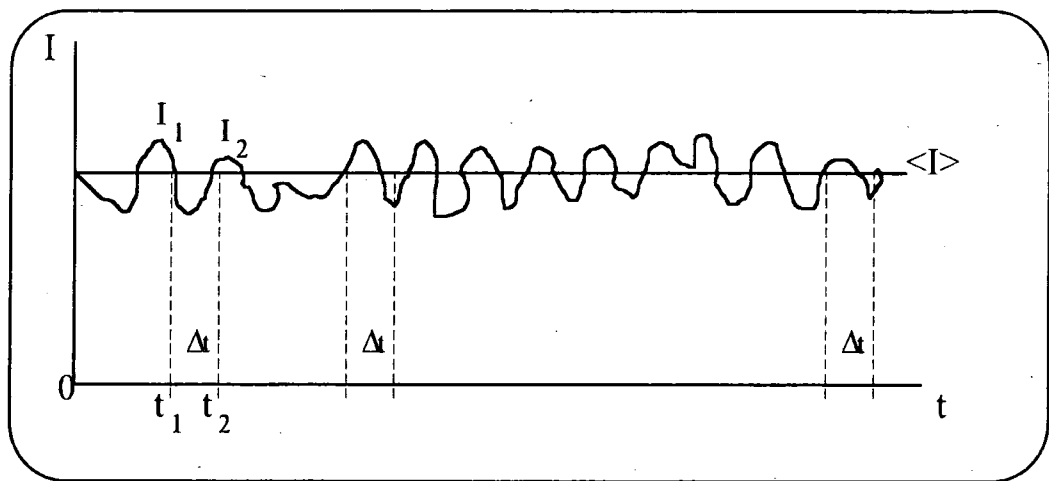


Figure 4.2.: Schematic Diagram of the Spectrum of the Scattered Intensity Arriving at the Detector.

Essentially the fluctuations in the scattered electric field are random, but the value at any given instant is mutually related (*correlated*) to the value at some previous instant. The strength of the correlation between the scattered intensity at points t_1 and t_2 falls off as the separation of the measurements (Δt) increases, until at large times with respect to the motion when the values are uncorrelated. It is from the nature of this decay that information on the motion giving rise to the fluctuations can be obtained.

The measure of the temporal correlation in the intensity (related to the square of the electric field of the scattered radiation) is described mathematically by the intensity autocorrelation function $G^2(\tau)$ which measures the similarity of the essentially random fluctuations in the scattered intensity and is given by equation 4.9.

$$G^2(\tau) = \langle I(t)I(t+\tau) \rangle = \lim_{t \rightarrow \infty} \frac{1}{t} \int_0^t I(t)I(t+\tau) dt \quad 4.9.$$

Initially at $t=0$, the autocorrelation function has a value of $\langle I^2 \rangle$. However with increasing time, values of $I(t)$ and $I(t+\tau)$ become uncorrelated and at infinite separation the autocorrelation function decays to $\langle I \rangle^2$. The relaxation time (τ) associated with the decay of the correlation function is the characteristic time of the decay and is a function of all the relaxation processes contributing to the decay of the autocorrelation function. The decay of the autocorrelation function is generally described by either a single or a combination of exponential decays, arising from the various decay modes within the system. It is from the relaxation rate of the decay that information is obtained on the diffusion of the scattering centres and hence the particle size of the molecules.

The intensity *autocorrelation* function $G^2(\tau)$ is the unnormalised form of the second order intensity *correlation* function $g^2(\tau)$ to which it is related by equation 4.10.

$$g^2(\tau) = \frac{G^2(\tau)}{\langle I \rangle^2} \quad 4.10.$$

2.3. Homodyne and Heterodyne Correlation Functions

For convenience two autocorrelation functions can be defined: The first order field autocorrelation function $G^1(\tau)$ (which contains information regarding the motion of the scattering centres within the solution) measures the correlation between values of the scattered electric field and the second order, intensity autocorrelation function $G^2(\tau)$ which measures the correlation between successive values of the square of the electric field of the scattered radiation (the intensity). Since a photo detector does not respond to the electric field incident upon it and instead responds to the square of the electric field (the intensity), it is the second order correlation function which is determined experimentally and no direct information is available in the detector output regarding the first order field correlation function.

In a homodyne QELS experiment where only light scattered by the fluctuations under consideration impinges on the photo detector, the autocorrelation function is simply $g^2(\tau)$ of the fluctuations. In this case where the scattering region is composed by many statistically independent contributions, the intensity correlation function is itself related to the first order field correlation function $g^1(\tau)$ (the normalised form of the first order autocorrelation function $G^1(\tau)$) by the Siegert equation^{14,15} given below in equation 4.11.

$$g^2(\tau) = 1 + |g^1(\tau)|^2 \quad 4.11.$$

Generally, the field impinging on the detector is not of this simple nature but it is possible to obtain a direct measurement of the field autocorrelation function in a heterodyne measurement. In this experiment, the light scattered from the fluctuations under consideration is mixed with unshifted light focused onto the photo detector.

Experimentally this can be achieved either by careful optical arrangement where a portion of light from the laser impinges directly onto the photo detector or where the unshifted beam arises from static scattering species present in the illuminated volume. If the amplitude of the reference beam is constant and much greater than that from the field arising from the fluctuations then the field and intensity correlation functions are related through equation 4.12^{14,15}.

$$g^2(\tau) = 1 + \left(\frac{2I_s}{I_r} \right) g_s^1(\tau) \quad 4.12.$$

where I_r is the intensity of the reference beam,

and I_s is the intensity of the scattered radiation from the fluctuations.

Equation 4.12. assumes that the reference and scattered fields are statistically independent and shows the measured second order correlation function to be directly related to the first order correlation function.

2.4. Data Reduction and Analysis

Interpretation of the correlation function obtained from an experiment can take one of a number of forms, depending upon the nature of the experiment performed and the system under study. Probably the most commonly applied QELS experiment measures the homodyne correlation function arising from the motion of a dilute solution of a scattering species.

The scattering species can be any one of a number of moieties including synthetic polymers, bio-organic macromolecules, latex suspensions or dispersions of small particles. QELS in this form is routinely used as a tool to determine the size of the scattering particle. Diffusion theory relates the field correlation function for a monodisperse solution of a polymer¹⁵ through equation 4.13.

$$g^1(\tau) = \exp(-\Gamma t) \quad 4.13.$$

where Γ is the relaxation rate of the decay of the fluctuations given by 4.14.

$$\Gamma = 2DQ^2 \quad 4.14.$$

where D is the experimental diffusion coefficient of the polymer chains.

Substituting equation 4.13. into the Siegert relationship (equation 4.11) gives equation 4.15. for the homodyne scattering arising from a monodisperse solution of a polymer.

$$g^2(\tau) = 1 + \exp(-\Gamma \tau) \quad 4.15.$$

However, experimentally the unnormalised correlation function will be of the form:

$$g^2(\tau) = A + B \exp(-\Gamma \tau) \quad 4.16.$$

where A and B are constants depending upon the instrument used.

Following the measurement of the diffusion coefficient of the scattering species it becomes possible to measure the hydrodynamic radius (R_h) of the scattering particle via the Stokes-Einstein relationship.

$$R_h = \frac{k_B T}{6\pi\eta_0 D} \quad 4.17.$$

where k_B is the Boltzmann constant,

T is the absolute temperature,

η_0 is the viscosity of the solvent,

and D is the translational diffusion coefficient.

The hydrodynamic radius gives the radius of a hypothetically impenetrable sphere having the same frictional effect in a hydrodynamic field as the polymer chain and as such differs in definition and usually in value from the radius of gyration of the polymer. Equations 4.16 and 4.17. form the basis of the use of QELS as a standard tool for the determination of particle size in such fields as biochemistry, colloid science and chemistry.

It is only in a few rare cases, as with many biological macromolecules that a single molecular weight species is present in the solution. Virtually all synthetic polymer solutions consist of a distribution of molecular weights and consequently the correlation function is made up of a distribution of exponential decays having different relaxation rates. The expression for the field correlation function given in equation 4.13 can therefore be modified to equation 4.18¹⁶

$$g^1(\tau) = \int G(\Gamma) \exp(-\Gamma\tau) d\Gamma \quad 4.18.$$

where $G(\Gamma)$ is the distribution of decay rates Γ .

$G(\Gamma)$ depends upon the distribution of molecular weights and as such can be used in the determination of the polydispersity of a polymer sample. Determination of $G(\Gamma)$ is essentially a problem of inverting the Laplace transform. The transform is known mathematically to be ill-conditioned and as such small changes in $g^1(\tau)$ such as those produced by the random noise fluctuations in the photo detector signal can result in dramatically different solutions of $G(\Gamma)$. As the result of the sensitivity of the transform

to the input data, all methods of performing the inversion place additional constraints on the least-squares fitting procedure which may involve assuming a particular shape of the distribution or simply excluding all solutions which force $G(\Gamma)$ negative or those where the distribution changes too rapidly.

2.4.1. Cumulants.

The method of cumulants^{21,22} gives the z average diffusion coefficient D_z , and the second moment of $G(\Gamma)$, μ_2 , providing a measure of the polydispersity of the sample. In the cumulants method, a polynomial of order two (or even three) is fitted to a plot of $\ln|g^1(\tau)|$ against τ and values of $\bar{\Gamma}$ and μ_2 obtained from the first and second coefficients of least-squares fit as given by equation 4.19.

$$\ln|g^1(\tau)| = -\bar{\Gamma}\tau + \frac{\mu_2\tau^2}{2!} - \frac{\mu_3\tau^3}{3!} + \dots \quad 4.19.$$

Where $\bar{\Gamma} = \int_0^{\infty} \Gamma G(\Gamma) d\Gamma$ is the mean relaxation time

and $\mu_2 = \int_0^{\infty} (\Gamma - \bar{\Gamma})^2 G(\Gamma) d\Gamma$ is the second moment of the distribution.

A measure of the polydispersity is given by the variance of the distribution which for a narrow polydispersity²² is given below in equation 4.20.

$$\frac{\mu_2}{\bar{\Gamma}^2} \approx \frac{1}{4} \left[\frac{M_z}{M_w} - 1 \right] \quad 4.20.$$

It has been noted that there are limitations associated with this type of analysis in the determination of polydispersity by QELS. Even in the absence of intermolecular interactions and internal motions the amplitude factor is proportional to M^2 and the presence of size ranges beyond the bandwidth limit of the measured correlation function will prevent the resolution of the motion of these molecules. Similarly, if the amplitude factors of these motions are buried in the experimental noise, the line width distribution

would disregard those size fractions. Hence there are practical upper and lower limits in the determination of the variance. Normally this range is given by: $(0.01 \leq \mu_2/\bar{\Gamma} \leq 2)$, implying a lower limit for almost monodisperse polymers as well as polydisperse samples.

2.4.2. The Kohlrausch-Williams-Watts Stretched Exponential Function.

Analysis of QELS data using a Kohlrausch-Williams-Watts (KWW) function provides a method of analysis similar to that of cumulants, allowing direct measurement of the diffusion coefficient and polydispersity of the autocorrelation function. The method involves fitting the experimental correlation function to a stretched exponential function of the type^{23,31} given below in equation 4.21.

$$g^2(\tau) = \exp(-\Gamma \tau^\beta) \quad 4.21$$

where Γ is the mean relaxation rate

and β is the variance and takes the value $(0 \leq \beta \leq 1)$.

The variance arising from the fit to the KWW function gives a measure of the polydispersity of the fit. Clearly, when $\beta=1$, the KWW function reduces to the more conventional single exponential decay given in equation 4.15. A more complex decay consisting of many more relaxation rates will therefore have a lower value of β indicating a more polydisperse fit. Although the KWW fit is not as widely used in the analysis of QELS data as the cumulants method, it has some distinct advantages in the resolution of polydisperse correlation functions where two distinct modes can be resolved³². In such cases data can be fitted to a double KWW function of the type given in equation 4.22.

$$g^2(\tau) = x_1 \exp(-\Gamma_1 \tau^{\beta_1}) + x_2 \exp(-\Gamma_2 \tau^{\beta_2}) \quad 4.22$$

where x_i measures the strength of mode i

The double KWW fit has been extensively used in the determination of the relaxation rates of semi-dilute and concentrated solutions of polystyrene in diethyl

phthalate⁶² where relaxation rates arising from the co-operative and viscoelastic modes have been resolved.

2.4.3. Inverse Laplace Transformation of QELS Data.

As noted earlier, it is often necessary to invoke other conditions in addition to the least-squares fitting procedures in order to obtain reliable and consistent approximations for $G(\Gamma)$. Regularisation techniques as typified by the CONTIN program^{24,25} perform the mathematically ill conditioned inverse Laplace transformation of QELS data, decomposing the correlation function into a distribution of relaxation modes given by equation 4.23.

$$g^l(\tau) = \sum_i A_i \exp\left(-\frac{t}{\tau_i}\right) \rightarrow \int_0^{\infty} \rho(\tau) \exp\left(-\frac{t}{\tau}\right) d\tau \quad 4.23$$

CONTIN penalises solutions for $G(\Gamma)$ that are either negative or change too rapidly. This is done since it is thought that although such solutions may be very interesting they are physically unlikely and it is therefore better to err on the side of caution rather than to account for an artefact that may only be noise. To this end, a term is added to the sum of the squares of the deviations between the experimental and fitted points, measuring the rate of change of $G(\Gamma)$. For CONTIN, this term is proportional to the integral of the second derivative of $G(\Gamma)$ over the distribution. The proportionality constant (α^2) is called the regularisation parameter and can be varied. Clearly the choice of α is crucial and within CONTIN several coarsely spaced values are employed in sequence before a finer examination of a smaller range of α . Increasing values of α are generally found to lead to broadening of peaks and a removal of fine (and possibly spurious detail). Great care must be taken in the use of programs such as CONTIN as small changes in input variables can lead to great changes in the output of the program³³.

3. Instrumentation.

QELS measurements were performed using a Malvern 4700 digital photon correlation spectrometer as shown schematically in figure 4.4. This spectrometer is a commercially available instrument designed to be used primarily for homodyne QELS

and intensity light scattering measurements. Although a full discussion is available in the manufacturers literature, a brief summary of its method of operation is given here.

For descriptive purposes the Malvern 4700 apparatus used can be divided into three distinct sections. The light source used, a 50mW Ion Laser Technologies model 5000 laser operates at a resonance frequency of 488nm. The incident power of the laser is monitored by the use of a photo diode power meter mounted at the head of the laser. The incident beam from the laser is focused onto the sample cell which is maintained in thermostatically controlled glass walled vat filled with xylene.

The xylene serves two purposes, firstly to provide precise control over the temperature of the cell during the duration of the experiment and secondly to "match" the refractive index of the fluid around the scattering cell to that of the glass. Xylene used within the vat was maintained within a closed system so as to exclude any dust which may cause secondary scattering. Dust was removed from the index matching fluid by constantly circulating the xylene through a 0.45 μ m PTFE filter between experiments.

Light scattered by the solution was collected by a photo multiplier (PM) tube mounted on a goniometer arm with an angular range from 10^o to 150^o. The scattered radiation passed through a 200 μ m pinhole before impinging upon the PM tube so as to ensure that light scattered by only one coherence area was measured by the detector²⁹. The autocorrelation function was computed from the analogue signal using a Malvern K7032 8 bit, 128 channel digital correlator. The K7032 correlator was controlled from a dedicated PC using Malvern Automeasure version 5.2 software²⁸.

The 128 channel correlator (including a further 4 delay channels used to measure the mean base-line) was split into 8 "sub-correlators" each of 16 channels. Each of the sub-correlators spanned delay times from $\tau = 2^n t$ to $\tau = 2^{(n+4)} t$ where $n=0, 1, 2, \dots, 7$ for sub-correlators 1, 2, 3, ... 8 respectively. This allows simultaneous measurement of multiples of

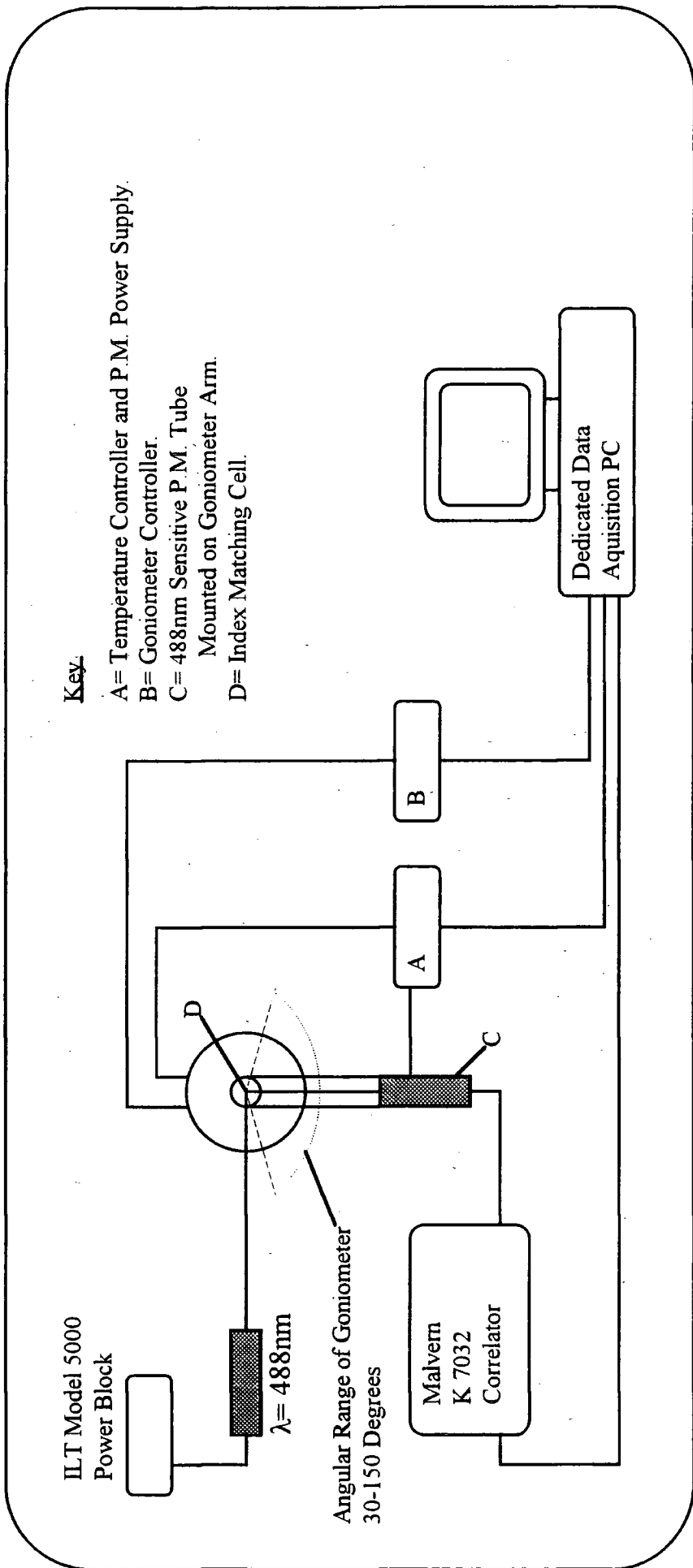


Figure 4.3.: Schematic Diagram of the Malvern 4700 digital Photon Correlation Spectrometer.

the sample time t from 1,2,3,4...16, (sub-correlator 1), 2,4,6...32, (sub-correlator 2), through to 128,256,384...2048 for sub-correlator number 8. This has the advantage of measuring a wide range of delay times simultaneously and prevents the need for the measurement and splicing together of several correlation functions as may be necessary with linearly spaced channels.

In most cases at least 5 data sets were collected from each sample, each of which was made up of at least 20 correlograms. These individual correlograms were automatically summed by the software and those outside one standard deviation deemed unacceptable and rejected. The remaining correlograms were then summed together and the data written and saved as an ASCII file.

In general for dilute solutions the measured and calculated baseline differed by no more than 2.5% with signal-to-noise ratios of around 25%. In those cases where the samples were of low molecular weight having a low refractive index increment, the amount of scattering was found to be very low and collection times were substantially longer, in some cases of the order of several hours. In these cases, the data set may be that of a single measurement. For semi-dilute solutions and swollen gels, scattering was found to be substantially stronger and collection times of around 10-30 seconds were satisfactory for the generation of the correlograms. In these cases upwards of 100 correlograms were summed together.

Some data analysis was possible using the Malvern software (second-order cumulants) however as this was limited in the number options available, data was analysed by a specialist program developed for use with data sets generated from the Automeasure software³⁰. Correlation functions generated by the Automeasure software were analysed and the data set then fitted to one of several functions using SIQELS. Several fitting options were available for use.

A single exponential function was used to fit the data arising from dilute solution measurements though a double exponential option was also available. A second order cumulants function was available for the analysis of more complex data sets produced by semi-dilute solutions and swollen gels, however data from these measurements were mostly analysed using either a single or double KWW stretched exponential function. The data produced by the software was then converted to a suitable format and transferred to a micro VAX computer where it was analysed by CONTIN so as to determine a distribution of diffusion coefficients.

3.1. Alignment of the Spectrometer.

Although the optical alignment of the spectrometer in QELS mode is not as crucial as that when used in intensity measurements, the same method and criteria were used in the alignment of the system. Three stages are necessary to correctly align the system. Firstly the beam from the laser is aligned through a pinhole at the front of the index matching vat and two pinhole attachments mounted on the goniometer arm (set to 0°). This ensures that the beam is parallel to the optical table and follows the optical axis of the instrument. The horizontal alignment of the beam can be confirmed by inserting a thin steel wire mounted to one of the scattering cells. If the optical alignment of the laser is central then as the beam strikes the wire a bright diffraction pattern will be seen.

The second stage of the alignment procedure centres around focusing the laser beam onto the centre of the scattering cell to produce a beam with a narrow "waist" (approx. $150\mu\text{m}$) at the centre of the scattering cell. This is obtained by inserting a lens between the laser head and the index matching cell, the correct position being found by inserting an opaque strip of melinex at the centre of the vat which when in focus produces a characteristic boiling pattern when moved within the beam.

The final stage of the alignment procedure centres around the alignment and focusing of the photo multiplier tube and its associated lenses. A strongly scattering solution is placed into the vat and the PM tube coarsely focused by moving the housing

toward the vat until an image from the scattered beam is in sharp focus. The PM tube housing is then locked to the goniometer arm and the correct focus achieved by adjusting the position of a pinhole located in front of the PM tube.

Finally the alignment of the apparatus was verified by measuring the scattered intensity of a Rayleigh scattering solution (in this case toluene) over the full range of θ available for the instrument. The counts at each angle, normalised to those at 90° as in equation 4.24 should be (1.0 ± 0.05) .

$$I_N = \frac{I_\theta}{I_{90}} \sin \theta \quad 4.24.$$

3.2. Calibration of the Spectrometer.

Although no calibration was required to extract the relaxation rate and hence diffusion coefficient from the decay of the autocorrelation function, it was necessary to calibrate the spectrometer in order to extract the longitudinal osmotic modulus from the absolute intensity of the autocorrelation function.

The theory of the scattering of light by swollen gels was first derived by Tanaka⁴³ who related the spectrum of the scattered light to the kinetics of the movements of the polymer lattice within the gel. In the Tanaka model, the lattice is considered to be an elastic continuum, the motion of which is stimulated by thermal fluctuations with the surrounding solvent.

The two cases of the network moving against the solvent, taking the form of either a longitudinal or a shear wave have been considered separately. The gel is characterised by the elastic retractive forces of the polymer network and a friction factor relating the velocity of the network relative to the solvent and the resistive force provided by the solvent. The field autocorrelation function of the scattered radiation is proportional to the autocorrelation function of the lattice displacements which itself is dependent upon the thermally induced concentration fluctuations within the gel.

Solutions were obtained for non propagating waves, corresponding to longitudinal and transverse displacements. Longitudinal displacements of the lattice refer to polarised scattering and transverse displacements to depolarised scattering.

However the depolarised spectrum is thought too weak to measure⁴³ and not considered further. The correlation function for the longitudinal displacements is predicted to be decay characterised by a single exponential decay of the form given above in equation 4.13. though the relaxation rate Γ is predicted to be related to the co-operative diffusion coefficient D_c through equation 4.25. below.

$$\Gamma = (D_c |q|^2) \quad 4.25.$$

For semi-dilute solutions and polymer gels, a correction procedure has been outlined by Geissler⁴⁴ to correct the measured diffusion coefficient for the effects of solvent back flow in order to calculate the co-operative diffusion coefficient of the polymer. This correction, given in equation 4.26, has been used in all cases of both semi-dilute solutions and swollen networks described in later in this chapter.

$$D_c = \frac{D_{obs}}{(1 - \phi_p)} \quad 4.26.$$

where ϕ_p is the volume fraction of polymer in the semi-dilute solution/gel.

Tanaka related the co-operative diffusion coefficient of the polymer network to the bulk (K) and shear (G) moduli and the friction coefficient (f), of the gel.

$$D_c = \frac{(K + \frac{4}{3}G)}{f} \quad 4.27.$$

The intensity, I, of radiation scattered by concentration fluctuations in a volume of solution V, at a temperature T in a direction perpendicular to the plane of polarisation of the incident beam (intensity I_0) measured by a photo detector at a distance d from the scattering cell is given by equation 4.28.

$$I = \frac{(\pi^2 T k_B I_o V)}{\lambda^4 d^2 \rho \left(\frac{\delta \mu}{\delta w} \right)} \left(\frac{\delta \epsilon}{\delta w} \right)^2 \quad 4.28.$$

where λ is the wavelength of the radiation,

ρ is the density of the solution,

ϵ is the relative dielectric constant,

$\delta\mu/\delta w$ is the gradient of the chemical potential per gram solvent,

and k_B is the Boltzmann constant.

From the Tanaka model it is in principle possible to measure the ratio $(K+4/3G)/f$ from the decay of the field autocorrelation function and $(K+4/3G)$ from the intensity of at zero delay time. The osmotic modulus appropriate to light scattering from gels is that due to plane waves and is given by the longitudinal modulus⁴⁵ defined below in equation 4.29.

$$M_{os} = w^2 \rho \left(\frac{\delta \mu}{\delta w} \right) = K + \left(\frac{4}{3} \right) G \quad 4.29.$$

where w is the weight fraction of polymer in the gel,

ρ is the density of the gel,

and M_{os} is the longitudinal osmotic modulus.

A procedure for the determination of the osmotic modulus from the intensity of the scattered radiation at zero time has been outlined by Geissler and Hecht^{44,46,47} for concentrated polymer solutions and polymer gels, where an optically heterodyned signal is measured at the photo detector. Such a case arises in solutions and gels which have not been filtered to remove dust and other inhomogeneities, which by their very nature scatter much more strongly than the thermodynamic fluctuations and act as ideal operators for optical heterodyning. In such a case, when the scattering from a reference beam is much more intense as compared to the concentration fluctuations, the time dependent part of the signal is given by equation 4.30.

$$I(t) = \frac{cI_0\Delta T}{\rho \left(\frac{\delta\mu}{\delta w} \right)} \left(\frac{\delta\varepsilon}{\delta w} \right)^2 \exp(-\Gamma t) \quad 4.30.$$

where c is a constant depending upon the wavelength, optics, detector and correlator,
 N is the number of pulses generated by the reference signal,
and Δ is the delay period of the correlator.

Although it is in principle possible to determine the system constant c , the procedure is considered tedious due to the many factors involved and gives rise to large errors. An alternative procedure proposed by Geissler is to calibrate the spectrometer with a semi-dilute solution for which the factor $(\rho\delta\mu / \delta w)$ is known. From this it would then be possible to determine the osmotic modulus and co-operative diffusion coefficient simultaneously. Here the spectrometer was calibrated using a solution of polystyrene in cyclohexane of known concentration (weight fraction 0.0995, M_w 145,000 gmol^{-1}) for which the osmotic modulus is known from ultra centrifugation measurements⁴⁸. For such a solution at 318K, the factor $(\delta\mu / \delta w)$ is quoted as 603.4 Nm/Kg, while the density of the solution ρ is predicted to be 778.96 Kg/m^3 from the formula quoted in reference 48.

Therefore for a calibrant solution, c can be determined with more precision than by explicit calculation by measurement of the intensity at zero time delay (relative to a calibrant solution). The decay of the autocorrelation function with time was analysed by fitting a single KWW function to the data, the excess intensity at zero time ($\text{Ex}_{(t=0)}$), was determined by extrapolation to zero time delay of the fit to the data and the value of the excess intensity normalised for the total number of counts received (N), the incident laser beam intensity I_0 and the delay period of the correlator Δ to give a value of the normalised excess intensity $I(0)$ as given by equation 4.31.

$$I(0) = \frac{\text{Excess}_{(t=0)}}{I_0 N \Delta} \quad 4.31.$$

From equations 4.30 and 4.31 the scattering of the calibrant solution at zero delay time is given by:

$$I(0) = C \frac{T_c}{\left[\rho \left(\frac{\delta \mu}{\delta w} \right)_c \right]} \left(\frac{\delta \varepsilon}{\delta w} \right)_c^2 \quad 4.32$$

$$\text{Where } \left(\frac{\delta \varepsilon}{\delta w} \right) = 2n \left(\frac{\delta n}{\delta w} \right) \quad 4.33.$$

and n is the refractive index of the sample at the wavelength of the incident beam.

By combination of equations 4.32. and 4.33., equation 4.34 is obtained.

$$I(0) = C' \frac{T_c}{\left[\rho \left(\frac{\delta \mu}{\delta w} \right)_c \right]} n_c^2 \left(\frac{\delta n}{\delta w} \right)_c^2 \quad 4.34.$$

It is assumed in this work that the refractive index of polystyrene gels and solutions is the same at any concentration of polymer. Hence using the same experimental geometry to measure the scattering from the calibrant, it is possible to determine the factor $(\rho \delta \mu / \delta w)$ for the gel and hence calculate the osmotic modulus of the gel from the absolute intensity using equation 4.35. The refractive index variation of the solution with polymer concentration has been taken from the literature^{2,44,47}.

$$\rho \left(\frac{\delta \mu}{\delta w} \right) = \left(\frac{I(0)_c}{I(0)} \right) \cdot \left(\frac{T}{T_c} \right) \cdot \left[\frac{n^2 \left(\frac{\delta n}{\delta w} \right)^2}{n_c^2 \left(\frac{\delta n}{\delta w} \right)_c^2} \right] \cdot \left[\rho \left(\frac{\delta \mu}{\delta w} \right)_c \right] \quad 4.35.$$

As the measurement of the osmotic modulus requires the measurement of the *heterodyne* correlation function it was eminently suitable for swollen networks prepared using unfiltered solvent where dust could not be excluded, however a heterodyne technique was found impractical in the measurement of semi-dilute solutions as dust was found to produce QELS spectra with relaxations which interfered with the resolution of

the those relaxations arising from the semi-dilute solution (discussed later in this chapter), thus making the heterodyne technique unsuitable for semi-dilute solutions.

4. Experimental.

Samples for QELS study were prepared by three different procedures, depending on the type of sample and the desired experiment to be carried out, though all of the methods used followed some similar principles in the preparation of solvent and glassware etc. The optical apparatus of the 4700 correlator was itself entirely contained on a gas damped optical table housed in a purpose built light scattering laboratory devoid of natural light, illuminated by dimmed tungsten filament bulbs so as to reduce the background scattering intensity.

4.1. Preparation of Solvents and Glassware for QELS Studies.

As noted earlier, homodyne QELS experiments rely upon measuring only the correlation function arising from the concentration fluctuations of the polymer system. Therefore it is essential that particulate matter, particularly small dust moieties are excluded from the sample in order not to affect the homodyne experiment. To this end solvents used in the measurement of the self diffusion coefficient have been carefully prepared to remove impurities.

Analar grade cyclohexane and toluene solvent (BDH) were refluxed for around 90 minutes over 3Å molecular sieves in order to remove any residual traces of water. The solvent was then doubly distilled into an appropriately sized flask which was immediately sealed with a self sealing rubber membrane. Quantities of solvents were then extracted from this stock source as required and were removed with a syringe equipped with an air tight PTFE plunger.

Glassware used in QELS experiments were scrupulously cleaned by a two stage process which firstly removed all traces of any organic residues by steeping in permanganic acid for at least 12 hours. Following the neutralisation of the acid with

large amounts of distilled water, all traces of dust were removed from the glassware by rinsing with large volumes of acetone (filtered through a 0.2 μ m membrane) and then sealed with a small covering of aluminium foil before being dried inverted in an oven at around 345K for 24 hours.

4.2. Dilute Solution Measurements of the Tracer Diffusion Coefficient.

Prior to the preparation of any solutions for QELS study, the "clean" solvent was filtered repeatedly (around 5-6 times at rates of approx. 1cm³min⁻¹) through a 0.2 μ m PTFE membrane filter (Millipore) in order to remove any dust present in the solvent. The appropriate quantity of polymer was then weighed directly into a "cleaned" volumetric flask and approximately 75% of the required solvent directly filtered into the flask. It was found that covering the neck of the volumetric flask with a small "membrane" of aluminium foil was a useful method of excluding dust from the flask.

Following 24 hours equilibration of the solution at around 315K the remainder of the solvent was added to the flask and the weight of the flask noted accurately. From the weights of both polymer and solvent and using the empirical calculation¹⁹ outlined below for the temperature dependence of the density of the solvent, the concentration of polymer in cyclohexane at any temperature in the range 308-323K could be determined.

$$\rho_t = \left[\rho_s + 10^{-3} \alpha (T - T_s) + 10^{-6} \beta (T - T_s)^2 + 10^{-9} \gamma (T - T_s)^3 \right] \quad 4.36.$$

where ρ_t is the density of the solvent at temperature T (in degrees Celsius),

ρ_s is the density of the solvent at the reference temperature of zero Celsius,

and $\alpha = -0.8879$, $\beta = -0.972$ and $\gamma = 1.55$.

Scattering cells used in the determination of the tracer diffusion coefficient were precision circular (10mm diameter) optical cells obtained from Hellma UK which allowed the measurement of the correlation function at a range of angles. Solutions for scattering were filtered directly into the cleaned cell through an aluminium foil membrane which was then immediately replaced by a PTFE stopper which made an intimate contact

with the walls of the scattering cell. Prior to scattering, the solution was allowed to come to thermal equilibrium within the vat for around 10 minutes, having been held at that temperature for at least one hour.

4.3. Preparation of Semi-Dilute Solutions for QELS Study.

In the measurement of the diffusion coefficient of semi-dilute solutions (and also those solutions containing a small fraction of probe chain) the scattering solution was prepared by weighing both the polymer and the cleaned solvent directly into a cleaned scattering cell. The high viscosity of such solutions prevented filtering the solution through a membrane filter into the cell. It was also found that the high polymer concentration required that the solution took upwards of 21 days to reach equilibrium (around 7 days after complete dissolution) which for cyclohexane solutions was necessarily performed at 313K. Therefore it was found necessary to seal the solutions into the cells so as to avoid solvent loss due to evaporation at elevated temperatures.

Cells were filled with solution and the stopper placed in position and immediately sealed with a rapid araldite adhesive which was designed to remain in place for the lifetime of the cell. Following full cure of the adhesive (approximately 24 hours) the weight of the cell was noted and the equilibration procedure started, the weight of the cell was then periodically checked so as to ensure that no solvent was lost. It was observed that some cells lost weight during this period and these cells were discarded and fresh samples prepared.

Cyclohexane solutions were allowed to equilibrate for around 24 hours at the measurement temperature before transfer to the scattering vat. Once placed in the instrument, around 30 minutes were allowed to bring the solution to final equilibrium. Although sealing the scattering cell with epoxy adhesive was found to prevent solvent loss on prolonged heating, it was not thought desirable to seal solutions into precision optical cells as those cells were very expensive and recovery of the cell could not be guaranteed following completion of the experiment. It was therefore necessary to use a

more cost effective method which was found to be the in-house manufacture of suitable cells.

To facilitate this, thick walled quartz glass tubing (10mm inner diameter, wall thickness 1mm) was cut into small sections of a length comparable to the precision cells and one end sealed using an acetylene/oxygen flame. Any jagged edges were then removed from the second end of the cell and the cell cleaned in the manner described above prior to use. For these experiments, where the scattering geometry was fixed at 90 degrees these cells were found to be entirely suitable for the purpose of the experiment. However, for those few experiments requiring multi-angle measurements, precision cells were used and carefully recovered after use.

4.4. Preparation of Swollen Gels for QELS Study.

As a result of the large quantities of unfiltered solvents used in the synthesis of the polymer networks it was thought to be unlikely that the gels could be studied by QELS in the homodyne mode. For this reason it was decided to study the swollen gels with heterodyne QELS. Therefore following cleaning of the scattering cells, gel samples were carefully inserted into the cell and the cell filled with solvent. No attempt was made to filter the solvent as it was advantageous to have dust present to act as a local operator for optical heterodyning. The cells used in the study were again precision optical cells purchased from Hellma. For these measurements it was chosen to study the scattering at 90 degrees and therefore square cells with a path length of 10mm were used in the measurements. It was not found to be necessary to seal the lids of the cells with adhesive as there was good contact between the cell and the PTFE stopper which minimised any solvent losses. Regardless of any solvent loss, the polymer in the gel automatically maintained its volume fraction and as the cell was filled with an excess of solvent it was only necessary to ensure that an excess was present in the cell.

Suitable samples of the network, dried to the bulk to remove all residual traces of benzene were cut to approximately the size of the scattering cell using a sharp razor

blade. The sample was then swollen for around 4 days before carefully cutting the swollen sample to the appropriate dimensions. In the case of those networks swollen in cyclohexane this procedure was carried out at a temperature of around 308K so as to minimise the effects of solvent expulsion occurring below the theta point. Cyclohexane swollen samples were then allowed to reach thermal equilibrium at 308K over a 7 day period before being transferred to the correlator where at least 30 minutes was allowed for final equilibration of the sample. A similar procedure was adopted for those samples swollen in toluene, these were allowed to reach equilibrium over a 10 day period at 298K before being transferred to the correlator. Again around 30 minutes was allowed for equilibration in the vat before beginning the experiment.

5. The Probe Chain Tracer Diffusion Coefficient.

In these experiments the tracer diffusion coefficients of those polymer molecules used within model networks as trapped probe chains were established in dilute solution. Although considerable effort has been focused upon the study of the dilute solution properties of both flexible and rigid polymers^{16, 34-41}, it was important within this work to determine the diffusion coefficient of the polymers in dilute solution so as to provide a comparison with the behaviour found when the probe chain interacts with the "matrix" of polymer chains in the swollen network or the semi-dilute solution.

Solutions for QELS studies were prepared as outlined in section 4 above and data collected in homodyne mode. As the QELS measurements focused upon the determination of the diffusion coefficients it was deemed to be unnecessary to study the diffusion as a function of scattering angle (dilute solutions of polystyrene in cyclohexane and toluene have been extensively studied^{16, 34-41} by QELS as a function of scattering angle and the results well documented) and therefore all QELS data was collected at a scattering angle of 90°. The dilute solution behaviour of five polymers (molecular weights 10,000, 52,000, 120,000, 330,000 and 1,008,000 gmol⁻¹) was studied in cyclohexane and toluene. Data was collected on the Malvern 4700 correlator utilising an

incident laser beam of intensity approximately 35mW (somewhat lower than the theoretical maximum power available due predominately to the age of the laser).

Dilute solutions of the probe polymer in cyclohexane were studied in the temperature range 308-333K. The scattering rate was found to be a maximum at the theta point and high quality data was collected in experimental times of the order of a few minutes. However for solutions at higher temperatures and lower concentrations the scattered intensity decreased and it was therefore necessary to increase counting times to the order of several hours in order to obtain a suitable correlogram. In such cases the data set making up the correlation function may consist of only a single correlogram.

Dilute solutions of polystyrene in toluene at 298K were prepared and the most concentrated solutions investigated by QELS. However it was found that the count rate obtained was considerably lower than for cyclohexane solutions of equivalent concentration and suitable quality data could not be obtained within reasonable experimental times. It was also found that during such long experiments in toluene there was a large interference from dust within the solution and satisfactory results could not be obtained. The necessity for long experimental times was thought to arise from a combination of a low incident laser intensity and a lower refractive index increment for the probe polymers in toluene.

A similar situation was also encountered in the QELS study of the lowest molecular weight polymers in cyclohexane solution. Again it was found that the count rates obtained from polymers "Probe 1" and "Probe 2" (molecular weights 10,000 and 52,000 gmol^{-1} respectively) were very low, even in the most concentrated solutions and it was found to be impossible to study effectively the behaviour of these polymers in dilute solution. Hence it was reasoned that it would also be impossible to study the behaviour of those polymers as probe chains within ternary semi-dilute solutions and when trapped within networks as it was anticipated that the scattering from the matrix would greatly outweigh that from the probe chain and resolution would be impossible.

From the results of these preliminary QELS measurements in dilute solution, it was decided not to prepare networks containing either probe 1 or probe 2 polymers as the trapped chain and the behaviour of these polymers was studied no further.

The diffusion coefficient measured by QELS, D_{obs} , is only a measure of the tracer (or self-diffusion) coefficient (D_t or D_s) in dilute solution where the polymer chains do not interact. In more concentrated systems such as semi-dilute solutions, the diffusion coefficient determined by QELS is a co-operative diffusion coefficient (D_{co}) measuring the relaxation of interacting particles. In the limit of infinite dilution, the co-operative and tracer diffusion coefficients become identical, however with increasing concentration, D_{co} becomes substantially larger than D_t which becomes vanishingly small and approximates to zero in concentrated systems. The tracer diffusion coefficient was determined by extrapolation of the observed diffusion coefficient to zero concentration following equation 4.37 which relates the tracer diffusion coefficient at any given concentration by a polynomial expansion in terms of the polymer concentration.

$$D_{obs} = D_t(1 + k_d c + k_d^1 c^2 + \dots) \quad 4.37$$

In the limit of a dilute solution equation 4.37. reduces to equation 4.38.

$$D_{obs} = D_t(1 + k_d c) \quad 4.38$$

Clearly the choice of the concentration regime studied is very important in the correct determination of the tracer diffusion coefficient. To ensure that only dilute solution behaviour was determined, a maximum concentration was chosen for each polymer this concentration being substantially below the overlap concentration c^* . In all cases this maximum concentration was chosen to be $c^*/5$. The behaviour of the polymer was then determined by studying upto six solutions within the range ($c^*/20 \leq c \leq c^*/5$) prepared by dilution of the $c^*/5$ stock solution.

Data collected on the spectrometer was analysed by two methods. Firstly data was fitted to a single exponential function (given in equation 4.13.) using a least-squares

fitting procedure, the criteria for a successful fit being a difference of less than 10^{-7} in successive values of chi-squared. Secondly data was analysed by directly inverting the Laplace transformation using CONTIN to produce a distribution of relaxation times and hence diffusion coefficients. Figure 4.4 below shows a typical single exponential fit to the QELS data arising from SIQELS, while figure 4.5 parts A and B show a typical fit to the normalised correlation function and the distribution of diffusion coefficients associated with the fit.

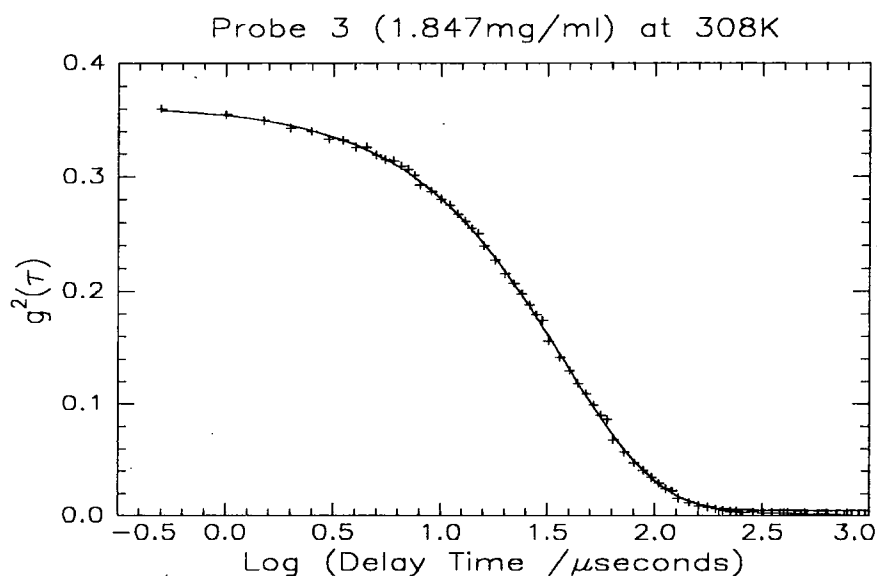


Figure 4.4.: Single Exponential Fit to Correlation Function from SIQELS.

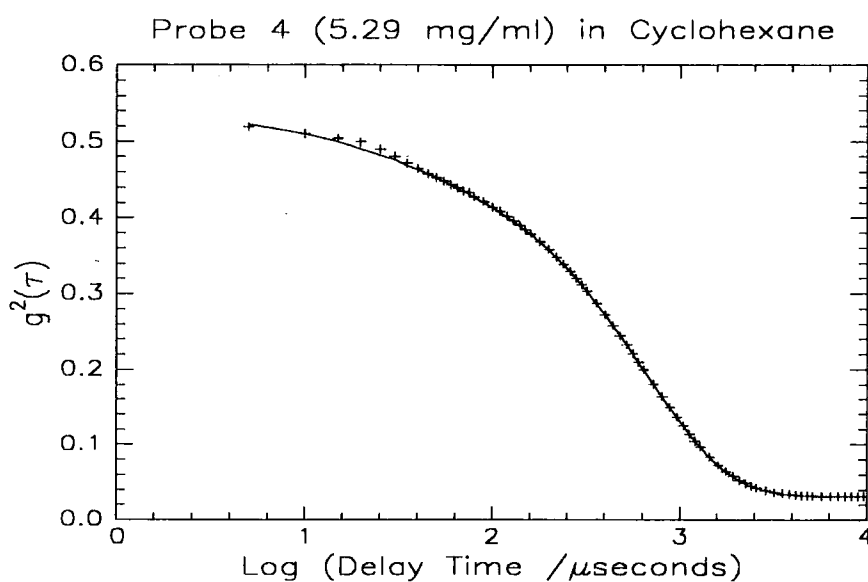


Figure 4.5.A. CONTIN Fit to data From Probe 4 Solution in Cyclohexane

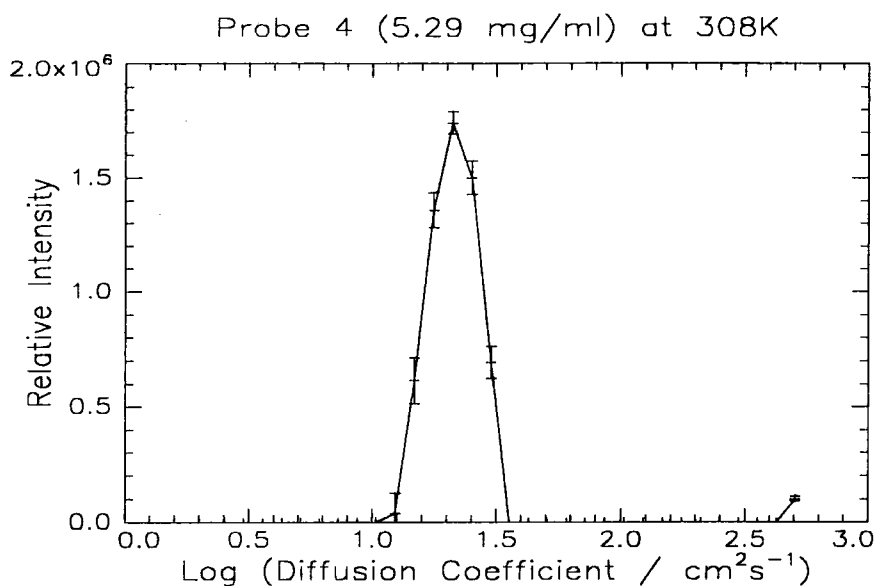


Figure 4.5.B.: Distribution of Diffusion Coefficients Arising from Figure 4.5.A.

Figure 4.5.B shows a single peak of narrow distribution ($D_w/D_n = 1.04$) in the spectrum of diffusion coefficients. This was found to be typical of all solutions investigated within the region of $10^{-8} < D_{\text{obs}} \text{ (cm}^2\text{s}^{-1}\text{)} < 10^{-6}$. However in certain cases peaks of low intensity (approximately 1-2%) having large errors were found at both the extreme fast and slow ends of the distribution spectra.

Such peaks have been found in previous QELS studies^{15,25,33} and have been variously attributed to small amounts of dust (peak at the slow end of the distribution) and small amounts of noise present in the spectra. Provencher²⁵ studied the peak at the fast extreme and found that the peak disappeared in simulated data without noise, whilst when noise is added to the spectra the small peak frequently appears. The presence of this peak does not affect the position or distribution of the main peaks in the spectra.

5.1. Tracer Diffusion Coefficients in Cyclohexane Solution.

The tracer diffusion coefficient of the probe polymers were determined in cyclohexane solution at temperatures of 308, 313, 318 and 323K. Results arising from fitting the data to a single exponential function and by Laplace transformation using CONTIN are given in appendices C1-C3 for polymers within the temperature range 308-323K.

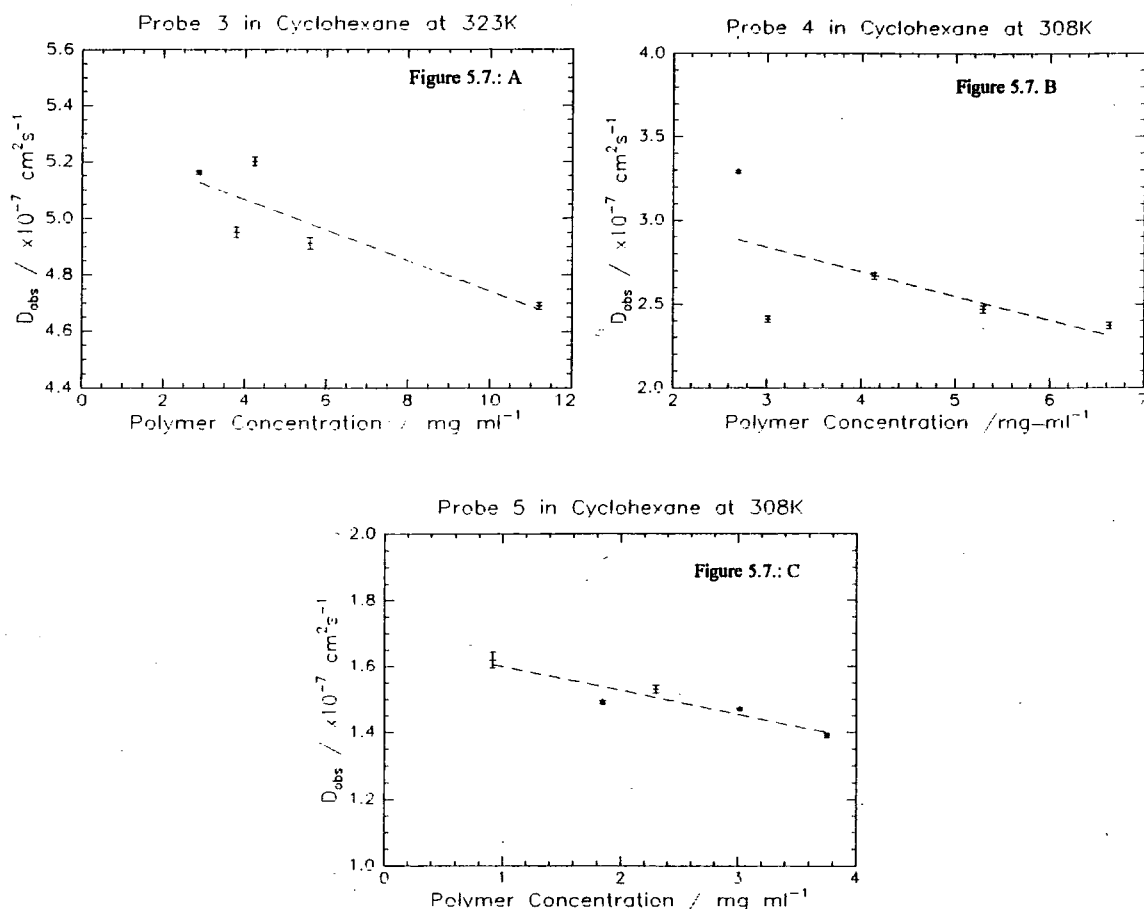


Figure 4.6. Parts A-C: Variation of Diffusion Coefficient with Polymer Concentration for the Probe Polymers in Cyclohexane Solution.

D_t was determined from the single exponential fits by extrapolation to zero concentration of a plot of D_{obs} against polymer concentration. Typical plots are given in figure 4.6, parts A-C, the tracer diffusion coefficient and the normalised slope (k_d) being determined from the intercept and ratio of the slope to intercept respectively.

Full results of the QELS experiments are given in appendix C, from which three noticeable features can be seen. Firstly in all cases within the molecular weight and temperature range studied, the diffusion coefficient of the probe chain decreases with increasing polymer concentration. This is clearly reflected in the values of k_d presented below in table 4.1 A-C, which show that in all cases regardless of probe chain molecular weight or temperature, k_d is negative leading to a decrease in the diffusion coefficient with increasing concentration.

Table 4.1. A.: Probe 3 QELS Results in Cyclohexane between 308K and 323K				
Temperature / K	308K	313K	318K	323K
$D_1 / \times 10^{-7} \text{ cm}^2 \text{ s}^{-1}$	4.23 ± 0.19	4.65 ± 0.08	4.91 ± 0.06	5.28 ± 0.11
$k_d / \text{ml mg}^{-1}$	-0.022 ± 0.017	-0.019 ± 0.011	-0.012 ± 0.006	-0.010 ± 0.009

Table 4.1. B.: Probe 4 QELS Results in Cyclohexane between 308K and 323K				
Temperature / K	308K	313K	318K	323K
$D_1 / \times 10^{-7} \text{ cm}^2 \text{ s}^{-1}$	3.27 ± 0.05	3.68 ± 0.05	4.23 ± 0.03	4.51 ± 0.03
$k_d / \text{ml mg}^{-1}$	-0.044 ± 0.006	-0.041 ± 0.009	-0.043 ± 0.003	-0.036 ± 0.003

Table 4.1. C.: Probe 5 QELS Results in Cyclohexane between 308K and 323K				
Temperature / K	308K	313K	318K	323K
$D_1 / \times 10^{-7} \text{ cm}^2 \text{ s}^{-1}$	1.67 ± 0.04	1.80 ± 0.05	1.97 ± 0.05	2.15 ± 0.06
$k_d / \text{ml mg}^{-1}$	-0.043 ± 0.001	-0.036 ± 0.001	-0.034 ± 0.001	-0.032 ± 0.001

Table 4.1. A-C : Tracer Diffusion Coefficients of Probe Chains.

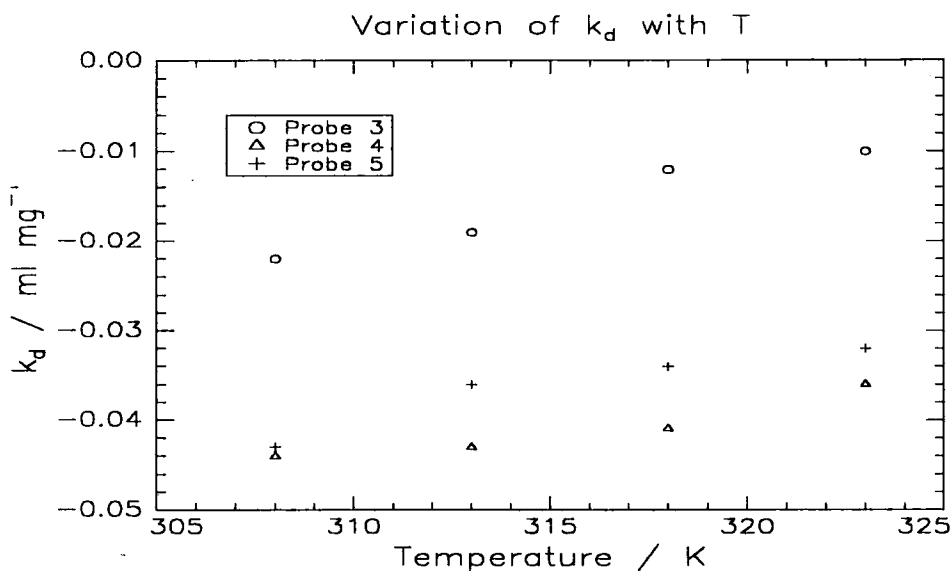


Figure 4.7. Variation of k_d with Temperature for Probe Polymers in Cyclohexane.

Values of k_d taken from table 4.1. A-C are plotted against the temperature of the system in figure 4.7, where it can be seen that k_d for the probe 3 polymer is somewhat less negative than those obtained for the higher molecular weight polymers, probes 4 and 5, indicating that at temperatures higher than those studied here the diffusion coefficient may become independent of concentration and eventually increase with concentration as

k_d initially becomes zero and finally greater than zero at a given temperature. Behaviour of this type has been seen by Caroline³⁹ who found that solutions of polystyrene (M_w 1,260,000 g mol^{-1}) in cyclohexane exhibited no concentration dependence at a temperature around 323K. Above this temperature, the diffusion coefficient was found to increase with concentration. The increase in the value of k_d with temperature has been rationalised by Caroline in terms of the intermolecular repulsion and the degree of excluded volume present in the system.

For a system at the theta point, although the excluded volume is zero, the slope is negative as the diffusing molecules occupy a finite volume. Increasing the temperature causes an increase in the excluded volume and hence intermolecular repulsion which begins to balance this volume effect.

Figure 4.8. below shows the tracer diffusion coefficient of the probe chain increases as the temperature of the system is increased above the theta point.

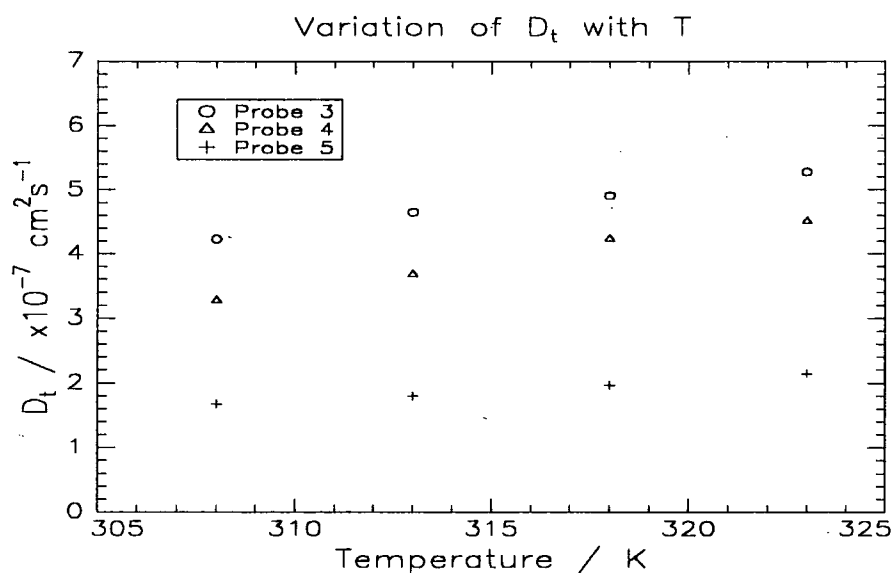


Figure 4.8.: Variation of the Tracer Diffusion Coefficient with Temperature for Probe Chains in Cyclohexane Solution

This increase in D_t with increasing temperature has been noted in previous studies of the diffusion of polystyrene in cyclohexane^{38,39}. Caroline has shown that the

hydrodynamic radius of the polymer (determined from the tracer diffusion coefficient using the Stokes-Einstein equation), increases in a smooth manner with temperature above the theta point. Although an increase in the hydrodynamic radius above its unperturbed value might be expected to lead to a decrease in the diffusion coefficient, both the increase in temperature and decrease in the solvent viscosity outweigh this increase in size and cause the increase in the diffusion rate.

Figure 4.8. also shows the tracer diffusion coefficient at any given temperature to be dependent on the molecular weight of the polymer, an increase in the polymer molecular weight corresponding to a decrease in the tracer diffusion coefficient. This can be more clearly seen below in figure 4.9. which shows the variation of the tracer diffusion coefficient with the molecular weight of the probe chain for the theta system at 308K in cyclohexane. From a least squares fit to the data, the following relationship was found between the tracer diffusion coefficient and the polymer molecular weight.

$$\text{Log}(D_t) = (2.88 \pm 0.55) - (0.44 \pm 0.09)\text{Log } M_w$$

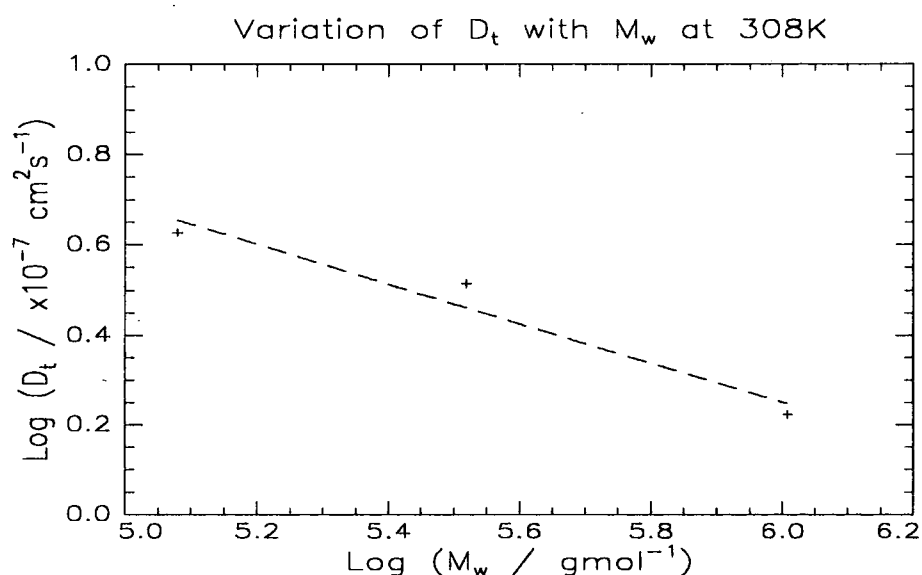


Figure 4.9. : Log-Log Representation of the Variation of the Tracer Diffusion Coefficient with Probe Chain Molecular Weight at the Theta Point.

This is in strong agreement with previous studies of the variation of D_t with M_w at the theta point for polystyrene in both cyclohexane which find that the diffusion coefficient at the theta point can be given by the following relationship³⁵ which is itself in good agreement with theoretical predictions for dilute solution behaviour⁴².

$$D_t(\theta) = (1.4 \pm 0.2) \times 10^{-4} M_w^{-(0.508 \pm 0.007)} \text{ cm}^2\text{s}^{-1}$$

Although considerable effort has previously been expended by several workers on the study of the properties of dilute solutions of polystyrene in cyclohexane, the results determined here allow the prediction of the probe chain diffusion coefficient at any concentration and temperature in dilute solution. This allows a direct comparison with the probe chain diffusion coefficient obtained from either the dilute solution of the probe trapped within a network or in the ternary semi-dilute solution.

6. Quasi-Elastic Light Scattering From Model Polystyrene Networks.

In this series of experiments the co-operative diffusion coefficient and longitudinal osmotic modulus of model polystyrene networks were determined as a function of the polymer volume fraction in gels swollen to equilibrium in cyclohexane and toluene using Quasi-Elastic Light Scattering. Networks suitable for QELS study were prepared using the method outlined in section 4 of this chapter. Networks synthesised in "clean" unfiltered solvent were thought unsuitable for study by homodyne QELS as it was felt that residual traces of dust present in the network (arising from the dusty solvent used in the preparation of the experiment) would interfere with the scattering from the concentration fluctuations under consideration in the homodyne experiment.

For these reasons it was decided to adopt a heterodyne QELS technique in the measurement of the diffusion coefficient as the presence of dust would be advantageous, acting as a local operator for optical heterodyning. To this end no effort was made to filter the solvent used to swell the network to ensure full heterodyne efficiency.

Generally it is not simple to distinguish between heterodyne and homodyne detection modes, except at low scattering angles where heterodyne signals are almost unavoidable. One test of heterodyne geometry utilises split beam geometry where radiation from an external oscillator is mixed with the scattered signal to prove the observations are made in heterodyne mode. For results made in heterodyne mode, the results should compare with those from the split beam technique. A second possible check of the nature of the signal follows the variation of the signal with the scattering angle. Where a heterodyne signal is contaminated by a homodyne signal, the ratio of the relaxation rate to the square of the scattering vector becomes dependent upon the scattering angle. However, it was found difficult to prepare gel samples which were in intimate contact with the walls of circular scattering cells to check this assumption. It is noted that measurements by other workers using split beam geometry indicate that the quasi elastic signal is fully heterodyned by local oscillators⁴⁹⁻⁵¹.

To ascertain the heterodyne nature of the signals measured here, a fine steel wire was carefully inserted into one of the swollen polymer networks. This wire was placed into the scattering volume defined by the intersection of the incident beam and the photo multiplier tube and when correctly aligned acted as a local oscillator providing a large unshifted beam which mixed with the frequency shifted radiation from the scattering particles. Considerable time was taken to achieve the correct positioning of the wire which was found when the scattering rate at the photo detector increased significantly as compared to the signal received without the inserted wire.

This procedure was only performed once in a gel sample swollen in cyclohexane at 308K to check the nature of the signal as the procedure was found to be time consuming. The spectra from both the raw gel and the gel plus wire are shown below in figure 4.10. As can be seen the two data sets are very similar, having almost identical relaxation rates and normalised scattering excesses, thus indicating that the spectra from the dusty, swollen gels are fully optically heterodyned.

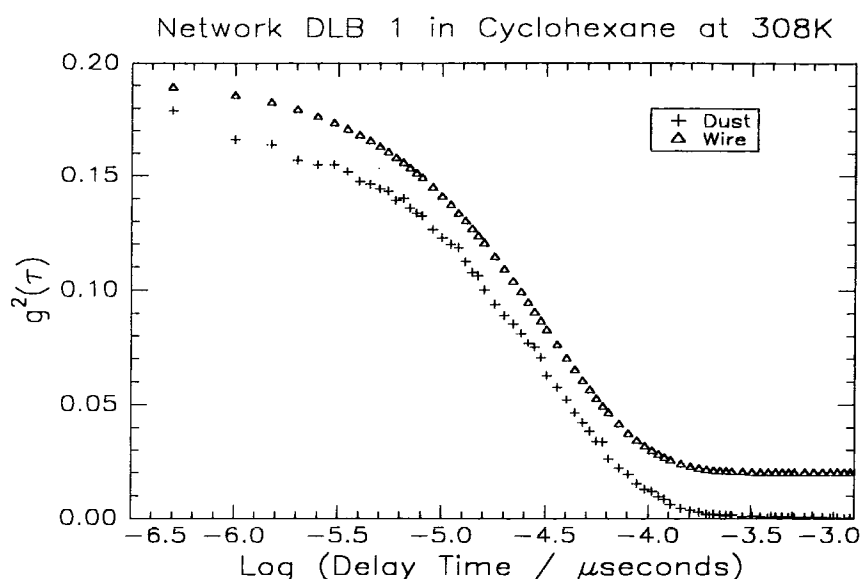


Figure 4.10.: Comparison of Heterodyne Signal Arising from Local Oscillation with Dust Compared to Thin Wire Technique. Data Sets Have Been Vertically Offset for Clarity.

QELS data from solvent swollen networks were generated in two experimental series. In the series of experiments performed in February/March 1993, QELS spectra were recorded from networks prepared using the AMS/DVB system. The incident laser power at the sample was measured as being 35-40mW and networks swollen in cyclohexane in the range 308-323K and in toluene at 298K were studied. In the series of experiments performed in June/July 1994, QELS spectra were recorded from networks prepared from the PBMPPD/DVB system which were again swollen in cyclohexane in the range 308-323K and in toluene at 298K. For this series of experiments, the incident laser power at the sample was measured to be 10-15mW which led to difficulties in the extraction of the relaxation rate of the gel due to the long count times necessary for the measurement of the correlation function.

This difference in the incident laser power was predominantly due to the advancing age of the laser at the time of measurement and may have lead to the production of spectra of lower quality than might have been attained with a laser of higher power. Unfortunately it was not possible to increase the output power of the

laser and time constraints prevented re-measurement of the spectra with a more powerful laser which subsequently became available.

Scaling theory has been used by de Gennes to relate the co-operative diffusion coefficient and hydrodynamic correlation length (ξ_h), showing the two to be inversely related through equation 4.39.

$$\xi_h = \frac{k_B T}{6\pi\eta_0 D_{co}} \quad 4.39.$$

where k_B is the Boltzmann constant,

T is the absolute temperature

and η_0 is the solvent viscosity.

As described in chapter 1, various scaling regimes have been introduced to relate the correlation length of the gel to the polymer concentration, different regimes existing for different polymer-solvent interactions. For a polymer gel in the theta state, the correlation length is predicted to be related to the polymer volume fraction through equation 4.40. while for a gel in a good solvent the correlation length is expected to depend less strongly on the concentration (equation 4.41.)

$$\xi_h = \phi_p^{-1} \quad 4.40.$$

$$\xi_h = \phi_p^{-3/4} \quad 4.41.$$

Therefore for the polystyrene-cyclohexane system at the theta point D_c is expected to be related to the polymer concentration by equation 4.40, while 4.41. is expected to relate the two in the polystyrene-toluene system.

6.1. General Features of the QELS Spectra.

Perhaps the most noticeable feature of the data collected from both series of networks was the relatively low statistical quality of the data obtained from both the AMS/DVB and PBMPPD/DVB series of networks compared to those obtained from solutions of equivalent concentration. This feature is most noticeably marked for the

PBMPPD/DVB series of networks which were studied using a much weaker incident laser beam. Spectra from these networks were obtained in experimental times of the order of 1500 to 1800 seconds which compared to acquisition times of around 60 seconds necessary for the generation of data from the AMS/DVB system.

Spectra were analysed by two methods. Firstly the normalised correlation functions were fitted to a single Williams-Watts (KWW) stretched exponential function using SIQELS. Fitting to the KWW function was found to be preferential over a two cumulant fit as the fit to the data was found to be consistently better with a more random distribution of the residuals. A typical KWW fit is shown below in figure 4.11. Although the theory of Tanaka predicts that the decay of the concentration fluctuations is described by a single exponential decay, this was found not to be the case with a significant amount of broadening of the decay modes. This is a feature that has also been noted by other workers who have studied randomly cross linked polystyrene networks swollen in cyclohexane^{44,52}.

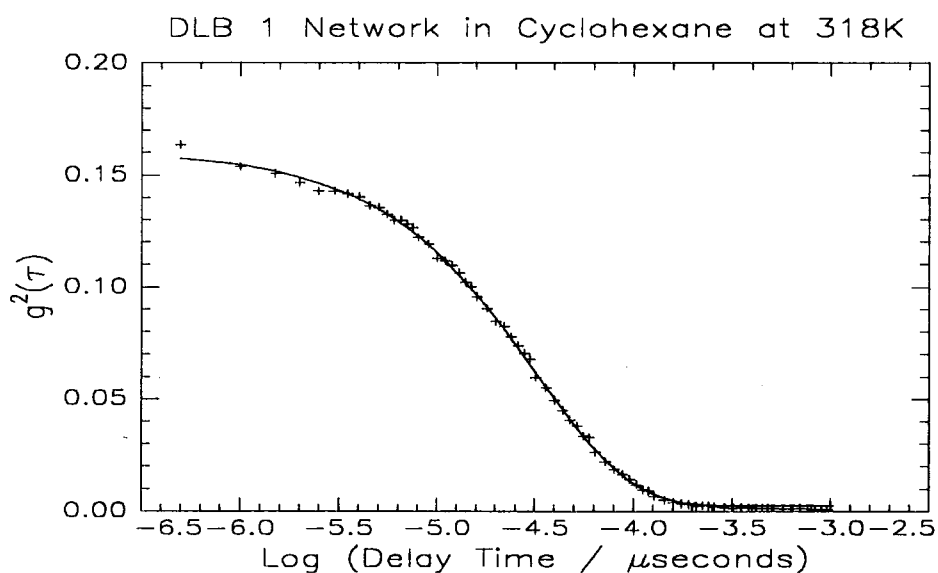


Figure 4.11.: Single KWW fit to QELS Data from Cyclohexane Swollen Network

Data was also analysed by direct determination of the inverse Laplace transform using CONTIN. Similarly to the ILT measurements described earlier this produced a distribution of decay times within the region ($10^{-9} < D_{\text{obs}} / \text{cm}^2 \text{s}^{-1} < 10^{-5}$).

One feature that was frequently noticed in the KWW fit to the data from AMS/DVB gels was a small deviation of the experimental data from the fit at high delay times as the experimental correlation function gently sloped into the baseline. This feature was found present in many spectra (though it did not correlate with any particular network cross link density or temperature) and may have indicated the presence of a second relaxation mode within the gel, however it was not possible to resolve the mode or infer any more information from the KWW fit. However within the CONTIN distribution of diffusion coefficients, a very large peak was found in nearly all cases at around $10^{-9} \text{ cm}^2\text{s}^{-1}$ as well as the peak arising from the decay of the concentration fluctuations at approximately $10^{-7} \text{ cm}^2\text{s}^{-1}$. From the large magnitude of the slow decay in the CONTIN analysis, it is thought that the small kink in the KWW fit was an artefact of the peak at $10^{-9} \text{ cm}^2\text{s}^{-1}$ which was a feature of the motion of the dust moieties within the gel.

This peak in the CONTIN spectra was also seen in networks prepared from the PBMPPD/DVB system, though in no cases was any deviation in the fit to the KWW function observed in SIQELS. A further artefact of the CONTIN spectra was the continued presence of a very small peak occurring at $10^{-5} \text{ cm}^2\text{s}^{-1}$. As explained in section 5 earlier, this is a small peak added by CONTIN to increase the "goodness of fit" and is particularly present in noisy spectra.

In all cases, some departure from the predicted single exponential decay was observed from both AMS/DVB and PBMPPD/DVB networks swollen in cyclohexane. A measure of the departure from the single exponential behaviour is given by both the polydispersity of the measured diffusion coefficient (CONTIN) and the variance of the KWW fit (the β parameter determined by SIQELS). Values of β and the polydispersity are given in appendix C(4-6) for networks swollen in cyclohexane and toluene. No correlation could be made for values of β or the polydispersity with either the cross link density of the network or the temperature for either the AMS/DVB or PBMPPD/DVB systems. In all cases, it was found that β was generally closer to unity for the

PBMPPD/DVB networks than for the AMS/DVB gels indicating that the AMS/DVB networks had a less exponential behaviour, possibly due to the presence of other decay modes in the AMS/DVB series of networks, though it is thought that lower values of β are more likely to arise as a result of the relatively poor quality of the AMS/DVB networks produced with a more open structure, containing large quantities of pendant chains within the network.

The homogeneity of networks produced from the AMS/DVB system, was determined by studying the spectrum of light from three independent regions of the gel when swollen in cyclohexane in the region 308 to 323K. Little variation was found in the values of the co-operative diffusion coefficient obtained from different regions of the gel and those values quoted in appendix C4-6 are a direct average of the fifteen measurements made at each temperature. Measurements of the longitudinal osmotic modulus from any one region of the gel were found to be very precise, though values determined from different regions were found to be somewhat more different.

Within a series of measurements from any one position within the gel the normalised intensity was found to vary by up to 15% and for different positions within the gel variations of up to 40% were observed. Values of the osmotic moduli of the AMS/DVB networks quoted in appendix C7 are a direct average of the fifteen measurements made at each temperature.

Unfortunately, time constraints prevented repeated QELS measurements of the scattered spectra from different regions of PBMPPD/DVB networks and those values quoted for D_c and M_{os} in appendix C7 are simply an average of 5 measurements from one position within the gel.

6.2. The Co-operative Diffusion Coefficient.

The decay constant was extracted from each spectra by fitting the data to the KWW model function as described earlier. The heterodyne D_{obs} was then extracted

from the decay constant through equation 4.25 and finally corrected for solvent back flow using equation 4.26 to give a value of the co-operative diffusion coefficient. Values of D_{co} were also extracted from CONTIN and a distribution of diffusion coefficients obtained. Results from both the AMS/DVB and PBMPPD/DVB series of networks are given in appendix C4-6, the results quoted are an arithmetic mean of at least five spectra, the error quoted for the data is the standard deviation about the mean which is most probably a conservative estimation of the error, the real error probably being larger.

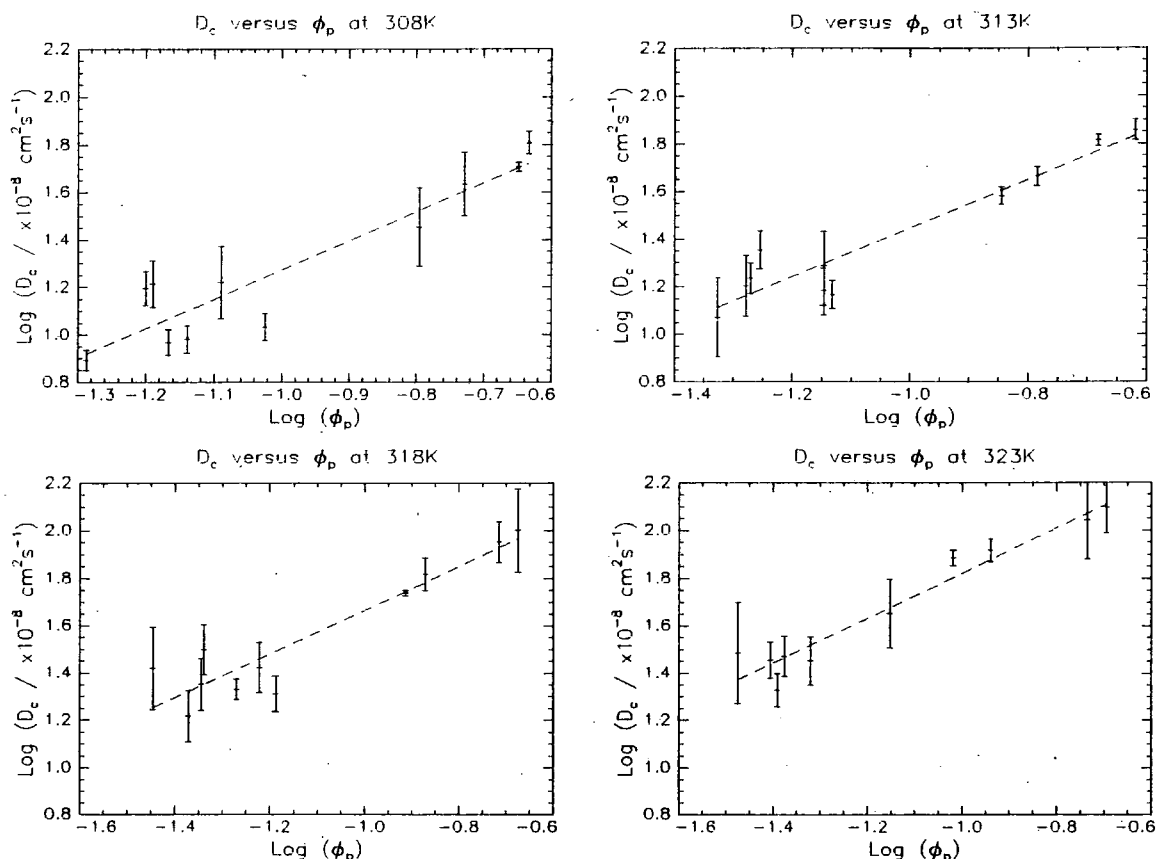


Figure 4.12.: Log-Log Plots of the Co-operative Diffusion Coefficient Against the Polymer Volume Fraction in AMS/DVB and PBMPPD/DVB Networks Swollen in Cyclohexane in the Temperature Range 308-323K.

For both series of networks it was found that the diffusion coefficient of the gel increased with the temperature of the system when swollen in cyclohexane, as might be expected from equation 4.39. where the factor T/η increases by a factor of nearly 1.5 in the temperature range 308-323K⁵³. At constant temperature the diffusion coefficient

can also be seen to increase with the polymer volume fraction. Results from SIQELS analysis for both series of gels are shown in figure 4.12. in double logarithmic format to allow the determination of the various scaling exponents.

The equations describing the curves shown in figure 4.12. are:

$$308\text{K: } \text{Log } D_c (\times 10^{-8} \text{ cm}^2\text{s}^{-1}) = (2.49 \pm 0.17) + (1.23 \pm 0.16) \text{Log } \phi_p$$

$$313\text{K: } \text{Log } D_c (\times 10^{-8} \text{ cm}^2\text{s}^{-1}) = (2.46 \pm 0.12) + (1.02 \pm 0.11) \text{Log } \phi_p$$

$$318\text{K: } \text{Log } D_c (\times 10^{-8} \text{ cm}^2\text{s}^{-1}) = (2.59 \pm 0.14) + (0.92 \pm 0.12) \text{Log } \phi_p$$

$$323\text{K: } \text{Log } D_c (\times 10^{-8} \text{ cm}^2\text{s}^{-1}) = (2.76 \pm 0.10) + (0.94 \pm 0.08) \text{Log } \phi_p$$

Figure 4.13. below shows the variation of the co-operative diffusion coefficient with polymer volume fraction for both series of networks swollen in toluene at 298K. From figure 4.13. the scaling relationship in toluene is found to be:

$$298\text{K: } \text{Log } D_c (\times 10^{-7} \text{ cm}^2\text{s}^{-1}) = (3.43 \pm 0.37) + (1.82 \pm 0.23) \text{Log } \phi_p$$

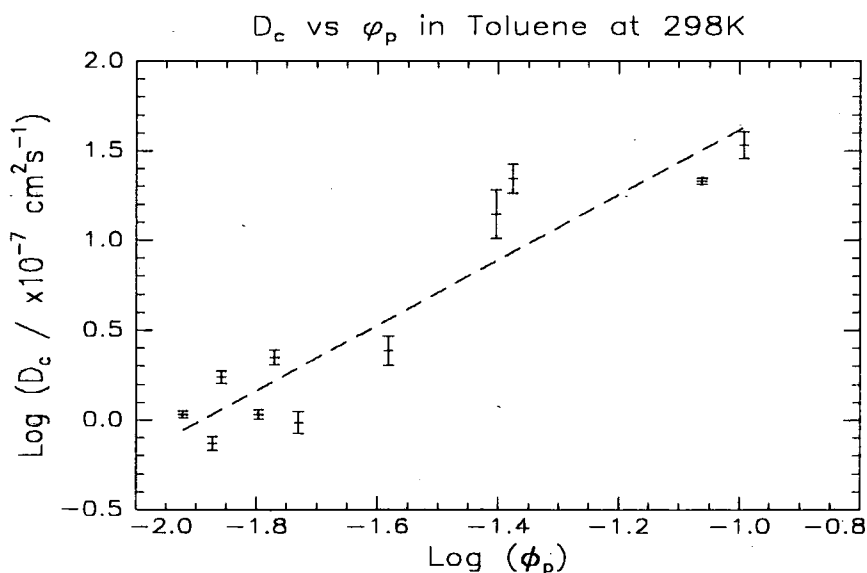


Figure 4.13.: Variation of Dc with Polymer Volume Fraction for PBMPPD/DVB and AMS/DVB Networks Swollen in Toluene at 298K.

For networks swollen in cyclohexane, it can be seen that the variation of D_c with the polymer concentration at the theta point is in very good agreement with the

behaviour predicted by scaling theory, and upon increasing the temperature and hence solvent quality of the system, the dependence of D_c upon ϕ_p decreases towards the value predicted for a polymer in a good solvent. However the results for the polystyrene-toluene system do not agree with values predicted from scaling theory with a scaling exponent of 1.82 being realised for gels in the good solvent compared to the value of 3/4 predicted by de Gennes. Again the relative poor quality of the AMS/DVB series of networks is thought to be the predominant reason for these results.

As can be seen below in tables 4.2. and 4.3., the hydrodynamic correlation length of the AMS/DVB networks in toluene is found to be around 15-20 times larger than that due to the PBMPPD/DVB series of networks, a feature which is thought to arise due to the more open structure associated with the poor quality AMS/DVB network. Therefore it can be seen that the co-operative diffusion coefficient associated with the AMS/DVB series of networks is correspondingly lower, which causes an increase in the magnitude of the scaling exponent in toluene swollen gels.

The hydrodynamic correlation length is extracted from the co-operative diffusion coefficient with equation 4.39. ξ_h differs from ξ (that measured by SANS) the correlation length describing the length scale where excluded volume interactions are screened out by the effects of neighbouring chains, in that ξ_h measures the length scale where hydrodynamic interactions are screened by polymer chains-i.e. the average distance between two nearest junction points.

Clearly for networks prepared in semi-dilute solution where chain entanglements provide excluded volume screening over relatively short distances, it would be expected that the hydrodynamic correlation length would be somewhat larger than the static correlation length. ξ_h has been determined using values of the solvent viscosity taken from *Polymer Handbook*.

Network	ξ_h for Cyclohexane Swollen Networks / Å (± Error)				Toluene
Mc (S.E.C.)	308	313K	318K	323K	298K
10,600	44.6 ± 2.1	45.2 ± 1.9	30.0 ± 4.2	39.5 ± 0.4	12.7 ± 0.9
17,800	56.2 ± 1.1	49.8 ± 1.2	41.4 ± 3.6	34.9 ± 3.7	20.2 ± 4.1
53,000	66.4 ± 13.6	70.7 ± 2.7	56.5 ± 3.9	49.2 ± 2.2	19.6 ± 1.6
102,800	101.8 ± 2.7	85.4 ± 3.2	82.6 ± 1.1	50.2 ± 1.5	30.8 ± 4.2

Table 4.2.: Hydrodynamic Correlation Length of PBMPPD/DVB Networks.

Network	ξ_h for Cyclohexane Swollen Networks / Å (± Error)				Toluene
Mc (S.E.C.)	308	313K	318K	323K	298K
10,400	184 ± 13	173 ± 25	139 ± 17	149 ± 5	178 ± 14
12,700	193 ± 11	188 ± 21	165 ± 16	234 ± 23	446 ± 26
20,100	170 ± 10	144 ± 11	122 ± 3	203 ± 7	399 ± 11
37,900	308 ± 15	193 ± 21	138 ± 6	102 ± 16	249 ± 9
48,700	269 ± 6	219 ± 12	176 ± 7	124 ± 7	195 ± 8
53,600	376 ± 26	254 ± 15	228 ± 17	139 ± 17	584 ± 22
109,900	305 ± 18	225 ± 4	186 ± 9	150 ± 7	400 ± 7

Table 4.3.: Hydrodynamic Correlation Length of AMS/DVB Networks.

Clearly the data in tables 4.2. and 4.3. shows the hydrodynamic correlation length to be substantially larger than the screening length determined from SANS. Two main features can be seen from the data. Firstly, both tables show a decrease of ξ_h with an increase in the solvent quality of the system most particularly marked for the increasing temperature of the cyclohexane swollen gels. This is not an unexpected feature as increasing temperature causes an increase in the thermal motion within the gel causing a decrease in ξ_h .

Some correlation can also be seen between ξ_h and the polymer concentration in table 4.2 for PBMPPD/DVB networks swollen in both cyclohexane and toluene. In a manner reminiscent of that seen in the static correlation length, ξ_h can be seen to decrease with the solvent quality of the system and unlike the static correlation length can be seen to be dependent upon the cross link density of the network. However at fixed temperatures no correlation can be seen between ξ_h and polymer concentration for

the AMS/DVB series of networks. This lack of scaling of the AMS/DVB series of networks again seems to be a feature of the poor quality of those gels. It should be noted that ξ_h measured for the AMS/DVB series of gels is at least four times greater than those values from the PBMPPD/DVB gels, indicating a much more open network structure in those networks where large quantities of sol fraction were extracted.

6.3. The Longitudinal Osmotic Modulus.

The relative intensity of the scattered radiation was extracted from each spectrum by fitting the data to the KWW model function as described earlier. An average normalised value was then determined from the fit to the data using equation 4.30 and from these results and those of the calibrant solution, a value of the osmotic modulus determined. Values of M_{os} are given in appendix C7, from which it can be seen that M_{os} generally decreased with increasing temperature in the system and increased with the polymer concentration at a given temperature.

The scaling predictions of de Gennes have been used to relate the osmotic modulus to the volume fraction of polymer within the gel for both theta and thermodynamically good solvents. For a theta system the osmotic modulus is expected to scale with the polymer concentration according to equation 4.42., while under good solvent conditions equation 4.43. is predicted to apply.

$$M_{os} \approx \phi_p^3 \quad 4.42.$$

$$M_{os} \approx \phi_p^{2.25} \quad 4.43.$$

Values of the osmotic modulus for both AMS/DVB and PBMPPD/DVB networks were determined for gels swollen in cyclohexane in the temperature range 308K to 323K, those values being correlated against the polymer volume fraction in a double logarithmic format in figure 4.14. However it was noted earlier that the measurement of the osmotic modulus by QELS was subject to large errors (upwards of 40%) and some anomalous values were found and the results determined from the intensity measurement were not as clear as the diffusion coefficient results from the

measurement of the decay constant. The large error in the measurement of the excess scattering intensity is reflected in the error associated with the osmotic modulus in the scaling relationships below.

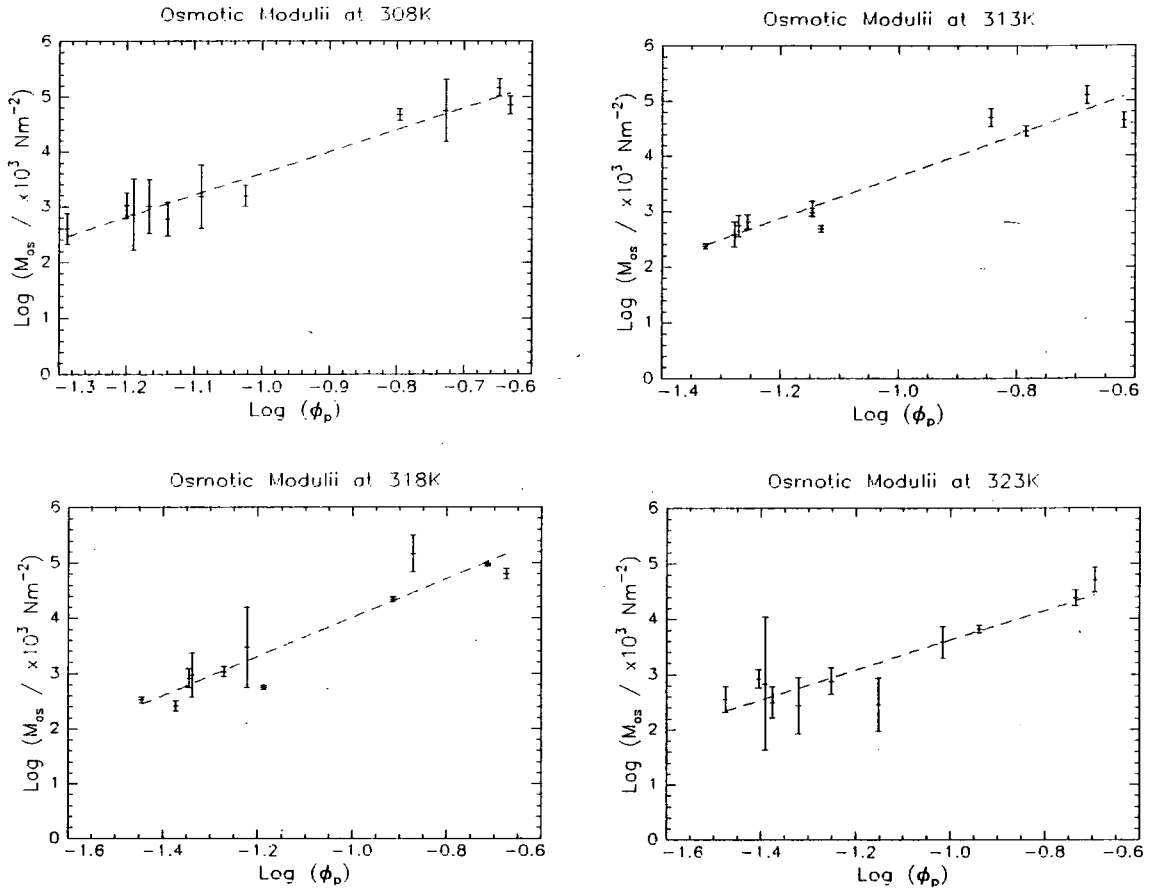


Figure 4.14. : Variation of the Longitudinal Osmotic Modulus Determined From QELS for Networks Swollen in Cyclohexane between 308K and 323K.

From the least-squares fit to the data, the following scaling relationships can be inferred for the osmotic modulus and polymer volume fraction.

$$308\text{K: } \text{Log } M_{\text{os}} (\times 10^5 \text{ Nm}^{-2}) = (7.59 \pm 0.28) + (3.98 \pm 0.27) \text{Log } \phi_p$$

$$313\text{K: } \text{Log } M_{\text{os}} (\times 10^5 \text{ Nm}^{-2}) = (7.44 \pm 0.37) + (3.81 \pm 0.35) \text{Log } \phi_p$$

$$318\text{K: } \text{Log } M_{\text{os}} (\times 10^5 \text{ Nm}^{-2}) = (7.54 \pm 0.47) + (3.52 \pm 0.41) \text{Log } \phi_p$$

$$323\text{K: } \text{Log } M_{\text{os}} (\times 10^5 \text{ Nm}^{-2}) = (6.31 \pm 0.46) + (2.69 \pm 0.39) \text{Log } \phi_p$$

Clearly the data above shows a much stronger dependence of the osmotic modulus on the polymer volume fraction for networks swollen in cyclohexane than predicted. Under theta conditions where a scaling exponent of 3 is predicted, the determined value is found to be somewhat stronger at 3.98, which is found to decrease as the temperature and solvent quality is increased. At the highest temperature studied 323K, a value of 2.69 is found which is intermediate between the value predicted for theta and good solvent conditions.

Values of the scaling exponents at all temperatures are thought to be somewhat higher than predicted due to the low values of M_{os} obtained for the AMS/DVB series of networks. M_{os} is found to be substantially lower for these networks than compared to the PBMPPD series networks and values of M_{os} from AMS/DVB gels are found to vary in an essentially random manner at a given temperature and to change little with the temperature of the system.

The low value of the osmotic modulus is again thought to arise from the more open network structure of the AMS/DVB networks arising from the relatively poor cross linking reactions used to prepare these networks which resulted in a large sol fraction for the network and a substantially less well cross linked network containing large amounts of pendant chains.

When results from the PBMPPD/DVB series of networks are considered alone, the scaling exponent is found to be somewhat lower (approximately 2 at 308K decreasing to 1.2 at 323K) than those obtained from both networks, though it is noted that the volume fraction range explored with these networks is rather small and therefore measurement of M_{os} subject to large errors.

Previous studies on the variation of the osmotic moduli of swollen polymer networks have focused on the determination of the modulus in randomly cross linked networks. Davidson^{52,53} has studied randomly cross linked polystyrene networks

swollen to equilibrium in cyclohexane within the temperature range 308K-333K and found remarkably little dependence of M_{os} with the temperature of the network. Data from three temperatures measured in the study was reduced to a single plot where a scaling exponent of 2.6 was found to describe the variation of the osmotic modulus with polymer concentration.

The osmotic modulus has also been measured in "good" solvent systems by Geissler⁴⁴ who studied poly(acrylamide) gels swollen in water where a scaling exponent of 2.35 was found for lightly cross linked gels within the region 0.025-0.12 gcm⁻³. The discrepancy between the predicted scaling exponent and that measured using QELS was attributed to water not being a truly good solvent for poly(acrylamide) networks.

Polystyrene networks swollen to equilibrium in benzene have been studied by Candau⁵⁴ who found good agreement with the osmotic modulus determined by QELS and that determined from mechanical measurements. In both cases, the good solvent prediction of 2.25 describing the variation of M_{os} with polymer concentration was observed. However when known fractions of pendant chains were deliberately introduced into the polymer network structure, the osmotic modulus of polystyrene network was found to decrease with an increasing content of pendant chains within the network.

When correlated with the results from the AMS/DVB networks provides some insight into the larger scaling exponents for M_{os} determined by QELS. Had the cross linking reactions employed in the AMS/DVB networks been more effective, then a substantially lower quantity of uncross linked polymer would have been extracted from the network and similarly less pendant chains incorporated into the network structure. Therefore it would seem reasonable that the osmotic modulus determined from the AMS/DVB networks would have been somewhat larger and values of the scaling exponent correspondingly lower.

7. The Co-operative Diffusion Coefficient of "Equivalent" Solutions.

In these experiments, the collective motions of a series of polymer solutions were studied within the semi-dilute region. The co-operative diffusion coefficient of the semi-dilute solution was studied as a function of the molecular weight of the polymer matrix, the polymer concentration and the quality of the solvent within the system. Four linear polystyrene polymers were studied PS13, PS14, PS18, and PS19, (molecular weights and distributions of the polymers are given in chapter 2), within the concentration range ($0.01 \leq \phi \leq 0.4$) at temperatures in the range 308-323K in cyclohexane and 298K in toluene. These conditions provided a complete examination of the variation of D_c with molecular weight and solvent quality over the entire semi-dilute concentration region, allowing a comparison to be made with the behaviour exhibited by the swollen networks under essentially the same conditions.

Solutions for study were prepared as outlined earlier in the chapter, using filtered solvent to prepare the solution, followed rapidly by sealing into scattering cells. Solutions were allowed to reach thermodynamic equilibrium over a period of upwards of 21 days before being held at the measurement temperature for 24 hours prior to QELS study. Spectra were recorded in homodyne mode using the Malvern correlator and data analysed by fitting the normalised correlation function to either a single or double KWW function and by ILT analysis using CONTIN.

7.1. General Features of the Spectra from Cyclohexane Solutions.

Perhaps the most evident difference between the spectra of polymer gels and semi-dilute solutions of equivalent concentration was the presence (at large decay times) of a second relaxation mode. This peak was not present in all spectra, though a correlation between its presence and molecular weight and concentration could be made. Figure 4.15. parts A and B show typical correlation functions obtained from solutions where only a single mode and from those where two modes were present, part A showing the spectrum from a low molecular weight matrix (10,000 g/mol) giving rise to a single mode, while part B shows the correlation function obtained from a solution of

the same concentration but having a matrix molecular weight of 100,000 g/mol which gives rise to a second relaxation mode.

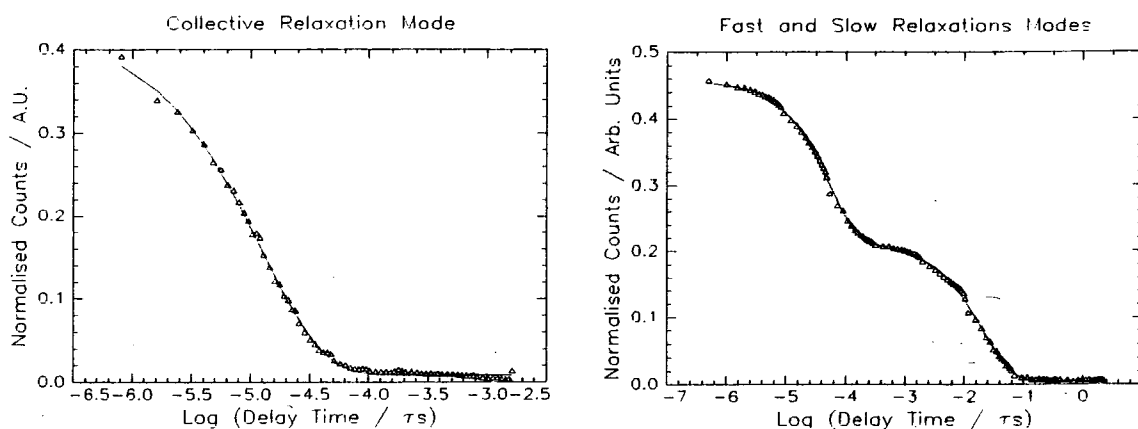


Figure 4.15. Parts A and B: Homodyne QELS Spectra Obtained From A:10,000 g/mol at 0.2 g/g in Cyclohexane at 308K, B:100,000 g/mol at 0.2 g/g in Cyclohexane at 308K.

Previous QELS studies on solutions of polymers within the semi-dilute region have shown the presence of at least two decay modes in the relaxation spectrum^{59,61}. The faster of these modes (identified with the collective motions of the polymer chains within the overlapping solution) has been found to be dependent upon the square of the scattering vector, and has been^{57,62}. The slower relaxation mode has been found to be independent of the scattering vector, the origin of the mode being the subject of considerable discussion, with some authors suggesting that the slow mode arises from the self diffusion of the polymer chains within the solution⁵⁶. However it is now widely thought that the mode arises from the viscoelastic properties of the transient network⁵⁷⁻⁶², of the entangled solution where chains are able to disentangle over relatively long time scales. Such behaviour has not been observed for polymer gels, where the cross links within the gel prevent the polymer chains from disentangling⁶³.

For the lowest molecular weight matrices (10,000 and 20,000 g/mol) there was no evidence of the slow relaxation in any solution over the entire concentration region

studied, while for the higher molecular weight polymers (60,000 and 100,000 g mol^{-1}) the relaxation was observed for all but the most dilute solutions.

Spectra were recorded from all four matrices in the temperature range 308-323K during August of 1993 using an incident laser power of around 35mW. This experimental set-up generally produced data of suitable quality within a few minutes, though spectra from polymers of lower molecular weight at the lower concentrations were found to take considerably longer, a feature that was noted in the earlier series of measurements of the tracer diffusion coefficient in dilute solution. While spectra from the more concentrated solutions of polymers of higher molecular weights were acquired in relatively short time spans, considerable effort was required to correctly configure the correlator to properly measure both the fast and slow decays and in some cases it was found that the large magnitude and relaxation time of the slow decay prevented measurement of the correlation function of the solution. In such cases where the slow decay could not be resolved the correlator was set-up such that only the fast decay mode was observed.

Results from fitting the experimental data to a double KWW fit are given in appendix C8-11, from which it can be seen that the relaxation time of the slow mode increases with concentration for a given polymer at a fixed temperature. At constant temperature and for solutions of equivalent concentration, the relaxation time associated with the 50,000 g/mol polymer can be seen to be substantially smaller than those from the 100,000 g/mol matrix. Increasing the temperature of the solution can also be seen to cause not only a decrease in the relaxation time of the slow decay, but also a decrease in the relative magnitude of the slow decay.

The variation of the relaxation rate of both fast and slow modes with scattering vector has been studied for one solution. As seen in figure 4.16., the fast mode associated with the 100,000 g/mol matrix at a nominal concentration of 0.2 g/g is found

to be linearly dependent upon the square of the scattering vector, while the slow mode is seen to be independent of the scattering vector.

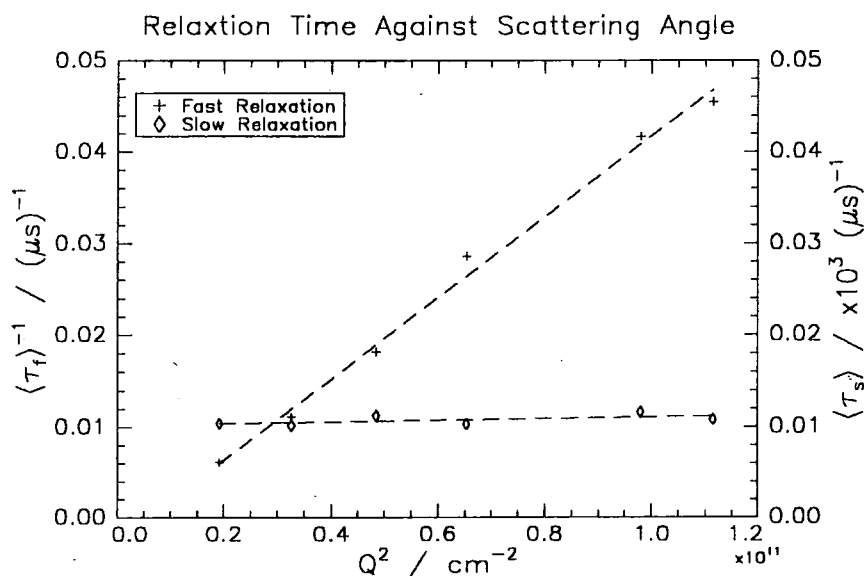


Figure 4.16. Variation of the Fast and Slow Decay Modes With Scattering Vector for a 0.2 g/g Solution of the 100,000 g/mol Matrix Polymer at 308K in Cyclohexane.

This observation has been noted by other authors^{61,62} and provides evidence for the theories of Brochard and de Gennes⁶³ who have described the influence of topological entanglements on the intensity autocorrelation function of the radiation scattered by the semi-dilute solution. de Gennes theory predicts the autocorrelation function to be a sum of two exponential decays, firstly a fast q^2 dependent mode arising from the collective motions of the polymer chains and secondly a slower q independent mode related to the disentangling of the entangled polymer chains of the transient network.

From the relaxation rate of the fast decay mode D_c can be determined, the results of which are given in appendix C8-11 together (where applicable) with the relaxation times obtained from the slow decay. Diffusion coefficients of the fast decay mode quoted in appendix C are determined from the KWW fit to the normalised correlation function as well as from the ILT of the normalised correlation function. Although CONTIN produced a distribution of diffusion coefficients which for the fast mode are

consistent with the values from the KWW fit, results from the slow mode were somewhat less consistent, with differences in some cases greater than 10^2 being observed. In all cases CONTIN was found to produce an estimate of the rate of diffusion coefficient equivalent of the slow mode somewhat faster than that obtained from the KWW fit.

Theoretical interpretation of the origins of the slow viscoelastic mode is however somewhat underdeveloped and with the limited amount of data available from this study, little can be said regarding the origins of the slow mode. It is noted that many examples of the slow relaxation mode could not be properly resolved as the decay mode often spanned times longer than the maximum decay time available with the Malvern K7032 correlator. This was found to be particularly prevalent for semi-dilute theta solutions where the amplitude of the slow decay was greatest and resolution most difficult, therefore allowing only a very limited interpretation of the available data. For these reasons the slow decay mode is considered no further.

One final point to note regarding the quality of the data obtained from the semi-dilute solutions was relative intensity of the normalised correlation function of the semi-dilute solution compared that from the swollen gel. For the semi-dilute solution, the amplitude of the correlation function was found to be much stronger than that arising from the gel. This is most probably due to the different data acquisition modes employed to record the spectra, as the heterodyne mode used to measure the swollen gels introduced a large baseline due to the scattering of the dust particles within the gel. For the semi-dilute solutions, dust was excluded from the scattering cell and as such the correlation function arose solely from the concentration fluctuations of the polymer solution.

7.2. General Features of the Spectra from Toluene Solutions.

QELS spectra from solutions of polystyrene in toluene were again recorded for solutions of various concentrations ($0.01 \leq \text{W.F.} \leq 0.4$) where the matrix molecular

weight ranged from 10,000 g/mol to 100,000 g/mol. The same polymers were utilised for these experiments, however spectra were not recorded for solutions of the 20,000 g/mol polymer in toluene as it was found to be impossible to exclude dust from the solutions. Spectra were recorded for the 10,000, 50,000 and 100,000 g/mol matrices, the results of which are presented in appendix 1. Measurements were again made using an incident laser power of around 35mW with experimental times of the order of 60-300 minutes needed for the generation of suitable data, these duration's being substantially longer than those needed for the measurement of solutions of equivalent concentration in cyclohexane. This was most evident for the 10,000 g/mol matrix in toluene at a nominal concentration of 0.01 g/g, where the data obtained was found to be subject to a large error and a large amount of experimental noise.

As with the semi-dilute solutions in cyclohexane, the most evident difference between the spectra of polymer gels and semi-dilute solutions in toluene was the presence at long decay times of a second relaxation mode. Although not present in all spectra, a correlation between the presence of the peak and the polymer molecular weight and concentration was again made.

Solutions of the lowest molecular weight polymer were found not to exhibit the slow relaxation while it was again found to have maximum intensity and relaxation time for solutions of the 100,000 g/mol matrix at the highest concentrations. For solutions of the two highest molecular weight polymers, the presence of the second exponential decay was often found to prevent resolution of the fast mode as the slow mode was found to be somewhat more massive than the fast mode. This can be seen graphically in figure 4.17. where the normalised correlation function obtained from the 0.4 g/g solution of the 50,000 g/mol matrix is shown.

Simultaneous measurement of both the fast and the slow decay modes was found to prevent the resolution of the fast mode due to the large magnitude of the slow mode, which was found to be of much larger intensity than the fast mode and as such prevented

the determination of the fast decay mode. A similar situation arose in the measurement of the fast mode in cyclohexane solution, though in those solutions it was found to be possible to configure the correlator in such a way so as to exclude the slow mode and measure only the relaxation due to the collective motions. This procedure was attempted for solutions in toluene, though it was not found to be satisfactory as only a very poor correlation function with a very low signal could be extracted from the resulting spectra. In these cases (see appendix 1), only relaxation times from the slow decay are quoted.

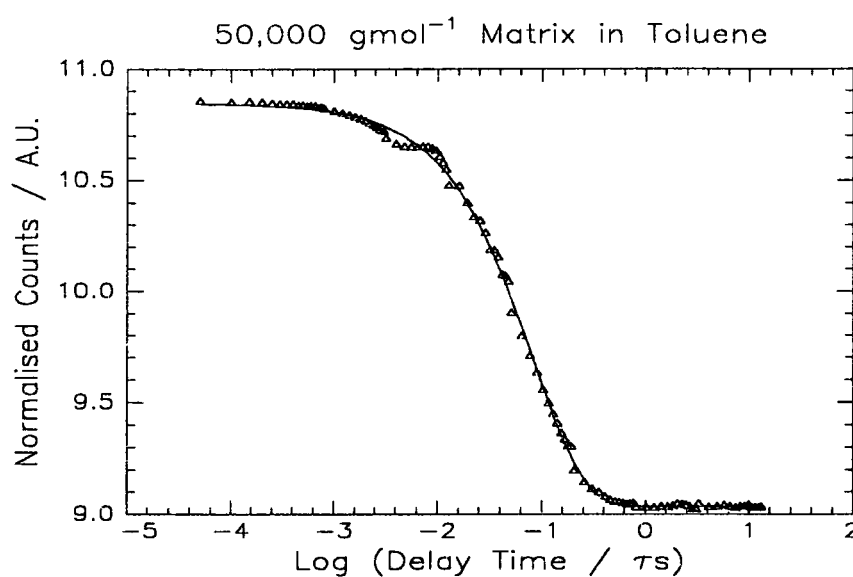


Figure 4.17.: Correlation function obtained from a 0.4 g/g solution of 50,000 g/mol polystyrene matrix in toluene.

Figure 4.17. shows only a single decay in the QELS spectra, the relaxation rate of the decay being consistent with both the relaxation times of the q -independent slow mode obtained from other solutions of polystyrene in toluene and cyclohexane. In a manner similar to that observed for solutions in cyclohexane, the relaxation time of the slow mode is again found to increase with both the polymer molecular weight and the concentration of the solution.

The presence of the slow decay mode in semi-dilute solutions of polystyrene in toluene has been observed by some authors^{56,68,69} previously though not unanimously

by all⁷⁰⁻⁷². The spectrum is generally resolved into two decay modes when the concentration of the solution is greater than 0.1 g/g. Below this concentration, most authors find the data to be adequately described by a single mode. As with the situation of the slow decay mode present in cyclohexane solutions, the origins of the slow decay mode in toluene solutions is somewhat unclear and taken in conjunction with the limited amount of data available here, the slow decay mode is considered no further.

7.3. The Co-operative Diffusion Coefficient.

The decay constant was extracted from each spectra by fitting the data to the KWW model function as described earlier and was corrected for solvent back flow following the procedure outlined earlier. Values of the hydrodynamic correlation length were determined from D_c using equation 4.39., values for the solvent viscosity being taken from the Polymer Handbook. Full results of the QELS experiments are given in appendix 1, the results quoted being an arithmetic mean of five spectra, the error quoted for the data is the standard deviation about the mean which is most probably a conservative estimation of the error, the real error probably being larger.

Above the polymer critical overlap concentration⁵⁷ defined by equation 4.44, D_c for a given polymer at constant temperature can be seen to increase with the polymer concentration. As data in the study of solutions of equivalent concentration to polymer gels was collected over the entire semi-dilute region, many spectra from polymers of lower molecular weight in cyclohexane under theta conditions were collected on or slightly below the chain overlap concentration (c^*). Values of the diffusion coefficient measured from these solutions are therefore modulated by the self diffusion coefficient and can be seen to be substantially higher than those values collected for polymer solutions of higher matrix molecular weight and of similar concentration.

$$c^* = \frac{M_w}{4/3\pi R_g^3 N_a} \quad 4.44.$$

Only the 100,000 g mol⁻¹ polymer was found to produce a series of solutions for which all solutions were above the overlap concentration. Figure 4.18 parts a-e show the variation of D_c with the polymer volume fraction for solutions in cyclohexane in the range 308-323K and in toluene at 298K. All data is shown in double logarithmic format which allow determination of the scaling exponents relating the collective diffusion coefficient to the polymer volume fraction in the solution.

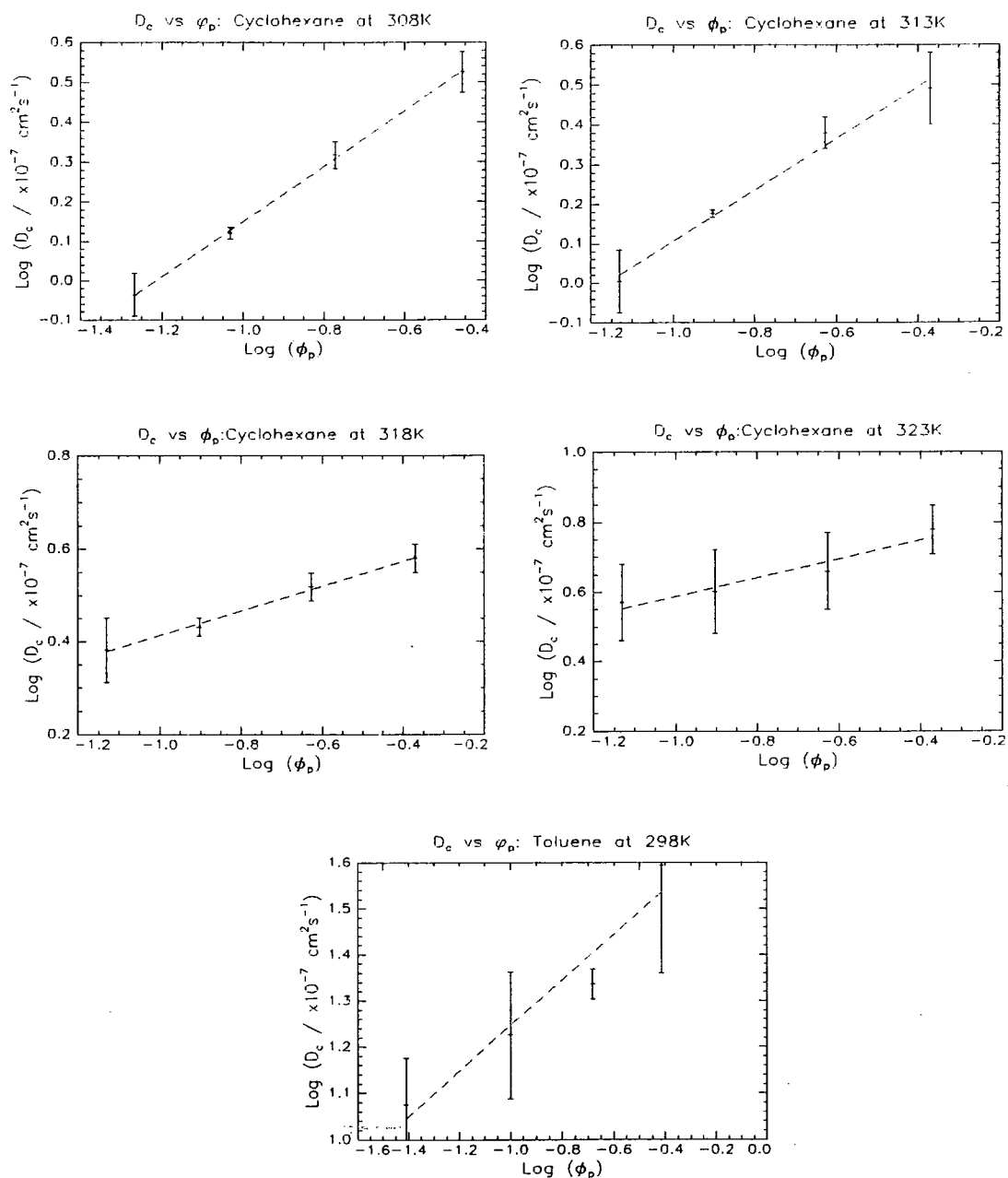


Figure 4.18. Parts A-E: Collective Diffusion Coefficient For Semi-Dilute Solutions of Matrix Molecular Weight 100,000 g/mol in Cyclohexane and Toluene.

From figure 4.18., the following scaling exponents were determined:

$$\text{Cyclohexane 308K: } \text{Log } D_c (\text{x}10^{-7} \text{ cm}^2\text{s}^{-1}) = (0.85 \pm 0.01) + (0.69 \pm 0.02) \text{ Log } \phi_p$$

$$\text{Cyclohexane 313K: } \text{Log } D_c (\text{x}10^{-7} \text{ cm}^2\text{s}^{-1}) = (0.79 \pm 0.12) + (0.57 \pm 0.13) \text{ Log } \phi_p$$

$$\text{Cyclohexane 318K: } \text{Log } D_c (\text{x}10^{-7} \text{ cm}^2\text{s}^{-1}) = (0.70 \pm 0.02) + (0.25 \pm 0.02) \text{ Log } \phi_p$$

$$\text{Cyclohexane 323K: } \text{Log } D_c (\text{x}10^{-7} \text{ cm}^2\text{s}^{-1}) = (0.88 \pm 0.03) + (0.26 \pm 0.04) \text{ Log } \phi_p$$

$$\text{Toluene 298K: } \text{Log } D_c (\text{x}10^{-7} \text{ cm}^2\text{s}^{-1}) = (1.74 \pm 0.09) + (0.49 \pm 0.09) \text{ Log } \phi_p$$

It can be seen that the dependence of D_c on the polymer concentration is found to be somewhat weaker than predicted by scaling theory, where exponents of 1 in theta solvents and 0.75 in good solvents are predicted. Similar results have been obtained by other authors who have studied polystyrene-diethyl phthalate solutions⁶² and who have found scaling exponents lower than predicted (0.62) for solutions in the semi dilute region bounded by ($c^* < c < 5c^*$).

Tables 4.4-4.8 below show the hydrodynamic correlation length of the semi-dilute solutions determined from the collective diffusion coefficient for matrix solutions in cyclohexane in the temperature range 308-323K and also in toluene at 298K. Data presented in bold face arises from those solutions which are above the overlap concentration c^* . From these results it can be seen that ξ_h decreases as a function of both the concentration of the semi-dilute solution and also the solvent quality of the system.

Comparison of the data presented earlier in table 4.2 (showing ξ_h for PBMPPD/DVB gels swollen in cyclohexane) and toluene under the same conditions as for those semi-dilute solutions measured here, shows ξ_h for the solution to be twice the magnitude of ξ_h in the cyclohexane swollen gel over the entire temperature range studied. A comparison of the results for semi-dilute solutions and gels in *toluene* at 298K shows the ratio of the hydrodynamic correlation lengths of the gel and the solution to be unity, within the margin of error associated with the measurement.

This is in direct contradiction to the results for the ratio of the hydrodynamic correlation length of both poly(acrylamide)⁶⁷ and poly(vinylacetate)⁶³ gels and semi-dilute solutions, where the ratio (gel to solution) in both cases was found to be 2:1. This is a feature which the authors have attributed to increased mobility in the semi-dilute solution allowing the polymer chains of the solution to adopt more flexible conformations, which are prevented when the polymer chains are cross linked. Clearly this is not the case for the results determined here.

Concentration / g g ⁻¹	Hydrodynamic Correlation Length (ξ_h) / Å ± Error			
	10,000 g/mol	20,000 g/mol	50,000 g/mol	100,000 g/mol
0.4	32.7 ± 1.2	43.7 ± 2.6	120.0 ± 1.5	85.8 ± 4.3
0.2	40.1 ± 0.8	51.4 ± 0.4	163.0 ± 0.8	138.0 ± 4.9
0.1	25.4 ± 0.4	39.7 ± 0.9	260.0 ± 2.7	217.0 ± 3.2
0.05	23.7 ± 1.1	34.1 ± 1.2	125.0 ± 0.4	312.0 ± 1.6
0.01	13.4 ± 1.1	27.9 ± 3.4	37.2 ± 1.2	92.0 ± 2.3

Table 4.4.: Hydrodynamic Correlation Length in Cyclohexane at 308K.

Concentration / g g ⁻¹	Hydrodynamic Correlation Length (ξ_h) / Å ± Error			
	10,000 g/mol	20,000 g/mol	50,000 g/mol	100,000 g/mol
0.4	33.4 ± 4.1	27.8 ± 0.7	95.4 ± 2.1	104.0 ± 2.4
0.2	37.1 ± 2.6	58.0 ± 0.5	126.0 ± 1.2	135.0 ± 2.9
0.1	26.6 ± 1.9	41.9 ± 1.6	161.0 ± 1.3	172.0 ± 1.3
0.05	23.1 ± 3.6	35.5 ± 0.8	113.0 ± 2.3	312.0 ± 1.6
0.01	5.5 ± 2.5	27.3 ± 3.8	35.0 ± 0.3	83.2 ± 0.9

Table 4.5.: Hydrodynamic Correlation Length in Cyclohexane at 313K.

Concentration / g g ⁻¹	Hydrodynamic Correlation Length (ξ_h) / Å ± Error			
	10,000 g/mol	20,000 g/mol	50,000 g/mol	100,000 g/mol
0.4	29.4 ± 4.3	27.7 ± 0.7	68.0 ± 4.1	85.9 ± 0.6
0.2	35.6 ± 3.3	35.9 ± 2.8	92.4 ± 1.2	99.3 ± 0.9
0.1	26.9 ± 2.7	38.6 ± 1.9	139.0 ± 2.6	121.0 ± 0.9
0.05	21.0 ± 3.6	28.5 ± 2.0	86.5 ± 10.5	136.0 ± 4.1
0.01	No Data	No Data	26.8 ± 3.8	78.2 ± 1.1

Table 4.6.: Hydrodynamic Correlation Length in Cyclohexane at 318K.

Concentration / g g ⁻¹	Hydrodynamic Correlation Length (ξ_h) / Å ± Error			
	10,000 g/mol	20,000 g/mol	50,000 g/mol	100,000 g/mol
0.4	50.4 ± 5.9	17.6 ± 6.7	60.7 ± 5.2	72.6 ± 4.5
0.2	36.9 ± 3.9	33.8 ± 11.5	89.4 ± 2.5	95.4 ± 2.3
0.1	27.1 ± 4.2	36.3 ± 0.9	122.0 ± 1.6	109.0 ± 3.4
0.05	18.9 ± 4.8	122 ± 1.6	94.9 ± 2.7	117.0 ± 1.9
0.01	No Data	No Data	25.1 ± 8.9	71.1 ± 1.2

Table 4.7.: Hydrodynamic Correlation Length in Cyclohexane at 323K.

Concentration /g g ⁻¹	Hydrodynamic Correlation Length (ξ_h) / Å ± Error		
	10,000 g/mol	50,000 g/mol	100,000 g/mol
0.4	No Data	No Data	7.8 ± 1.8
0.2	16.3 ± 3.5	No Data	15.0 ± 1.5
0.1	17.4 ± 1.7	No Data	19.4 ± 2.6
0.05	19.5 ± 1.07	21.9 ± 2.9	27.4 ± 2.6
0.01	5.2 ± 1.2	20.6 ± 3.3	35.6 ± 2.1

Table 4.8.: Hydrodynamic Correlation Length in Toluene at 298K.

One possible explanation can be advanced for these results. In this series of experiments, the correlation length has been measured for polystyrene networks prepared in semi-dilute solution and as described earlier the screening length of the gel is found to be constant over the entire range of polymer gel concentration studied which is thought to be due to the fact that the cross linking reactions are in all cases performed on semi-dilute solutions of 10% concentration, thus *freezing in* the screening length associated with the semi-dilute solution into the gel structure. As the temporary chain entanglements present within the transient network are still present within the cross linked gel and control the screening length, it might seem reasonable that chain mobility within the gel would be influenced by the presence of these chain entanglements and thus the mobility of the gel should be the same as that for the semi-dilute solution of equivalent concentration.

8. QELS from Networks and Semi-Dilute Solutions Containing Probe Chains.

One of the central aims of this work has been the determination of the dynamic processes controlling the motion of polymer chains diffusing through polymer networks. Evaluation of the diffusion coefficient of the probe polymer and the ability to relate it to the probe chain molecular weight, the cross link density of the network and the solvent quality, would provide fundamental understanding of the mechanism of diffusion through swollen gels. In order to study this, a series of polymer networks having a range of cross links densities, have been prepared containing a number of trapped probe chains. These trapped chain containing networks, described in chapter 2 contain combinations of networks and trapped polymers which provide the molecular weight and cross link density range necessary to study the dynamic processes of the trapped chain.

Networks with cross link densities of 10,000, 50,000 and 100,000 g/mol (molecular weight between cross links) containing probes chains with molecular weights of 120,000, 330,000 and 1,018,000 g/mol, have been prepared in benzene solution and subsequently dried to the bulk before being re swollen in filtered cyclohexane and toluene. These networks have then been allowed to reach swelling equilibrium over a period of upto 7 days prior to QELS experiments to determine the correlation function of the gel, the diffusion of trapped probe chains being studied in cyclohexane within the temperature range 308-323K and in toluene at 298K.

In order to ascertain any differences between the dynamic behaviour of probe chains within gels and semi-dilute solutions, a series of ternary semi-dilute solutions were also prepared containing matrix polymers of equivalent molecular weight to the polymer gels at a nominal matrix concentration of $5c^*$ (defined by equation 4.44.) and a probe concentration of $c^*/5$. It was initially intended to study the dynamics of the probe polymer in these ternary solutions as a function of both the probe molecular weight, matrix molecular weight and concentration by increasing the concentration of the matrix to values of circa. $10c^*$ and $15c^*$, however as will be described later, both pressures of time and experimental difficulties prevented these experiments during this work.

Determination of the diffusion coefficient of the probe chain from the autocorrelation function of the gel centres around the use of the ILT method to separate the collective motions of the gel from the self-diffusive motions of the probe chain. In principle, for a system containing two polymers of different molecular weights, the autocorrelation function of the gel is described by two exponential decays with different relaxation rates. Where these decays are sufficiently separated (as in the previous section) these two modes present themselves readily for resolution and analysis, however for decays of similar relaxation rates analysis relies upon the use of programs such as CONTIN to deconvolute the correlation function into its constituent modes.

Such procedures have been used by Brown⁶⁶ who used a modified version of CONTIN to deconvolute the QELS spectra of ternary poly(isobutylene) semi-dilute solutions into the constituent self diffusive mode of the probe chains and the collective mode of the semi-dilute matrix. Analysis of the normalised correlation function using SIQELS to fit the data to a KWW exponential function yielded only a single decay mode.

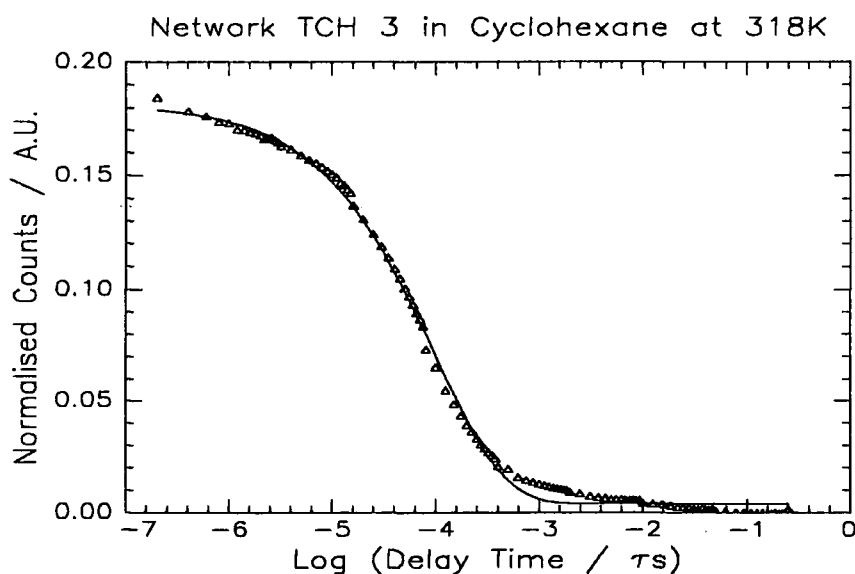


Figure 4.19. Normalised Correlation Function and Associated Single KWW Fit From Network TCH 1 ($M_c = 9,000$ g/mol, Probe = 1,018,000 g/mol) Swollen in Cyclohexane at 318K.

Similarly to the data obtained from PBMPPD/DVB networks, the correlation function from the gel was found to be well described by a single decay, i.e. the relaxation rate of the probe chain is sufficiently similar to the network that a single stretched exponential decay mode satisfactorily fitted the autocorrelation function. A typical spectrum obtained from a trapped chain network is shown above in figure 4.19. As can be seen, the autocorrelation function is described by a single exponential decay, the single KWW fit to the data being shown in the figure. However it is noted that the variance of the decay (β in the KWW function) was slightly lower for trapped chain containing networks than for 'blank' networks, thus indicating the decay mode was slightly broader. It was also noted that the relaxation times of the decay was slightly slower than for blank PBMPPD/DVB networks of similar concentration. These features are most probably due to the presence of the trapped chain within the network causing a broadening of the decay.

Resolution of the decay spectrum to determine the diffusion coefficient of the probe chain therefore relied upon the use of CONTIN to produce a distribution of decay time from which the relaxation of the probe chain could be isolated.

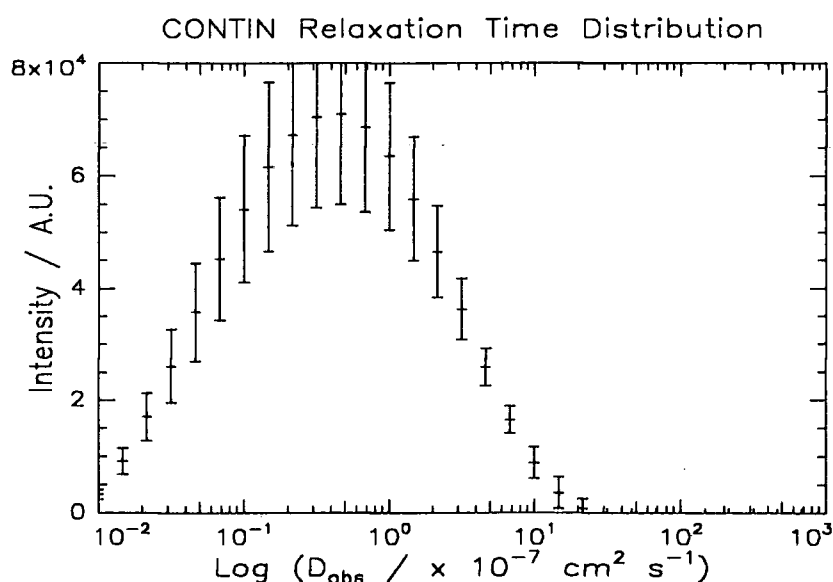


Figure 4.20.: Distribution of Decay Times Arising From CONTIN Analysis of Network TCH 1 ($M_c = 9,000 \text{ g/mol}$, Probe = $1,018,000 \text{ g/mol}$) Swollen in Cyclohexane at 318K.

A typical example of the diffusion coefficient distribution obtained is shown above in figure 4.20. where it can be seen that the errors associated with the peak are quite large. As typified by figure 4.20., CONTIN analysis of all QELS spectra obtained, (not only those obtained from networks containing probe chains but also from ternary semi-dilute solutions containing equivalent amounts of probe chains) was found to produce a single peak in the distribution of diffusion coefficients, which ranged from $(1.0 \times 10^{-9} \leq D_{\text{obs}} (\text{cm}^2\text{s}^{-1}) \leq 1.0 \times 10^{-6})$, and had associated with itself a large error.

This broad peak was found in all cases, regardless of probe chain size, cross link density or solvent quality and attempts to modify the input parameters of the program to produces a distribution of diffusion coefficients met with no success. Similar behaviour was found for ternary semi-dilute solutions over the entire range of matrix polymer weight and solvent quality studied. Unfortunately time constraints prevented any further re-analysis of the data generated in this study and as such no information regarding the diffusion of the probe chain through the network was available.

It has however been noted by other authors⁶⁵ that when CONTIN tries to resolve multi peak solutions, it cannot resolve peaks where the ratio of the sizes of the two species are less than a factor of two apart and instead of providing a solution with two discrete peaks will instead smooth the peaks together producing a single broad peak.

From the co-operative diffusion coefficient data of *blank* networks prepared from the PBMPPD/DVB system given in appendix 1, a value of the hydrodynamic correlation length ξ_h can be determined. The ratio of this correlation length has been compared with the hydrodynamic radius of the probe measured in dilute solution and has for many of the combinations of networks and probes studied here been found to be close to unity. This is most prevalent for highly cross linked networks containing "low" molecular weight probe polymers and can be seen to rise to approximately 4 for networks containing the highest molecular weight probe polymers.

Therefore, in many cases CONTIN can be seen to be making an attempt to resolve relaxation modes which are directly overlapping and in other cases where the molecular weights of the probe polymer and the network are most suited to allow a separation of the individual combinations, CONTIN can be seen to be operating on its resolution limit and hence it is thought resolution of the decay modes is impractical when using CONTIN to resolve the decay modes.

9. Conclusions.

QELS has been used to follow the dynamic behaviour of a series of polystyrene networks swollen in cyclohexane within the temperature range 308K to 323K and in toluene at 298K. Differences between the dynamic behaviour of the polymer chains in the cross linked gel and when uncross linked in semi-dilute solution have been followed by measuring the QELS spectrum of a series of polystyrene solutions having a concentration equivalent to that of the polymer gel. The collective diffusion coefficient of the swollen gel has been determined from the relaxation of the QELS spectrum and scaling exponents relating the diffusion coefficient to the polymer concentration have been determined.

For polystyrene networks under theta conditions (308K in cyclohexane), good agreement has been found between the measured scaling exponent (1.23) and that predicted by renormalisation group theory (1). Increasing the solvent quality has been found to decrease the scaling exponent towards that predicted for a good solvent (0.75), however when measured in toluene at 298K the scaling exponent has been found to be considerably greater than that predicted at 1.82.

The longitudinal osmotic modulus has also been measured by QELS and related to the renormalisation group predictions of de Gennes. Under theta conditions where a scaling exponent of 3 is predicted, a somewhat larger value of 3.98 has been found. This difference has been attributed to the low quality of the AMS/DVB series of networks used in part to complete this work. Values of the osmotic modulus determined from

these networks are found to be considerably lower than those obtained from PBMPPD/DVB networks and are found to change in an essentially random manner, changing little with the temperature of the system. These features are thought to be due to the open structure of these networks formed during the relatively poor cross linking reactions which produced networks containing large fractions of pendant chains. When considered alone, the scaling exponents obtained from the PBMPPD/DVB series of networks was found to be somewhat lower than predicted by renormalisation group theory, however the polymer concentration range explored with these networks is noted to be rather low and the measurement subject to large errors. Increasing the quality of the solvent is found to decrease the scaling exponent towards a value predicted for a polymer-good solvent system.

The collective motions of a series of solutions entangled in the semi-dilute region have been studied by QELS and differences established between the solutions and polymer gels. In the gels, only a single relaxation mode due to collective motion is found, while in semi-dilute solutions a second mode was frequently found. The origins of the mode are somewhat unclear however it seems likely that the mode arises from the viscoelastic properties of polymer chains in entangled solutions. Unlike the cross linked gels, the chains of the solution can disentangle over relatively long time scales, causing the second relaxation mode. For semi dilute solutions of a high molecular weight polymer, scaling exponents relating the co-operative diffusion coefficient to the polymer volume fraction have been determined and found to be somewhat lower than predicted, also decreasing with the solvent quality as predicted by renormalisation group theory.

In toluene based solutions and gels the ratio of the hydrodynamic radii of the gel and solution has been measured and has been found to be unity. This is a feature not found in previous studies of swollen gels/solutions and is attributed to the method of synthesis of the networks. As 10% solutions of polymer were end linked to form a network, the temporary chain entanglements along the chain backbone become frozen into the network structure. These entanglements have been shown to control the

screening length of the network and as such it would seem reasonable that these chain entanglements might also influence the chain mobility within the swollen network after cross linking.

QELS has been used in an attempt to extract the tracer diffusion coefficient of a series of probe chains trapped within networks swollen to equilibrium in cyclohexane and toluene and has also been used to determine the "free" diffusion coefficient in dilute solution for comparative purposes with the tracer diffusion coefficient in swollen networks.

Determination of the tracer diffusion coefficient centres on the assumption that ILT routines such as CONTIN are able to deconvolute the relaxation spectrum into its components. Such an analysis has been performed previously for poly(isobutylene) semi-dilute solutions. In principle the relaxations of the swollen network and the probe chain should be more easily resolved due to the differences in the molecular weights of the components. However this has not found to be the case and the relaxation rates of the network and probe have not been able to be resolved. This is thought to be due to the similarities of the hydrodynamic radii for the probe chain and the chains of the swollen network. The ratio of these has been found in many cases to be only slightly larger than unity and it has been reported that programs such as CONTIN cannot resolve separate decays where this ratio is less than two.

10. References.

- 1 Cowie J.M.G., *Polymers: Chemistry and Physics of Modern Materials*, Intertext, Aylesbury, 1973.
- 2 Huglin M.B., *Light Scattering from Polymer Solutions*, Academic Press, New York, 1972.
- 3 Kratochvil P., *Classical Light Scattering from Polymer Solutions*
- 4 Katime I.A. and Quintana J.R., in *Comprehensive Polymer Science Volume 1* (Ed Allen G.), Pergamon, Oxford, 1989.
- 5 Lord Rayleigh, *Philos. Mag.* **12(5)**, 81, (1881).
- 6 Einstein A., *Ann. Phys. (Leipzig)*, **33**, 1275, (1910).
- 7 Smoluchowski M., *Ann Phys. (Leipzig)*, **25**, 205, (1908).
- 8 Smoluchowski M., *Philos. Mag.*, **23(6)**, 165, (1912).
- 9 Debye P., *The Collected Papers of P. Debye.*, Wiley Interscience, New York, 1954.
- 10 Debye P., *J. Appl. Phys.*, **15**, 338, (1944).
- 11 Kratochvil P., in *Light scattering from Polymer Solutions*, (Ed Huglin M.B.), Academic Press, London, 1972.
- 12 Burchard W., in *Applied Fibre Science Volume 1*, (Ed. Happey F.), Academic Press, New York, 1978.
- 13 Zimm B.H., *J. Chem. Phys.*, **16**, 1099, (1948).
- 14 *Measurement of Suspended Particles By QELS* (Ed. Dahneke B.E.), Wiley Interscience, New York, 1983.
- 15 Berne B.J. and Pecora R., *Dynamic Light Scattering*, Wiley Interscience, New York, 1976.
- 16 Caroline D., in *Developments in Polymer Characterisation Volume 5*, (Ed. Dawkins J.V.), Elsevier, London, 1986.
- 17 King T.A., in *Comprehensive Polymer Science Volume 1*, (Ed. Allen G.), Pergamon, Oxford, 1989.
- 18 Chu B., in *Comprehensive Polymer Science Volume 1*, (Ed. Allen G.), Pergamon, Oxford, 1989.

- 19 International Critical Tables Reference
- 20 Koppel D.E., J. Chem. Phys., 57, 4814, (1972)
- 21 Pusey P.N., Koppel D.E., Schaeffer D.W. and Camerini-Otero R.D.,
Biochemistry, 13, 952, (1974)
- 22 Pusey P.N. and Brown J.C., J. Phys. D., Appl.Phys., 7, L31, (1974)
- 23 Williams G. and Watts D.C. Trans. Farad. Soc., 66, 80, (1970)
- 24 Provencher S.W., Makromol. Chem. 180, 201, (1979)
- 25 Provencher S.W., Comput. Phys. Commun., 27, 213, (1982)
- 26 Provencher S.W., CONTIN Users Manual, Version 2, Max-Planck Institut,
Göttingen, F.R.G., 1984
- 27 Malvern 4700 Spectrometer User Guide, Malvern Instruments, Malvern, 1990
- 28 *Automeasure* Version 5.2 User Manuel, Malvern Instruments, Malvern, 1992
- 29 Ford N.C. in *Measurement of Suspended Particles by QELS*, (Ed. Dahneke
B.E.), Wiley Interscience, New York, 1983.
- 30 Richards R.W., *SIQELS-a Program for Analysing QELS data*, University of
Durham, 1993
- 31 Williams G, Watts D.C., Dev S.B. and North A.M., Trans. Farad. Soc., 67, 1323,
(1971)
- 32 Wang C.H. and Zhang X.Q., Macromolecules, 26, 707, (1993)
- 33 Johnson R.M. and Brown W., in *Laser Light Scattering in Biochemistry*,
(Eds. Harding S.E., Sattelle D.B. and Bloomfield V.A.) Royal Society of
Chemistry, Cambridge, 1992
- 34 Han C.C. and Akcasu A.Z., Polymer, 22, 1165, (1981)
- 35 Caroline D. and Jones G., Chem. Phys., 37, 187, (1979)
- 36 King T.A., Knox A., Lee W.I. and McAdam J.D.G., Polymer, 14, 151, (1973)
- 37 Adam M. and Delsanti M., J. Physique, 41, 713, (1980)
- 38 Caroline D. and Pritchard M.J., Macromolecules, 13, 957, (1980)
- 39 Caroline D. and Pritchard M.J., Macromolecules, 14, 424, (1981)
- 40 Novotny V.J., J. Chem. Phys., 78(1), 183, (1983)
- 41 Han C.C. and McCrackin F.L., Polymer, 20, 427, (1979)

- 42 Yamakawa H., *Modern Theory of Polymer Solutions*, Harper and Row, New York, 1971
- 43 Tanaka T., Hocker L.O., and Benedek G.B., *J. Chem. Phys.*, **59**, 5151, (1973)
- 44 Geissler E. and Hecht A-M., *J. Phys. (Paris)*, **39**, 631, (1978)
- 45 Landau L.D. and Lifshitz E.M., *Theory of Elasticity*, Pergamon, New York, (1970)
- 46 Geissler E. and Hecht A-M., *Chem. Phys. Letts.*, **37(2)**, 343, (1976)
- 47 Geissler E. and Hecht A-M., *J. Chem. Phys.*, **65(1)**, 103, (1976)
- 48 Scholte T.G., *J. Polym. Sci. A2*, **8**, 841, (1970)
- 49 Munch J.P., Lemarechal P., Candau S. and Herz J., *J. Phys (Paris)*, **38**, 1499, (1977)
- 50 Bastide J., Picot C. and Candau S., *J. Polym. Sci. (Polym.Phys.)*, **17**, 1441, (1979)
- 51 Candau S., Butler I. and King T.A., *Polymer*, **24**, 1601, (1983)
- 52 Davidson N.S., PhD Thesis, University of Strathclyde, 1984
- 53 Davidson N.S. and Richards R.W. *Polymer*, **26**, 1643, (1985)
- 54 Candau S., Young C.Y., Tanaka T., Lemarechal P. and Bastide J., *J. Chem. Phys.*, **70**, 4694, (1979)
- 55 *Polymer Handbook*, Eds. Immergut and Brandrup, Wiley Interscience
- 56 Amis E. and Han C.C., *Polymer*, **23**, 1403, (1982)
- 57 Brown W. and Stepanek P., *Macromolecules*, **26**, 6884, (1993)
- 58 Brown W. and Fang W., *Macromolecules*, **25**, 6897, (1992)
- 59 Brown W., Nicolai T, Hvidt S, and Heller K., *Macromolecules*, **23**, 5088, (1990)
- 60 Brown W., Nicolai T, Hvidt S, and Stepanek P., *Macromolecules*, **23**, 357, (1990)
- 61 Brown W. and Nicolai T., *Macromolecules*, **23**, 3150, (1990)
- 62 Wang C.H. and Zhang X.Q., *Macromolecules*, **26**, 707, (1993)
- 63 Brown W., Fang L. and Stepanek P., *Macromolecules*, **24**, 3201, (1991)
- 64 Brochard F. and de Gennes P.G., *Macromolecules* **10**, 1157, (1977)
- 65 Sorlie S.S. and Pecora R., *Macromolecules*, **21**, 1437, (1989)

- 66 Brown W. and Zhou P, *Macromolecules*, **22**, 4031, (1989)
- 67 Geissler E., Hecht A.M. and Duplessix R., *J. Polym. Sci., Polym. Phys.*, **20**, 225, (1982)
- 68 Brown W., Johnsen R.M. and Stilbs P., *Polym. Bull. (Berlin)*, **9**, 305, (1983)
- 69 Brown W., *Polymer* **25**, 680, (1984)
- 70 Munch J.P., Candau S., Herz J. and Hild G., *J. Phys. (Orsay)*, **38**, 971, (1977)
- 71 Munch J.P., Lemarchel P., Candau S. and Herz J. *J. Phys. (Orsay)*, **38**, 1499, (1977)
- 72 Wiltzus P. and Cannel D.S., *Phys. Rev. Lett.*, **56**, 61, (1986)

CHAPTER 5.

CONCLUSIONS AND SUGGESTIONS FOR FUTURE WORK.

The objective of this work was to prepare and characterise the behaviour of model polymeric networks containing a known fraction of trapped chains. Studies of the behaviour of these trapped chains were focused on the determination of the conformation of the probe chain in solvent swollen gels as well as in the bulk networks, while studies of the hydrodynamic behaviour of the probe chains were initiated for networks swollen to equilibrium under a range of thermodynamic conditions so as to test theories describing the diffusion of trapped chains in concentrated media.

5.1. General Discussion

To study the behaviour of trapped chains, it was necessary to prepare a series of high quality model networks, which contained no macromolecular sol fraction usually associated with polymeric networks. Polymeric networks containing no trapped chains (so called blank networks) were prepared using a conventional difunctional anionic polymerisation initiator (di-sodium tetramer of α -methyl styrene) and contrary to the reports published in the literature were unable to be cross linked with a reasonable efficiency. Networks produced from the system were found to contain a large macromolecular sol fraction and the cross link density of the network was not able to be predicted with any degree of accuracy.

However using a novel difunctional organo-lithium initiator system based on 1,3-bis(1-phenylethenyl)benzene it has been found possible to prepare high quality model polymer networks containing only a very small fraction of macromolecular sol. Such networks have been prepared efficiently, the cross link densities of which have been predicted with great consistency.

Characterisation of the properties of these networks has been undertaken and the properties of the networks examined in terms of the scaling models of de Gennes. The

swelling of the network has been examined as a function of the quality of the swelling solvent and in the good solvent limit at 298K in toluene. The scaling predictions relating the volumetric swelling of the network and the cross link density have been found to be consistent with experimental observations. In solvents of relatively poor quality, the scaling exponents were found to be somewhat lower than the good solvent value, however progressively increasing the solvent quality was found to lead to behaviour approaching that of a good solvent.

The collective motions of the solvent swollen gels have been studied using QELS in the good solvent limit in toluene at 298K as well as under theta conditions in cyclohexane at 308K. In theta conditions, the scaling exponent relating the co-operative diffusion coefficient to the polymer volume fraction was found to be in excellent agreement with the predicted value, progressive increases in the solvent quality through increasing the temperature of the gel were found to bring about a decrease the scaling exponent towards the good solvent value. However in the good solvent limit, the scaling exponent was found to be substantially different to that predicted by theory, a difference which is thought to be due to the limited range of the data points available from the PBMPPD networks.

The collective motions of a series of semi-dilute solutions of concentrations equivalent to that of the solvent swollen networks have also been studied by QELS and differences between the two systems quantified. The autocorrelation function from the swollen network is in all cases, found to be composed of a single stretched exponential decay, while that obtained from the semi-dilute solutions is found to be composed of upwards of two decays depending on the concentration of the solution and the molecular weight of the polymer. For solutions of high molecular weight and/or high concentration a second decay, over three decades longer than that due to the collective chain motions has been found which has been attributed to the viscoelastic properties of the overlapping semi-dilute chains. This relaxation is not present in swollen polymer networks as the chains of the network are prevented from dis-entangling over long time scales, unlike the

chains of the semi-dilute solution. The collective motions of semi-dilute solutions of the $100,000 \text{ gmol}^{-1}$ matrix polymer have been found to be dependent on the polymer concentration, although the scaling exponents have been found to be somewhat smaller than that predicted by theory. Increasing the solvent quality has been found to lead to a decrease in the magnitude of the scaling exponent as predicted by scaling theory.

The longitudinal osmotic modulus of the polymer networks swollen in cyclohexane in the temperature range 308-323K has also been extracted from the autocorrelation function of the QELS spectrum. Again, scaling trends following those predicted by de Gennes have been observed, though the magnitudes of the scaling exponents differ from those predicted by theory. This is a feature attributed to the relative magnitudes of the osmotic moduli obtained from the AMS/DVB and PBMPPD/DVB series of networks. Values obtained from the relatively open structured AMS/DVB series of networks were found to vary little with either solvent quality or the polymer concentration, while results obtained from the PBMPPD/DVB series of networks were found to be dependent on both solvent quality and polymer volume fraction. Hence as the solvent quality increases and the osmotic moduli of the PBMPPD/DVB series decreases, the scaling exponent decreases towards that of the good solvent limit.

While scaling behaviour consistent with theoretical predictions has been found for the collective diffusion coefficient and hence the hydrodynamic correlation length, the correlation length describing the excluded volume interactions has been measured by SANS and has been found to be independent of the polymer concentration, dependent only on the solvent quality of the network. The explanation advanced for this behaviour centres on the method of preparation of the networks.

All networks regardless of cross link density were prepared from a 10% solution of polystyrene in the good solvent benzene. For such a semi-dilute solution, the excluded volume correlation length is dependent only on the polymer concentration and

describes the separation of entanglements on the backbone of the polymer chain. Over long time scales these entanglements can disentangle, however by the introduction of a cross linking agent joining the chain ends, it is postulated that these entanglements become "frozen" into the networks structure and therefore the correlation length of the network is controlled by that of the semi-dilute solution at the moment of cross linking.

To investigate the conformation of the probe chains within the networks, a perdeuterated polystyrene polymer has been incorporated into the reaction medium prior to cross linking the network. This probe polymer has been trapped within networks where the cross link density has been tightly controlled between a range between 50,000 gmol^{-1} and 10,000 gmol^{-1} . In the bulk state, the hydrogenous network and the perdeuterated probe chain have not been found to exist in separate phases, the molecular weights of the probe chains indicating that the trapped chains exist as non-aggregated particles, regardless of the cross link density of the network.

However, the cross link density has been found to influence the radius of gyration of the probe chain. Theoretical predictions of the probe chain in a random medium suggest that the probe chain should contract below the unperturbed dimensions as the cross link density of the network is increased. However, increasing the cross link density of the medium has been found to cause an increase in the radius of gyration of the probe chain. No explanation for this behaviour can be advanced at present as only a limited amount of data was collected in the short amount of experimental time available.

The size of the probe chain has also been determined in networks swollen to equilibrium in cyclohexane in the temperature range 308-318K. The radius of gyration of the probe chain has been found to be independent of the cross link density of the network and for networks swollen at the theta point, the radius of gyration of the probe chain has been found to be in line with the unperturbed dimensions of the chain. Increasing the temperature of the system and hence the solvent quality have been found to lead to an increase in the size of the chain. Behaviour of this type has been identified

as being similar to that of a semi-dilute chain in a theta solvent (region III of the polymer phase diagram), as might be expected following the c^* theorem of de Gennes relating the behaviour of semi-dilute solutions with that of swollen networks.

The hydrodynamic properties of the probe chain within the network have been studied using the decay of the autocorrelation function from a QELS experiment to provide an estimate of the self diffusion coefficient of the probe chain. Previous studies of ternary solutions have shown the possibility of deconvoluting the autocorrelation function into its components to measure the tracer diffusion coefficient of the dilute chain relative to that of the matrix. In principle the two relaxation's of the gel and the probe should have been more easily resolved as compared to that of a ternary solution, the difference in the molecular weight of the network and the probe being larger than a semi-dilute matrix. A series of networks containing a number of different high molecular weight probe molecules have been prepared and studied by QELS, however it has not been found possible to extract the diffusion coefficient of the probe chain from the QELS spectrum as the two relaxation's overlap too closely, the ratio of the hydrodynamic radii of probe and gel being close to unity. Hence no information has been obtained regarding the applicability of the reptation model for the probe chain diffusing through the cross linked network.

5.2. Conclusions.

In summary a series of high quality model polystyrene networks have been prepared and characterised. The volumetric swelling ratio, co-operative diffusion coefficient and longitudinal osmotic modulus of the networks have been examined as a function of the solvent quality and polymer concentration. The predictions of scaling theory have been confirmed for these networks and in the main scaling exponents in line with those predicted have been found for the swollen networks.

Two series of probe polymer chains have been *trapped* within these model networks. A perdeuterated probe polymer has been incorporated into the networks so as

to measure the size of the chain as a function of the cross link density in the bulk network and when swollen with solvent. In the bulk, the predictions of the chain in a random medium have been found to be inapplicable as the size of the chain increased with the cross link density. No evidence for phase separation between the probe polymer and the network was found. In the solvent swollen networks, the size of the chain was found to be independent of the cross link density of the network, the radius of gyration being dependent only on the temperature of the cyclohexane swollen gel. For networks swollen at the theta point unperturbed chain dimensions were found, while increasing the temperature was found to increase the size of the probe chain. This behaviour has been identified with that of a semi-dilute solution at the theta point, the so-called region III of the polymer phase diagram.

A second series of networks containing high molecular weight hydrogenous polymers have been prepared in an attempt to study the hydrodynamic properties of probe chains in polymer gels and in solutions of equivalent concentration. However, deconvolution of the two decays in the QELS spectrum has not been possible as was first thought possible and the mechanism of diffusion of the probe chain within the network remains unknown.

5.3 Suggestions for Future Work.

Clearly, from the results presented above, the properties of the model networks prepared have been found to be described well by the scaling predictions of de Gennes and as such little further work can be envisaged on this subject. However, the properties of polymer chains trapped within these networks remain not well understood. The conformation of the one probe chain trapped within the network indicates an increase in the size of the chain and as noted earlier no explanation for this increase has as yet been advanced.

Theoretical work to model the size of a polymer in such a situation should help to provide some insight into this chain expansion, which could be determined more

thoroughly by further SANS studies utilising probe polymers of different molecular weight trapped in networks where the cross link density is chosen to be in the critical region around $5\text{-}20,000\text{ gmol}^{-1}$. Although no evidence for phase separation was found using a low molecular weight perdeuterated probe polymer, this would appear surprising and phase separation might be found for probe polymers of higher molecular weight. This again is an area that could be studied by SANS.

Perhaps the most important result which might have been obtained from this study was the determination of the mode of diffusion of the probe polymer within the network. Although this has not been found possible using QELS, the ability to prepare trapped polymer containing networks has been demonstrated and as such the self-diffusive motions of a suitably tagged polystyrene polymer might be studied by techniques such as quasi-elastic neutron scattering, pulsed field gradient NMR or forced Rayleigh scattering. Similar experiments to those performed here might help to alleviate many of the questions posed surrounding the diffusion of polymer chains within concentrated, entangled systems.

Appendix A

Glossary of Terms and Symbols Used

Glossary of Terms and Symbols Used.

Chapter 1.

A_2	Second Virial Coefficient
c^*	Critical Overlap Concentration
C_∞	Characteristic Ratio
D_{co}	Collective Diffusion Coefficient
D_s	Self Diffusion Coefficient
D_t	Tracer Diffusion Coefficient
g	Number of Monomers per 'Blob'
k_B	The Boltzmann Constant
M_{os}	Longitudinal Osmotic Modulus
M_c	Molecular Weight Between Cross Links In a Network
M_n	Number Average Molecular Weight
M_w	Weight Average Molecular Weight
N	Number of Segments in the Polymer Chain
N_A	Avagadro's Number
R	Universal Gas Constant
R_g	The Radius of Gyration of the Polymer
R_h	The Hydrodynamic Radius of the Polymer
$\sqrt{r^2}$	Root Mean Square End-to End Distance
T	The Absolute Temperature of the System
T_r	Reptation Time
V_o	Unswollen Undeformed Volume of the Network
\bar{V}_1	Molar Volume of Solvent
α	Linear Expansion Factor
χ	Flory-Huggins Interaction Parameter
η	Shear Viscosity
η_o	Solvent Viscosity
$[\eta]$	Intrinsic Viscosity
μ	Chain Mobility
μ_e	The Number of Elastically Effective Cross Links in the Network
ν	Excluded Volume Exponent
ν_e	Number Of Chains Connecting two Elastically Effective Junctions
π	Osmotic Pressure
ρ	The Bulk Density
ρ_o	Mean Obstacle Density of a Random Medium
τ	Reduced Temperature
υ	Specific Volume
ξ	Correlation Length

ζ	Monomer Friction Coefficient
ζ_N	Cycle Rank of the Polymer Network

Chapter 2.

c_o	The Concentration of Polymer at the Point of Cross Linking
DP	Degree of Polymerisation
M_n	Number Average Molecular Weight
M_w	Weight Average Molecular Weight
Q	Equilibrium Volumetric Swelling Ratio
V_d	Volume of the Dry Network
V_o	Volume of the System at the Point of Cross Linking
\bar{V}_s	Molar Volume of Solvent
ϕ_p	The Polymer Volume Fraction in the Swollen Network

Chapter 3.

b	Scattering Length
I	Intensity of Radiation
\bar{k}	Wave Vector
m	Neutron Mass
M_z	Z-Average Molecular Weight
n	Refractive Index
P(Q)	Particle Form Factor
\bar{Q}	Scattering Vector
Q(Q)	Normalised Interference Term
S(Q)	Structure Factor
z	Number of Segments in the Polymer Chain
λ	Wavelength of Radiation
θ	Scattering Angle
ρ	Scattering Length Density
σ	Scattering Cross Section
v_o	Reference Scattering Volume

Chapter 4.

D_{obs}	Measured Diffusion Coefficient
D_{co}	Collective Diffusion Coefficient
D_s	Self Diffusion Coefficient
D_t	Tracer Diffusion Coefficient
E_o	Electric Field of the Radiation Incident on a Particle
f	Friction Coefficient of the Swollen Gel
G	Shear Modulus of a Swollen Network

$G^1(\tau)$	Field Autocorrelation Function
$g^1(\tau)$	Field Correlation Function
$G^2(\tau)$	Intensity Autoorrelation Function
$g^2(\tau)$	Intensity Correlation Function
K	Bulk Modulus of a Swollen Network
M	Molecular Weight of the Scattering Centre
M_{os}	Longitudinal Osmotic Modulus
N	Number of Pulses Generated by Reference Signal in Heterodyne QELS
$R(\theta)$	Rayleigh Ratio
r	Observer Distance in a Light Scattering Experiment
w	Weight Fraction of Polymer in a Swollen Network
V	Volume of the Scattering Region
Δ	Delay Period of the Correlator
Γ	Relaxation Rate of the Decay of the Autocorrelation Function
$\bar{\Gamma}$	Mean Relaxation Rate of a Cumulant Distribution
α	Molecular Polarisability
β	Variance
μ	Induced Dipole Moment
μ_2	Second Moment of a Cumulant Distribution
ξ_h	Hydrodynamic Correlation Length

Appendix B

Volumetric Swelling Results

SAMPLE	Dry Wt.	Run 1	Run 2	Run 3	Average	Std. Dev.	% Error	Q	Err Q	Phi P	Err Phi P
AMS 4	0.21318	2.3749	2.1142	2.04795	2.179017	0.172844	7.932192	13.58221	1.107653	0.072472	0.006372
AMS 5	0.07655	0.5881	0.5969	0.6273	0.6041	0.020568	3.404724	10.39921	0.367064	0.094654	0.00369
AMS 6	0.04295	0.3891	0.3909	0.3971	0.392367	0.004197	1.069618	12.09849	0.133492	0.081359	0.000977
AMS 7	0.06347	0.7254	0.7263	0.7258	0.725833	0.000451	0.062125	15.2412	0.009706	0.064583	4.4E-05
AMS 11	0.05012	0.537	0.5386	0.5579	0.5445	0.011632	2.136324	14.45987	0.317067	0.068073	0.001602
AMS 16	0.04448	0.6226	0.6355	0.6441	0.634067	0.010821	1.706671	19.0927	0.332366	0.051555	0.000946
AMS 19	0.07456	0.8704	0.8679	0.8765	0.8716	0.004424	0.507549	15.58829	0.081056	0.063145	0.00035
TCH 1	0.19638	0.6515	0.6452	0.6522	0.649633	0.003855	0.593458	4.137445	0.02682	0.237907	0.002024
TCH 2	0.12596	0.5769	0.57545	0.57825	0.576867	0.0014	0.242742	5.874795	0.015187	0.167551	0.00052
TCH 3	0.06523	0.4606	0.4612	0.4818	0.467867	0.01207	2.579869	9.416945	0.252795	0.104527	0.003134
TCH 4	0.20035	0.61595	0.6125	0.6177	0.615383	0.002646	0.429961	3.81435	0.018042	0.258059	0.001645
TCH 5	0.18082	0.9652	0.9872	0.99713	0.983177	0.016341	1.662041	7.046349	0.123459	0.139693	0.002845
TCH 6	0.12782	0.8653	0.86699	0.8941	0.875463	0.016162	1.8461	8.975162	0.172739	0.109672	0.002371
TCH 7	0.21917	0.747	0.7437	0.7442	0.744967	0.001779	0.238746	4.261755	0.011086	0.230967	0.000781
TCH 8	0.17111	0.89576	0.8993	0.9003	0.898453	0.002385	0.26551	6.791444	0.019046	0.144936	0.000475
TCH 9	0.29493	1.61312	1.6801	1.7245	1.672573	0.05607	3.35233	7.365703	0.259722	0.133636	0.005439
TCD 1	0.06874	0.6048	0.59765	0.6193	0.60725	0.011031	1.816547	11.68672	0.219231	0.084226	0.001725
TCD 2	0.14477	0.7111	0.7047	0.6858	0.700533	0.013155	1.877797	6.228872	0.124135	0.158026	0.00374
TCD 4	0.13928	0.5376	0.5337	0.51833	0.529877	0.010188	1.922724	4.815539	0.099931	0.204406	0.005332
TCD 5	0.10794	0.42925	0.4303	0.4295	0.429683	0.000548	0.127648	5.056475	0.006942	0.194666	0.000332
TCD 6	0.06364	0.19675	0.1983	0.19755	0.197533	0.000775	0.392407	3.858581	0.01664	0.255101	0.001477
DLB 1	0.1568	0.55145	0.5475	0.54132	0.546757	0.005106	0.933824	4.381884	0.044485	0.224635	0.002941
DLB 2	0.3332	1.3737	1.35791	1.38581	1.372473	0.01399	1.019356	5.245422	0.057362	0.187654	0.002526
DLB 3	0.31214	1.47142	1.50123	1.50069	1.491113	0.017057	1.143915	6.144343	0.074654	0.1602	0.002318
DLB 4	0.30478	1.0455	1.0191	1.01331	1.02597	0.017159	1.67251	4.216984	0.076915	0.233419	0.005554
Constants											
Specific Volume, Bulk Polystyrene (cm3/g)							0.957				
Specific Volume, Cyclohexane @35 Degrees							1.3074				
Partial Specific Volume, PS in Cyclohexane							0.942				

Appendix B1: Swelling Results in Cyclohexane at 308K

SAMPLE	Dry Wt.	Run 1	Run 2	Run 3	Average	Std. Dev.	% Error	Q	Err Q	Phi P	Err Phi P
AMS 4	0.21318	2.3256	2.0796	1.9778	2.127667	0.178813	8.404173	13.33009	1.153092	0.073842	0.006897
AMS 5	0.07655	0.7732	0.788	0.8067	0.7893	0.016788	2.126922	13.78415	0.301481	0.07141	0.001682
AMS 6	0.04295	0.4444	0.4462	0.4399	0.4435	0.003245	0.731679	13.80484	0.103863	0.071303	0.000578
AMS 7	0.06347	0.8477	0.8313	0.828	0.835667	0.010551	1.262583	17.70953	0.228526	0.055582	0.000759
AMS 11	0.05012	0.6732	0.6903	0.723	0.6955	0.025304	3.638239	18.68608	0.694048	0.052677	0.002065
AMS 16	0.04448	0.7043	0.6515	0.7105	0.688767	0.032422	4.707316	20.89685	1.002057	0.047104	0.00237
AMS 19	0.07456	0.9993	1.0131	1.0368	1.0164	0.018967	1.866052	18.34966	0.349699	0.053643	0.00108
TCH 1	0.19638	0.6853	0.6884	0.6849	0.6862	0.001916	0.279179	4.413197	0.013411	0.223041	0.000872
TCH 2	0.12596	0.6536	0.6547	0.6595	0.655933	0.003137	0.478312	6.768393	0.034241	0.14543	0.000861
TCH 3	0.06523	0.5714	0.5776	0.5689	0.572633	0.004479	0.782213	11.67778	0.094399	0.084291	0.000744
TCH 4	0.20035	0.6451	0.6529	0.6457	0.6479	0.004341	0.669935	4.055215	0.029783	0.242731	0.002354
TCH 5	0.18082	1.1353	1.13882	1.13125	1.135123	0.003788	0.333716	8.239568	0.0288	0.119463	0.000474
TCH 6	0.12782	1.0112	1.1001	1.0802	1.063833	0.046655	4.38557	11.05121	0.501779	0.08907	0.00444
TCH 7	0.21917	0.765	0.766	0.7589	0.7633	0.003843	0.503495	4.397304	0.024106	0.223848	0.001581
TCH 8	0.17111	1.0027	0.9899	1.0043	0.998967	0.007893	0.790078	7.635399	0.06341	0.128916	0.001229
TCH 9	0.29493	2.00039	1.99683	2.0316	2.009607	0.01913	0.951917	8.976689	0.089167	0.109654	0.001223
TCD 1	0.06874	0.7027	0.7218	0.7318	0.718767	0.014785	2.057029	13.98403	0.295686	0.070389	0.001601
TCD 2	0.14477	0.7275	0.7364	0.7653	0.743067	0.019762	2.659542	6.665655	0.187658	0.147671	0.004878
TCD 4	0.13928	0.5586	0.5585	0.5586	0.558567	5.77E-05	0.010336	5.122743	0.00057	0.192148	2.65E-05
TCD 5	0.10794	0.456	0.4464	0.4335	0.4453	0.01129	2.535428	5.280908	0.143792	0.186393	0.006238
TCD 6	0.06364	0.2067	0.2044	0.2041	0.205067	0.001422	0.693647	4.039339	0.030727	0.243685	0.002451
DLB 1	0.1568	0.5806	0.59018	0.58275	0.58451	0.005027	0.859978	4.734188	0.04407	0.207919	0.002444
DLB 2	0.3332	1.56028	1.5332	1.5447	1.54606	0.013591	0.879082	5.98833	0.056074	0.164374	0.001842
DLB 3	0.31214	1.64082	1.6548	1.65255	1.64939	0.007507	0.455115	6.873781	0.03306	0.1432	0.000804
DLB 4	0.30478	1.03362	0.97351	0.9759	0.994343	0.034036	3.42292	4.094607	0.153518	0.240396	0.011865
Constants											
Specific Volume, Bulk Polystyrene (cm ³ /g)							0.957				
Specific Volume, Cyclohexane @40 Degrees							1.3156				
Partial Specific Volume, PS in Cyclohexane							0.942				

SAMPLE	Dry Wt.	Run 1	Run 2	Run 3	Average	Std. Dev.	% Error	Q	Err Q	Phi P	Err Phi P
AMS 4	0.21318	2.4214	2.3716	No Data	2.3965	0.035214	1.469389	15.15251	0.228513	0.064961	0.001048
AMS 5	0.07655	1.0284	1.0457	No Data	1.03705	0.012233	1.179591	18.34216	0.22107	0.053665	0.000683
AMS 6	0.04295	0.5304	0.5129	No Data	0.52165	0.012374	2.372159	16.40287	0.398569	0.060009	0.001551
AMS 7	0.06347	1.0215	0.9838	No Data	1.00265	0.026658	2.658747	21.4546	0.581033	0.045879	0.001302
AMS 11	0.05012	0.9938	1.0249	No Data	1.00935	0.021991	2.178731	27.46048	0.606984	0.035845	0.000822
AMS 16	0.04448	0.8185	0.7006	No Data	0.75955	0.083368	10.97596	23.22393	2.592849	0.042384	0.004941
AMS 19	0.07456	1.2151	1.173	No Data	1.19405	0.029769	2.493128	21.75533	0.552337	0.045245	0.001203
TCH 1	0.19638	0.7339	0.7265	0.7148	0.725067	0.00963	1.3282	4.708623	0.06784	0.209048	0.003808
TCH 2	0.12596	0.762	0.7727	0.7567	0.7638	0.00815	1.067093	7.989555	0.089514	0.123202	0.001574
TCH 3	0.06523	0.7081	0.7147	0.7388	0.720533	0.01616	2.242773	14.88188	0.342717	0.066143	0.001631
TCH 4	0.20035	0.6865	0.6741	0.7267	0.695767	0.027497	3.952065	4.405101	0.189864	0.223451	0.012402
TCH 5	0.18082	1.5008	1.46562	1.4576	1.474673	0.022979	1.55824	10.88311	0.175803	0.090445	0.001606
TCH 6	0.12782	1.3381	1.3263	1.30483	1.323077	0.016868	1.274876	13.92049	0.182557	0.070711	0.000998
TCH 7	0.21917	0.8069	0.8056	0.8027	0.805067	0.00215	0.267083	4.682464	0.013572	0.210215	0.000771
TCH 8	0.17111	1.0906	1.1055	1.1556	1.117233	0.034051	3.04784	8.633519	0.275299	0.114012	0.004103
TCH 9	0.29493	2.31835	2.32006	2.2927	2.31037	0.015327	0.66338	10.43786	0.07189	0.094303	0.000717
TCD 1	0.06874	0.8786	0.8252	0.8764	0.860067	0.030215	3.513152	16.9097	0.608083	0.058211	0.002223
TCD 2	0.14477	0.8206	0.8021	0.8046	0.8091	0.010037	1.240567	7.332496	0.095915	0.134242	0.002028
TCD 4	0.13928	0.5867	0.5856	0.5816	0.584633	0.002684	0.459075	5.407756	0.026658	0.182021	0.001097
TCD 5	0.10794	0.4872	0.4815	0.48	0.4829	0.003799	0.78664	5.789906	0.048685	0.170007	0.001722
TCD 6	0.06364	0.2175	0.2078	0.2091	0.211467	0.005265	2.489894	4.197734	0.114455	0.23449	0.008352
DLB 1	0.1568	0.62586	0.61748	0.62543	0.622923	0.004719	0.757552	5.096751	0.041634	0.193128	0.001955
DLB 2	0.3332	1.8653	1.86261	1.84293	1.856947	0.012213	0.657697	7.310644	0.050706	0.134643	0.001079
DLB 3	0.31214	1.92042	1.91057	1.88763	1.906207	0.016825	0.882634	8.049133	0.074567	0.12229	0.001291
DLB 4	0.30478	1.13092	1.10043	1.1046	1.111983	0.016532	1.486681	4.648193	0.075037	0.211765	0.004337
Constants											
Specific Volume, Bulk Polystyrene (cm3/g)							0.957				
Specific Volume, Cyclohexane @45 Degrees							1.3239				
Partial Specific Volume, PS in Cyclohexane							0.942				

Appendix B3: Swelling Results in Cyclohexane at 318K

SAMPLE	Dry Wt.	Run 1	Run 2	Run 3	Average	Std. Dev.	% Error	Q	Err Q	Phi P	Err Phi P
AMS 4	0.21318	2.4727	2.0457	2.0792	2.1992	0.237449	10.79708	13.95687	1.551003	0.070526	0.008432
AMS 5	0.07655	1.1408	1.1693	No Data	1.15505	0.020153	1.744733	20.60269	0.366583	0.047777	0.000893
AMS 6	0.04295	0.6129	0.5283	0.5221	0.554433	0.050728	9.149599	17.56706	1.64466	0.056032	0.005557
AMS 7	0.06347	1.1111	1.0617	No Data	1.0864	0.034931	3.215305	23.42652	0.766357	0.042018	0.001435
AMS 11	0.05012	1.1192	1.0259	No Data	1.07255	0.065973	6.151048	29.39035	1.83292	0.033491	0.002161
AMS 16	0.04448	0.8075	0.817	No Data	0.81225	0.006718	0.827025	25.01989	0.210296	0.039342	0.000344
AMS 19	0.07456	1.3232	1.3173	No Data	1.32025	0.004172	0.315995	24.24873	0.077915	0.040593	0.000136
TCH 1	0.19638	0.7363	0.6971	0.7116	0.715	0.01982	2.77202	4.661718	0.140538	0.211151	0.008069
TCH 2	0.12596	0.8204	0.8135	0.8198	0.8179	0.003822	0.467331	8.633661	0.042255	0.11401	0.00063
TCH 3	0.06523	0.7923	0.7685	0.7734	0.778067	0.012568	1.615228	16.20138	0.268282	0.060756	0.001071
TCH 4	0.20035	0.7035	0.7064	0.7051	0.705	0.001453	0.20604	4.491754	0.010096	0.219141	0.000631
TCH 5	0.18082	1.4984	1.46608	1.4545	1.472993	0.022752	1.544602	10.93522	0.17521	0.090014	0.001585
TCH 6	0.12782	1.46491	1.44911	1.4333	1.449107	0.015805	1.090672	15.37848	0.17218	0.064007	0.000766
TCH 7	0.21917	0.8382	0.8341	0.8227	0.831667	0.008031	0.965699	4.875767	0.051027	0.201881	0.002647
TCH 8	0.17111	1.2303	1.2401	1.2455	1.238633	0.007705	0.62209	9.671727	0.062706	0.101774	0.000735
TCH 9	0.29493	2.51181	2.57598	2.54448	2.54409	0.032087	1.261228	11.60346	0.151494	0.08483	0.00121
TCD 1	0.06874	0.9667	0.9526	0.9424	0.9539	0.012202	1.279175	18.91514	0.247179	0.052039	0.000717
TCD 2	0.14477	0.8448	0.8623	0.8124	0.839833	0.025318	3.014651	7.669823	0.243523	0.128338	0.004675
TCD 4	0.13928	0.586	0.5724	0.5748	0.577733	0.007259	1.256465	5.367841	0.072573	0.183375	0.003036
TCD 5	0.10794	0.4765	0.4741	0.4839	0.478167	0.005108	1.068281	5.760423	0.065898	0.170877	0.002358
TCD 6	0.06364	0.2117	0.2078	0.2065	0.208667	0.002706	1.296885	4.157585	0.059212	0.236754	0.004418
DLB 1	0.1568	0.65405	0.64832	0.64435	0.648907	0.004877	0.751501	5.354523	0.043307	0.183831	0.001822
DLB 2	0.3332	2.1576	2.13931	2.1254	2.14077	0.01615	0.754381	8.538344	0.067491	0.115283	0.00103
DLB 3	0.31214	2.4445	2.37085	2.32564	2.38033	0.059994	2.520424	10.21065	0.267639	0.096402	0.002796
DLB 4	0.30478	1.13792	1.1773	1.14703	1.154083	0.020616	1.786329	4.864616	0.094189	0.202344	0.004912
Constants											
Specific Volume, Bulk Polystyrene (cm3/g)							0.957				
Specific Volume, Cyclohexane @50 Degrees							1.3326				
Partial Specific Volume, PS in Cyclohexane							0.942				

Appendix B4: Swelling Results in Cyclohexane at 323K

SAMPLE	Dry Wt.	Run 1	Run 2	Run 3	Average	Std. Dev.	% Error	Q	Err Q	Phi P	Err Phi P	Mc
AMS 4	0.23571	15.7384	No Data	No Data	15.7384			80.1996		0.011961		430331.3
AMS 5	0.11135	5.3059	5.1842	No Data	5.24505	0.086055	1.640688	56.50587	0.931114	0.016976	0.000285	233624.2
AMS 6	0.04741	1.4633	1.4398	No Data	1.45155	0.016617	1.144777	36.64196	0.422228	0.026179	0.00031	108201.2
AMS 7	0.07535	3.7884	3.7508	No Data	3.7696	0.026587	0.705306	60.02835	0.425116	0.015981	0.000115	259778.4
AMS 11	0.05083	2.9855	2.8713	No Data	2.9284	0.080752	2.757533	69.16534	1.914028	0.013869	0.000389	332746
AMS 16	0.05787	3.4273	3.4729	No Data	3.4501	0.032244	0.934584	71.58274	0.671295	0.013401	0.000127	353256
AMS 19	0.05352	2.2856	2.3175	No Data	2.30155	0.022557	0.980066	51.56541	0.507782	0.018603	0.000187	198859.6
TCH 1	0.03671	0.3224	0.3124	0.3081	0.3143	0.007337	2.33436	10.06963	0.240794	0.095261	0.002518	9167.266
TCH 2	0.07483	1.5613	1.5315	1.534	1.542267	0.016531	1.071843	24.58583	0.266154	0.039016	0.00044	52219.37
TCH 3	0.03763	1.7665	1.7461	1.7382	1.750267	0.014603	0.834322	55.79305	0.467542	0.017193	0.000147	228468.9
TCH 4	0.20149	1.4883	1.4856	1.4882	1.487367	0.001531	0.10292	8.64813	0.009153	0.11092	0.000132	6666.746
TCH 5	0.31547	8.58796	8.9218	9.05564	8.855133	0.240862	2.720026	33.57295	0.919872	0.028572	0.000806	92399.35
TCH 6	0.13034	5.5738	5.5243	5.49927	5.532457	0.037929	0.685565	50.89408	0.350596	0.018848	0.000132	194311.9
TCH 7	0.10001	0.8603	0.8485	0.8435	0.850767	0.008626	1.013946	10.00351	0.10392	0.095891	0.001102	9043.2
TCH 8	0.14549	3.8936	3.8797	No Data	3.88665	0.009829	0.252886	31.9399	0.081392	0.030033	7.89E-05	84410.85
TCH 9	0.40574	8.6425	9.5224	10.3038	9.489567	0.831137	8.758425	27.93281	2.467982	0.034341	0.003142	66084.96
DLB 1	0.29813	2.7932	2.80456	2.8076	2.801787	0.00759	0.2709	11.07706	0.030673	0.086598	0.000263	11148.34
DLB 2	0.18131	3.4523	3.44936	3.5056	3.469087	0.031656	0.912506	22.80656	0.210352	0.04206	0.000405	45404.85
DLB 3	0.36504	7.0315	7.3277	7.9605	7.4399	0.474554	6.378505	24.30967	1.566257	0.03946	0.002647	51135.91
DLB 4	0.4631	3.7741	3.6576	3.72708	3.719593	0.05861	1.575703	9.431381	0.15248	0.101708	0.001831	8001.011
Constants												
Partial Specific Volume, Bulk Polystyrene (cm ³ /g)								0.957				
Partial Specific Volume, Toluene @ 25 Degrees								1.153				
Partial Specific Volume, PS in Toluene								0.918				
Chi, Polystyrene in Toluene								0.42				
Molar Volume of Toluene @ 25 Degrees (cm ³ /mol)								106.2374				
Density of Bulk Polystyrene (g/cm ³)								1.044932				
Partial Specific Volume, PS in Benzene								0.9185				
Concentration at Crosslinking (g/cm ³)								0.1				

Appendix B5. Swelling Results in Toluene at 298K

Appendix C

Quasi-Elastic Light Scattering Results

Concentration	SIQELS Results	CONTIN Results / $\times 10^{-7} \text{ cm}^2 \text{ s}^{-1}$		
/ gcm^{-3}	$D_z / \times 10^{-7} \text{ cm}^2 \text{ s}^{-1}$	D_n	D_w	D_z
11.423	3.38 ± 0.02	4.19	4.27	4.34
5.714	3.50 ± 0.03	3.69	3.81	3.93
4.319	3.85 ± 0.04	5.04	5.25	5.59
3.862	3.88 ± 0.02	3.71	3.85	4.01

Probe 3 QELS Results at 308K

Concentration	SIQELS Results	CONTIN Results / $\times 10^{-7} \text{ cm}^2 \text{ s}^{-1}$		
/ gcm^{-3}	$D_z / \times 10^{-7} \text{ cm}^2 \text{ s}^{-1}$	D_n	D_w	D_z
11.352	3.69 ± 0.02	4.68	4.78	4.92
5.679	4.05 ± 0.02	4.07	4.28	4.48
4.292	4.24 ± 0.02	4.29	4.35	4.40
3.838	4.35 ± 0.03	4.27	4.36	4.43
2.901	4.47 ± 0.01	4.56	4.72	4.88

Probe 3 QELS Results at 313K

Concentration	SIQELS Results	CONTIN Results / $\times 10^{-7} \text{ cm}^2 \text{ s}^{-1}$		
/ gcm^{-3}	$D_z / \times 10^{-7} \text{ cm}^2 \text{ s}^{-1}$	D_n	D_w	D_z
11.280	4.26 ± 0.01	4.79	4.89	5.02
5.643	4.54 ± 0.02	4.48	4.58	4.66
4.265	4.62 ± 0.03	4.76	4.92	5.08
3.813	4.73 ± 0.02	5.43	5.61	5.78
2.883	4.77 ± 0.02	5.25	5.29	5.57

Probe 3 QELS Results at 318K

Concentration	SIQELS Results	CONTIN Results / $\times 10^{-7} \text{ cm}^2 \text{ s}^{-1}$		
/ gcm^{-3}	$D_z / \times 10^{-7} \text{ cm}^2 \text{ s}^{-1}$	D_n	D_w	D_z
11.208	4.69 ± 0.02	5.47	5.67	5.85
5.607	4.91 ± 0.02	5.17	5.29	5.41
4.238	4.95 ± 0.01	4.46	4.56	4.68
3.789	5.20 ± 0.02	6.44	6.56	6.66
2.864	5.16 ± 0.01	5.21	5.41	5.61

Probe 3 QELS Results at 323K

Appendix C1: Dilute Solution QELS Results from the Probe 3 Polymer.

Concentration	SIQELS Results	CONTIN Results / $\times 10^{-7} \text{ cm}^2 \text{ s}^{-1}$		
/ gcm^{-3}	$D_z / \times 10^{-7} \text{ cm}^2 \text{ s}^{-1}$	D_n	D_w	D_z
6.632	2.37 ± 0.02	2.49	2.54	2.58
5.299	2.47 ± 0.02	2.22	2.30	2.36
4.135	2.67 ± 0.02	2.35	2.44	2.52
3.018	2.41 ± 0.02	2.96	3.02	3.07
2.697	3.29 ± 0.01	2.90	3.05	3.18

Probe 4 QELS Results at 308K

Concentration	SIQELS Results	CONTIN Results / $\times 10^{-7} \text{ cm}^2 \text{ s}^{-1}$		
/ gcm^{-3}	$D_z / \times 10^{-7} \text{ cm}^2 \text{ s}^{-1}$	D_n	D_w	D_z
6.591	2.80 ± 0.02	2.54	2.62	2.71
5.267	2.80 ± 0.03	2.57	2.67	2.77
4.109	3.00 ± 0.04	2.62	2.75	2.88
2.999	2.78 ± 0.01	3.06	3.13	3.19
2.680	3.76 ± 0.03	3.11	3.24	3.35

Probe 4 QELS Results at 313K

Concentration	SIQELS Results	CONTIN Results / $\times 10^{-7} \text{ cm}^2 \text{ s}^{-1}$		
/ gcm^{-3}	$D_z / \times 10^{-7} \text{ cm}^2 \text{ s}^{-1}$	D_n	D_w	D_z
6.549	3.16 ± 0.04	2.93	3.07	3.21
5.233	3.18 ± 0.01	2.78	2.89	3.00
4.083	3.42 ± 0.01	2.82	2.97	3.11
2.980	3.52 ± 0.19	2.98	3.18	3.31
2.663	3.99 ± 0.32	3.14	3.26	3.37

Probe 4 QELS Results at 318K

Concentration	SIQELS Results	CONTIN Results / $\times 10^{-7} \text{ cm}^2 \text{ s}^{-1}$		
/ gcm^{-3}	$D_z / \times 10^{-7} \text{ cm}^2 \text{ s}^{-1}$	D_n	D_w	D_z
6.507	3.55 ± 0.05	3.04	3.19	3.33
5.199	3.55 ± 0.03	3.08	3.21	3.33
4.057	3.87 ± 0.02	3.09	3.23	3.34
2.961	3.81 ± 0.1	3.12	3.38	3.63
2.646	4.32 ± 0.08	3.91	4.05	4.07

Probe 4 QELS Results at 323K

Appendix C2: Dilute Solution QELS Results from the Probe 4 Polymer.

Concentration / gcm ⁻³	SIQELS Results	CONTIN Results / x10 ⁻⁷ cm ² s ⁻¹		
	D _z / x10 ⁻⁷ cm ² s ⁻¹	D _n	D _w	D _z
3.753	1.39 ± 0.01	1.33	1.36	1.38
3.032	1.47 ± 0.01	1.41	1.45	1.49
2.301	1.53 ± 0.01	1.37	1.48	1.53
1.848	1.49 ± 0.01	1.49	1.53	1.56
0.917	1.62 ± 0.02	1.55	1.63	1.70

Probe 5 QELS Results at 308K

Concentration / gcm ⁻³	SIQELS Results	CONTIN Results / x10 ⁻⁷ cm ² s ⁻¹		
	D _z / x10 ⁻⁷ cm ² s ⁻¹	D _n	D _w	D _z
3.729	1.54 ± 0.01	1.57	1.58	1.62
2.997	1.63 ± 0.01	1.44	1.52	1.59
2.287	1.69 ± 0.01	1.47	1.60	1.71
1.836	1.63 ± 0.01	1.56	1.61	1.65
0.911	1.75 ± 0.01	1.72	1.82	1.89

Probe 5 QELS Results at 313K

Concentration / gcm ⁻³	SIQELS Results	CONTIN Results / x10 ⁻⁷ cm ² s ⁻¹		
	D _z / x10 ⁻⁷ cm ² s ⁻¹	D _n	D _w	D _z
3.706	1.73 ± 0.02	1.48	1.52	1.55
2.978	1.78 ± 0.01	1.57	1.63	1.67
2.272	1.86 ± 0.02	1.62	1.70	1.77
1.825	1.79 ± 0.02	1.80	1.91	1.89
0.906	1.94 ± 0.01	1.84	1.94	2.04

Probe 5 QELS Results at 318K

Concentration / gcm ⁻³	SIQELS Results	CONTIN Results / x10 ⁻⁷ cm ² s ⁻¹		
	D _z / x10 ⁻⁷ cm ² s ⁻¹	D _n	D _w	D _z
3.682	1.81 ± 0.01	1.54	1.59	1.65
2.959	1.98 ± 0.01	1.60	1.68	1.77
2.258	2.02 ± 0.01	1.77	1.81	1.86
1.813	1.96 ± 0.02	1.87	1.99	2.09
0.899	2.11 ± 0.01	1.95	2.06	2.17

Probe 5 QELS Results at 323K

Appendix C3: Dilute Solution QELS Results from the Probe 5 Polymer.

Volume	SIQELS Results		CONTIN Results / $\times 10^{-7} \text{ cm}^2 \text{ s}^{-1}$		
Fraction	$D_z / \times 10^{-7} \text{ cm}^2 \text{ s}^{-1}$	Variance	D_n	D_w	D_z
0.233	6.36 ± 0.29	0.877	5.24 ± 0.48	5.32 ± 0.50	5.40 ± 0.54
0.224	5.16 ± 0.96	0.842	4.86 ± 0.26	5.14 ± 0.34	5.40 ± 0.38
0.187	4.32 ± 0.93	0.907	3.12 ± 0.06	3.22 ± 0.04	3.50 ± 0.16
0.160	2.84 ± 0.83	0.802	3.00 ± 0.12	3.12 ± 0.14	3.62 ± 0.20

Heterodyne QELS from PBMPPD/DVB Networks at 308K

Volume	SIQELS Results		CONTIN Results / $\times 10^{-7} \text{ cm}^2 \text{ s}^{-1}$		
Fraction	$D_z / \times 10^{-7} \text{ cm}^2 \text{ s}^{-1}$	Variance	D_n	D_w	D_z
0.240	6.90 ± 0.29	0.896	6.20 ± 0.24	6.52 ± 0.32	6.78 ± 0.34
0.208	6.80 ± 0.15	0.898	5.60 ± 0.20	5.80 ± 0.14	5.98 ± 0.10
0.164	4.60 ± 0.19	0.918	3.86 ± 0.14	4.12 ± 0.30	4.60 ± 0.30
0.143	3.81 ± 0.15	0.829	4.10 ± 0.20	4.90 ± 0.28	5.60 ± 0.32

Heterodyne QELS from PBMPPD/DVB Networks at 313K

Volume	SIQELS Results		CONTIN Results / $\times 10^{-7} \text{ cm}^2 \text{ s}^{-1}$		
Fraction	$D_z / \times 10^{-7} \text{ cm}^2 \text{ s}^{-1}$	Variance	D_n	D_w	D_z
0.212	12.1 ± 1.71	0.664	7.32 ± 0.54	7.56 ± 0.53	7.79 ± 0.55
0.193	9.18 ± 0.77	0.842	6.86 ± 0.18	7.29 ± 0.14	7.81 ± 0.16
0.134	7.06 ± 0.48	0.797	4.72 ± 0.32	5.89 ± 1.0	6.88 ± 1.5
0.122	4.5 ± 0.06	0.812	4.57 ± 0.06	4.95 ± 0.10	5.31 ± 0.1

Heterodyne QELS from PBMPPD/DVB Networks at 318K

Volume	SIQELS Results		CONTIN Results / $\times 10^{-7} \text{ cm}^2 \text{ s}^{-1}$		
Fraction	$D_z / \times 10^{-7} \text{ cm}^2 \text{ s}^{-1}$	Variance	D_n	D_w	D_z
0.202	12.5 ± 0.14	0.605	9.66 ± 0.7	10.57 ± 0.9	11.33 ± 1.1
0.184	11.0 ± 0.18	0.518	8.44 ± 0.34	9.85 ± 0.3	11.03 ± 0.3
0.115	8.26 ± 0.39	0.475	6.78 ± 0.24	7.52 ± 0.68	8.11 ± 0.94
0.096	7.69 ± 0.25	0.381	6.68 ± 0.18	8.08 ± 0.18	9.22 ± 0.2

Heterodyne QELS from PBMPPD/DVB Networks at 323K

**Appendix C4: QELS Results from PBMPPD/DVB Networks Swollen
in Cyclohexane In The Temperature Range 308-323K.**

Volume	SIQELS Results		CONTIN Results / $\times 10^{-7} \text{ cm}^2 \text{ s}^{-1}$		
Fraction	$D_z / \times 10^{-7} \text{ cm}^2 \text{ s}^{-1}$	Variance	D_n	D_w	D_z
0.051	0.78 ± 0.34	0.661	1.83 ± 0.13	1.88 ± 0.13	1.92 ± 0.13
0.063	1.57 ± 0.11	0.684	0.98 ± 0.01	1.65 ± 0.62	2.32 ± 0.61
0.064	1.64 ± 0.16	0.730	0.93 ± 0.05	1.45 ± 0.17	1.95 ± 0.32
0.068	0.93 ± 0.50	0.695	1.85 ± 0.03	1.90 ± 0.05	1.98 ± 0.02
0.072	0.96 ± 0.09	0.620	2.46 ± 0.04	2.56 ± 0.04	2.68 ± 0.04
0.081	1.66 ± 0.25	0.662	2.79 ± 0.1	2.89 ± 0.05	3.04 ± 0.04
0.094	1.08 ± 0.60	0.668	4.25 ± 0.15	4.41 ± 0.14	4.56 ± 0.14

Heterodyne QELS from AMS/DVB Networks at 308K

Volume	SIQELS Results		CONTIN Results / $\times 10^{-7} \text{ cm}^2 \text{ s}^{-1}$		
Fraction	$D_z / \times 10^{-7} \text{ cm}^2 \text{ s}^{-1}$	Variance	D_n	D_w	D_z
0.047	1.18 ± 0.19	0.681	1.63 ± 0.05	1.71 ± 0.04	1.78 ± 0.02
0.053	1.60 ± 0.20	0.747	3.17 ± 0.01	3.23 ± 0.02	3.31 ± 0.03
0.054	1.72 ± 0.11	0.647	1.45 ± 0.06	1.49 ± 0.07	1.52 ± 0.08
0.056	2.26 ± 0.18	0.736	1.26 ± 0.67	1.88 ± 0.72	2.39 ± 0.62
0.071	1.53 ± 0.15	0.721	2.80 ± 0.20	2.92 ± 0.23	3.04 ± 0.25
0.071	1.89 ± 0.29	0.667	2.24 ± 0.28	2.38 ± 0.35	2.51 ± 0.33
0.074	1.47 ± 0.08	0.605	2.45 ± 0.24	2.59 ± 0.26	2.72 ± 0.27

Heterodyne QELS from AMS/DVB Networks at 313K

Volume	SIQELS Results		CONTIN Results / $\times 10^{-7} \text{ cm}^2 \text{ s}^{-1}$		
Fraction	$D_z / \times 10^{-7} \text{ cm}^2 \text{ s}^{-1}$	Variance	D_n	D_w	D_z
0.036	2.63 ± 0.46	0.748	1.74 ± 0.63	1.86 ± 0.64	1.97 ± 0.67
0.042	1.65 ± 0.18	0.662	2.57 ± 0.13	2.65 ± 0.10	2.73 ± 0.06
0.045	2.25 ± 0.25	0.556	2.09 ± 0.12	2.24 ± 0.15	2.39 ± 0.18
0.046	3.16 ± 0.33	0.560	2.12 ± 0.13	2.15 ± 0.14	2.17 ± 0.14
0.053	2.14 ± 0.09	0.721	1.97 ± 0.61	2.38 ± 0.21	2.67 ± 0.05
0.06	2.65 ± 0.28	0.684	1.76 ± 0.17	2.33 ± 0.36	2.62 ± 0.43
0.064	2.05 ± 0.16	0.657	2.51 ± 0.11	2.64 ± 0.13	2.75 ± 0.15

Heterodyne QELS from AMS/DVB Networks at 318K

**Appendix C5: QELS Results from AMS/DVB Networks Swollen
in Cyclohexane In The Temperature Range 308-318K.**

Volume	SIQELS Results		CONTIN Results / $\times 10^{-7} \text{ cm}^2 \text{ s}^{-1}$		
Fraction	$D_z / \times 10^{-7} \text{ cm}^2 \text{ s}^{-1}$	Variance	D_n	D_w	D_z
0.071	4.49 ± 0.65	0.689	3.61 ± 0.79	4.75 ± 0.97	5.51 ± 1.30
0.056	2.71 ± 0.46	0.634	3.21 ± 0.15	3.38 ± 0.25	3.55 ± 0.35
0.047	2.83 ± 0.29	0.795	2.82 ± 0.08	3.03 ± 0.06	3.24 ± 0.13
0.042	2.97 ± 0.25	0.786	3.60 ± 0.28	3.83 ± 0.33	4.05 ± 0.37
0.041	2.10 ± 0.15	0.687	3.32 ± 0.47	3.44 ± 0.48	3.57 ± 0.51
0.039	2.80 ± 0.22	0.895	2.33 ± 0.35	2.61 ± 0.46	2.92 ± 0.39
0.033	3.06 ± 0.66	0.801	4.89 ± 0.38	5.22 ± 0.49	5.54 ± 0.61

Heterodyne QELS from AMS/DVB Networks at 323K

Volume	SIQELS Results		CONTIN Results / $\times 10^{-7} \text{ cm}^2 \text{ s}^{-1}$		
Fraction	$D_z / \times 10^{-7} \text{ cm}^2 \text{ s}^{-1}$	Variance	D_n	D_w	D_z
0.0119	1.08 ± 0.19	0.663	1.76 ± 0.43	2.38 ± 0.97	3.20 ± 1.84
0.0134	0.74 ± 0.03	0.538	1.32 ± 0.54	1.37 ± 0.61	1.44 ± 0.68
0.0138	1.74 ± 0.60	0.867	2.05 ± 0.23	2.26 ± 0.26	2.49 ± 0.29
0.0159	1.08 ± 0.30	0.461	4.27 ± 0.36	4.32 ± 0.49	4.38 ± 0.55
0.0169	2.23 ± 0.92	0.57	1.76 ± 0.29	1.89 ± 0.33	2.03 ± 0.36
0.0186	0.97 ± 0.06	0.502	2.91 ± 0.49	2.95 ± 0.66	2.98 ± 0.79
0.0262	2.43 ± 0.19	0.583	2.11 ± 0.41	2.45 ± 0.56	2.79 ± 0.74

Heterodyne QELS from AMS/DVB Networks at 298K in Toluene.

Volume	SIQELS Results		CONTIN Results / $\times 10^{-6} \text{ cm}^2 \text{ s}^{-1}$		
Fraction	$D_z / \times 10^{-6} \text{ cm}^2 \text{ s}^{-1}$	Variance	D_n	D_w	D_z
0.102	3.41 ± 0.25	0.63	2.54 ± 0.57	2.77 ± 0.19	3.01 ± 0.27
0.087	2.14 ± 0.04	0.603	1.89 ± 0.27	2.04 ± 0.16	2.31 ± 0.31
0.042	2.25 ± 0.18	0.694	1.69 ± 0.39	1.94 ± 0.64	2.18 ± 0.45
0.039	1.57 ± 0.19	0.556	1.49 ± 0.13	1.67 ± 0.09	1.76 ± 0.29

Heterodyne QELS from PBMPPD/DVB Networks at 298K in Toluene.

Appendix C6: QELS Results from AMS/DVB Networks Swollen in Cyclohexane at 323K, in Toluene at 298K and from PBMPPD/DVB Networks Swollen in Toluene at 298K.

Volume	Longitudinal Osmotic Modulus Results (M_{os}) \pm Error / Nm^{-2}			
Fraction	308K	313K	318K	323K
0.051	395 \pm 66	234 \pm 11	261 \pm 24	8249 \pm 1003
0.063	705 \pm 294	544 \pm 106	830 \pm 139	62188 \pm 27826
0.064	694 \pm 234	644 \pm 86	941 \pm 373	32317 \pm 8229
0.068	571 \pm 401	382 \pm 87	339 \pm 18	3758 \pm 384
0.072	593 \pm 215	486 \pm 28	568 \pm 20	24686 \pm 1539
0.081	1447 \pm 559	1122 \pm 152	2989 \pm 2179	7865 \pm 1684
0.094	1266 \pm 339	940 \pm 76	1087 \pm 98	22176 \pm 1539

Longitudinal Osmotic Modulus Results From AMS/DVB Networks.

Volume	Longitudinal Osmotic Modulus Results (M_{os}) \pm Error / Nm^{-2}			
Fraction	308K	313K	318K	323K
0.233	160196 \pm 10350	127269 \pm 20772	92391 \pm 2120	24185 \pm 3394
0.224	65064 \pm 7355	43906 \pm 6078	63571 \pm 5850	51252 \pm 11155
0.187	56428 \pm 3889	28778 \pm 2687	146577 \pm 48509	6590 \pm 477
0.160	47331 \pm 4035	50597 \pm 8178	22111 \pm 826	3850 \pm 1098

Longitudinal Osmotic Modulus Results From PBMPPD/DVB Networks.

Volume Fractions Quoted Are Those Measured In Cyclohexane at 308K.

**Appendix C7: Longitudinal Osmotic Modulus Results from AMS/DVB
and PBMPPD/DVB Series Networks in Cyclohexane
in the Temperature Range 308-323K.**

Polymer	Relaxation Time / μ seconds and Variance		Z-Average D_c	
Mass Fraction	Fast Relaxation	Slow Relaxation	$\times 10^{-7} \text{cm}^2 \text{s}^{-1}$	
0.37	12.4 ± 0.4	0.853	Not Applicable	8.79 ± 0.31
0.186	12.5 ± 0.3	0.840	Not Applicable	7.15 ± 0.15
0.103	7.3 ± 0.1	0.820	Not Applicable	11.3 ± 0.18
0.056	6.6 ± 0.3	0.784	Not Applicable	12.1 ± 0.6
0.013	3.6 ± 0.3	0.709	Not Applicable	21.5 ± 1.8

SIQELS Results from 10,000 g/mol matrix solutions in cyclohexane at 308K

Polymer	Relaxation Time / μ seconds and Variance		Z-Average D_c	
Mass Fraction	Fast Relaxation	Slow Relaxation	$\times 10^{-7} \text{cm}^2 \text{s}^{-1}$	
0.409	17.5 ± 1.1	0.590	Not Applicable	6.56 ± 0.39
0.207	16.3 ± 0.1	0.699	Not Applicable	5.59 ± 0.05
0.101	11.5 ± 0.3	0.546	Not Applicable	7.73 ± 0.16
0.054	9.56 ± 0.3	0.667	Not Applicable	8.40 ± 0.29
0.010	7.5 ± 0.9	0.682	Not Applicable	10.3 ± 1.2

SIQELS Results from 20,000 g/mol matrix solutions in cyclohexane at 308K

Polymer	Relaxation Time / μ seconds and Variance		Z-Average D_c	
Mass Fraction	Fast Relaxation	Slow Relaxation	$\times 10^{-7} \text{cm}^2 \text{s}^{-1}$	
0.364	45.1 ± 0.6	0.811	Not Resolved	2.40 ± 0.03
0.199	51.2 ± 0.3	0.954	$8.1e^3 \pm 1.5e^2$ 0.910	1.76 ± 0.01
0.106	75.4 ± 0.8	0.65	Not Applicable	1.10 ± 0.01
0.050	34.7 ± 0.1	0.597	Not Applicable	2.3 ± 0.01
0.010	10.0 ± 0.3	0.699	Not Applicable	7.70 ± 0.20

SIQELS Results from 50,000 g/mol matrix solutions in cyclohexane at 308K

Polymer	Relaxation Time / μ seconds and Variance		Z-Average D_c	
Mass Fraction	Fast Relaxation	Slow Relaxation	$\times 10^{-7} \text{cm}^2 \text{s}^{-1}$	
0.427	35.2 ± 0.7	0.715	Not Resolved	3.35 ± 0.17
0.236	44.3 ± 0.2	0.914	$1.9e^4 \pm 5.1e^2$ 0.884	2.08 ± 0.07
0.125	63.8 ± 0.9	0.56	Not Resolved	1.32 ± 0.02
0.074	88.1 ± 0.5	0.754	Not Resolved	0.92 ± 0.05
0.019	24.9 ± 0.1	0.825	Not Applicable	3.12 ± 0.01

SIQELS Results from 100,000 g/mol matrix solutions in cyclohexane at 308K

Appendix C8: QELS Results from Equivalent Solutions in Cyclohexane at 308K

Polymer	Relaxation Time / μ seconds and Variance		Z-Average D_c	
Mass Fraction	Fast Relaxation	Slow Relaxation	$\times 10^{-7} \text{cm}^2 \text{s}^{-1}$	
0.37	11.2 ± 1.4	0.697	Not Applicable	9.75 ± 1.20
0.186	10.2 ± 0.7	0.599	Not Applicable	8.76 ± 0.60
0.103	6.8 ± 0.5	0.565	Not Applicable	12.2 ± 0.9
0.056	5.7 ± 0.9	0.469	Not Applicable	14.1 ± 2.2
0.013	1.3 ± 0.6	0.403	Not Applicable	59.7 ± 27.6

SIQELS Results from 10,000 g/mol matrix solutions in cyclohexane at 313K

Polymer	Relaxation Time / μ seconds and Variance		Z-Average D_c	
Mass Fraction	Fast Relaxation	Slow Relaxation	$\times 10^{-7} \text{cm}^2 \text{s}^{-1}$	
0.409	9.8 ± 0.3	0.497	Not Applicable	11.7 ± 0.3
0.207	16.3 ± 0.1	0.699	Not Applicable	5.60 ± 0.05
0.101	10.7 ± 0.4	0.655	Not Applicable	7.77 ± 0.29
0.054	8.8 ± 0.2	0.592	Not Applicable	9.17 ± 0.21
0.010	6.5 ± 0.9	0.492	Not Applicable	11.9 ± 1.6

SIQELS Results from 20,000 g/mol matrix solutions in cyclohexane at 313K

Polymer	Relaxation Time / μ seconds and Variance		Z-Average D_c	
Mass Fraction	Fast Relaxation	Slow Relaxation	$\times 10^{-7} \text{cm}^2 \text{s}^{-1}$	
0.364	31.8 ± 0.7	0.808	$1.1e^5 \pm 7.1e^2$ 0.906	3.41 ± 0.07
0.199	35.0 ± 0.3	0.882	$6.1e^3 \pm 1.7e^2$ 0.888	2.62 ± 0.02
0.106	41.4 ± 0.3	0.755	Not Applicable	2.01 ± 0.02
0.050	27.7 ± 0.6	0.677	Not Applicable	2.91 ± 0.06
0.010	8.4 ± 0.8	0.614	Not Applicable	9.22 ± 0.88

SIQELS Results from 50,000 g/mol matrix solutions in cyclohexane at 313K

Polymer	Relaxation Time / μ seconds and Variance		Z-Average D_c	
Mass Fraction	Fast Relaxation	Slow Relaxation	$\times 10^{-7} \text{cm}^2 \text{s}^{-1}$	
0.427	37.8 ± 1.1	0.830	$9.1e^5 \pm 5.6e^5$ 0.649	3.10 ± 0.09
0.236	38.5 ± 0.7	0.842	$1.3e^4 \pm 6.5e^2$ 0.919	2.40 ± 0.04
0.125	44.7 ± 0.3	0.802	Not Resolved	1.90 ± 0.01
0.074	80.1 ± 0.6	0.798	Not Resolved	1.01 ± 0.08
0.019	19.9 ± 0.2	0.684	Not Applicable	3.90 ± 0.05

SIQELS Results from 100,000 g/mol matrix solutions in cyclohexane at 313K

Appendix C9: OELS Results from Equivalent Solutions in Cyclohexane at 313K

Polymer	Relaxation Time / μ seconds and Variance		Z-Average D_c	
Mass Fraction	Fast Relaxation	Slow Relaxation	$\times 10^{-7} \text{cm}^2 \text{s}^{-1}$	
0.37	9.9 ± 1.5	0.816	Not Applicable	11.1 ± 1.6
0.186	9.8 ± 0.9	0.765	Not Applicable	9.15 ± 0.84
0.103	6.9 ± 0.7	0.664	Not Applicable	12.1 ± 1.2
0.056	5.2 ± 0.9	0.546	Not Applicable	15.5 ± 2.7
0.013	No Data Obtained		No Data Obtained	No Data Obtained

SIQELS Results from 10,000 g/mol matrix solutions in cyclohexane at 318K

Polymer	Relaxation Time / μ seconds and Variance		Z-Average D_c	
Mass Fraction	Fast Relaxation	Slow Relaxation	$\times 10^{-7} \text{cm}^2 \text{s}^{-1}$	
0.409	9.8 ± 0.3	0.497	Not Applicable	11.7 ± 0.03
0.207	10.1 ± 0.8	0.556	Not Applicable	9.06 ± 0.72
0.101	9.9 ± 0.5	0.472	Not Applicable	8.42 ± 0.42
0.054	7.1 ± 0.5	0.523	Not Applicable	11.4 ± 0.8
0.010	No Data Obtained		No Data Obtained	No Data Obtained

SIQELS Results from 20,000 g/mol matrix solutions in cyclohexane at 318K

Polymer	Relaxation Time / μ seconds and Variance		Z-Average D_c	
Mass Fraction	Fast Relaxation	Slow Relaxation	$\times 10^{-7} \text{cm}^2 \text{s}^{-1}$	
0.364	22.7 ± 0.4	0.886	$4.6e^4 \pm 2.7e^4$ 0.901	4.79 ± 0.29
0.199	25.8 ± 0.3	0.946	$4.6e^3 \pm 2.5e^2$ 0.935	3.52 ± 0.05
0.106	35.9 ± 0.7	0.685	Not Applicable	2.33 ± 0.04
0.050	21.3 ± 2.6	0.591	Not Applicable	3.76 ± 0.05
0.010	6.4 ± 0.9	0.503	Not Applicable	12.2 ± 1.7

SIQELS Results from 50,000 g/mol matrix solutions in cyclohexane at 318K

Polymer	Relaxation Time / μ seconds and Variance		Z-Average D_c	
Mass Fraction	Fast Relaxation	Slow Relaxation	$\times 10^{-7} \text{cm}^2 \text{s}^{-1}$	
0.427	31.2 ± 0.2	0.902	$1.7e^5 \pm 1.9e^3$ 0.653	3.80 ± 0.03
0.236	28.3 ± 0.3	0.914	$1.1e^4 \pm 5.2e^2$ 0.691	3.30 ± 0.03
0.125	31.6 ± 0.3	0.545	Not Resolved	2.70 ± 0.02
0.074	34.1 ± 1.0	0.687	Not Applicable	2.41 ± 0.07
0.019	18.8 ± 0.3	0.661	Not Applicable	4.16 ± 0.06

SIQELS Results from 100,000 g/mol matrix solutions in cyclohexane at 318K

Appendix C10: QELS Results from Equivalent Solutions in Cyclohexane at 318K

Polymer	Relaxation Time / μ seconds and Variance		Z-Average D_c	
Mass Fraction	Fast Relaxation	Slow Relaxation	$\times 10^{-7} \text{cm}^2 \text{s}^{-1}$	
0.37	12.7 ± 1.5	0.805	Not Applicable	8.66 ± 1.01
0.186	7.6 ± 0.8	0.596	Not Applicable	11.8 ± 1.3
0.103	5.2 ± 0.8	0.506	Not Applicable	16.1 ± 2.5
0.056	3.5 ± 0.9	0.495	Not Applicable	23.1 ± 5.9
0.013	No Data Obtained		No Data Obtained	No Data Obtained

SIQELS Results from 10,000 g/mol matrix solutions in cyclohexane at 323K

Polymer	Relaxation Time / μ seconds and Variance		Z-Average D_c	
Mass Fraction	Fast Relaxation	Slow Relaxation	$\times 10^{-7} \text{cm}^2 \text{s}^{-1}$	
0.409	4.6 ± 1.8	0.579	Not Applicable	24.6 ± 9.47
0.207	7.1 ± 2.4	0.699	Not Applicable	12.9 ± 4.38
0.101	9.3 ± 0.3	0.546	Not Applicable	8.96 ± 0.25
0.054	6.5 ± 1.3	0.564	Not Applicable	12.5 ± 2.5
0.010	No Data Obtained		No Data Obtained	No Data Obtained

SIQELS Results from 20,000 g/mol matrix solutions in cyclohexane at 323K

Polymer	Relaxation Time / μ seconds and Variance		Z-Average D_c	
Mass Fraction	Fast Relaxation	Slow Relaxation	$\times 10^{-7} \text{cm}^2 \text{s}^{-1}$	
0.364	15.2 ± 1.3	0.811	$5.7e^4 \pm 2.2e^3$ 0.679	7.17 ± 0.62
0.199	18.7 ± 0.5	0.802	$3.1e^3 \pm 3.4e^2$ 0.705	4.88 ± 0.14
0.106	23.5 ± 0.3	0.703	Not Applicable	3.58 ± 0.05
0.050	17.5 ± 0.5	0.654	Not Applicable	4.60 ± 0.13
0.010	4.5 ± 1.6	0.457	Not Applicable	17.3 ± 6.2

SIQELS Results from 50,000 g/mol matrix solutions in cyclohexane at 323K

Polymer	Relaxation Time / μ seconds and Variance		Z-Average D_c	
Mass Fraction	Fast Relaxation	Slow Relaxation	$\times 10^{-7} \text{cm}^2 \text{s}^{-1}$	
0.427	19.7 ± 1.2	0.689	$6.8e^4 \pm 9.3e^3$ 0.653	6.01 ± 0.07
0.236	20.2 ± 0.5	0.701	$1.1e^4 \pm 2.6e^3$ 0.556	4.57 ± 0.11
0.125	21.4 ± 0.6	0.756	$1.6e^3 \pm 3.1e^2$ 0.601	3.99 ± 0.12
0.074	22.0 ± 0.3	0.803	Not Applicable	3.72 ± 0.11
0.019	12.8 ± 0.2	0.889	Not Applicable	6.13 ± 0.10

SIQELS Results from 100,000 g/mol matrix solutions in cyclohexane at 323K

Appendix C11: OELS Results from Equivalent Solutions in Cyclohexane at 323K

Polymer	Relaxation Time / μ seconds and Variance			Z-Average D_c
Mass Fraction	Fast Relaxation		Slow Relaxation	$\times 10^{-7} \text{cm}^2 \text{s}^{-1}$
0.441	Not Resolved		$1.9e^4 \pm 1.3e^3$ 0.508	Not Resolved
0.255	4.9 ± 1.1	0.625	$1.2e^4 \pm 4.2e^3$ 0.478	20.0 ± 4.3
0.152	4.7 ± 0.5	0.572	$6.4e^3 \pm 1.7e^3$ 0.403	18.7 ± 1.8
0.057	4.8 ± 2.7	0.505	546 ± 51 0.345	16.7 ± 9.2
0.015	1.2 ± 0.3	0.469	Not Applicable	62.6 ± 1.5

SIQELS Results from 10,000 g/mol matrix solutions in toluene at 298K

Polymer	Relaxation Time / μ seconds and Variance			Z-Average D_c
Mass Fraction	Fast Relaxation		Slow Relaxation	$\times 10^{-7} \text{cm}^2 \text{s}^{-1}$
0.389	Not Resolved		$8.2e^4 \pm 2.9e^3$ 0.906	Not Resolved
0.199	Not Resolved		$3.8e^3 \pm 2.3e^1$ 0.963	Not Resolved
0.998	Not Resolved		$1.2e^3 \pm 7.9e^1$ 0.772	Not Resolved
0.049	5.4 ± 0.7	0.553	Not Applicable	14.8 ± 1.9
0.010	4.9 ± 0.8	0.478	Not Applicable	15.8 ± 2.6

SIQELS Results from 50,000 g/mol matrix solutions in toluene at 298K

Polymer	Relaxation Time / μ seconds and Variance			Z-Average D_c
Mass Fraction	Fast Relaxation		Slow Relaxation	$\times 10^{-7} \text{cm}^2 \text{s}^{-1}$
0.439	3.2 ± 0.7	0.715	Not Resolved	39.3 ± 9.2
0.248	4.5 ± 0.4	0.914	$1.3e^4 \pm 3.0e^2$ 0.884	21.7 ± 0.7
0.123	5.1 ± 0.7	0.464	Not Applicable	16.8 ± 2.3
0.049	6.7 ± 0.6	0.494	Not Applicable	11.9 ± 1.2
0.013	8.5 ± 0.6	0.552	Not Applicable	9.14 ± 0.5

SIQELS Results from 100,000 g/mol matrix solutions in toluene at 298K

Appendix C12: QELS Results from Equivalent Solutions in Toluene at 298K

Appendix D

Lectures, Conferences and Courses Attended

University of Durham
Board of Studies in Chemistry
Colloquia, Lectures and Seminars Given by Invited Speakers

1991

October	17	Dr. J.A. Salthouse, (University of Manchester) Son et Luminere-A Demonstration Lecture
October	31	Dr. R. Kceley, (Metropolitan Police Forensic Science) Modern Forensic Science
November	6	Prof. B.F.G. Johnson, (University of Edinburgh) Cluster Surface Analogies
November	7	D. A.R. Butler (University of St. Andrews) Traditional Chinese Herbal Drugs: A Different Way of Treating Disease
November	13	Prof. D. Gani (University of St. Andrews) The Chemistry of PLP Dependant Enzymes
November	20	Dr. R. More O'Farrall (University College, Dublin) Some Acid Catalysed Rearrangements in Organic Chemistry
November SCI Lecture	28	Prof. I.M. Ward (IRC in Polymer Science, University of Leeds) The Science and Technology of Oriented Polymers
December	4	Prof. R. Grigg (University of Leeds) Palladium Catalysed Cyclisation and Ion Capture Processes
December	5	Prof. A.L. Smith (Ex Unilever) Soap, Detergents and Black Puddings
December	11	Dr W.D. Cooper (Shell Research) Colloid Science: Theory and Practice

1992

January	22	Dr. K.D.M. Harris (University of St. Andrews) Understanding the Properties of Solid Inclusion Compounds
January	29	Dr. A. Holmes (University of Cambridge) Cycloaddition Reactions in the Service of the Synthesis of Piperadine and Indolizidine Natural Products
January	30	Dr. M. Anderson (Shell Research) Recent Advances in the Safe and Selective Chemical Control of Insect Pests
February	12	Prof. D.E. Fenton (University of Sheffield) Polynuclear Complexes if Molecular Clefts as Models for Copper Biosites
February	13	Dr. J. Saunders (Glaxo Group Research) Molecular Modelling in Drug Discovery
February	19	Prof. E.J. Thomas (University of Manchester) Applications of Organostannanes to Organic Synthesis
February Musgrave Lecture	20	Prof. E. Vogel (University of Cologne) Porphyrins: Molecules of Interdisciplinary Interest

February Tilden Lecture	25	Prof. J.F. Nixon (University of Sussex) Phosphaalkynes: New Building Blocks in Inorganic and Organometallic Chemistry
February	26	Prof. M.L. Hitchman (University of Strathclyde) Chemical Vapour Deposition
March	5	Dr. N.C. Billingham (University of Sussex) Degradable Plastics-Myth or Magic?
March	11	Dr. S.E. Thomas (Imperial College) Recent Advances in Organoiron Chemistry
March	12	Dr. R.A. Hann (ICI Imagedata) Electronic Photography-An Image of the Future
March	18	Dr. H. Maskill (University of Newcastle) Concerted or Stepwise Fragmentation in a Deamination-type Reaction
April	7	Prof. D.M. Knight (University of Durham) Interpreting Experiments: The Beginning of Electrochemistry
May	13	Dr. J.C. Gehert (Ciba Geigy, Basel) Some Aspects of Industrial Agrochemical Research
October	15	Dr M. Glazer and Dr. S Tarling (University of Oxford and Birbeck College) It Pays to be British! The Chemists Role as an Expert Witness in Patent Litigation
October	20	Dr. H.E. Bryndza (Du Pont Research) Synthesis, Reactions and Thermochemistry of Metal(alkyl)cyanide Complexes and Their Impact on Olefin hydrocyanation Catalysis
October Ingold-Albert Lecture	22	Prof. A.G. Davies (University College, London) The Behaviour of Hydrogen as a Pseudometal
October	28	Dr. J.K. Cockroft (University of Durham) Recent Developments In Powder Diffraction
October	29	Dr. J Emsley (Imperial College, London) The Shocking History of Phosphorous
November	4	Dr T. Kee (University of Leeds) Synthesis and Coordination Chemistry of Silylated Phosphites
November	5	Dr. C.J. Ludman (University of Durham) Explosions, A Demonstration Lecture
November	11	Prof. D Robins (University of Glasgow) Pyrrolizidine Alkaloids: Biological Activity, Biosynthesis and Benefits
November	12	Prof. M.R. Truter (University College, London) Luck and Logic in Host Guest Chemistry
November	18	Dr. R.Nix (Queen Mary College, London) Characterisation of heterogeneous Catalysts
November	25	Prof. Y. Vallee (University of Caen) Reactive Thiocarbonyl Compounds

November	25	Prof. L.D. Quinn (University of Massachusetts, Amherst) Fragmentation of Phosphorous Heterocycles as a Route to Phosphoryl Species with Uncommon Bonding
November	26	Dr. D. Humber (Glaxo, Greenford) AIDS-The Development Of A Novel Series Of Inhibitors Of HIV
December	2	Prof. A.F. Hegarty (University College, Dublin) Highly Reactive Enols Stabilised by Steric Protection
December	2	Dr. R.A. Aitken (University of St. Andrews) The Versatile Cycloaddition Chemistry of $\text{Bu}_3\text{P} \cdot \text{CS}_2$
December SCI Lecture	3	Prof. P. Edwards (University of Birmingham) What is a Metal?
December	9	Dr. A.N. Burgess (ICI, Runcorn) The Structure of Perfluorinated Ionomer Membranes
1993		
January	20	Dr. D.C. Clary (University of Cambridge) Energy Flow in Chemical Reactions
January	21	Prof. L. Hall (University of Cambridge) NMR-A Window to the Human Body
January	27	Dr. W. Kerr (University of Strathclyde) Development of Pauson-Khand Annulation Reaction: Organocobalt Mediated Synthesis of Natural and Unnatural Products
January	28	Prof. J. Mann (University of Reading) Murder, Magic and Medicine
February	3	Prof. S.M. Roberts (University of Exeter) Enzymes in Organic Synthesis
February	10	Dr. D. Gillies (University of Surrey) NMR and Molecular Motion in Solution
February Tilden Lecture	11	Prof. S. Knox (University of Bristol) Organic Chemistry at Polynuclear Metal Centres
February	17	Dr. R.W. Kemmitt (University of Leicester) Oxatrimethylenemethane Metal Complexes
February	18	Dr. I. Fraser (ICI Wilton) Reactive Processing of Composite Materials
February	22	Prof. D.M. Grant (University of Utah) Single Crystals, Molecular Structure and Chemical Shift Anisotropy
February	24	Prof. C.J.M. Stirling (University of Sheffield) Chemistry on the Flat-Reactivity of Ordered Systems
March	3	Dr. K.J.P. Williams (BP) Raman Spectroscopy for Industrial Analysis
March	10	Dr K.P. Baker (University College of North Wales, Bangor) An Investigation of the Chemistry of Highly Versatile 7 Coordinate Complexes

March	11	Dr. R.A. Jones (University of East Anglia) The Chemistry of Wine Making
March	17	Dr. R.J.K. Taylor (University of East Anglia) Adventures in Natural Product Synthesis
March	24	Prof. I.O. Sutherland (University of Liverpool) Chromogenic Reagents for Chiral Amine Selectors
May Boys-Rahamnn Lecture	13	Prof. J.A. Pople (Carnegie Mellon University, Pittsburgh) Applications of Molecular Orbital Theory
May	21	Prof. L. Weber (University of Bielfeld) Metallo-phospha Alkenes as Synthons in Organometallic Chemistry
June	1	Prof. J.P. Konopelski (University of California, Santa Cruz) Synthetic Adventures with Enantimerically Pure Acetals
June	7	Prof. R.S. Stein (University of Massachusetts) Scattering Studies of Crystalline and Liquid Crystalline Polymers
June	16	Prof. A.K. Covington (University of Newcastle) Use of Ion Selective Electrodes as Detectors in Ion Chromatography
June	17	Prof. O.F. Nielson (University of Copenhagen) Low Frequency IR and Raman Studies of Hydrogen Bonded Liquids
September	13	Dr. K.J. Wynne (Office of Naval Research Washington) Polymer Surface Design for Minimal Adhesion
September	14	Prof. J.M. DeSimone (University of North Carolina) Homogeneous and Heterogeneous Polymerisation in Environmentally Responsible Carbon Dioxide
September	28	Prof. H. Ila (North Eastern Hill University, India) Synthetic Strategies for Cyclopentanoids via Oxoketene Dithioacetals
October	4	Prof. F.J. Fehler (University of California, Irvine) Bridging the Gap Between Surfaces and Solutions with Sessilquioxanes
October	14	Dr. P. Hubberstey (University of Nottingham) Alkali Metals: Alchemist's Nightmare, Biochemist's Puzzle and Technologist's Dream
October	20	Dr. P. Quayle (University of Manchester) Aspects of aqueous ROMP Chemistry
October	23	Prof. R.Adams (University of South Carolina) The Chemistry of Metal Carbonyl Cluster Complexes Containing Platinum and Iron, Ruthenium or Osmium and the Development of a Cluster Based Alkyne Hydrogenation Catalyst
October	27	Dr. R.A.L Jones (University of Cambridge) Perambulating Polymers
November	10	Prof. M.N.R. Ashfold (University of Bristol) High Resolution Photofragment Translational Spectroscopy: A New Way to Watch Photodissociation

November	17	Dr. A. Parker (Rutherford Appellton Laboratory) Applications of Time Resolved Resonance Raman Spectroscopy to Chemical and Biochemical Problems
November	24	Dr. P.G. Bruce (University of St. Andrews) Synthesis and Applications of Inorganic Materials
November	25	Dr. R.P. Wayne (University of Oxford) The Origin and Evolution of the Atmosphere
December	1	Prof. M.A. McKervy (Queens University, Belfast) Functionalised Clixerenes
December	8	Prof. O. Meth Cohn (University of Sunderland) Friedel's Folly Revisited-A Super Way to Fused Pyridines
December	16	Prof. R.F. Hudson (University of Kent) Close Encounters of the Second Kind
1994		
January	26	Prof. J. Evans (University of Southampton) Shining Light on Catalysts
February	2	Dr. A. Masters (University of Manchester) Modelling Water Without Using Pair Potentials
February	9	Prof. D. Young (University of Sussex) Chemical and Biological Studies of the Coenzyme Tetrahydrofolic Acid
February	16	Prof. K.H. Theopold (University of Delaware) Paramagnetic Chromium Alkyls : Synthesis and Reactivity
February	23	Prof. P.M. Maitlis (University of Sheffield) Across the Border: From Homogeneous to Heterogeneous Catalysis
March	2	Dr. C. Hunter (University of Sheffield) Noncovalent Interactions between Aromatic Molecules
March	9	Prof. F. Wilkinson (Loughborough University of Technology) Nanosecond and Picosecond Laser Flash Photolysis
March	10	Prof. S.V. Ley (University of Cambridge) New Methods for Organic Synthesis
March	25	Dr. J. Dilworth (University of Essex) Technetium and Rhenium Compounds with Applications as Imaging Agents
April	28	Prof. R.J. Gillespie (McMaster University, Canada) The Molecular Structure of some Metal Fluorides and Oxofluorides: Apparent Exceptions to the VSEPR Model
May	12	Prof. D.A. Humphreys (McMaster University, Canada) Bringing Knowledge to Life

**The Following Lectures in the IRC in Polymer Science and Technology
International Seminar Series have also been Attended.**

1992

March	17	Prof. Sir S.F. Edwards (University of Cambridge) at Leeds University Phase Dynamics and Phase Changes in Polymer Liquid Crystals
March	25	Prof. H. Chedron (Hoechst AG) at Durham University Structural Concepts and Synthetic Methods in Industrial Polymer Science
May	11	Prof. W. Burchard (University of Freiburg) at Durham University Recent Developments in the Understanding of Reversible and Irreversible Network Formation
September	21	Prof. E.L. Thomas (MIT, Cambridge, Massachusetts) at Leeds University Interface Structures in Copolymer-Homopolymer Blends

1993

March	16	Prof. J.M.G. Cowie (Heriot-Watt University) at Bradford University High Technology in Chains: The Role of Polymers in Electronic Applications and Data Processing
April	1	Prof. H.W. Speiss (Max-Planck Institut, Mainz) at Durham University Multidimensional NMR Studies of Structure and Dynamics of Polymers
June	2	Prof. F. Ciardelli (University of Pisa) at Durham University Chiral Discrimination in the Stereospecific Polymerisation of α -olefins
June	8	Prof. B.E. Eichinger (BIOSYM Technologies) at Leeds University Recent Polymer Modelling Results and a Look into the Future
July	6	Prof. C.W. Macosko (University of Minnesota) at Bradford University Morphology Development in Immiscible Polymer-Polymer Blending
September	13	Prof. A.D. Schluter (Freie Universitat, Berlin) at Durham University Synthesis and Characterisation of Molecular Rods and Ribbons

The Following Conferences and Courses Have Been Attended.

March 1992: Macro Group (UK) Family Meeting, Durham University

September 1992: IRC Club Meeting, Leeds University

January 1993: IRC Polymer Engineering Course, Bradford University

March 1993: IRC Polymer Physics Course, Leeds University

April 1993: Macro Group (UK) Family Meeting, Lancaster University

July 1993: The Polymer Conference, Cambridge University

September 1993: IRC Club Meeting, Durham University

April 1994: Macro Group (UK) Family Meeting, Birmingham University

July 1994: MacroAkron '94 IUPAC Meeting, University of Akron, Ohio, USA

